Union de Normalisation de la Mécanique

# EN 13445 "Unfired pressure vessels"

# Background to the rules in Part 3 Design

**Editors:**

**Guy BAYLAC**
**Consultant and Technical Advisor to EPERC**
**114 avenue Félix Faure**
**F-75015 PARIS**
**guy.baylac@wanadoo.fr**

**Danielle KOPLEWICZ**
**Technical Director**
**Union de Normalisation de la Mécanique**
**F-92038 PARIS LA DEFENSE**
**d.koplewicz@unm.fr**

**Issue 2 – 20 August 2004**

92038 Paris La Défense cedex
45, rue Louis Blanc
92400 Courbevoie - France
Site internet : www.unm.fr
Tél. : + 33 1 47 17 67 67
Fax : + 33 1 47 17 67 99

## Introduction

The European standard EN 13445 "Unfired pressure vessels" provides a precedent in that after 10 years of discussion between experts, a European consensus was achieved in the field of pressure equipment. Part 3 which was prepared by a group of leading European experts under the guidance of Dr. Fernando LIDONNICI, Sant'Ambrogio, (Milano, Italy), represents a major advance in European technical convergence. The adoption of the first issue of EN 13445 in May 2002 was the first step of a continuous process for development & improvement.

This new standard benefits from the contribution of all the European expertise; as such, it includes innovative capacities and supplies solutions for modern subjects.

The CEN Design rules promote Limit Analysis and Design By Analysis – Direct Route. Design has a strategic importance for the future and the competitiveness of the pressure equipment industry. Optimum design allows substantial advantages such as: thickness reduction and damage control in service with safety increase and drastic maintenance cost reduction.

The objective of this book is to explain the background of these rules, to help industry to apply them in the most effective way. It was initiated by EPERC, the European Pressure Equipment Research Council, and and was awarded a contract of CEN, the European Standardization Committee, with support of the European Commission.

The release of this booklet was made possible by the co-operative efforts of the experts involved in the discussion of Part 3, namely:

| | |
|---|---|
| - Guy BAYLAC | Design criteria |
| - Matteo CANNEROZZI | Openings in shells |
| - Joris DECOCK | Additional non-pressure loads |
| - Richard FAWCETT | Shell under internal pressure, shell under external pressure, Design of flanges and domed ends |
| - Alain HANDTSCHOEWERCKER | Simplified assessment of fatigue life, Design by Analysis based on stress categories |
| - Fernando LIDONNICI | Flat ends |
| - Stephen MADDOX | Detailed assessment of fatigue life |
| - Olavi VALTONEN | Rectangular pressure vessels |
| - Francis OSWEILLER | Heat exchangers, Expansion bellows |
| - Joachim WOELFEL | Advanced design for flanges, Advanced design of tubesheets |
| - Josef ZEMAN | Design by Analysis – Direct Route |

UNM, which leads the maintenance Help desk of EN 13445 (EN 13445/MHD), provides its logistical support to compile and format the contributions, and agrees to put the booklet on the EN 13445/MHD website for free uploading.

## Presentation

This book shows the background to Part 3 "Design" of the European standard EN 13445 "Unfired pressure vessels". To facilitate for the reader the cross-referencing between the explanations provided and the normative content of the standard itself, the booklet is organized according to the same clause numbering than the standard. In each clause, a different numbering, with letters, is provided.

Each explanatory clause address the following topics:

- Background and references to the rules (with, where relevant a bibliography included in each clause)
- Detailed description of the method and comparison to other methods
- Future developments

The following clauses are included:

# 1 Scope

Part 3 of EN 13445 gives the rules to be used for design and calculation under internal and/or external pressure (as applicable) of pressure bearing components of Pressure Vessels, such as shells of various shapes, flat walls, flanges, heat exchanger tubesheets, including the calculation of reinforcement of openings. Rules are also given for components subject to local loads and to actions other than pressure.

For all these components the DBF (Design by Formulae) method is generally followed, i.e. appropriate formulae are given in order to find stresses which have to be limited to safe values. These formulae are generally intended for predominantly non-cyclic loads, which means for a number of full pressure cycles not exceeding 500.

However general prescriptions are also given for DBA (Design by Analysis) which can be used either to evaluate component designs or loading situations for which a DBF method is not provided, or, more generally, as an alternative to DBF.

Methods are also given where a fatigue evaluation is required, due to a number of load cycles being greater than 500. There are two alternative methods: a simplified method based on DBF (valid mainly in case of pressure variations) and a more sophisticated method based on a detailed determination of total stresses using, for example, FEM or experimental methods. This can be used also in the case of variable loads other than pressure.

For certain components (such as flanges and tubesheets) also an alternative DBF method (based on limit analysis) has been provided; the choice of which method has to be used in each particular case is left to the Designer.

For the time being, the scope of Part 3 is limited to steel components working at temperatures lower than the creep range of the specific material concerned.

# 2 Normative references

Clause 2 includes the list of the referenced documents cited in EN 13445-3 in such a way as to make them indispensable for the application of the standard. These references are dated, that means that subsequent amendments to, or revisions of, dated references will need to be incorporated by amendment of the document referring to them.

# 3 Terms and definitions

Clause 3 gives the definition of terms applicable to the whole Part 3 such as calculation pressure/temperature, design pressure/temperature, governing weld joint. Specific definitions are also found in the clause of the standard where they are used.

# 4 Symbols and abbreviations

Clause 4 establishes symbols and units, needed to apply Part 3. Specific symbols are also found in the clause of the standard where they are used. The units are SI-units, consistent with the ISO 31 standard series.

# 5 Basic design criteria

## 5A General

Basic design criteria for Part 3 are given in Clause 5.

It is essential to remember that:

- EN 13445-3:2002 does not contain rules to design in the creep range. Creep design rules are under development and will be introduced later, probably in 2006.

- The rules are not applicable in case of localised corrosion. In this case the material shall be changed or adequate protection provided.

Clause 5 deals successively with:

- Corrosion, erosion and protection
- Load cases
- Design methods
- Weld joint coefficient
- Design of welded joints

## 5B Corrosion, erosion and protection

In the standard "corrosion" is a very general term to be understood as all forms of wastage. Thus, it is impossible to give rules to protect against corrosion, due to the multitude of cases to consider; only general advice can be provided in informative notes.

The two cases where the standard can be prescriptive are:

[1] When an additional thickness is sufficient to protect against corrosion during lifetime. Then the design shall take into consideration the corroded condition at the end of life.

[2] Or when an adequate coating or lining is a reliable protection against corrosion.

Figure 3-1 of the Standard gives the relation between the various thicknesses. This figure is applicable to plates. It is relatively complex since it aims at providing guidance to order the plates.

## 5C Load cases

Load cases to consider are in conformity with the requirements of Annex I of the Directive on Pressure Equipment [1]. The classification of the load cases in three categories is classical, but may be modified in the future.

## 5D Design methods

This Part provides currently two design methods:

[1] Design by formulae which is used in Clause 7 to 16

[2] Design by analysis, which is covered by Annexes B and C. Annex C uses the classical approach of stress portioning while Annex B Design by Analysis – Direct Route is totally new.

A new amendment is in preparation on experimental techniques.

This Standard mainly addresses welded construction and the communication between Part 3 and the other parts [2] is ensured by the testing groups.

This architecture has been built from elements borrowed from the German Code AD-Merkblatt [3], the British Specification for unfired pressure vessels PD 5500:2000 [4] and the French Code CODAP 2000 [5].

In Part 1 of the Standard, the testing group of a weld is defined as "one of the four groups designed to specify the extent of non destructive testing and destructive testing necessary in association with weld joint coefficient, material grouping, welding process, maximum thickness, service temperature range".

The table of testing groups is given in annex (Table 1). Testing groups are classified from 1 to 4 in decreasing extent of NDT. The manufacturer may select a high extent of NDT (testing groups 1 or 2), a reduced extent of NDT (testing group 3), or just a visual inspection (testing group 4).

However testing groups are designed to offer the same safety by a combination of several factors, as represented in table 1. Material grouping of the table is per CR ISO/TR 15608:1999 [6]. More detailed information on testing groups can be found in EPERC Bulletin Nr 2 [7].

When the weld is a governing one (longitudinal weld on a cylinder or a cone, or main weld on a sphere or a dished end), the testing group controls the thickness of the weldment and generally the thickness of adjacent plates by the weld joint efficiency factor.

It is intended that a single testing group shall be applied to the entire vessel. Nevertheless, where there is more than a single governing joint on a vessel and provided the requirements of table 1 are met, combinations of testing groups 1 and 2 or 1, 2 and 3 are permissible. Thus the concept of testing group is more flexible than the concept of vessel category used in certain codes.

However testing group 4 cannot coexist with any other testing group on the same vessel.

## 5D-1 PRESSURE LOADING OF NON-CYCLIC NATURE

Many pressure vessels are designed for pressure loading of non-cyclic nature. The requirements specified in the Design By Formulae (DBF) section of EN 13445-3 provide satisfactory designs when the number of full pressure cycles or equivalent full pressure cycles is less than 500. This value is similar to the value 1000 of the ASME Code [8], but reduced to take account of a higher nominal design stress (safety coefficient of 2,4 instead of 4 on the ultimate strength)

$$n_{eq} \leq 500 \qquad \text{(5D-1)}$$

Then no fatigue analysis is necessary and the standard requirements of non destructive testing given in EN 13445-5 shall be applied.

For $n_i$ pressure cycles of pressure range $\Delta P_i$ less than the full calculation pressure $P$, the number of equivalent full pressure cycles is given by:

$$n_{eq} = \Sigma\, n_i \cdot \left( \frac{\Delta P_i}{P_{max}} \right)^3 \qquad \text{(5D-2)}$$

In the above formula, the exponent 3 is the exponent related to the design fatigue curve, $P_{max}$ is the maximum permissible pressure based on the analysis thickness. $P_{max}$ is greater than the calculation pressure $P$. This increases the number of allowed full pressure cycles.

For usual components, $P_{max}$ expression is generally given in the different clauses of the DBF section. If necessary, $P_{max}$ may be replaced by the calculation pressure $P$.

Pressure vessels to testing group 4, are intended for non-cyclic operation and are limited to 500 full pressure cycles or equivalent full pressure cycles.

## 5D-2 PRESSURE LOADING OF CYCLIC NATURE

If the number of full pressure cycles or equivalent full pressure cycles is likely to exceed 500, the calculations of vessels of testing groups 1, 2 and 3 shall be completed by a simplified fatigue analysis, as given in clause 17 of EN 13445-3 or, if necessary, by a detailed fatigue analysis, as given in clause 18.

In addition clauses 17 and 18 specify limiting values $D_{max}$ of the cumulative damage for the determination of critical zones where additional requirements on weld imperfections and NDT shall be applied, as defined in Annex G of EN 13445-5.

Figure 5D-1 shows the correlation between fatigue analysis and NDT.

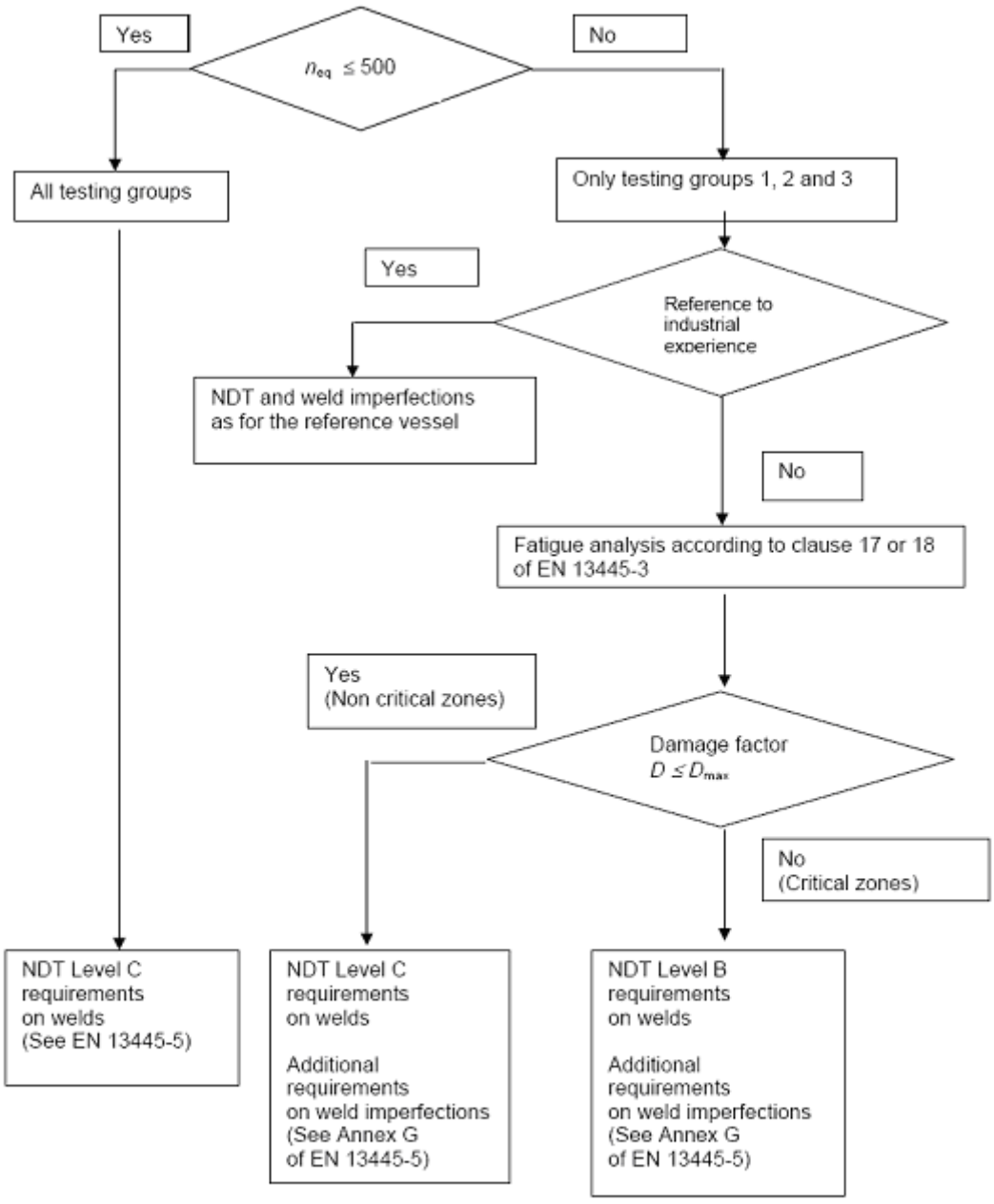


**Figure 5D-1 Fatigue analysis and NDT**

## 6 Maximum allowed values of the nominal design stress for pressure parts

Table 6.6.1-1 of Part 3 gives the maximum value of the nominal design stress for ductile steels, according to the definition of ductility given in EN 13445-2. This value is to be used in the DBF section of EN 13445-3 for pressure components other than bolts.

**Table 6.6.1-1Testing groups for steel pressure vessels**

| Requirements | Testing group a | | | | | | |
|---|---|---|---|---|---|---|---|
| | 1 | | 2 | | 3 | | 4 |
| | 1a | 1b | 2a | 2b | 3a | 3b | [b,j] |
| Permitted materials [g] | 1 to 10 | 1.1, 1.2, 8.1 | 8.2, 9.1, 9.2, 9.3, 10 | 1.1, 1.2, 8.1 | 8.2, 9.1, 9.2, 10 | 1.1, 1.2, 8.1 | 1.1, 8.1 |
| Extent of NDT for governing welded joints [e,h] | 100 % | 100 % | 100 % - 10% [d] | 100 % - 10 % [d] | 25 % | 10 % | 0 % |
| NDT of other welds | Defined for each type of weld in Table 6.6.2-1 | | | | | | |
| Joint coefficient | 1 | 1 | 1 | 1 | 0,85 | 0,85 | 0,7 |
| Maximum thickness for which specific materials are permitted | Unlimited [f] | Unlimited [f] | 30 mm for groups 9.1, 9.2<br>16 mm for groups 9.3, 8.2 [i], 10 | 50 mm for groups 1.1, 8.1<br>30 mm for group 1.2 | 30 mm for groups 9.2, 9.1<br>16 mm for groups 8.2, 10 | 50 mm for groups 1.1, 8.1<br>30 mm for group 1.2 | 12 mm for groups 1.1, 8.1 |
| Welding process | Unlimited [f] | Unlimited [f] | Fully mechanical welding only [c] | | Unlimited [f] | Unlimited [f] | Unlimited [f] |
| Service temperature range | Unlimited [f] | Unlimited [f] | Unlimited [f] | Unlimited [f] | Unlimited [f] | | Limited to (-10 to +200) °C for group 1.1<br>(-50 to+300) °C for group 8.1 |

[a] All testing groups shall require 100 % visual inspection to the maximum extent possible
[b] Testing group 4 shall be applicable only for:
- Group 2 fluids; and
- $P_S \leq 20$ bar; and
- $P_S\ V \leq 20\ 000$ bar·L above 100 °C; or
- $P_S\ V \leq 50\ 000$ bar·L if temperature is equal or less than 100 °C;
- higher pressure test (See clause 10);
- maximum number of full pressure cycle less than 500;
- lower level of nominal design stress (See EN 13445-3).

[c] Fully mechanised and/or automatic welding process (See EN 1418:1997).
[d] First figure: initially, second figure: after satisfactory experience. For definition of “satisfactory experience", see 6.6.1.1.4
[e] Testing details are given in Table 6.6.2-1
[f] Unlimited means no additional restriction due to testing. The limitations mentioned in the table are limitations imposed by testing. Other limitations given in the various clauses of the standard (such as design, or material limitations , etc.) shall also be taken into account.
[g] See EN 13445-2 for permitted materials.
[h] The percentage relates to the percentage of welds of each individual vessel
[i] 30 mm for group 8.2 material is allowed if delta ferrite containing welding consumables are used for depositing filling passes up to but not including the capping run.
[j] Limited to single compartment vessels and single material group.

For ferritic steels, the safety factor of 2,4 put on the ultimate strength at 20° C impedes efficient use of the new modern high yield strength steels (Thermo-Mechanically rolled and Quenched and Tempered steels). Therefore Annex B of EN 13445-3, DBA Direct Route, allows the use of a reduced safety equal to 1,875, but still giving a margin of safety of 2 towards burst for vessels with moderate notch effect (e.g. weld details of testing group 1 in accordance with Annex A of EN 13445-3).

For austenitic steels with a rupture elongation greater or equal than 35 %, the nominal design stress based on the ultimate strength at calculation temperature $T$ is safe, but may induce large strains. Therefore the nominal design stress cannot exceed the value:

$$\left( \frac{R_{\mathrm{p1,0}/T}}{1{,}2} \right) \qquad (6\text{-}1)$$

Many pressure vessels are built to testing group 4 without NDT, except for the cone to cylinder junction when the cone angle is greater than 30°. Although these vessels are built from easy-to-weld steels belonging to material groups 1.1 and 8.1, the nominal stress is limited 90 % of the current nominal design stress.

A safety equivalent to the vessels of other testing groups has been obtained by:

1. Reducing the manufacturing tolerances (peaking and excess weld of the longitudinal weld)

2. Increasing the test pressure to reduce residual stresses, obtain crack blunting and correction of shape imperfections.

The beneficial effect of a higher test pressure was shown by the Research and Development programme HYDFAT, sponsored by DG Research of the European Commission. For more information, see EPERC Bulletin Nr 4 [9].

## 6A Bibligraphy


[1] Directive 97/23/EC of the European Parliament and of the Council of 29 May 1997 on the approximation of the laws of the Member States concerning pressure equipment, Official Journal of the European Communities, No L 181/1, 9 July 1997.

[2] EN 13445, Unfired pressure vessels, Issue 1(2002-05), Part 1: General, Part 2: Materials, Part 3: Design, Part 4: Manufacture, Part 5 Inspection and Testing, Part 6: Requirements for design and fabrication of pressure vessels and vessel parts constructed of spheroidal cast iron.

[3] AD-Merkblatt, 2000 edition, English translation, Carl Heymans Verlag KG, D-50939 Köln.

[4] PD 5500:2000, Specification for unfired fusion welded pressure vessels, British Standards Institution, London, UK.

[5] CODAP 2000, French code for the construction of pressure vessels, SNCT, F-92400 Courbevoie

[6] CR ISO/TR 15608:1999(E), Welding – Guidelines for a metallic grouping system for fabrication purposes.

[7] EPERC Bulletin Nr 2, October 1999, European Approach to Pressure Equipment Inspection, Ed. Jean-Bernard Veyret, Guy Baylac, European Commission JRC, NL-1755 ZG Petten, S.P.I. 192.

[8] ASME Code, Section VIII, Division 2, Alternative Rules, 2000.

[9] EPERC Bulletin Nr 4, June 2001, European R&D on fatigue strength and hydrotest for pressure equipment, European Commission JRC, NL-1755 ZG Petten, S.P.P.01.42.


# 7 Shells under internal pressure

## 7A Introduction

Rules for cylinders, spheres and cones as given in EN 13445-3 clauses 7.4.2, 7.4.3, and 7.6.4 require no comment, the equations being standard and familiar. It is only when one comes to the intersection of a sphere and a cone (on the same axis) in 7.6.5 to 7.6.9 that comment is needed, as described below under 7B.

Dished ends are used in most pressure vessels so their economic design is of importance. They are dealt with in sections 7.5 and 7.7 of part 3 of EN 13445-3, and explained under 7C.

## 7B Cones and conical ends

There are three situations to consider: the large end of the cone, with and without a knuckle, and the small end. In each case it is necessary to consider gross deformation and shakedown criteria, for which limit analysis and elastic analysis with a stress limit of 2f are used respectively. Not only must the rules give a minimum thickness but they must also tell the user how far from the junction the thickness has to extend.

Rules for determining the minimum thickness are, it will be seen, all based on limit analysis based procedures supplied by the German delegation. They are taken from the East German pressure vessel code [1]

### 7B-1 The large end of a cone without a knuckle

This has traditionally been dealt with by limiting the stress at the junction to 3f. However it is found that the limit pressure is close to but slightly less than the 3f pressure for all D/e ratios and angles, the difference becoming greater at greater angles. The method based on stress analysis has therefore been replaced by a formula provided by Germany and based on limit analysis.

The formula originally supplied was

$$e = \frac{pD\beta}{2f} \text{ where } \beta = 0{,}4\sqrt{\frac{D}{e}}\frac{\tan(\alpha)}{1+1/\sqrt{\cos(\alpha)}} - 0{,}25$$

and α is the cone semi-angle. The formula is an approximation to a fuller and far more complicated solution.

It was accepted that deformation by the internal pressure loading results in a more favourable shape and that there has been successful experience with rules based on the 3f criterion. It was therefore decided to replace the above equation for β by:

$$\beta = \tfrac{1}{3}\sqrt{\frac{D}{e}}\frac{\tan(\alpha)}{1+1/\cos(\alpha)} - 0{,}15$$

which brings us very close to the 3f method. The upper limit on angle is set at 60°, though it has been established that the formula is safe up to 90°.

While a formula based on limit analysis for intersections in which the thicknesses of cone and cylinder are different exists, it has not been used. Stresses hardly come down at all as the thickness of one member is increased, so the stress limit soon becomes controlling and the stress would have to be compared with 3f.

Once it is realised that the limit load controls design, fresh thought has to be given to the distance over which the increased thickness must be maintained.

Looking first at the minimum distance along the cylinder, conventional elastic stress analysis shows no increase in stress even when the junction thickness is maintained only for a distance well below $\sqrt{D \cdot e}$ However work carried out by the author using a thin shell limit analysis computer code (named LASH - details in 7B-5) showed unacceptable loss of limit load - about 15% - with junction thickness extending for a distance $\sqrt{D \cdot e}$ but only a minor loss of < 5% for a distance of $1{,}4\sqrt{D \cdot e}$ , which has therefore been adopted as the minimum for the new standard.

It is also necessary to consider the acceptable distance between two major features, such as two cone/cylinder intersections. Calculations of typical examples with LASH showed that this distance could be $2\sqrt{D \cdot e}$ and not the $2{,}8\sqrt{D \cdot e}$ that might be expected. One reason for this observation is the importance in these problems of shell bending, so that any thinning of the shell greatly reduces the available moment in the limit analysis at the point where thickness changes.

### 7B-2 The large end with a knuckle

The method is again based on limit analysis and has been modified to tie in with the formula without a knuckle. It

$$e = \frac{pD\beta}{2f\gamma}$$

where β is given above

$$\gamma = 1 + \frac{\rho}{1{,}2\left(1 + 0{,}2/\rho\right)},$$

$$\rho = \frac{0{,}028r}{\sqrt{D \cdot e}} \times \frac{\alpha}{1 + 1/\cos(\alpha)}$$ and $r$ is the radius of the knuckle.

Use of LASH showed that the distance over which the thickness calculated above had to be maintained could be measured, not from the tangent line with the knuckle but from the junction, as defined in the standard.

### 7B-3 The small end of the cone

Turning now to the small end of the cone, we find a situation where the limit load controls at all times and stress concentrations are moderate. It is therefore possible to provide a method allowing for different thicknesses of shell and cone. It is also found that the limit load improves only little with the introduction of a knuckle, so no separate method need be given for it.

The method now is the CEN draft again comes from East Germany. As before, it is an acceptable approximation to the full analysis, and better in that respect than other sets of formulae such as area replacement methods.

### 7B-4 Future work

Recommendations were submitted to CEN TC 54 WG"C" for removing the angle limitation, allowing the rules for angles up to 90°, but there is little incentive to make the change to the text of EN13445-3. Of course as the cone becomes very flat the cone rules become very conservative due to the cos(α) factor, but it is then possible to turn to the flat plate rules as given in clause 10.

Confirming the various minimum distance rules would make a nice masters degree project.

### 7B-5 Thin Shell Limit Analysis Program LASH

The computer program LASH was written to carry out a limit analysis on an axisymmetric thin shell. The thin shell itself is modelled by a sandwich of four shells, each representing 1/4 of the total thickness. The four shells individually can only take membrane loads but can combine to give the full plate the ability to accept a bending moment. (Shear is also of course allowed). The normal Tresca yield criterion is applied to each of the layers. The shell is split up into 'finite elements' about $0{,}25\sqrt{(re)}$ long.

The equations relating the loads in the elements to bending moments and direct loads in the whole plate and the equations balancing the various loads are all linear. In lower bound limit analysis one is trying to find a stress distribution that maximises the applied load without infringing the yield condition. We therefore have a linear programming problem, which can be solved by computer, though with much more effort than required for an elastic analysis.

How good a model does the 4 layer sandwich provide? Considering direct load and bending in one direction only, the sandwich approximation to the shell replaces the well known yield parabola by two straight lines. The parabola referred to is:

$$\left(N/N_0\right)^2 + M/M_0 = 1$$

There is a maximum departure from the true curve of 5%, always on the safe side. The 4 layer sandwich also gives a good approximation to the interaction between direct load in one direction and bending in the other, which is important in this class of problem.

## 7C Dished ends

### 7C-1 Introduction

Dished ends are used in most pressure vessels so their economic design is of importance. It is found that two modes of failure have to be considered in drawing up design rules – excessive axisymmetric plastic deformation and, for thin ends, buckling of the knuckle under the compressive circumferential stresses found there. Over the years the problem has attracted the attention of many workers and a number of different design rules are to be found in pressure vessel codes. There is a great fund of experience of the use of dished ends.

However it is only very recently that the power of the computer has enabled us to produce consistent design rules. The rules provided in the UPVS to protect against excessive deformation are based on one report, Welding Research Council Bulletin 364 [2] by Kalnins and Updike (known here as K&U) modified by the CEN committee to take account of European experience.

A number of papers have been produced on the phenomenon of buckling in dished ends but the latest one to suggest design rules is by Galletly (1986) [3] and these rules have been adopted as they stand.

The question of a nozzle in or intruding into the knuckle region is dealt with in this part of the standard since the solution is to increase thickness over the whole of the knuckle region.

### 7C-2 Review of EN 13445-3 rules for dished ends

Dished ends are dealt with in sections 7.5 and 7.7 of part 3 of EN 13445-3.

The limitations in 7.5.3.1 follow from the data used, except that the committee considered a limitation by Galletly of his method to ambient temperatures only could be ignored. Galletly argued from the fact that the experimental work was all at ambient, but the committee considered the extensive computer work justified a different view.

Equation (7.5-1) and (7.5-6) are concerned with the membrane stress in the spherical cap.

Equations (7.5-2) and (7.5-7), together with (7.5-9) to (7.5-17) are the main part of the method and are intended to prevent excessive deformation.

The K&U results appear in the method as polynomials that closely match the data in their report. These polynomials are the expressions in brackets in equations (7.5-13), (7.5-15) and (7.5-17).

The modifications made by the CEN committee appear in the standard as factor N in equations (7.5-13) and (7.5-15), the 0,95 and 0,5 in equation (7.5-19) and the factor $\{(0,75\,R + 0,2\,D)$ (replacing $R$) in equations (7.5-2) and (7.5-7).

Equations (7.5-3) and (7.5-8) are based on Galletly's method.

The rules in 7.5.4 for ellipsoidal ends provide for a nominally equivalent torisphere. The simple formulae therein are approximations to the two well-known equivalence formulae, namely

$$(0,5/K - 0,08) \cong \left\{K^2 + 1 - \left(K-1\right)\sqrt{K^2+1}\right\}/\left(4K^2\right)$$

and $$(0,44\,K + 0,02) \cong \left\{K^2 + 1 + \left(K-1\right)\sqrt{K^2+1}\right\}/\left(4K\right)$$

Moving now to section 7.7 on nozzles in the knuckle region, the rules are based on AD2000-Merkblatt B-3, the main difference being that formulae have been found (equations (7.7-3) to (7.7-10) that are close to the crude graphical method in the ADM. These rules are limited to the two standard ends since there is no way of interpolating when two shape variables are involved.

A note on the standard German ends – the method in section 7.5 is a complicated calculation and to supplement the graphs the following tabulation for factor $C = \frac{ef}{pR}$ is provided.

| e/R | 0,001 | 0,002 | 0,003 | 0,004 | 0,006 | 0,008 | 0,01 | 0,012 |
|---|---|---|---|---|---|---|---|---|
| Kloepper | 1,082 | 1,044 | 0,990 | 0,941 | 0,862 | 0,802 | 0,758 | 0,726 |
| Korbogen | 0,809 | 0,788 | 0,760 | 0,734 | 0,692 | 0,659 | 0,634 | 0,615 |

| e/R | 0,014 | 0,016 | 0,02 | 0,024 | 0,028 | 0,032 | 0,036 | 0,04 |
|---|---|---|---|---|---|---|---|---|

| | | | | | | | | |
|---|---|---|---|---|---|---|---|---|
| Kloepper | 0,703 | 0,685 | 0,654 | 0,624 | 0,595 | 0,568 | 0,545 | 0,524 |
| Korbogen | 0,603 | 0,593 | 0,578 | 0,563 | 0,550 | 0,537 | 0,527 | 0,518 |

## 7C-3 Basis for design rules

### *7C-3a Excessive plastic deformation*

Although there are a number of available methods for dished end design in current use and many papers on the subject, the method presented in this standard is based on the work of Kalnins and Updike. The first task here is to state what they did, then how it was adapted for CEN use. It is not the purpose here to provide a general review of the history of dished end design or to show that other failure mechanisms are catered for; that is done already by K&U.

Failure of dished ends is difficult to define. Those made of typical ductile pressure vessel materials will deform into stronger and stronger shapes, eventually taking on a nearly spherical form, before bursting. The shape improvement on hydro-test also goes to reduce stresses in subsequent operation, of importance when considering shakedown and fatigue.

The failure criterion chosen by K&U was the twice elastic slope criterion (as prescribed by ASME) applied to the deformation of the centre of the head.

The theoretical model included shape change. There was no work hardening. The ratio of Young's modulus to yield was set at 1000. The von Mises yield criterion was used.

Geometries studied were for just three values of *r/D* (inside knuckle radius/inside diameter) of 0,06, 0,1 and 0,2. The value of *e/R* (thickness/inside crown radius) covered the range from 0,002 to 0,04. There was no straight flange of thickness equal to that of the end – the thickness of the whole cylinder was set in the calculations at the minimum required by code rules.

Results were presented in the form $\frac{p}{f} = func\left(\frac{e}{R}, \frac{r}{D}\right)$. Note that the number of dimensionless variables is one less than expected. It was found that results varied little with *R/D* and so in the interests of ease of use this variable was omitted.

The arguments used to justify the modifications made by committee are in the next section.

Interpolation has to be used in a design procedure between the values of *r/D* considered by K&U. A simple but conservative interpolation rule is needed. The one chosen is a linear interpolation for β since it is more conservative than interpolation for 1/β.

In the absence of other data, design for *e/R*>0,04 is dealt with by using the value at 0,04.

### *7C-3b CEN modifications to K&U*

Since the Kloepper form is used so much in Europe and is typical of shapes used elsewhere, comparison is concentrated on it. It also happens to be close to one of the shapes considered by K&U, who looked at *r/D* values of 0,06, 0,1 and 0,2. There is a slight difference because their *D* was the internal diameter whereas the Kloepper *r/D* is based on the external diameter.

The attached graph shows how the ratio *C = (e/R)/(p/f)* varies according to the above data. It is seen that ASME/CODAP is closest to the K&U data.

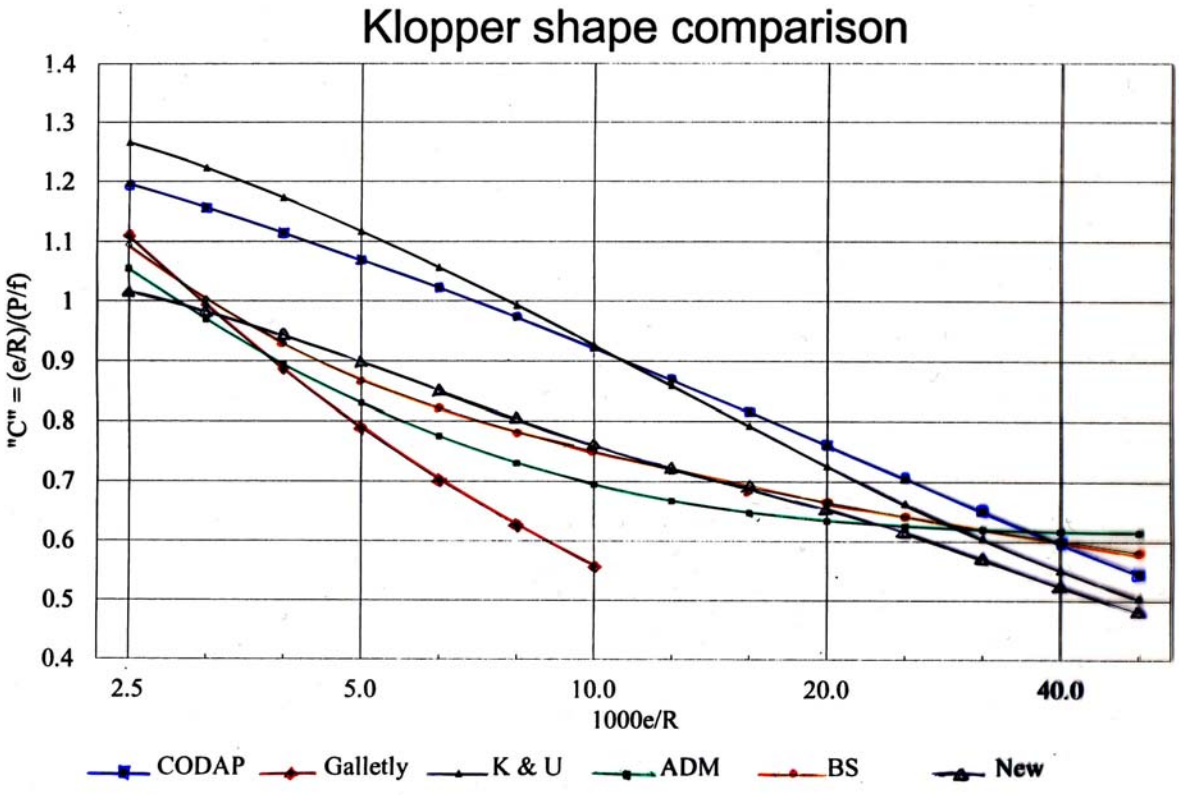


**Figure 7C-1 Klopper shape comparison**

PD 5500 and ADM are relatively close to each other and, in the middle of the range, well below the other lines.

Faced with the difference between Kalnins and Updike's results and the ADM rules in particular, of which there has been such wide experience, it is first necessary to consider how German ends can be satisfactory when theory suggests they are not. The difference is greatest at $e/R$ = 0,007, the values of $C$ being 1,028 and 0.754 respectively, a ratio of 1,36

It was considered that the two may be reconciled as follows:

The ADM rules are only tested to a pressure 1,3 times design, whereas K&U were aiming for the conventional 1,5 safety factor.

K&U's failure criterion was based on deflection at the centre of the end using the twice elastic slope criterion. However dished ends continue to behave in an acceptable manner well past that point, to say 3 or 4 times elastic slope. This is worth another 17% approximately, based on the observed shape of load deflection curves.

The comparison is about the ability of a certain thickness to carry pressure, the pressure allowed according to K&U being lower. Unlike previous workers in this field K&U did not work with a cylinder thickness equal to the thickness of the end, rather they used the cylinder thickness corresponding to the $p/f$ for the end. Thus the actual geometry on which the ADM experience is based would have had a thicker cylinder. This is worth another 4%.

K&U's figure is for all $R/D$, an approximation. Although they found that $C$ is nearly constant as $R/D$ varies, it is greater at $R/D$ = 0,8 than at 1,0. It is estimated that this accounts for another 5% of the difference. ($R/D$ is 1,0 for the Kloepper shape.)

Design is based on minimum thickness after forming. Actual heads are of non-uniform thickness, worth another 5% say.

Most heads will also have the benefit of a corrosion allowance, reduced design stresses for elevated temperatures and greater yield stress than that specified by up to 50%.

Multiplying the factors in 1) to 5) above together gives an overall factor of 1,55, much greater than the ratio of 1,36 that had to be explained. The academic calculation and experience can be reconciled. The problem is to go from there to a design method.

Note that we do not wish to use the German rules directly. They cover only certain geometries and we wish to be able to permit a higher pressure than 1,3*p* at pressure test, namely 1,43*p*.

It was decided that it is reasonable to adjust the K&U data by the 17% in 2) above together with an additional term to take credit for the variation of '*C*' with *R/D* in 4) above. It was also agreed that the nominal factor of safety could be reduced by 2,5% giving an overall adjustment factor of $\frac{1,17}{0,975(0,75+0,2\times D/R)} = \frac{1,2}{0,75+0,2\times D/R}$.

In the Kloepper case this is worth 1,2/0,95 = 1,26. The Kloepper experience would justify a slightly smaller factor, namely 1,36*1,3/1,43=1,24.

This credit is extended to *r/D* = 0,06 and to *e/R*<0,007. Above *e/R* of 0,007 the 1,2 adjustment tapers away to unity because shape change is less for such geometries and '*C*' is getting closer to the membrane limit for the crown.. For *r/D* = 0,2, the same comment about the crown applies but it was still felt possible to make a small adjustment to the K&U data as well as retaining the *D/R* factor.

### *7C-3c Instability*

The paper by Galletly concludes with a suggested design equation, namely

$$\frac{P}{\sigma_y} = \frac{80\left(r/D\right)^{0,825}\right)}{\left(D/e\right)^{1.5}\left(R/D\right)^{1,15}} \cdot$$

This was modified slightly for use in EN 13445-3 to give equations (7.5-3) and (7.5-8).

The basis of the equation is a curve fit to the results of many large deflection plastic buckling calculations, with a knock-down factor based on the lower bound of a limited number of test results. Bearing in mind the difficulty of modelling the actual shape, thickness profile and work hardening found on actual fabrications, theory and practice were in reasonably close accord. The paper confirms that the thickness to be used in the formula is the minimum at the knuckle after forming and the proof stress is that in the plate as received, both in conformance with definitions of these quantities in the standard.

The graphs referred to above also show the Galletly design equation on the same basis as the other criteria. The comparison is a fair one for carbon steel since the same value of yield is used as in the main calculation but the comparison becomes more complicated for stainless steel. Ends that are not cold spun require the 0,2% proof stress, somewhat lower than the 1% proof stress, so that stability becomes important at slightly larger e/R. On the other hand with cold spun ends the design stress is multiplied by 1,6, in which case stability no longer controls. There may be doubt about the extrapolation of Kalnins and Updike's results to e/R< 0,002, but on the other hand the increase in yield observed for cold spun ends will more than compensate for this uncertainty.

## 7C-4 Nozzle in Knuckle rules

As mentioned above, the ADM contain rules for increased thickness if there is a nozzle intruding into the knuckle region. It is a crude rule - a thickness adjustment that takes no account of the location of the branch or its wall thickness. It was reviewed by the CEN working group and compared with available stress analysis data and experience. It was concluded that the ADM adjustment should continue to be used in the new code. The curves in the ADM are incomplete and leave doubts about interpolation but equations have been fitted to them.

It is frequently said that some other codes prohibit the use of this arrangement. That is not strictly true; they merely fail to provide design rules for them. Those who carry out a Design by Analysis or use strain gauges are surprised at how low the stresses turn out to be.

Unfortunately no method has been found for applying the curves to other than the standard German geometries.

Recent work described in The Design by Analysis Manual [4] found that there is an area of large deformation if the nozzle gets close to the tangent line with the cylinder, so the arbitrary penalty in the last paragraph of 7.7.2 was imposed.

## 7C-5 Future work

The following items are suggested, in no particular order

K & U themselves clearly recognised the conservative and arbitrary nature of their failure criterion. Since with a dished end “gross deformation” is not an intimation of failure by any other mode and merely makes the end less like the shape on the drawing, there is a need to reconsider in this case what end deflection can really be accepted.

There is a large gap between two of the values of *r/D* selected by K & U. Their work should be repeated at *r/D*=0,14

The rules limit *R/D* to be less than 1,0. This is traditional and therefore K & U did not consider working with values greater than unity. Industry tends to press to be able to continue doing what it has been doing rather than seek improvements. It seems probable that the rules can safely be applied as written to R/D>1, without limit, but this has yet to be properly demonstrated. This could be of interest to manufacturers of ends for low pressures.

There is a need to look at thicker ends (*e/R*>0,04)

The nozzle in knuckle rules consider only pressure. The absence of information on stresses due to pipe loads is a severe restriction on their use in much of industry

Galletly noted the lack of a sufficient number of tests and felt that with more there could be scope for less conservative rules. In particular it might be possible to consider the effect of work hardening on the resistance of spun stainless steel dished ends to axisymmetric failure.

### 7D Bibliography


[1]. Fachbereitstandard, Behalter und Apparate, Festigskeitsberechnung, Kegelschalen, TGL32903/06. Standardsversand, Leipzig, April 1989

[2]. KALNINS A and UPDIKE D P; New design curves for torispherical heads, Welding Research Council Bulletin 364, June 1991

[3]. GALLETLY G D; Design equations for preventing buckling in fabricated torispherical shells subjected to internal pressure. Proc I Mech E, London 1986.

[4]. Design by Analysis Manual. Pressure Equipment Directive Joint Research Centre. To be found at http://ped.eurodyn.com/jrc/jrc_design.html.


## 8 Shells under external pressure

### 8A Introduction

Rules for external pressure design have to cover a variety of components and modes of failure. They are therefore complicated. The rules in clause 8 of EN 13445-3 are based almost entirely on the rules in British Standards Institution (BSI) document PD 5500 [1], itself a continuation of the previous BS 5500. The rules have been in BS 5500, the British Standard for unfired pressure vessels, since about 1973.

The British rules were rewritten for EN 13445-3 and some modifications made, mainly in presentation. The safety factor is now shown explicitly in the formulae and the distinction between light and heavy stiffeners is clearer. The values of elastic limit (yield stress) have been changed slightly.

A number of documents have been produced to justify or as an aid to understanding the rules in PD5500. The author of this paper has drawn heavily on PD 6550: Part 3: 1989, an explanatory supplement to BS 5500 on external pressure, published by BSI [2]. Other papers are in the list of references.

Although the rules are said to be rules for design, the user will in all cases have to choose a thickness or in the case of stiffeners a complete set of dimensions. Application of the rules will then tell the user whether his proposal is adequate for the pressure.

The rules are discussed in the order in which they appear in EN 13445-3 clause 8.

### 8B General comments

**8.2.2 and 8.2.3.** A typical ‘heavy stiffener’ would be a girth flange. If it is designated as a heavy stiffener then the cylinder is split into two and the two shorter cylinders are calculated independently. However the girth flange may not be stiff enough to meet the requirements of 8.5.3.7. It would then be permissible to redesignate it a ‘light stiffener’ and recalculate, to see if a more favourable result is obtained. A worked example is appended to assist in the understanding of this point.

**8.4.2 and 8.4.3** The important strength parameter in stability studies is the elastic limit. In the case of low alloy steels with a distinct yield point, elastic limit and yield are the same. In most places where design against external pressure is discussed, as in the rest of this paper, the word yield is used instead of elastic limit

However in the case of austenitic stainless steels and others materials with stress/strain curves showing work hardening and great plasticity, there is no such thing as a yield point. The elastic limit for these materials is not generally available from a standard tensile test - indeed it is difficult to define and measure precisely - and so design is based on the nearest readily available parameter, the 0,2% proof stress. Study of some typical stress/strain curves for stainless steel gave the factor 1,25 in equations (8.4.3-1) and (8.4.3-2).

The possibility of increasing the nominal elastic limit while at the same time taking account of the consequential reduction in Young's modulus was considered, but calculations showed there was no benefit from so doing.

The tolerance on radius (deviation from theoretical shape) is an important feature of the method. The experimental results that went into deriving figure 8.5-5 were limited to those for cylinders that met the 0,5% tolerance, so it is not possible to apply the rules to cylinders outside the specified tolerance without further consideration. In the case of stiffener design the tolerance appears explicitly in the equations, for example equation (8.5.3-46).

Measurements of diameter are not sufficient to demonstrate circularity - one only has to consider a three lobed shape to see this. They may however be considered as evidence of good workmanship.

**8.5.1.2 and 8.5.1.3** The simple safe rule in 8.5.1.2 can be applied at the design stage whereas 8.5.1.3 and Annex F are for use after fabrication is complete and the actual out of tolerance shape is known.

**8.5.2.1** The simple rules for L when the vessel end is a cone, a sphere or a dished end, namely the 0.4h term and the effect of the cone angle, are based on computer instability studies of many geometries.

Equation (8.5.2-6) is the well known Mises equation. Other versions of it appear but this is the most accurate. It is possible to replace the calculation of ε by a simple formula not containing $n_{cyl}$, but this lacks accuracy at low values of $n_{cyl}$.

Curve 1) of Figure 8.5-5 represents the lower bound of 700 well documented tests available at the time of the study. It gives the pressure above which failure might occur as a function of the Mises instability pressure and the pressure to circumferential yield.

The knock down factor at the 'slender' end (low $p_m / p_y$) is 2,0. There was much scatter in that part of the plot of test results. Those on the line were checked and proved to be good experimental results.

**8.5.3.1** Attention is drawn to the note in 8.5.3.1 and to the comments above on paragraphs 8.2.2 and 8.2.3.

**8.5.3.4** It was found that the particular pressure at yield calculated in equation (8.5.3-15) (the maximum circumferential stress in the cylinder) gave the best correlation of experimental results.

**8.5.3.5** Equation (8.5.3-23) is the result of a limit analysis of the shell, considering it as a flat plate fully supported at the ends, and taking account of the weakening effect of the circumferential membrane stress.. For guidance on the use of heating/cooling channels as shell stiffeners, reference may be made to PD 5500 clause 3.11.4

**8.5.3.6.2** The first term in equation (8.5.3-24) represents the contribution of the shell and the second term the contribution of the stiffener. Ignoring the first term and setting $n$=2 leads to equation (8.5.3-51) for a heavy stiffener.

Equation (8.5.3-31) is only a preliminary filter before going on to 8.5.3.6.4.

Factor $S_f$ adds an additional safety factor for stiffeners to cover any interaction between inter-stiffener and overall collapse. It is made larger still when residual stresses may be high.

**8.5.3.6.3** The full precise method for calculating Le, the length of shell acting with the stiffener is extremely long and complicated but the method provided here is a close approximation..

**8.5.3.6.4** Here the stress in the stiffening ring is calculated, the first term in equation (8.5.3-46) being the direct stress and the second term the bending stress due to out of round, magnified by the effect of external pressure. This stress is limited to the nominal elastic limit. Note that the resulting allowable external pressure is a lower bound, not a prediction of failure, so no experimental knock down factor is called for.

**8.5.3.7** The method for heavy stiffeners is based on that for light stiffeners with the omission of the effect of the shell ( first term in equation (8.5.3-24) and setting $n$=2).

**8.5.3.8** Equation (8.5.3-60) is a simple but conservative result derived from energy considerations. The stiffener is assumed to be hinged at the junction with the shell. Note that $\sigma_{es}\left(P/P_{ys}\right)$ gives the direct stress in the stiffener. It is necessary to be more precise with flat bar stiffeners and most of the calculation has been done for us and presented in table 8.5-5.

**8.6** The necessary modifications to the methods for cylinders are presented here. Rules for heavy stiffeners have been omitted in error, though the capable user should be able to work them out for himself from what he has been told already.

**8.6.5.1 and 8.6.5.2** The rules provided here for the large and small ends of the cone are based on extensive computer stability analysis, which shows them to be safe. .

**8.7.1** The method for spherical shells is similar to that for cylinders - the two theoretical formulas are compared with experimental results and a lower bound curve to the experimental results is drawn, as shown in figure 8.5-5. The elastic instability pressure $p_m$ is much greater than the equivalent pressure for a cylinder of the same thickness and diameter, due to the benefit of the double curvature, but the knockdown factor is much greater.

**8.7.2** Conforming to the design shape is again important, though in the case of spheres it is only the local shape that matters. The requirement that the sphere should be spherical to 1% on radius is only a quality control measure. The requirement for a maximum on the local radius of curvature is vital.

**8.8** With vessel ends we have to determine the maximum radius of curvature and then apply the rules for a sphere. For an ellipsoid the maximum radius of curvature occurs at the centre.

The general rule that internal pressure rules shall be applied without modification using the external deign pressure, does not apply to torispherical ends since the method in clause 7 claims some benefit from the improvement in shape that occurs under pressure, and under external pressure the shape should get worse. That is why we have the rule N=1 introduced.

## 8C Future work

Three items that require no further technical development

1. Add heavy stiffeners to the rules for cones.

2. Add something about use of heating/cooling coils as stiffeners along the lines of PD 5500 clause 3.11.4

3. Add something about the fact that a short cylindrical flange forming part of a dished end and thinner than the rest of the cylinder, is permissible - see PD 5500 3.6.4 final paragraph.

Three items that may be possible with further work.

3. Rules for cylinders of variable thickness - for example a tall column.

4. Less onerous rules for measurement of tolerances in which measurements of departure from design shape are more related to predicted deformed shape.

5. More precise design for inter-stiffener collapse of cylinders, based on separation of the two failure mechanisms associated with circumferential and longitudinal loads respectively. Longitudinal compressive loads on cylinders suffer in the same way as spheres under external pressure from a large knock-down factor. Maybe a study of test results will show that the circumferential load acting alone has a low knockdown factor, resulting in more economic design for longer cylinders.

## 8D Bibliography


[1] PD 5500:2003 Specification for unfired fusion welded pressure vessels, British Standards Institution

[2] PD 6550: Part 3: 1989. Explanatory supplement to BS 5500: 1988 ‘Specification for unfired fusion welded pressure vessels’, section three ‘Design’ Part 3. Vessels under external pressure.

[3] ‘Collapse of stiffened cylinders under external pressure’, by S.B. Kendrick, Institution of Mechanical Engineers Paper C190/72, Proceedings of Conference on ‘Vessels under Buckling Conditions’ December 1972

[4] ‘Collapse of domes under external pressure’, by C.N. Newland, Institution of Mechanical Engineers Paper C190/73, Proceedings of Conference on ‘Vessels under Buckling Conditions’ December 1972

[5] ‘The technical basis for the external pressure section of BS 5500’ by S.B. Kendrick. Journal of Pressure Vessel Technology , ASME volume 106, May 1984.

# 9 Openings in shells

## 9A Introduction

**9A-1** The first proposal of CEN/TC54/WG'C' was to use 'Area Replacement Method' that was present in ASME VIII Div. 1 and in a few European national Codes (based on method of replacement of cross sectional missing area of openings with cross sectional areas of material reinforcement of shell and nozzles), but during standardization works it was decided to adopt the 'Pressure-Area Method' because this one was well known and widely used in continental Europe.

The Pressure-area method is based on ensuring that the reactive force provided by the material is greater than, or equal to, the load from the pressure. The former is the sum of the product of the average membrane stress in each component and its stress loaded cross-sectional area (see Figure 9A-1). The latter is the sum of the product of the pressure and the pressure loaded cross-sectional areas. If the reinforcement is insufficient, it shall be increased and the calculation repeated.

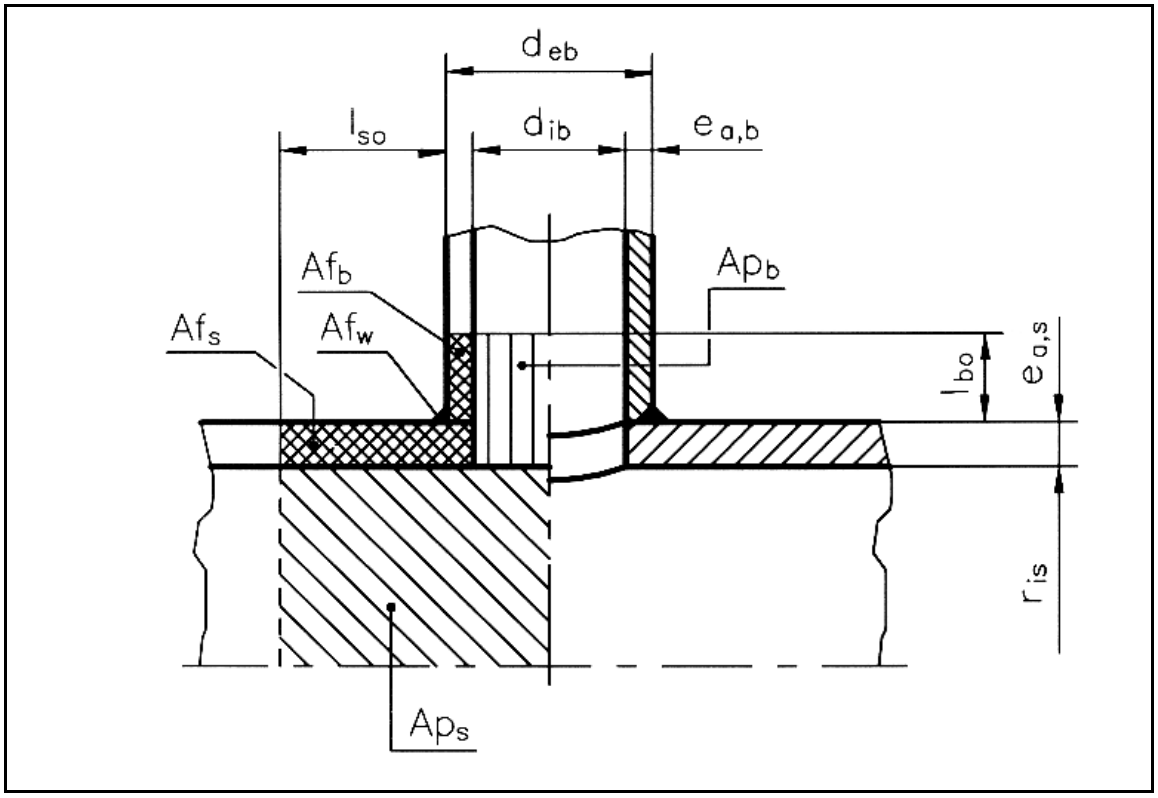


**Figure 9A-1 Cylindrical shell with isolated opening and set-on nozzle (identical to Figure 9.4-7 in EN 13445)**

**9A-2** It was decided to start with Code ISO 5730 (International Code for shell boilers) based on balance between cross sectional pressure areas and stress compensation of cross sectional areas of shells and nozzles, but it seemed to be good only for the working conditions and limits of shell boilers. Therefore it was decided to increase and expand the rules also for all possible stress situations of unfired pressure vessels, and the rules of

CODAP have been taken to complete and expand the code of ISO 5730 ( with some other integrations by Belgian rules for limitations of calculation thickness of nozzles for too large openings).

After this decision, the Working Group spent a lot of time just to put into the code more possible stress situations and stress limitations ( more general and comprehensive formulas for each geometrical possible situation).

**9A-3** Actually in Clause 9 there are no restrictions on size of circular openings and some restrictions on shape of elliptical openings ( coming from inclined circular nozzles), unless reinforcing pads are used.

Present rules include allowing openings close to a discontinuity and also small adjacent openings.

This makes EN 13445 Part 3 Clause 9 more comprehensive than ASME VIII DIV. 1 "Area Replacement " approach. Calculation of stress is not included.

## 9B Contents of Clause 9

### 9B-1 General

The design method specified in this clause is applicable to circular, elliptical or obround openings in dished ends or cylindrical, conical or spherical shells under internal or external pressure.

This clause is applicable to openings, nozzles and reinforcing plates in dished ends which are completely located inside the central area limited by a radius equal to $0{,}4D_e$ . For different locations (i.e. nozzles in knuckle regions) the relevant design rules are given in Clause 7.

Design for non-pressure loads is covered by Clause 16.

A shell containing an opening shall be adequately reinforced in the area adjacent to the opening. This is to compensate for the reduction of the pressure bearing section. The reinforcement shall be obtained by one of the following methods:

- increasing the wall thickness of the shell above that required for an unpierced shell,
- using a reinforcing plate,
- using a reinforcing ring,
- increasing the wall thickness of the nozzle above that required for the membrane pressure stress,
- using a combination of the above.

### 9B-2 General equation and its derivates

General equation for the reinforcement of an isolated opening is given (see Figures 9A-1 and 9B-1) by:

$$(Af_s + Af_w)\,(f_s - 0{,}5P) + Af_p\,(f_{op} - 0{,}5P) + Af_b\,(f_{ob} - 0{,}5P) \geq P\,(Ap_s + Ap_b + 0{,}5\,Ap_\varphi)$$

where, in general:

| | | |
|---|---|---|
| Ap | Pressure loaded area. | $mm^2$ |
| Af | Stress loaded cross-sectional area effective as reinforcement. | $mm^2$ |
| fs | Nominal design stress of shell material. | MPa |
| P | Internal pressure of shell. | MPa |

and $P_{max}$ shall be obtained as follows:

$$P_{max} = \frac{(Af_s + Af_w)\cdot f_s + Af_b \cdot f_{ob} + Af_p \cdot f_{op}}{(Ap_s + Ap_b + 0{,}5Ap_\varphi) + 0{,}5\,(Af_s + Af_w + Af_b + Af_p)}$$

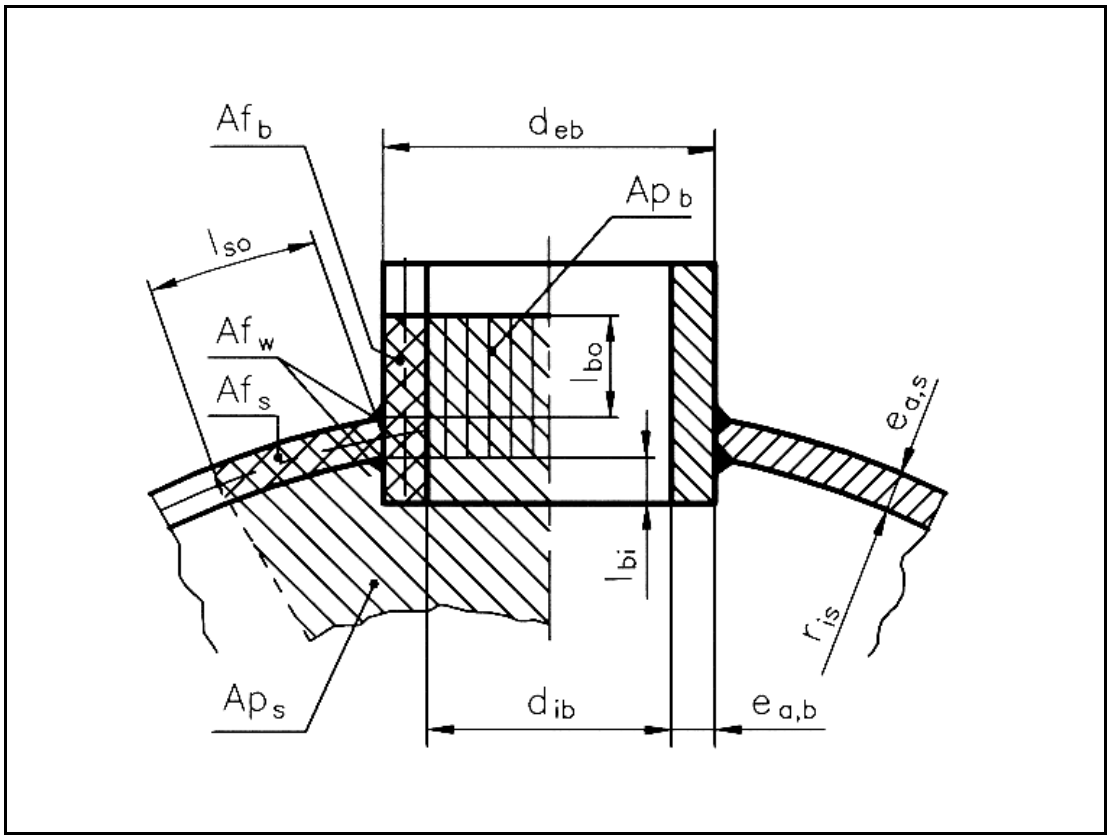


**Figure 9B-1 Spherical shell or dished end with isolated opening and set-in nozzle (identical to Figure 9.4-8 in EN 13445)**

### 9B-3 Single openings

In Clause 9 the general equation is adapted to each of the following configurations:

- Shells with openings without nozzle or reinforcing ring (with or without reinforcing pads) on cylindrical, conical and spherical shell, longitudinal and transverse cross-section.
- Shells with openings without nozzle, reinforced by reinforcing rings, on all same cases.
- Nozzles normal to the shell, with or without reinforcing pads, on all same cases.
- Nozzles oblique to the shell, with or without reinforcing pads, on all same cases.

### 9B- 4 Multiple openings

In Clause 9 the general equation is adapted also to each of the following configurations:

- Ligament check of adjacent openings.
- Openings in cylindrical and conical shells.
- Openings in spherical shells and dished ends.
- Overall check of adjacent openings.

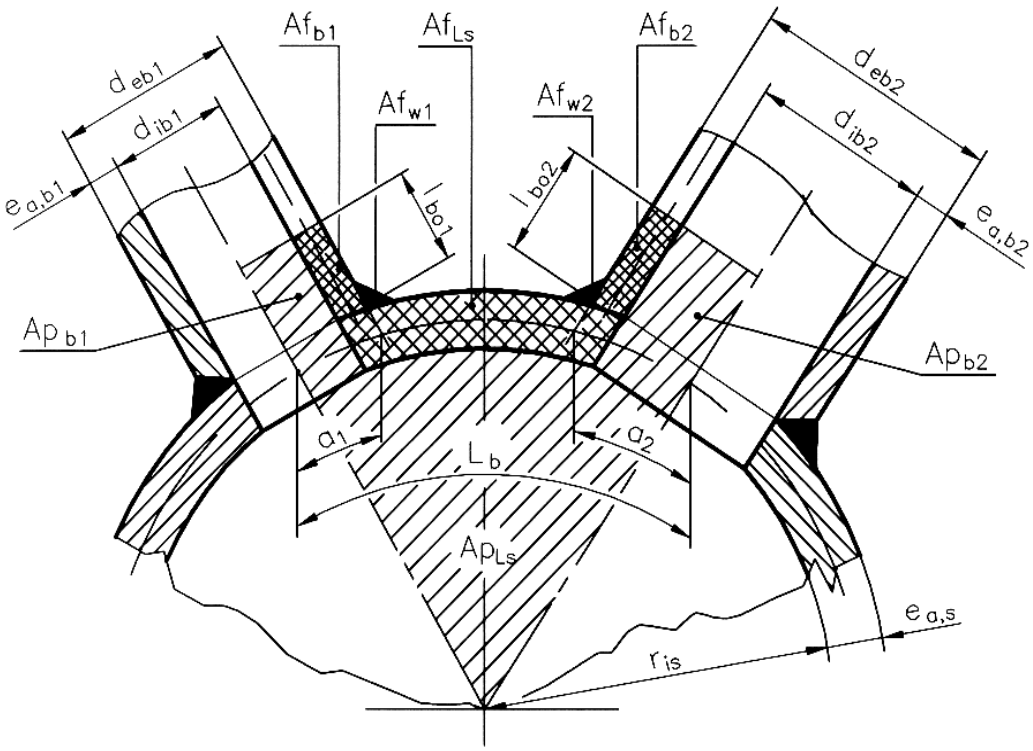


**Figure 9B-2 Ligament check of adjacent nozzles normal to a spherical shell (identical to Figure 9.6-3 in EN 13445)**

### 9B-5 Openings close to a shell discontinuity

In Clause 9 there are rules giving minimum distances of openings from discontinuities.

$$w \geq w_{\min} = \max\ (0{,}2\sqrt{(2r_{is} + e_{c,s}) \cdot e_{c,s}}\,; 3e_{a,s})$$

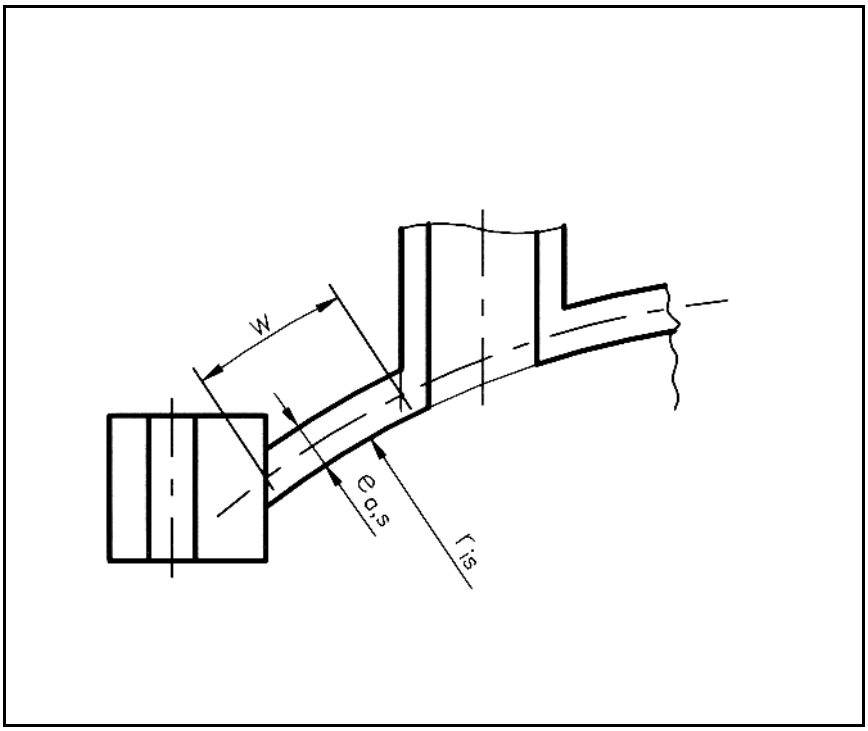


**Figure 9B-3 Opening in a domed and bolted end close to the junction with the flange (identical to Figure 9.7-11 in EN 13445)**

**9B-6 Future work**

There are other two items that need to be implemented:

- Openings with non circular nozzles,
- Openings in non circular walls.

# 10 Flat ends

The rules for flat ends are based partly on the rules of the French Pressure Vessel code (CODAP, in their 1995 ed. version) and partly on the rules of the Italian Pressure Vessel Code ISPESL/VSR. They deal with ends of both circular and non circular shape, either welded or bolted. The main purpose of the equations contained in the rules is to assure that a failure due to gross plastic deformation can never happen. For circular welded flat ends, this is achieved by setting the allowable pressure of the end to its limit pressure divided by 1,5.

The limit pressure calculations on which the rules are based take into account the support brought by the connected shell. For bolted flat ends, gross plastic deformation is prevented by limiting the bending stress in the centre of the end to a value equal to 1,5 times the nominal design stress (which assures that the yield strength of the material will not be exceeded, when the nominal design stress is limited by this material characteristic). In the case of circular welded flat ends, prevention of cyclic plasticity has also been considered, and for this reason the corresponding equations and graph are intended to guarantee that the primary+secondary stress induced in the cylindrical shell does not exceed three times the lower value between the nominal design stress of the shell and the nominal design stress of the end (the so-called shakedown criterion, which is typically used in all the standards that provide design-by-analysis rules based on stress categorization).

The need of fulfilling the shakedown criterion has been contested in other clauses of EN 13445.3: however not in this one, where it was decided to stay in line with the selected source (Clause C3 of CODAP); but in the next issue of Clause 10, which is now ready for the shortened approval procedure provided by the CEN rules (the so-called UAP route), it will be permitted to waive the shakedown criterion under the condition that a simplified fatigue analysis is performed. In other words application of the shakedown criterion (which limits to 3*f* the primary+secondary stress range in the shell) will be required only in those cases where no fatigue analysis is made (note that EN 13445-3 states that no such analysis is needed when the number of full pressure cycles is less

than 500). For vessels subjected to a small number of cycles, a higher primary+secondary stress in the shell will then be tolerated, resulting in much smaller thickness for the end.

It has to be noted that the shakedown criterion was up to now one of the main principles on which the traditional stress analysis of Pressure Vessels was based for years; and the fact that the primary+secondary stress range should be limited to 3 times the nominal design stress in all kind of Pressure Vessels, whatever their actual loading condition might be, was taken on board by all the main national Pressure Vessel Codes. With the introduction of the so-called "Direct Route" for Design By Analysis (that is, with the introduction of elastic-plastic calculations directed to finding the limit load of a given structure instead of the calculation of fictitious elastic stresses that in reality do not exist), it is possible to investigate the real behaviour of the same structure when it is subject to load variations; and therefore to predict which post-elastic behaviour will occur when the shakedown criterion is ignored: cyclic plasticity or incremental collapse. As far as the Design-By-Formulas rules are concerned, cyclic plasticity is assumed to be the only mechanism that is likely to occur, due to the uniqueness of the loading (pressure loading). So failure due to cyclic plasticity is in fact a failure due to fatigue, more specifically in the low cycle regime.

Looking at other clauses of EN 13445.3 (particularly flanges and tubesheets, where new methods based on limit analysis have been presented as an alternative to the traditional methods based on stress categorization) it is clear that this new standard is marking an important transition between these two different ways to consider Pressure Vessel design; probably the next issue of clause 10 will be the first clause in the standard where a synthesis of these two approaches will be made.

Coming back to the actual content of Clause 10, it has to be noted that the method used for opening reinforcement in circular (and non circular) flat ends is not based on area replacement (like in the case of openings in shells): the method, which comes from the Italian Pressure Vessel Code ISPESL/VSR, and has been successfully used for at least 30 years, is based on the replacement of the section modulus (which is also a rough approximation, but at least more logical, considering that we deal with walls subject to bending and not to tension). This rule aims to control the stress level in the end. In addition, there is also the need for a replacement of the moment of inertia, so that the overall bending behaviour of the pierced end is similar to that of the unpierced end, in order to assure similar bending stresses in the connected shell in both cases.

Clause 10 gives also the possibility of calculating ends of non-circular shape (that is, rectangular, elliptical or obround; even ends in form of a circular crown have been considered). The correlations used in this kind of calculations are also taken from the Italian Code.

# 11 Flanges

## 11A Introduction

Two sets of rules are provided for flange design in EN 13445-3, the traditional rules (in clause 11) and a new radical set of rules (in annex G).

The traditional rules are taken from the British PD 5500 and include a wide range of flange types apart from the common narrow face arrangement, namely full face flanges, reverse flanges, split flanges and welded flanges. The rules for narrow face flanges are based on the traditional Taylor Forge analysis.

Since Taylor Forge is so much used, it is not intended to explain or defend it here. Space will be devoted to listing some of its faults and the way it has been changed from the version still in the ASME code. Design stresses have been reduced at larger diameters in the light of wide experience of leakage problems when higher design stresses are used.

The new rules, known as the Alternative Method, cover narrow face joints only. While new to most countries, the method is based on a method used successfully in East Germany for some years. While most aspects of flange design were considered afresh by the authors of this method, the most notable features must be the use of limit analysis, the recognition that the bolt load has its own tolerance, the calculation of the way the bolt load changes as pressure (or other loads) are applied and the detailed analysis of gasket behaviour.

Any method that wishes to supplant Taylor Forge must be complete and attractive economically. It has to include taper hub flanges. It should assist understanding of what is happening in a flange assembly as an aid to good design and trouble-shooting. The Alternative Method does these things.

The Alternative Method as provided in EN 13445-3 includes a great deal of information on the mechanical model (see clause G.4.2), which there is no need to repeat here. Further explanation for many of the equations would be unduly complicated and not helpful to the user. It is nevertheless difficult for a new user to understand

what is going on and have confidence in what he is doing, so some space is given in this paper to describing the overall structure of the method. The treatment of the gasket is especially novel and a simplified treatment is included below.

Although the Alternative Method is able to take account of thermal expansion effects due to differences in bolt temperature and/or material, no guidance is given on determining flange and bolt temperatures. This is also discussed below.

## 11B The Taylor Forge method

The Taylor Forge method goes back over 60 years. Many alternatives have appeared over the years and many papers have explained the faults in the method, but it has continued to be the choice in many national pressure codes. Its success has been put down to the fact that it is a complete method, including gasket parameters, and it gives answers that work most of the time. Its strong point is the elastic stress analysis of taper hub flanges. However it has many weaknesses.

## 11B-1 Weaknesses of Taylor Forge

a. The decision as to whether a flange is thick enough depends in the Taylor Forge method on a stress calculation which has nothing to do with leakage and is only indirectly associated with permanent deformation (yielding). A stress is useful for the study of cyclic failure, but that is not the normal problem with a flanged joint. Indeed, there are geometries where it will be found that the an increase in thickness of the cylinder or the hub can result in an increase in stress and consequent down-rating of the flange.)

b. The calculation fails to consider the behaviour of the bolt load as pressure is applied.

c. Neither differential thermal expansion between bolt and flange nor non-pressure loads are covered

d. The theoretical model ignores the effect of pressure directly on the shell.

e. The theoretical model for the flange applies the moment as equal and opposite loads at the two edges of the flange rather than at the bolt circle etc.

f. Not all flanges are best modelled as thin plates. Some can be closer to thin cylinders.

g. The weakening effect of the bolt holes is ignored. This is especially important in loose flanges in which the stresses are circumferential. On the other hand the weakening effect of any groove is greatly magnified.

h. Although the bolts are given low design stresses to compensate for uncertainty over actual bolt loads, the same logic has not been applied to the flange, which also has to carry those same uncertain bolt loads. The consequence is that if the bolts are over-tightened it is the flange that suffers, not the bolts.

i. The “optional” flange may be calculated in either of two ways but the integral flange of the same dimensions may be calculated in only one of those ways. This seems “unfair” on the integral flange.

j. Maximum gasket pressures are not provided.

k. The stub flange in a lap joint is not considered

l. The gasket factors m and y are not scientifically defined. They seem to be based on guess work.

m. All methods of bolt tightening are treated alike. No credit is given for close control of bolt load.

n. No change is made when a flange is mated to a flat cover, even though the elastic behaviour of a flat cover is very different.

### 11B-2 Changes made to Taylor Forge Method

The major modifications made to the original Taylor Forge method as it appears in the ASME code follow. Note that only the first two modify the basic Taylor Forge method.

a. Following poor experience with simple substitution of the higher design stresses used in Europe, increased safety factors at larger diameters have been introduced.

b. Bolt stresses have been increased to reduce the disparity between flange strength and bolt strength mentioned in 8) above.

c. The complicated table for the calculation of effective gasket width has been removed. The biggest difference is the removal of the 1/64 in nubbin. The 1/64" nubbin is found in practice to have only a short life at higher temperature duties as it quickly gets worn away, so it is better removed from the standard.

d. The "loose" calculation may be applied to "integral" flanges.

e. For simplicity, the same moment is used in "loose" and "integral" calculations.

f. Formulae have been moved from the list of symbols into the text, making the method easier to apply.

g. Machining tolerances have been added.

h. Flange pairs of different design conditions (as found with a trapped tube sheet) are included.

i. Rules are provided for the stub flange in a lap joint.

## 11C Review of rest of Clauses 11 and 12

### 11C-1 Lap joints

The basis of the method for lap joints is that both components (stub flange and loose flange) are designed individually as flanges. The problem is to choose the diameter of the reaction force between the two. A rule is provided for calculating a diameter but, rather as in the use of limit analysis in the Alternative Method, it is permissible to choose an optimum. Note also that, in common with other traditional methods, no attempt is made to analyse the actual behaviour of the flange pair. The method is safe and may be very over-conservative when applied to existing designs.

### 11C-2 Full face flange with soft gasket

The method starts with some arbitrary but unimportant assumptions about gasket behaviour. Equation (11.6-16) is concerned with radial stress in the flange at the line of the bolt holes and inequality (11.6-17) is concerned with the flange being sufficiently stiff to be able to exert a pressure on the gasket over the whole span between bolt holes. The failure mechanism that equation (11.6-18) is aimed at preventing is rotation (twisting) of the complete flange assembly.

### 11C-3 Seal welded flanges

The method here follows Taylor Forge and therefore has the same weaknesses. In particular there is no check that the loss of bolt load on pressurisation will not be excessive.

### 11C-4 Reverse narrow face flanges

The only important piece of explanation needed to understand the logic of the rules is already in a note in the text. The method is simpler than that in ASME; results are the same for values of $K$ not much greater than 1,0 but at higher values of $K$ the CEN method is more conservative.

### 11C-5 Reverse full face flanges

As stated in a note in the text, two alternative design methods are provided for reverse full face flanges. The first follows the approach of clause 11.5 at the operating condition and assumes resistance to rotation comes from the flange itself; the second follows clause 11.6 and requires a larger bolt area.

Once again crude simplifying assumptions are made in order to get a design method without really studying the actual behaviour of the flange assembly. In particular such a flange is usually bolted to a flat cover which will bend under pressure, thereby tending to open up the joint. Unfortunately the Alternative Method does not deal with full face joints though the methods therein could be applied to the study of this problem.

### 11C-6 Full face flanges with metal to metal contact outside the bolt circle

This set of rules is based on the same model and understanding of the problem as lie behind the ASME method in Division 1 appendix Y. The relative simplicity of the CEN version is achieved by neglecting the stiffening effect of the shell and the stresses in the shell. This is similar to applying the loose method instead of the integral method when there is a gasket present. As usual the American method is preoccupied above all with determining stresses, not with understanding real behaviour. Results from the two methods are normally close with the CEN method tending to give the greater thickness. Neither method considers whether the opening up of the gap between the flanges at the point where the gasket is located might be excessive.

Note that if the gap is considered to be a problem it can be prevented from opening up by a slight modification to the flange. It can be given a concave surface, so that contact is made only at the inner and outer edges.

This design of flange can be a very attractive alternative to the narrow face approach, especially if bolt stresses higher than recommended in clause 11.4.3 are used. Users could consider applying the principles for bolting in the Alternative Method. The situation is completely different from that with the narrow face flange - the bolt load cannot decrease as pressure is applied (unless there is a thermal expansion effect).

The main practical problem with the metal to metal full face flange is that the type of gasket normally used requires a high quality finish in the groove.

The failure mechanism that equation (11.10-7) is guarding against is rotation (twisting) of the complete flange assembly.

# 12 Bolted domed ends

The method for spherically domes and bolted ends is the same as that in BS 5500. Notes in the text inform the user of the significance of the equations used.

# 13 Heat Exchanger Tubesheets

## 13A Introduction

During the last five decades, TEMA standards have been extensively used for the design of tubesheet heat exchangers. Due to their simplicity, these rules do not account for several effects (e.g. unperforated rim, tube expansion) and ignore some others (e.g. the connection of the tubesheet with shell and channel) that have a significant impact on the calculated thickness of the tubesheet.

For this reason, the author has developed a more rational treatment, which led in 1980 to the publication of new tubesheet design rules in the French Pressure Vessel Code, CODAP (F. OSWEILLER - 1991).

ASME, at approximately the same time, followed the same approach and new rules were published in ASME Section VIII - Div. 1 in 1982 for U-tubes, and in 1992 for fixed tubesheets. Both organisations, without having any contact at that time, came to the same conclusion that it was necessary to develop a more refined analysis than TEMA.

In 1991 CEN/TC54 decided to adopt CODAP tubesheet rules for its draft Unfired Pressure Vessel Standard (UPV).

NOTE: These UPV tubesheet rules provide also an alternative method based on limit load analysis. This aspect is not covered by the present paper which deals only with methods based on classical elastic theory of thin shells.

In 1992 ASME and CODAP decided to reconcile their tubesheet design rules as they were based on the same approach. This approach was extended to UPV and the author, as member of the three organizations, took

responsibility for the reconciliation which is now effective with the publication of new common rules in UPV, CODAP and ASME codes.

The purpose of this paper is to explain the basis of this consistency both on the editorial and analytical aspects. Design rules devoted to U-tube tubesheet, fixed tubesheets and floating heads are presented and benchmark results provided. A comparison to TEMA outlines the limits of this code.

A special attention is given to U-tube tubesheet rules which have been entirely reviewed after the comments received from the 6 months enquiry of EN-13445.

## 13B Analytical treatment of tubesheets

The analytical treatment has the same basis in UPV, CODAP and ASME rules, and has been widely presented in many papers (A.I. SOLER- 1990, F. OSWEILLER - 1991). It can be summarised in four steps (see Figure 13B-1):

1 - The tubesheet is disconnected from the shell and channel. A shear force $V_E$ and a moment $M_E$ are applied at the tubesheet edge as shown in Figure 13B-1b.

2 - The perforated tubesheet is replaced by an equivalent solid plate of effective elastic constants E* and ν*.

3 - The tubes are replaced by an equivalent elastic foundation of modulus $k_w$. In U-tube heat exchangers the tubes do not act as an elastic foundation ($k_w = 0$).

4 - Classical thin plate theory is applied to this equivalent tubesheet to determine the maximum stresses in the tubesheet, the tubes, the shell and the channel.

These maximum stresses are limited to a set of maximum allowable stresses derived from the concept of primary and secondary stresses, based on EN 13445 Part 3 Appendix C.

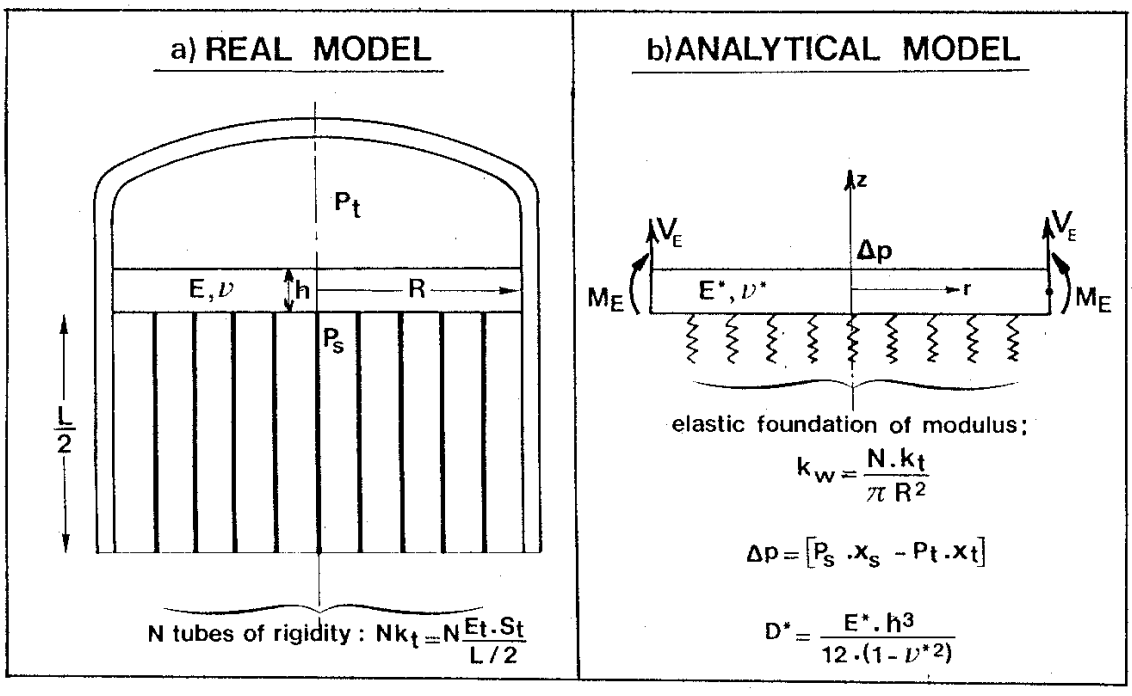


**Figure 13B-1: Analytical model used in design method**

## 13C Main basis of consistency

As explained above, the consistency of the rules has been performed both for the analytical and the editorial aspects, which are briefly presented below.

**13C-1 Analytical aspect is based on the three following items**

***13C-1a - Ligament efficiency μ****

ASME ligament efficiency $\mu^*$ has been adopted by UPV. It accounts (see Figure 13C-1) for an untubed diametral lane of width $U_L$ (through the effective tube pitch $p^*$) and for the degree of tube expansion ρ (through the effective tube diameter $d^*$). UPV has improved this concept by proposing a more general formula for $p^*$, which accounts for more than one untubed lane.

***13C-1b Effective elastic constant E* and ν****

CODAP and UPV effective elastic constants $E^*$ and ν*, given by curves as a function of $\mu^*$, have been adopted by ASME (Figure 13C-2). These curves account for the ratio $h/p$, which has a significant effect on the results (F. OSWEILLER - 1989), and was ignored in the ASME rules. Polynomial equations are provided with a discrepancy less than 0,5 %, which is below the reading error of the curves.

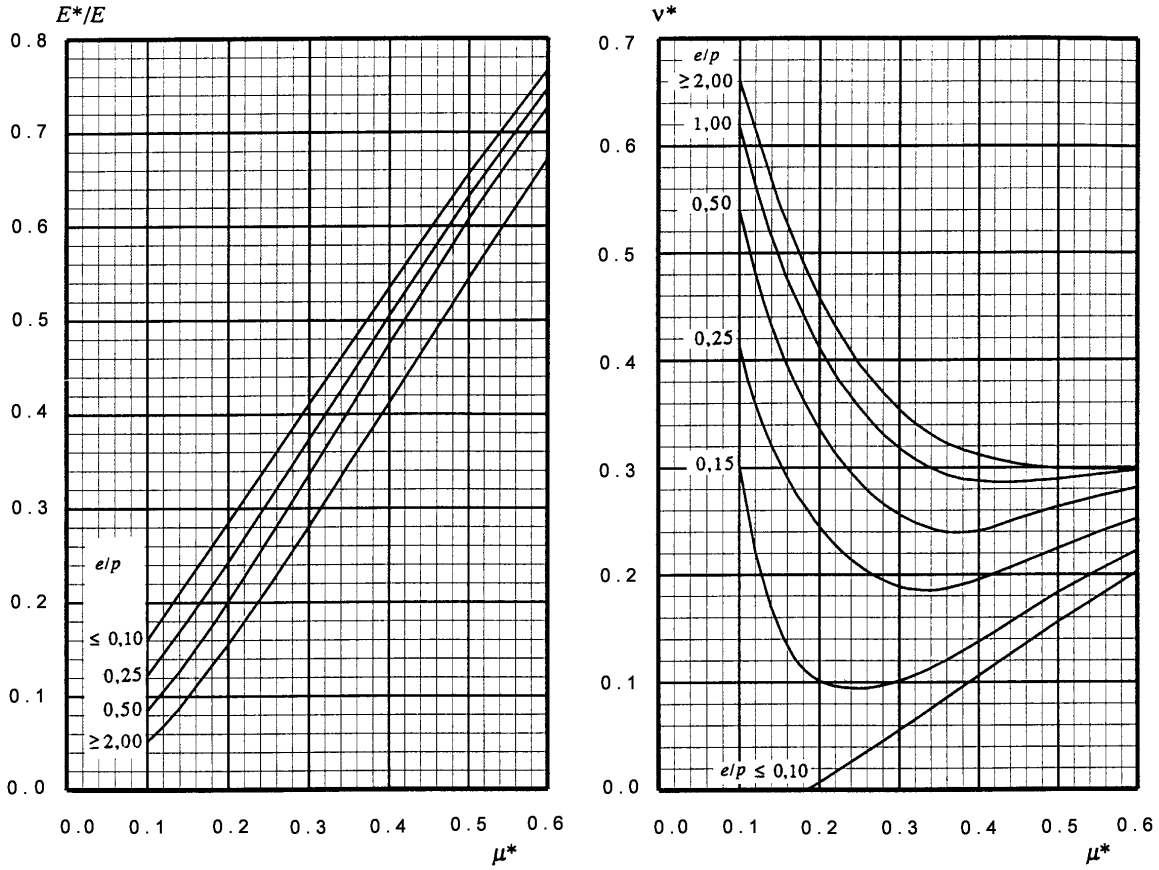


a): $E^* / E$ (equilateral triangular pattern)

b): $\nu^*$ (equilateral triangular pattern)

Polynomial equations given below can also be used.

NOTE: - These coefficients are only valid for $0{,}1 \leq \mu^* \leq 0{,}6$.

- For values of $e/p$ lower than 0,1 use $e/p = 0{,}1$.

- For values of $e/p$ higher than 2,0 use $e/p = 2{,}0$.

a) Equilateral triangular Pattern

$$E^* / E = \alpha_0 + \alpha_1 \mu^* + \alpha_2 \mu^{*2} + \alpha_3 \mu^{*3} + \alpha_4 \mu^{*4}$$

| $e / p$ | $\alpha_0$ | $\alpha_1$ | $\alpha_2$ | $\alpha_3$ | $\alpha_4$ |
|---|---|---|---|---|---|

| | | | | | |
|---|---|---|---|---|---|
| 0.10 | 0.0353 | 1.2502 | -0.0491 | 0.3604 | -0.6100 |
| 0.25 | 0.0135 | 0.9910 | 1.0080 | -1.0498 | 0.0184 |
| 0.50 | 0.0054 | 0.5279 | 3.0461 | -4.3657 | 1.9435 |
| 2.00 | -0.0029 | 0.2126 | 3.9906 | -6.1730 | 3.4307 |

b) Equilateral triangular Pattern

$$\nu = \beta_0 + \beta_1 \mu^* + \beta_2 \mu^{*2} + \beta_3 \mu^{*3} + \beta_4 \mu^{*4}$$

| e / p | $\beta_0$ | $\beta_1$ | $\beta_2$ | $\beta_3$ | $\beta_4$ |
|---|---|---|---|---|---|

**Figure 13C-2: Curves for the determination of *E**/*E* and ν* (equilateral triangular pattern) (identical to Figure 13.7.8-1 in EN 13445)**

### *13C-1c - Local thickening of the shell*

When the tubesheet is integral with the shell, the UPV method allows thickening of the shell at its connection to the tubesheet when the bending stress in the shell exceeds the allowable limit. This is also an efficient mean of reducing the tubesheet thickness significantly, even if the shell is not overstressed.

At the request of ASME SWG-HTE this principle has been extended to the situation in which the shell has a different material adjacent to the tubesheet.

The details of the reconciliation involved in the design rules devoted to U-tube tubesheets, fixed tubesheets and floating heads are presented further in the sections dealing with these three types of heat exchangers.

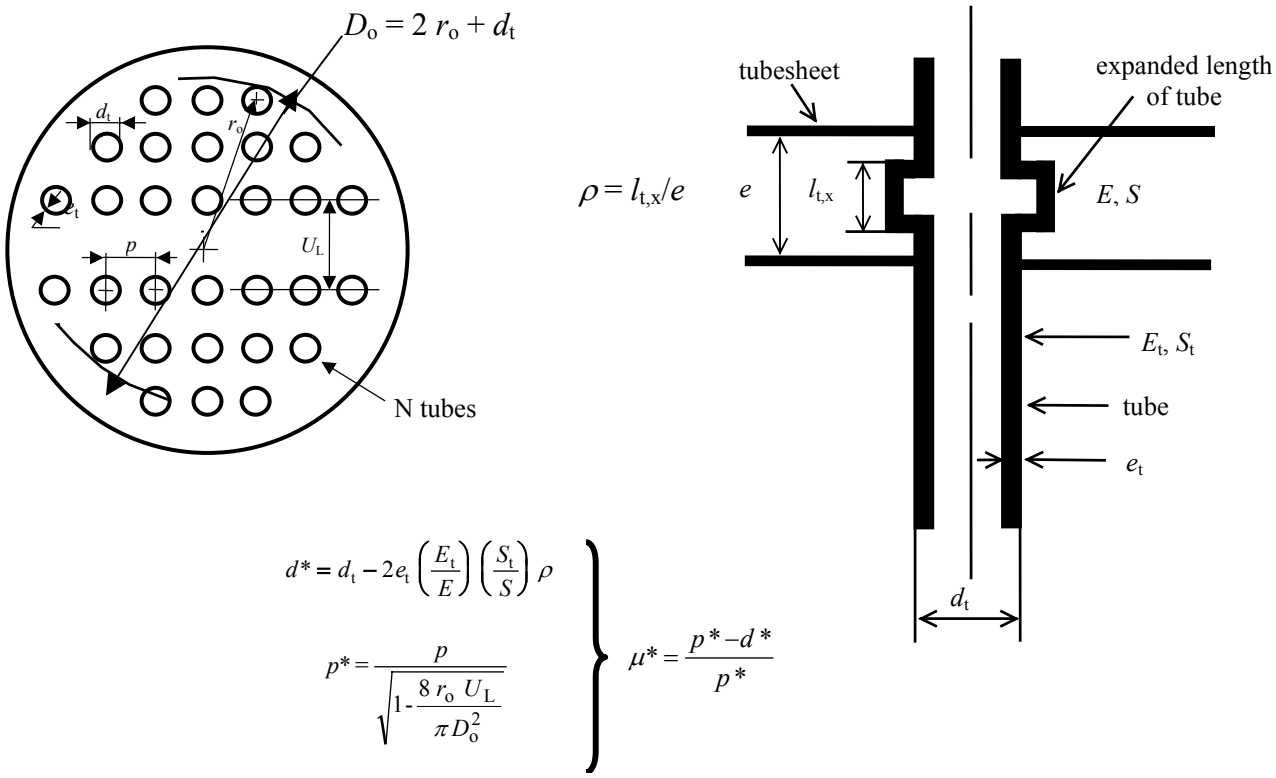


### 13C-2 Editorial aspect

This is an important issue as it is well known that differences in notation, terminology and presentation of the rules are significant barriers to the use and dissemination of foreign codes.

### *13C-2a Notations*

This is probably the most significant improvement.

English notations, based on TEMA, has been adopted by UPV, CODAP and ASME. Following subscripts are systematically used:

- *t* for tubes
- *s* for shell
- *c* for channel
- no subscript for tubesheet

However the following notations will remain different in US codes (ASME, TEMA) and European codes (CODAP, UPV):

- Tubesheet thickness: *h* in US - *e* in Europe
- Shell and channel thickness: $t_s$, $t_c$ in US - $e_s$, $e_c$ in Europe
- Nominal design stress: *S* in US - *f* in Europe

Aside from these exceptions, the notations are the same in all three codes and are shown on Figures 13D-1, 13D-2, 13E-1, 13F-1.

### *13C-2b Design equations*

Due to these common notations, the design equations are the same in the three codes.

The charts that are involved in these equations are presented in the same way. Equations or numerical tables are provided for these charts.

### *13C-2c Tubesheet configuations*

The same terminology of tubesheet configurations has been adopted, independently of the heat-exchanger type (see Figure 13C-3):

a : tubesheet integral both sides

b : tubesheet integral shell side, extended as a flange on channel side

c : tubesheet integral shell side, gasketed on channel side

d : tubesheet gasketed both sides

e : tubesheet integral channel side, extended as flange on shell side

f : tubesheet integral channel side, gasketed on shell side

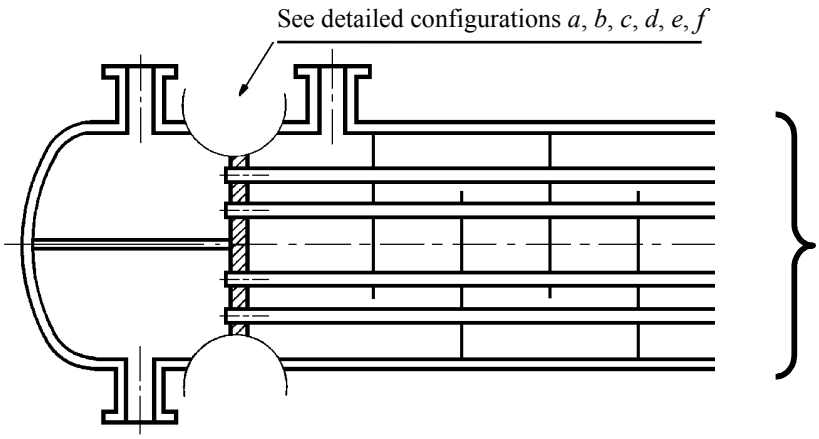


| | | |
|---|---|---|
| 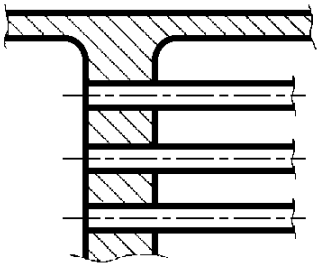 **a** | 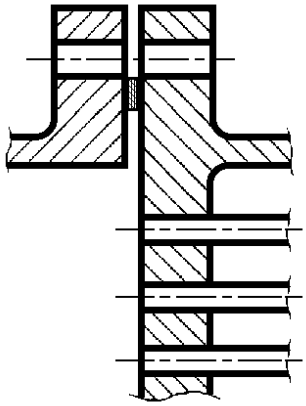 **b** | 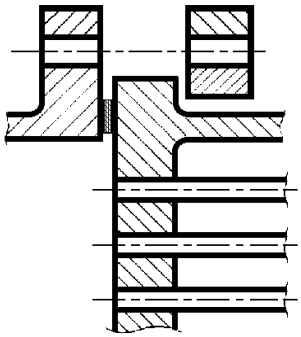 **c** |
| TUBESHEET INTEGRAL with SHELL and CHANNEL | TUBESHEET INTEGRAL with SHELL, GASKETED with CHANNEL, EXTENDED AS A FLANGE | TUBESHEET INTEGRAL with SHELL, GASKETED with CHANNEL, NOT EXTENDED AS A FLANGE |

| | | |
|---|---|---|
| 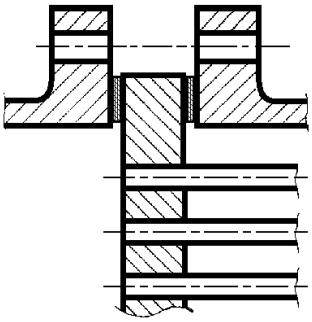 **d** | 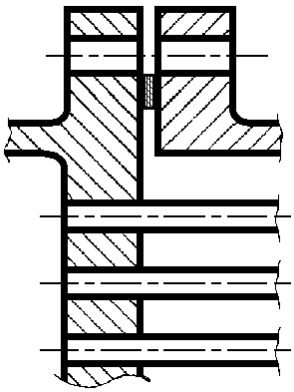 **e** | 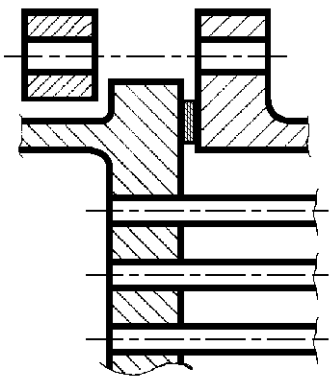 **f** |
| TUBESHEET GASKETED with SHELL and CHANNEL, NOT EXTENDED AS A FLANGE | TUBESHEET INTEGRAL with CHANNEL, GASKETED with SHELL, EXTENDED AS A FLANGE | TUBESHEET INTEGRAL with CHANNEL, GASKETED with SHELL, NOT EXTENDED AS A FLANGE |

**Figure 13C-3: Configurations of tubesheets**

**(identical to Figure 13.6.1-2 in EN 13445)**

### *13C-2d - Design loading cases*

The seven loading cases to be considered for the design have the same reference number, based on TEMA:

1. Tubeside pressure acting only, without thermal expansion.
2. Shellside pressure acting only, without thermal expansion.
3. Tubeside and shellside pressures acting simultaneously, without thermal expansion
4. Thermal expansion acting alone.
5. Tubeside pressure acting only, with thermal expansion.
6. Shellside pressure acting only, with thermal expansion.
7. Tubeside and shellside pressures acting simultaneously, with thermal expansion.

For U-tube tubesheets and floating heads, only the three first loading cases are to be considered.

### *13C-2e Structure and presentation of the rules*

Structure and presentation of the rules have been made consistent as far as possible. In the three codes, each of the three types of heat exchangers (U-tube, floating head, fixed tubesheets) is covered by independent and self supporting rules.

## 13D U-Tube tubesheet heat exchanger

### 13D-1 Selection of a design rule

At the request of CEN/TC54, the author has undertaken an extensive work to select a design rule for U-tube tubesheets. Seven methods were reviewed and compared, both on the analytical and numerical points of view: TEMA, ASME, BS 5500, CODAP, STOOMWEZEN, AD-MERKBLATT, TGL.

From this comparison (F. OSWEILLER - 1996) it was decided to adopt the ASME method for the following reasons:

- Tubesheet design formula is straightforward.
- It accounts for an unperforated rim and an unperforated diametral lane.
- Design rule for tubesheet extended as a flange is covered in a more satisfactory way than other code rules.
- Tubesheet thickness obtained is generally lower than by other rules.

The ASME method has been initially adopted by UPV with the same structure: three clauses cover the three common tubesheet configurations:

- Tubesheet integral both sides (configuration a)
- Tubesheet gasketed both sides (configuration d)
- Tubesheet gasketed one side, integral other side (configurations b and e)

However this set of rules was critized during the 6$^{th}$ month enquiry of Pr EN 13445 for the following reasons:

- 3 different rules, based on different analytical approaches, were proposed to cover configurations a, d, b and e.
- Rule for configuration "d" covered only the case were the tubesheet was not extended as a flange, with gaskets both sides of same diameter.

- Rule for configuration "a" used the same formula, corrected by TEMA coefficient F to account for the degree of restraint of the tubesheet by the shell and channel. That approach is not satisfactory for reasons explained by F. OSWEILLER (1999).
- Configurations c and f (gasketed tubesheet not extended as a flange) were not covered.

For these reasons, the author developed in 2000 a more refined, and unique, approach to cover the six tubesheet configurations. This approach is based on ASME method for configuration b – e, with some improvements:

- Treatment of configurations c and f where the tubesheet is not extended as a flange.
- Accounting for local pressures acting on shell and channel, when integral with tubesheet.
- Use of Poisson's ration ν in all formulas, rather than using ν = 0,3 which leads to odd coefficients.
- Derivation of more condensed formulas, providing formulas more consistent with fixed tubesheet rules, and improving the clarity of the rules.

The next section explains the basis of this new approach.

### 13D-2 Basis of analytical treatment

Figure 13D-1 shows, for a tubesheet integral both sides (configuration a), the free body of the component parts (perforated tubesheet, unperforated tubesheet rim, shell, channel), together with the relevant discontinuity forces and moments applied on these components. All loads are by unit of circumferential length in this figure, which shows the sign conventions. Subscript "s" is used for the shell, subscript "c" for the channel, no subscript for the tubesheet.

The analytical treatment follows the stress analysis already used for the treatment of fixed and floating tubesheet heat-exchangers.

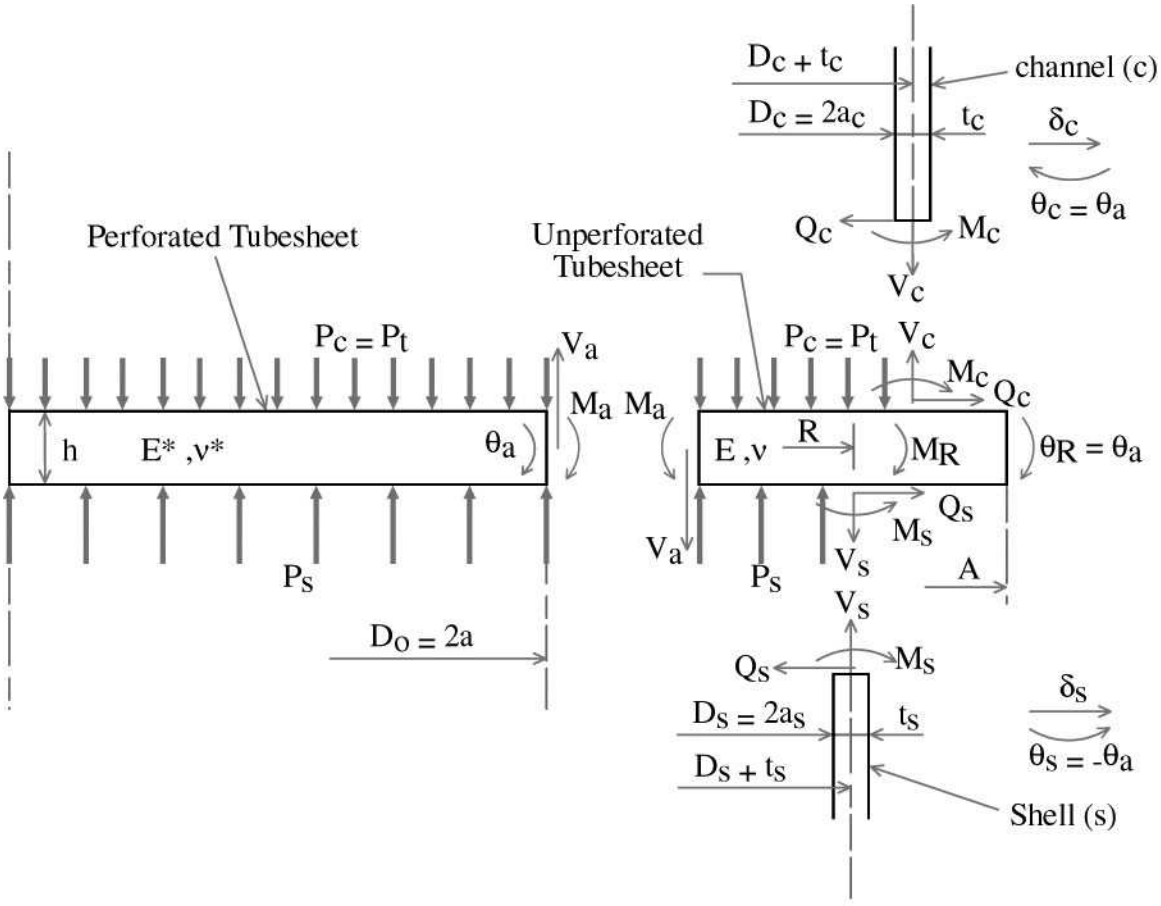


**Figure 13D-1: Analytical model for tubesheet integral both sides (configuration a)**

The main steps of the analytical treatment of this structure are described below. For more details see F. OSWEILLER (2002).

***13D-2a For channel***

- determination of edge displacements ( $\delta_c$, $\theta_c$) depending of $Q_c$ and $M_c$
- use of compatibility equations: $\delta_c = \frac{h}{2}\theta_c$ $\qquad\qquad$ $\theta_c = \theta_a$
- determination of $Q_c$ and $M_c$ as a function of $\theta_a$
- determination of $V_c$ from static equilibrium: $V_c = \frac{a_c}{2} P_c$

***13D-2b For shell: same treatment***

***13D-2c For perforated tubesheet***

The perforated tubesheet which extends over radius a is treated as a solid circular plate of effective elastic constants $E^*$ and $\nu^*$, which are given by curves (as a function of the ligament efficiency).

a) Rotation of the tubesheet at radius a is given by:

$$\theta_a = \frac{12(1-\nu^*)}{E^* h^3}\left[a M_a + \frac{a^3}{8}(P_s - P_c)\right]$$

b) Equilibrium equation writes : $2\pi a V_a + \pi a^2 (P_s - P_c) = 0$

which leads to : $V_a = -\frac{a}{2}(P_s - P_c)$

***13D-2d For unperforated tubesheet rim***

The unperfored rim of the tubesheet is assumed to behave as a rigid ring without distortion of the cross-section. Rotation is given by:

$$\theta_R = \frac{12}{E h^3}\frac{R \cdot M_R}{LnK} = \theta_a$$

where *R* is the centroidal radius of ring, $M_R$ the unit moment acting on ring, and $K = A / D_o$.

The equilibrium of moments acting on the rigid ring enables to determine the bending moments acting on the tubesheet and on shell and channel.

***13D-2e Determination of maximum bending stress in tubesheet***

The maximum bending moments in the perforated tubesheet will appear either at periphery ($M_a$) or at center ($M_o$), which enables to determine the maximum bending stress:

$$\sigma = \frac{6\ MAX(M_a, M_o)}{\mu^* e^2}$$

This primary bending stress is limited to $\sigma_{alw} = \Omega f = 2{,}0\ f$ instead of the traditional 1,5 f. This is justified by the fact that limit load analysis applied to circular plates leads to $\Omega = 1{,}9$ if the tubesheet is simply supported and $\Omega = 2{,}1$ if the tubesheet is clamped.

NOTE: In ASME the maximum allowable stress $\sigma_{alw} = 1{,}5\ S$.

***13D-2f Determination of maxium bending stresses in shell and channel***

$$\sigma_s = \frac{6 M_s}{e_s^2} \qquad\qquad \sigma_c = \frac{6 M_c}{e_c^2}$$

These primary bending stresses are limited to 1,5 $f_s$ and 1,5 $f_c$ respectively.

***13D-2g This new method has been adopted in 2002 by UPV, CODAP and ASME.***

**13D-3 Comparison to TEMA**

New TEMA formula appeared for the first time in 1988 (7th Edition):

$$T = F\frac{G}{3}\sqrt{\frac{P}{\eta S}}$$

A ligament efficiency $\eta$ was introduced, based on the mean ligament efficiency width (see Figure 13D-2) which leads to:

- $\eta_{tr} = 1 - 0{,}907\left(\frac{d_t}{P}\right)^2$ for triangular pitch

- $\eta_{sq} = 1 - 0{,}785\left(\frac{d_t}{P}\right)^2$ for square pitch

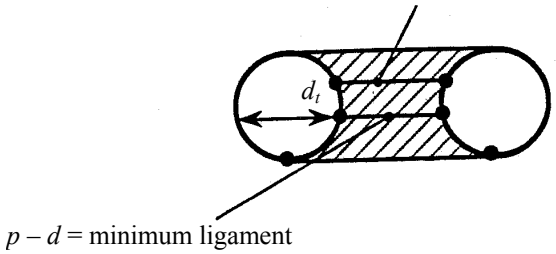


**Figure 13D-2: Ligament efficiency**

Therefore, for a given value of ligament efficiency $\mu$, $\eta_{sq} > \eta_{tr}$, and the tubesheet thickness is lower for square pitch than for triangular pitch. For more details, see F. OSWEILLER (1986).

The minimum value $\mu = 0{,}2$ imposed by TEMA leads to the minimum values of $\eta$:

$$\eta_{tr} \geq 0{,}42 \quad \eta_{sq} \geq 0{,}50$$

These values of $\eta$ are generally significantly higher than the effective ligament efficiency $\mu^*$ used in UPV, CODAP or ASME $(0{,}25 \leq \mu^* \leq 0{,}4)$, as $\mu^*$ is based on the minimum ligament efficiency (see Figure 13D-2).

**13D-4 Numerical comparisons**

Numerical comparisons have been performed on four U-tube tubesheet heat exchangers which are presently treated in the 4 examples of current Appendix AA of ASME Section VIII (Addenda July 2002).

NOTE: For this comparison the maximum allowable stress is written under the form $\sigma_{alw} = \Omega S$.

For each of these examples, Table 13D-1 shows the results obtained for the tubesheet thickness from:

— Classical circular plate, using the ASME ligament efficiency $\mu^*$ and values $\Omega = 1{,}5$ and 2,0.

— TEMA: old formula (6th Edition), and new formula (7th and 8th Editions).

— ASME: old method (July 2001 Edition), and new method (July 2002 Edition) presented in this paper, using $\mu^*$ and $\Omega = 1{,}5$.

— UPV - CODAP: use of new method with $\mu^*$, and Ω = 2,0 or 3,0.

For reasons explained above $\sigma_{alw}$ = 2,0 f is used in the French Code, with following consequences:

— If the yield stress controls (safety factor 1,5 applied on yield stress): $f = S$ and $\Omega = 2{,}0$.

— If the ultimate strength controls (safety factor 2,4 on ultimate strength, instead of 3,5 in ASME Section VIII – Div. 1): $f = 1{,}5\ S$ and $\Omega = 3{,}0$.

Examination of Table 13D-1 shows that, for these 4 examples:

1) TEMA new formula leads to lower thickness than the old formula (except Example 2 for which $\eta = 0{,}37$ is below the TEMA minimum).

   TEMA formula generally leads to lower tubesheet thickness than ASME, due to the high ligament efficiency $\eta$ used by TEMA, and Ω = 1,5 in ASMẼ

   Using $\mu^* = \eta$ will lead to an ASME tubesheet thickness reduced by about 25 %, which becomes close to TEMA thickness.

2) New UPV rules obtains generally a lower tubesheet thickness than TEMA due to the maximum allowable stress, 2 *S* or 3 *S*, used for the tubesheet.

3) New ASME rule leads to lower tubesheet thickness than the old rule, but higher thickness than UPV-CODAP rule due to Ω = 1,5.

4) The classical circular plate formula generally leads to tubesheet thickness higher than TEMA, even with $\Omega = 2{,}0$.

5) In the 4 examples TEMA considers the tubesheet as simply supported (*F* = 1,25). However new method shows that in example 1 the tubesheet is rather clamped (high value of coefficient *F*) due to the high bending rigidities of the shell and channel as compared to the tubesheet bending rigidity.

| Thicknesses ($h$, $T$) are in mm | | | | | | $h_o = C\frac{G}{2}\sqrt{\frac{P}{\mu^*\Omega}}$ | | $T_{new} = F\frac{G}{3}\sqrt{\frac{P}{\eta S}}$ | | | No direct formula: iterative calculations to obtain the optimized tubesheet thickness $h$ | | | | | |
|---|---|---|---|---|---|---|---|---|---|---|---|---|---|---|---|---|
| **EXAMPLE** | | | **LIGAMENT EFFICIENCIES** | | | **CIRCULAR PLATE FORMULA** (using μ*) | | **TEMA** (using η) | | | **ASME** (using μ*) | | | (using η) | **UPV-CODAP** (using μ*) | |
| **N°** | **Config.** | Pitch (Δ, □) | μ 1- $d_t/p$ | **μ*** (ASME) (CODAP) (UPV) | **η** (TEMA) | $h_o$ Ω = 1.5 (ss, cl) | $h_o$ Ω = 2.0 (ss, cl) | $F$ (ss, cl) | $T$ old | ***T*** **new** | $F$ (ss, cl) | $h$ old Ω = 1.5 | ***h*** **new Ω = 1.5** | $h$ new Ω = 1.5 | ***h*** **new Ω = 2.0** | $h$ new Ω = 3.0 |
| **1** | ***a*** | □ | 0.25 | **0.35** | **0.56** | 17.2 (cl) | 14.9 (cl) | 1.21 (ss) | 17.3 | **15.5** | 3.90 (cl) | 20.6 | **15.0** | 11.9 | **13.2** | 11.0 |
| **2** | ***d*** | Δ | 0.17 | **0.28** | **0.37** | 40.9 (ss) | 35.6 (ss) | 1.25 (ss) | 29.5 | **32.3** | 0.43 (ss) | 38.1 | **37.6** | 33.2 | **32.5** | 26.4 |
| **3** | ***d*** | Δ | 0.2 | **0.24** | **0.42** | 131.3 (ss) | 113.8 (ss) | 1.25 (ss) | 87.4 | **89.7** | 0.46 (ss) | 124.2 | **121.4** | 95.0 | **105.2** | 86.3 |
| **4** | ***e*** | □ | 0.25 | **0.39** | **0.56** | 108.7 (ss) | 94.2 (ss) | 1.25 (ss) | 103.3 | **92.2** | 0.86 (ss) | 109.5 | **103.1** | 89.4 | **87.8** | 69.2 |

ss = simply supported Δ: triangular pitch

cl = clamped □: square pitch

**Table 13D-1: Comparison of TEMA, ASME and UPV-CODAP tubesheet thickness on 4 U-tube Heat Exchangers**

## 13E Fixed tubesheet heat exchanger

### 13E-1 Analytical treatment of tubesheets

Configurations a, b, c and d of Figure 13C-3 are covered.

The stresses are calculated according to the four steps procedure described above and illustrated in Figure 13B-1.

These stresses depend on a dimensionless parameter, $X$, which represents the ratio of the axial tube bundle rigidity to the bending rigidity of the tubesheet. It is a fundamental parameter which governs the mechanical behaviour of the exchanger. It may vary from almost zero (tube bundle rigidity very low as compared to the tubesheet rigidity) to about 50 (very stiff tubes as compared to the tubesheet). Common values generally range between 2 and 8.

A second parameter $Z$, which represents the degree of rotational restraint of the tubesheet by the shell and channel, is also important. It may vary from zero, when the tubesheet is simply supported, to infinity when it is fully clamped.

### 13E-2 Differences between UPV and ASME

Some theoretical differences remain between the two design rules, although they rest on the same analytical treatment:

- the tubesheet unperforated rim is treated as a solid ring in ASME method. In the UPV method the tubes are assumed to be uniformly distributed over the whole tubesheet. The main consequence is that the fundamental parameter $X$ of the tubesheet will always be higher in UPV rule than in ASME rule,
- in UPV method the radial displacement of the tubesheet at its connection with shell and channel is ignored,
- when the tubesheet is extended as a flange, ASME method considers the loads due to the gasket and to the bolts, while UPV ignores it.

For more details see F. OSWEILLER (1991).

These differences may have a more or less significant impact on the numerical results and explain the discrepancies obtained between the two methods.

### 13E-3 Numerical comparisons

A benchmark comparison was performed on 10 industrial fixed tubesheet heat exchangers (see Table 13E-1):

- in cases 1 to 6, the tubesheet is integral both sides. Two of them have an expansion bellows set-up on the shell;
- in cases 7 to 10, the tubesheet is integral with the shell and extended as a flange with the channel. Three of them have an expansion bellows set-up on the shell.

Calculations have been performed according to TEMA, ASME, CODAP 95 and UPV – CODAP 2000.

The same allowable stress, taken from ASME Section VIII - Div. 1 has been used, to determine the optimised tubesheet thickness.

Additional calculations will be necessary to account for the fact that the tubes, the shell, or the channel may be overstressed in some cases. It is also possible to obtain lower values for the tubesheet thickness by thickening the shell or using the elastic-plastic solution proposed by the ASME method.

Results shown in table 13E-1 show that:

- UPV and ASME rules lead to similar results for cases 1, 2, 3, 5 and 8. More significant discrepancies appear for the other cases due to the differences between the 2 methods mentioned above.
- CODAP 2000 leads to lower tubesheet thicknesses (10 to 15 %) than CODAP 95, due to the ligament efficiency which is higher in CODAP 2000.
- Thicknesses obtained by TEMA are, in several cases, quite different for the reasons explained below.

| | SI Units | DATA | | | | | | TUBESHEET OPTIMIZED THICKNESS (in mm) (exclusive of corrosion allowance and partition grooves) | | | | |
|---|---|---|---|---|---|---|---|---|---|---|---|---|
| | CAS | Dimensions (mm) | | Pressures (MPa) | | Temperatures (°C) | | | TEMA 1 | ASME 2 | CODAP 95 3 | CODAP 99-EUPV 4 |
| | N° (Type) | ***D* x *L*** | Yes No | $P_t$ | $P_s$ | $T_t$ | $T_s$ | **X** | ***T*** (mm) | ***h*** (mm) | ***e*** (mm) | ***e*** (mm) |
| **INTEGRAL CHANNEL** | **1** (NEN) | 1524 x 13995 | No | 23,44 | 0,0 | 149 | 149 | 1,8 | 314,6 | 330,7 | 360,3 | 324,0 |
| | **2** (NEN) | 3251 x 7010 | No | 6,14 | 5,0 | 260 | 260 | 7,5 | 230,2 | 185,9 | 169,1 | 149,1 |
| | **3** (NEN) | 2743 x 5994 | No | 5,5 | 5,2 | 275 | 265 | 8,4 | 234,9 | 113,5 | 126,3 | 114,4 |
| | **4** (NEN) | 2565 x 1702 | No | -0,1 | 0,34 | 185 | 185 | 41,1 | 43,2 | 5,8 | 12,0 | 11,8 |
| | **5** (NEN) | 2007 x 4775 | Yes | 0,55 | 0,86 | 204 | 232 | 19,2 | 77,3 | 27,4 | 25,4 | 23,2 |
| | **6** (NEN) | 635 x 4877 | Yes | 0,0 | 1,38 | 177 | 93 | 14,6 | 11,9 | 14,2 | 7,6 | 6,0 |
| **GASKETED CHANNEL** | **7** (AEL) | 1803 x 4572 | No | 0,28 | 0,28 | 149 | 149 | 12,3 | 66,6 | 26,2 | 32,5 | 33,2 |
| | **8** (AEL) | 914 x 4267 | Yes | 2,76 | 1,03 | 288 | 288 | 5,4 | 80,8 | 60,2 | 55,2 | 49,6 |
| | **9** (AEL) | 610 x 5486 | Yes | 1,72 | 2,59 | 135 | 186 | 4,0 | 49,5 | 25,9 | 39,4 | 36,3 |
| | **10** (AEL) | 152 x 3658 | Yes | 0,86 | 0,86 | 49 | 163 | 2,5 | 16,7 | 7,4 | 11,4 | 10,5 |

**Table 13E-1 : Fixed tubesheet heat exchanger**

### 13E-4 Comparison to TEMA

The TEMA design method assumes that the weakening effect of the holes is balanced by the stiffening of the tubes. The consequence is that the coefficient $F$ which appears in the TEMA tubesheet formula,

$$T = F \frac{G}{3} \sqrt{\frac{P}{\eta S}}$$

has a constant value:

$F = 1{,}0$ if the tubesheet is simply supported.

$F = 0{,}8$ if the tubesheet is clamped.

Writing the UPV formula in the same way, we obtain:

$$T = F_{\text{UPV}} \frac{G}{3} \sqrt{\frac{P}{\eta S}}$$

were $F_{\text{UPV}}$ depends strongly on the fundamental parameter $X$, which represents the ratio of tube bundle axial stiffness to tubesheet bending stiffness (see Figure 13E-1).

This figure shows that:

- When $X$ is low ($X < 2$), the tubesheet thickness obtained by TEMA will be lower than UPV - CODAP or ASME thickness. This happens for case 1 ($X = 1{,}8$).
- When $X$ is high ($X > 5$), the tubesheet thickness obtained by TEMA will be higher than UPV - CODAP or ASME thickness. This happens in cases 2, 3 and 6. The discrepancy will increase dramatically when $X$ is very high, like in case 4 ($X = 41$, which is quite unusual), case 5 ($X = 19$) or case 7 ($X = 12$).
- in the intermediate range ($2 \leq X \leq 5$) UPV - CODAP and TEMA thicknesses will be about the same. Cases 8 ($X = 5$), 9 ($X = 4$) and 10 ($X = 2{,}5$). In this range the above assumption made by TEMA is acceptable.

The main consequence is that TEMA does not provide the same design margin for all heat exchangers, leading to over thickness when the $X$ value is high and underthickness when the $X$ value is low.

For more details see A.I. SOLER (1990) and F. OSWEILLER (1986).

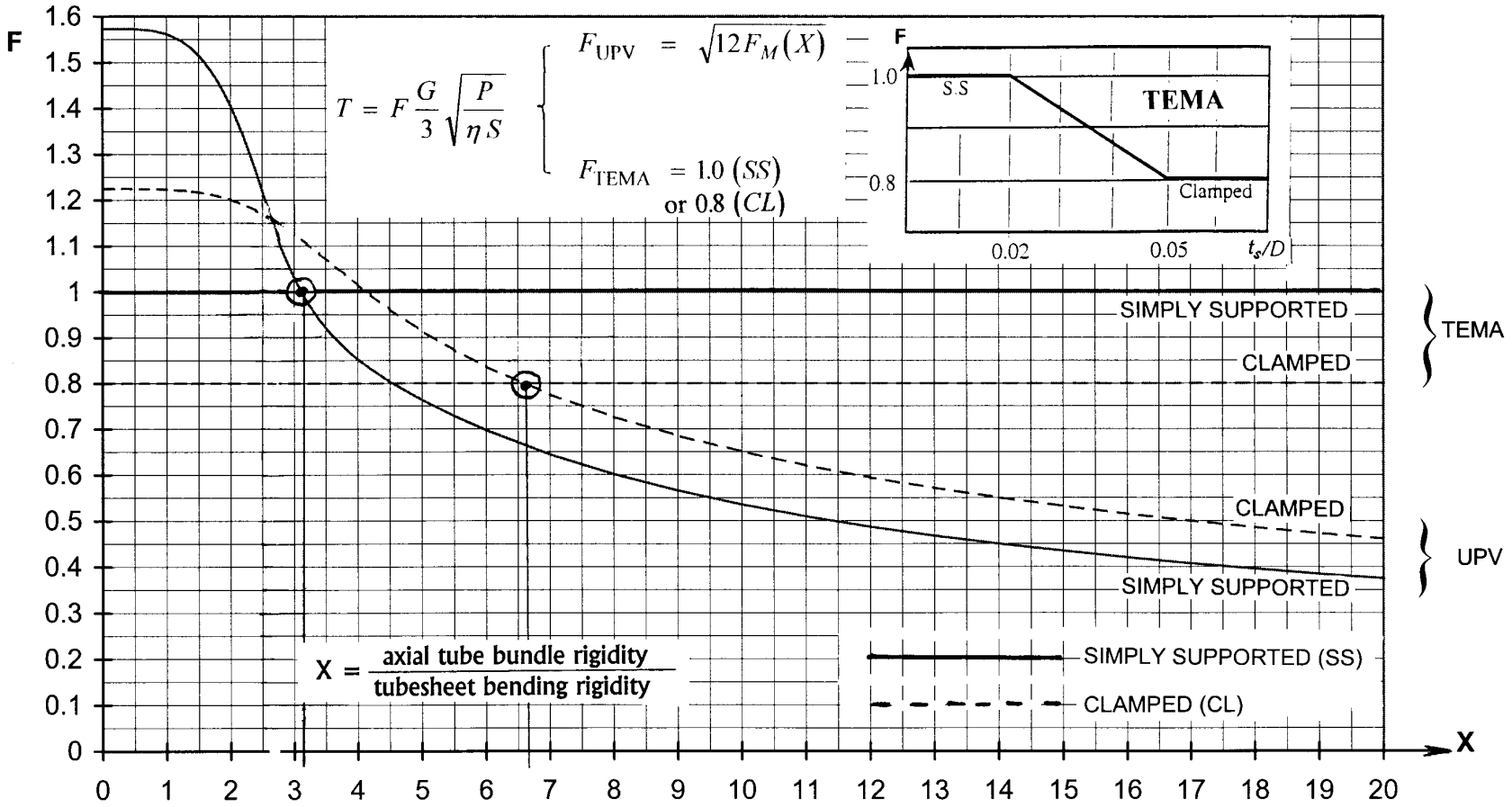


**Figure 13E-1: Comparison of TEMA and UPV-CODAP 99 rules for fixed tubesheets**

## 13F Floating head heat exchanger

### 13F-1 UPV rule

Until recently the CODAP 95 rule for floating heads was based on K. GARDNER (1969) method. This method has the following drawbacks:

- the connection of the tubesheet with shell and channel is not treated correctly (the tubesheet is considered as either simply supported or clamped),
- tubesheet thicknesses obtained are generally high,
- some of the charts provided for the calculation of tube stresses were not usable in certain ranges of $X$.

It was therefore decided to adapt the fixed tubesheet approach to cover floating tubesheet heat exchangers, with the following benefits:

- better consistency with the fixed tubesheet rules,
- correct treatment of tubesheet - shell - channel connection,
- reduced tubesheet thickness,
- possibility of covering new tubesheet configurations.

On the other hand this method does not account for the unperforated rim and the two tubesheets are assumed identical.

Three types of heat exchangers are covered (Figure 13F-1):

- immersed floating head,
- externally sealed floating head,
- internally sealed floating tubesheet.

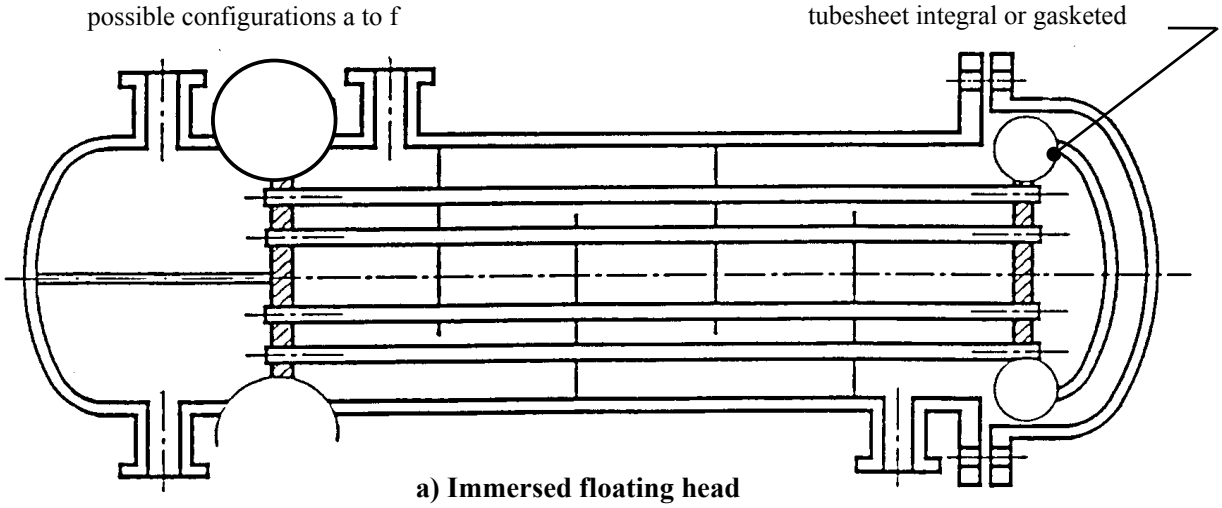


**a) Immersed floating head**

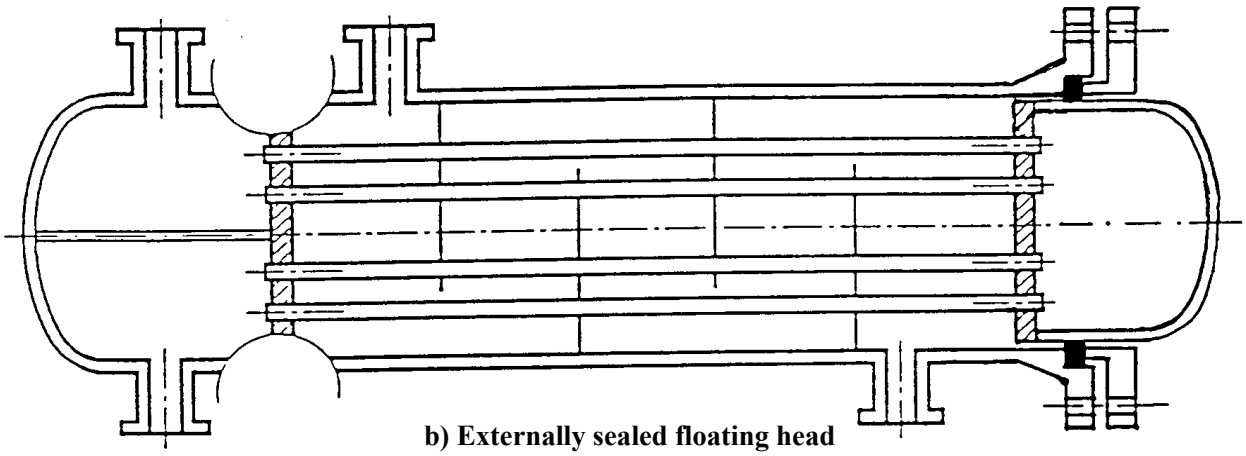

**b) Externally sealed floating head**

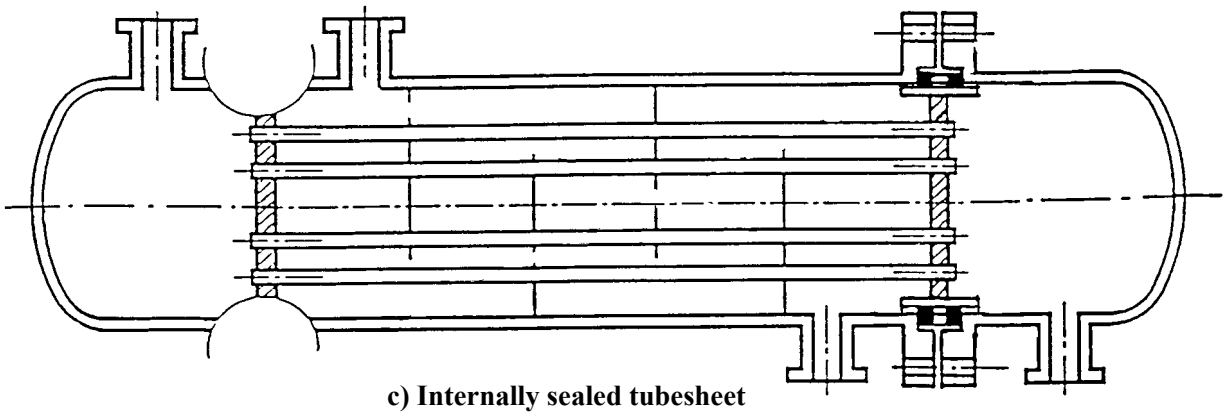

**c) Internally sealed tubesheet**

**Figure 13F-1: Types of floating head heat exchangers**
**(identical to Figure 13.6.1-1 in EN 13445)**

The stationary tubesheet may have any of the configurations a to *f*. The floating tubesheet may be gasketed to the floating head (extended as a flange, or not) or integral with the floating head.

The design procedure is similar to the fixed tubesheet procedure.

### 13F-2 ASME rule

Like UPV, ASME rule is based on the fixed tubesheet method.

## 13G Conclusion

TEMA design rules do not ensure the same safety level for all heat exchangers: they often lead to tubesheet over-thickness, occasionally to under-thickness, which may be detrimental to the safety of the vessel.

This is the main reason why UPV, CODAP and ASME decided to develop a more rational approach and to reconcile their heat exchanger design rules both on the analytical and editorial aspects. This reconciliation work is now achieved with the publication of consistent rules in:

- EN 13443 Part 3- Clause 13 in July 2002.
- ASME Code Section VIII - Div. 1 Appendix AA in July 2002 Addenda.
- CODAP Section C7 in January 2000.

These rules propose a better treatment of the mechanical behaviour of the various components of the heat exchanger. They lead to reduced tubesheet thicknesses, while ensuring a consistent safety margin for all heat exchangers.

Use of common notations, common tubesheet configurations and common terminology will facilitate an easy correspondence among these three codes, while ensuring a progressive transition from TEMA to these new design rules.

It is the opinion of the author that these new rules will gradually replace TEMA design rules both in US and Europe. This is based on the facts that ASME rule will become mandatory in US and Canada in July 2003 (non-mandatory Appendix AA replaced by new mandatory Part UHX) and EN 13445 should be widely used in Europe.

At the dawn of the new millennium, these rules should find increased use in national and international markets, thus following the new trends of market globalisation.

### 13H Bibliography


[1]. TEMA Standards (Tubular Exchangers Manufacturers Association): 7th Edition - 1998

[2]. CODAP 95: Code français de Construction des Appareils à Pression - Section C7 - revised on 01 January 1999

[3]. ASME Section VIII - Division 1 - Appendix AA: 1998 Edition (1 July 1998)

[4]. A. I. SOLER - S. CALDWELL (1990) "A proposed ASME Section VIII, Division 1, tubesheet design procedure" Proceedings of the 1990 ASME PVP Conference - Nashville - Vol. 186 (HOO605)

[5]. F. OSWEILLER (1986) "Analysis of TEMA tubesheet design rules - comparison with-up-to date Code methods" Proceedings of the 1986 ASME PVP Conference - Vol. 107 (G00358)

[6]. F. OSWEILLER (1989) "Evolution and synthesis of the effective elastic constants concept for the design of tubesheets" Journal of Pressure Vessel Technology - August 1989 - Vol. 111 - p. 209-217

[7]. F. OSWEILLER (1996) "U-tube heat exchangers: A comparison of Code Design Rules"Proceeding of ASME - 8th ICPVT Conference - Montreal - July 1996 - Vol. 2 (H10708)

[8]. K. GARDNER (1969) "Tubesheet design: a basis for standardization" 1969 Delft Conference (p. 621-648)

[9]. F. OSWEILLER (1991) "New design rules for fixed tubesheets heat exchangers: A comparison of CODAP and ASME approaches" Proceedings of the 1991 ASME PVP Conference - Vol. 110-2 (H00637)

[10]. F. OSWEILLER (2002) "New common design rules for U-tube heat-exchangers in ASME, CODAP and UPV Codes" Proceedings of the 2002 ASME PVP Conference - Vol. 439 (H01237)


## 14 Expansion bellows

Special rules are provided in Chapter 14 for the design of expansion joints, including consideration of fatigue. These follow the route originally proposed by the Expansion Joints Manufacturers Association (EJMA), which presents design S-N curves modelled on those in ASME. However, for EN 13445 use has been made of the larger database from fatigue tests now available. These were analysed to produce the same form of S-N relationship incorporating safety factors on the fitted mean S-N curve of 1,25 on stress and 3 on life. The stress used with the S-N curves is the equivalent stress range arising from cyclic pressure and deflection of the convolutions. As distinction is drawn between austenitic stainless steel, nickel alloy and copper-nickel alloy expansion joints that have or have not experienced cold work. On the basis that cold work increases the yield strength of the steel, the fatigue resistance of the latter is assumed to be higher than that of the former. However, no distinction seems to be drawn between joints that do or do not include longitudinal weld seams. Even so, both design curves are within the band of curves provided in Chapter 18 for assessing plain steels. In the case of expansion joints made from ferritic steel, the user of Chapter 14 is directed to Chapter 18.

# 15 Pressure vessels of rectangular section

## 15A Introduction to Fundamental theory

Where there is no relevant code, the procedure outlined in this article follows the same logic, based on fundamental engineering theory as used in the codes and should therefore be equally acceptable. Such procedure should be regarded as evidence of good modern day general engineering practice in this field. It is hoped that it will promote a better understanding of the problems associated with such vessels which are often either ignored or not given the consideration and attention which they deserve. Such vessels can be quite complex in their detailed design and unawareness on the part of the designer and/or fabricator, to appreciate the various aspects can lead to costly ramifications later on. These vessels although they appear to be very simple indeed, can nonetheless cause considerable embarrassment if not assessed adequately at the outset.

Comparison of the rectangular vessels with the equivalent size cylindrical (circular cross-section) vessels indicate that the former are rather inefficient. Cylindrical vessels will sustain considerably higher pressures, for the same wall thicknesses and size. However, practical consideration will often force the designer to select a rectangular shape as the best available option e.g. air cooler headers in oil refineries, many vessels in pulp and paper industry and maybe the most well known, the autoclaves for medical and pharmaceutical applications.

The fundamental theory is applicable to both external and internal pressure. Worked examples given in the text refer to internal pressure for the simple reason that, for the external pressure application, considerable gaps still exist in the knowledge of the allowable compressive stress levels which will not cause buckling or plastic collapse in rectangular and other non-circular vessels. The theory of flat plates is not applicable to rectangular vessel sides (except to plates between stiffeners). The adjacent side dimensions are having effect on the moments and stresses of the other side.

## 15B Fundamental theory for rectangular section pressure vessels [Ref. 6]

Figure 15B-1 shows that the basic geometry of the rectangular vessel with sharp corners and which is subjected to a uniform pressure of $p$.

Where $h$ = the longer span

$H$ = the shorter span

$I_1$ = second moment of area longer beam about its neutral axis

$I_2$ = second moment of area of shorter beam about its neutral axis

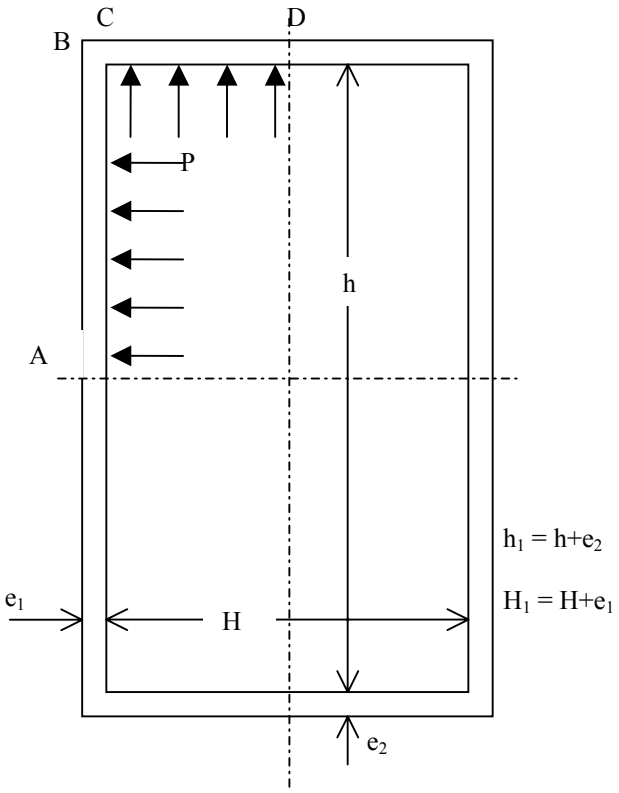


**Figure 15B-1**

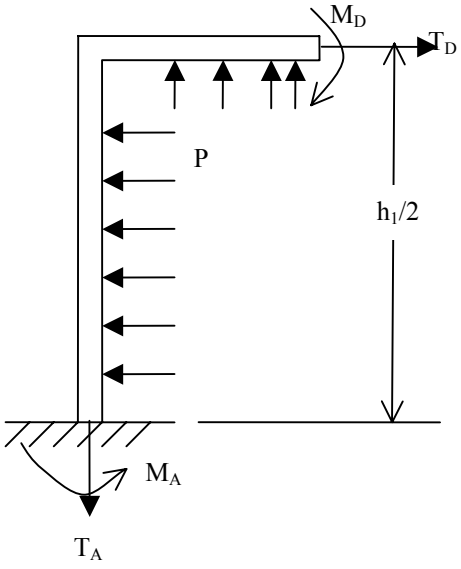


**Figure 15B-2.**

Due to symmetry about axes at *A* and *D* it will be convenient to analyse one quadrant only of the cross-section shown. This quadrant is in equilibrium under the action of the loads and moments indicated in Figure 15B-2.

Clearly from the balance of the horizontal and vertical forces acting on the quadrant we obtain

$$T_D = \frac{Ph}{2}$$

which represents the direct tensile load in member CD and

$$T_A = \frac{PH}{2}$$

the tensile load in member AB respectively. In evaluating these tensile forces the thicknesses $e_1$ and $e_2$ are considered to be negligible in comparison with dimensions H and $h$, i.e.

$\left(\frac{H}{2} - \frac{e_2}{2}\right)$ effectively equals to $\frac{H}{2}$

In beams and frames having rigid joints, as in this particular case, the strain energy due to the direct and shear forces is so small in comparison with that due to bending that only the latter need to be considered when evaluating statically indeterminate moments.

In any member of a structure subjected to bending the total strain energy is given by

$$U = \int_0^1 \frac{M^2 dx}{2EI} \qquad \text{(15B.1)}$$

where $M$ is the bending moment at any point on the member caused by the combined effect of the imposed loads and the supporting forces and moments whether statically determinate or not. The integration must be taken over the entire length of each member, of which $dx$ is an element of length.

Two further postulates (Castigliano's theory) help to solve the problem. These are:

1. The partial differential coefficient of the strain energy in a structure, is equivalent to the displacement of $F$ along its line of action, i.e.

$$\frac{\partial U}{\partial F} = \int_0^1 \frac{2M\partial M}{2EI\partial F} dx = \int_0^1 \frac{M\partial M}{EI\partial F} dx = \delta \qquad \text{(15B.2)}$$

2. The partial differential coefficient of the strain energy with respect to a moment acting on a structure is equivalent to the angle through which that portion of the structure rotates when the moment is applied

$$\frac{\partial U}{\partial M_X} = \int_0^1 \frac{M\partial M}{EI\partial M_X} dx = \phi \qquad \text{(15B.3)}$$

When, as in this case, the support of structure at this point of support and the two expressions just quoted can be equated to zero.

By setting down the equation for moments along $AB$ and CD and by considering the strain energy due to bending (by integrating along $AB$ and $CD$ respectively) it can be shown that the moments at the three important points $A$, $B$ & $C$ *and* $D$ become for a general case (observation: reference [6]. equations have been slightly corrected and negative sign added to midspan moments, because internal pressure is causing tensile stress in outside surface; shall be corrected also in equation 15.6.5-3 of standard).

$$M_A = -\frac{Ph^2}{8} * \left[1 - \frac{1}{3}\left(\frac{1 + 3k - 2\alpha^2 k}{k+1}\right)\right] \qquad \text{(15B.4)}$$

$$M_{B,C} = \frac{Ph^2}{24}\left(\frac{1 + 3k - 2\alpha^2 k}{k+1}\right) \qquad \text{(15B.5)}$$

$$M_D = -\frac{Ph^2}{8} * \left[\alpha^2 - 1 + \frac{1}{3}\left(\frac{1 + 3k - 2\alpha^2 k}{k+1}\right)\right] \qquad \text{(15B.6)}$$

where

$$k = \frac{I_2}{I_1}\frac{H}{h} \qquad \text{and} \qquad \alpha = \frac{H}{h}$$

Notice that

$$M_A = \frac{Ph^2}{8} - \frac{Ph^2}{24}\left(\frac{1+3k-2\alpha^2 k}{k+1}\right)$$

where the first term denotes the bending moment at mid span for a simply supported long side beam under the action of uniform load *P* and second term is the moment at corner.

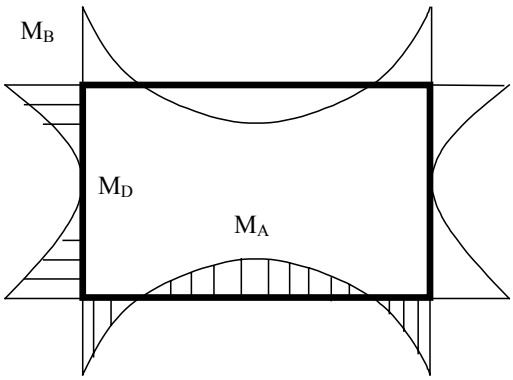


**Figure 15B-3 Moment distribution at rectangular frame**

So far we have dealt essentially with uniform wall rectangular vessels. The preceding basic theory is equally applicable to rectangular vessels which have peripheral stiffeners spaced along the length of the vessel, P must be substituted by $P*b_R$ ($b_R$ is the pitch between stiffeners). Evaluating the equation (15B.4), we are getting the equation (15.6.5-3) of Clause 15 of EN 13445-3. Same way from equation (15B.5) we are getting equations. (15.6.5-5) and (15.6.5-7). From equation (15B.6) we are getting equation (15.6.5-9). $\alpha$ shall be replaced by $\alpha_1$ every where in the equations, but in (15B.4) the first $\alpha$ remains.

Because the bending stresses shall be summed to membrane stresses, the stresses must be calculated both inside the vessel and outside the stiffener (see the calculation example).

In such cases we have to check not only the strength of the stiffeners but also the stress levels in wall panels between these stiffeners.

The strength of the peripheral stiffeners can be determined by the method described above, as for the plain rectangular vessels. Equations (15B.4), (15B.5) and (15B.6) can be used directly for a general case where the second moments of area of the stiffeners $I_1$ an $I_2$ and the wall thicknesses $e_1$, $e_2$ of the two main sides are different.

For **unreinforced rectangular vessels** with round corners (see Fig.15.5-1 in standard) there have been given the equations for calculating stresses directly. The theory equals to that described above, but the corner radius influence has been taken into account. The stresses in the corner can be calculated in the wanted position by using the applicable angle $\theta$.

The **wall panels between the stiffeners** can be treated as rectangular panels fixed (built-in) at all four edges and subjected to a uniform pressure load P over the entire area. E.g. Roark's Formulas for Stress and Strain (Reference [7]) covers this particular case and gives the maximum bending stress, which occurs at the centre of long edges, as

$$\sigma = C\frac{Pb^2}{e^2}$$

where the value of *C* depends solely on the ratio of the two sides *g/b*, *b* is the width or the shorter span and e is the panel plate thickness. Table 15.6-2 gives the variables C for various *g/b* ratios. Notice that for *g/b* values above 2.15 the parameter $\beta$=0.5, giving (observe that the heading of the last column in the table shall be >2.15, to be corrected in standard later)

$$\sigma = 0.5\frac{pb^2}{e^2} \qquad \text{or} \qquad \sigma = 0.5\frac{Ph^2}{e^2}$$

This represents the same situation that occurs for a built-in beam of span *b*. Here the end moment

$$M_B = \frac{Ph^2}{12}$$

and the plate section modules for an unit width strip

$$Z = \frac{e^2}{16}$$

Hence the bending stress at the built in edge

$$\sigma = \frac{M}{Z} = \frac{6Ph^2}{12e^2} = 0.5\frac{Ph^2}{e^2}$$

i.e. the same as above. This confirms that for wall panels whose g/*b* ratio exceeds 2.15 we can treat the central portion of such panels as fixed-in beam of span equal to the width of the panel. Standard EN 13445-3 Clause 15 combines this bending stress with the membrane stress acting perpendicular to stiffeners (axial membrane stress). This is not done e.g. in ASME, Appendix 13.

## 15C Allowable stresses

The **membrane stresses** are limited to material nominal design stress *f* (defined in Clause 1 of EN 13345-3) multiplied by the possible weld joint factor.

The sum of **membrane and bending stresses** are limited to *1.5 f* . On the basis of limit analysis this allowable stress seems to be conservative in corners of the unreinforced vessel for cases where the stresses at midspan are below *1.5f.*

For reinforced rectangular vessels the limitation *1.5f* may be unconservative, if the stiffener profile has very thin webs. This unconservatism has been compensated with the requirement for shear stresses at stiffener webs, see equations. (15.6.2.3-1) and (15.6.2.3-2) in clause 15 of standard. (Observe that in the first issue the stiffener pitch $b_R$ is missing as multiplier in the latter equation, to be corrected in later versions).

In reference [5] there has been presented a method that corrects the calculation weakness of the rectangular vessel reinforced by thin web profiles. Because of plasticity the corners of the stiffener frame are not theoretically stiff, but they yield. This is causing the effect that the real corner moment is decreasing (10-30 %) and the midspan moments are increasing respectively from the values calculated by the standard formulas. The effect of this has more importance, when the calculated stresses in corners of the vessel are smaller than the midspan stresses (especially in flat sections). In addition the stress range has more importance in fatigue assessments. However the designer shall design the corners by good engineering practice so, that the structure is able to conduct all the shear forces to webs (see Eurocode rules for steel constructions) and no excessive yielding happens.

In reference [5] there have been presented a correction method for calculating the corner moment $M_B$. This equation adds the shear rigidity to denominator of equation 15B.5 (this may be added to future version of EN 13445-3).

$$M_{B,C} = \frac{Ph^2}{24}\left(\frac{1+3k-2\alpha^2 k}{k+1+\dfrac{2SE}{hGA_w}}\right)$$

where S is the section modulus (firs moment of area to neutral axis)

E is the elastic modulus

G is the shear modulus (by steel appr. E/2.6)

$A_w$ is cross sectional area of corner webs

There is not any special **buckling** analysis for panel or stiffener parts subjected to compression stresses. Instead in table 15.6-1 (mistake in the end of chapter 15.6.3) there have been given limit lengths of stiffener parts

depending on the thickness. By these lengths it is supposed that no buckling of compressed parts may happen. There is missing the effective width $b_e$ to be calculated to the effective stiffener section, in Figure 15.6-1 shall be written $b_e \leq 10\ e$.

### 15D Bibliography

In the preparation the rules for design of rectangular pressure vessels in standard EN 13445-3 the following references have been used:


[1] BS 3970: Part1: 1990, Sterilizing and disinfecting equipment for medical products, Part 1. Specification for general requirements

[2] Swedish Pressure Vessel Code, TKN 1987

[3] ASME VIII, Div. 1, Appendix 13, Vessels of noncircular cross section

[4] Design manual for structural stainless steel, Euro inox, European Stainless Steel Development & Information Group

[5] Int. Journal for Pressure Vessels & Piping 30 (1987): The stress Analysis of Rectangular Pressure Vessels having thin-walled reinforcing members, Zhao-jing Zeng

[6] British Engine Technical Report 1981, Volume XIV

[7] Roark: Formulas for Stress and Strain, Mc Graw Hill


The basic equations are mainly from reference [1]. Calculation rules for vessels having central partition plate have been based on reference [3]. Reference [4] has been used to define the allowable flange and web dimensions of stiffeners and plates subjected to compressive stresses.

## 16 Additional non-pressure loads

### 16A Introduction

Generally the predominant loading in pressure vessels is internal and/or external pressure. However in most cases additional non-pressure loads do occur and their effects must be evaluated in order to guarantee the integrity of the pressure vessel. Potential areas for concern are the external loads on nozzles, the reaction forces at supports and the global loads such as wind loading.

At nozzle intersections relatively high stresses occur which are intensified by external loads on the nozzles. As such the problem at nozzles is different from other areas and is dealt with in a different way.

### 16B Background

Existing available methods, which are used frequently, are: BS 5500 [ref. 1], the methods published in WRCB 107 [ref. 2] and WRCB 297 [ref. 3] . Both BS 5500 and WRCB 107 are based on the theoretical work developed by Bijlaard [ref. 4 to 7]. For nozzle to cylinder intersections the following assumptions were made by Bijlaard:

the external load is applied directly to the cylindrical surface

the nozzle-cylinder intersection is in a flat plane

the circular loaded surface is replaced by an equivalent square loaded area

As such the validity of Bijlaard's work is restricted to smaller diameter ratios (up to about d/D ~ 0.30).

In WRCB 107 the available graphs are based partially on the work of Bijlaard and partially on some experimental data so that the ratio d/D could be extended to values of about 0.57.

The method in WRCB 297 is an analytical method developed by C.R. Steele [ref. 8] on the basis of thin shell theory. A large number of graphs are presented by which the stresses can be derived both in the shell and in the nozzle. The method covers a much broader field of application than BS 5500 and WRCB 107.

Although each of those methods has it own merits, there are some drawbacks which must be considered when applying those methods:

The methods are based on an elastic stress analysis and as such a stress categorisation must be applied.

In both WRCB methods the interaction with pressure is not considered and it is up to the user how to take into account the influence of pressure.

For nozzles located in cylindrical shells and subjected to a bending moment which is not along one of the main axes, the maximum stress is not found always.

In BS 5500 and WRCB 107 the nozzle thickness does not affect the stresses at the intersection

In BS 5500 a linear interaction with internal pressure is assumed and as such a rather conservative result is obtained.

If the resulting stresses are interpreted by means of the ASME VIII – Division 2 [ref. 9] a maximum stress of 3f may be allowed, whereas in BS 5500 the maximum allowable stress is 2.25 f

## 16C Method of EN 13445

In order to get rid of those drawbacks the method in the new EN 13445 has been based as much as possible on limit analysis.

## 16C-1 Nozzles in spherical shells (section 16.4 of EN 13445-3)

### *16C-1a Load ratios*

In a design method based on limit analysis, the main objective is to define the maximum allowable individual loads and the corresponding load ratios. A load ratio is defined as the ratio between the actual load and the maximum allowable load. As such each considered load ratio never may be greater than unity.

$\Phi_P$ = load ratio due to internal pressure <= 1.0

$\Phi_Z$ = load ratio due to axial nozzle load <= 1.0

$\Phi_B$ = load ratio due to bending moment applied to the nozzle <= 1.0

A solution to define the maximum allowable axial nozzle force is based on the theoretical work made by Dr. Kiesewetter and Dr. Wölfel [ref. 10]. The maximum allowable axial nozzle load is a function of a reinforcement rate factor $\kappa$ and the geometrical parameter $\lambda$ (equations 16.4-4, 16.4-5 and 16.4-7). Due to some simplifications the obtained value is situated between 0 % and 10 % below the true limit load and hence the equation yields a conservative estimation.

A similar expression is found for a bending moment applied to the nozzle. The bending moment can be transformed to an equivalent axial force and consequently the maximum allowable moment is obtained (equation 16.4-8).

Actually there are no such simple expressions available for internal or external pressure. However it is logical to base the maximum allowable pressure on the rules for reinforcement of openings (section 9). The latter value is obtained by equation 16.4-7.

Shear forces and twisting moments have not been considered as there are strong indications that, at least for the actual field of application, they can be ignored.

### *16C-1b Interaction of loadings*

The interaction of different loading and pressure is complicated and by now is not completely solved. Based on comparisons and several considerations (such as safety, lack of sufficient knowledge, etc...), following approximate solution was accepted:

$$\max\left(\left|\Phi_P+\Phi_Z\right|;\left|\Phi_Z\right|;\left|\Phi_P-0{,}2\Phi_Z\right|\right)+\left|\Phi_B\right|\le 1{,}0$$

This equation is based on a linear interaction between pressure plus axial load and the bending moment. It yields a conservative result. Most probably a circular interaction is more realistic but further theoretical and/or experimental data must be awaited before this will be accepted.

### *16C-1c Shakedown analysis*

As limit analysis is applied an additional check is required to insure that the shakedown limit has not been exceeded. In most cases a structure shakes down to elastic action if the maximum stress does not exceed twice the yield stress. The maximum stress is found by a quadratic interaction for the mechanical loads plus a linear

interaction with thermal stresses. For the mechanical loads the effects of both the axial nozzle load and the bending moment are similar and hence are added algebraically. The thermal stresses considered are those produced by temperature differences between nozzle and shell.

The elastic stresses are obtained by the charts found in figures 16.4-3 to 16.4-8, which have been reproduced from BS 5500 and which are based on the work made by Leckie and Penny [ref. 11].

### 16C-2 Nozzles in cylindrical shells (section 16.5 of EN 13445-3)

#### *16C-2a Load ratios:*

The problem no longer is axi-symmetric, but a true three-dimensional problem. Also two bending moments must be considered: one in the longitudinal plane of symmetry and one in the transverse plane of symmetry.

A true limit analysis is not possible and actually for nozzles in cylindrical shells no "simple" solutions are available to define the maximum allowable individual loads. To overcome this problem an approximate limit analysis is applied, which is derived from the existing design method in WRCB 297. It is assumed that the limit load is reached when the maximum stress due to each individual load is equal to 2.25 f .

The actual design charts in WRCB 297 are combined and after some simplification put into another form (see figures 16.5-2 to 16.5-4 and table 16.5-1). From this new charts the factors $C_1$, $C_2$ and $C_3$ are derived and relatively simple expressions are available to define the maximum allowable load components (equations 16.5-3 to 16.5-8).

Here also the maximum allowable pressure is based on the rules for reinforcement of openings (section 9) and is obtained by equation 16.5-2.

#### *16C-2b Interaction of loadings:*

Although the quadratic interaction of both moments is correct only for a nozzle in a spherical shell, it is still an acceptable approximation for nozzles in cylindrical shells.

Basically the same global interaction expression, applied to nozzles in spherical shells, also can be applied to nozzles in cylindrical shells. However in the latter case a quadratic interaction is accepted because the basis for defining the individual external loads already is rather conservative. As such too conservative results are avoided. Also an additional factor $C_4$ is introduced. For cases where the nozzle is connected to a piping system with due allowance for expansion or thrusts a value of $C_4$ up to 1.1 may be accepted and the standard prescribes that value. For rigid attachments the value of $C_4$ shall be equal to 1. Thus for a nozzle in a cylindrical shell the following condition is applied:

$$\sqrt{\left[\max\left(\left|\frac{\Phi_P}{C_4}+\Phi_Z\right|;\left|\Phi_Z\right|;\left|\frac{\Phi_P}{C_4}-0{,}2\Phi_Z\right|\right)\right]^2+\Phi_B^2} \quad \leq \quad 1{,}0$$

#### *16C-2c Shakedown analysis*

The maximum stress is found by a quadratic interaction for the mechanical loads plus a linear interaction with thermal stresses (equation 16.5-25).

For the mechanical loads the equation 16.5-25 is different from the corresponding equation for nozzles in spherical shells. This is based on the results from experimental tests, which indicate that it is more realistic to add stresses due to an axial nozzle load with those to pressure. The pressure stresses are obtained by equation 16.5-21, which is based on a large number of experimental stress measurements and fatigue tests [ref. 12].

### 16C-3 Allowable nozzle loads (section 16.4-8 and 16.5-8)

The external loads applied to the nozzle are considered as global loads. The load factors are obtained easily, while a linear interaction is assumed. An additional check is required for the longitudinal instability of the nozzle.

### 16C-4 Basis for calculation of line loads, lifting eyes, saddle supports and bracket supports

The design method is based on a work developed by Dr.-Ing. Ziegenbalg [ref. 13], and published in [ref. 14]. It has widely been applied in Eastern Germany and other countries from Eastern Europe [ref. 15].

### *16C-4a Line loads*

The solution is based on the theory of elasticity. Stresses are calculated in shells with radial line loads, applied in longitudinal and circumferential direction. Those line loads result in local normal forces and bending moments in both longitudinal and circumferential direction. The solutions are directly applicable for lifting eyes without reinforcing plate. Superposition of these solutions provides the basis for brackets with and without reinforcing plate and for saddles also.

The limitations of stresses include allowable local plastic deformations in the cross section of the shell. Formally this partially plastic deformation is seen in the so called "Bending-Limit-Stress" $\sigma_{b,all}$ , which mostly is higher then the allowable design stress $f$ . It is obtained as follows:

a) Elastic stresses:

$\sigma_b = 6\,M / e^2$

and $\sigma_m = N / e$

b) Limit load for a strip of shell:

$|M| / M_{max} + (N / N_{max})^2 \le 1$

with $M_{max} = f\,e^2 / 4$

and $N_{max} = f\,e$

c) Substitution of $M$ and $N$ with $\sigma_b$ and $\sigma_m$ :

$$\frac{2\sigma_b}{3f} + \left(\frac{\sigma_m}{f}\right)^2 \le 1$$

$\sigma_m = \sigma_{m,loc} + \sigma_{m,glob} = \sigma_b\,\upsilon_1 + f\,\upsilon_2$

with $\upsilon_1 = \sigma_{m,loc} / \sigma_b$ (section 16.6)

and $\upsilon_2 = \sigma_{m,glob} / f$

d) Equations for limitation of $\sigma_b$ and calculation of $K_1 = \sigma_{b,all} / f$

$$\frac{2\,\sigma_b}{3f} + \left(\frac{\sigma_b}{f}\upsilon_1 + \upsilon_2\right)^2 \le 1$$

$$\frac{2}{3}K_1 + \left(K_1\upsilon_1 + \upsilon_2\right)^2 = 1$$

### *16C-4b Lifting eyes (section 16.7 of EN 13445-3)*

The design method is a direct application of the line load method explained in the previous section. Once the factors $\upsilon_1$ and $\upsilon_2$ are defined the maximum allowable load on the lifting eye is easily obtained.

### *16C-4c Saddle supports (section 16.8 and 16.9 of EN 13445)*

For a long time the method developed by Zick [ref. 16] has been used in most design codes. However both experimental and analytical data indicate that the method is too conservative for thin walled shells or low pressure applications.

Based on line loads, and confirmed by experimental results, a new TGL standard [ref. 15] was developed. This standard is used as a basis for the new design methods with some modifications. An additional check is required for the risk of instability in the middle between the two saddles.

In section 16.9 a new method is available for the design of horizontal vessels on ring supports, based on a limit analysis developed by Dr. Wölfel [ref.17]. Besides the vertical loads, horizontal forces too may be considered.

*16C-4d Bracket, supporting legs, skirts and ring supports (section 16.10 to 16.13 of EN 13445-3)*

The methods are based on existing design methods or codes, such as TGL [ref.15] and AD-Merkblatt [ref. 18], with some minor modifications.

For skirts an elastic stress method is applied as no valid alternatives are available for the time being.

*16C-4e Global loads (section 16.14 of EN 13445-3)*

A linear interaction is accepted between the global loads and internal or external pressure. For the risk of instability of shells the rules of ECCS are included, which are conservative. Also he effect of deviation from the perfect shape is included in the calculations. Some guidance for earthquake loads is included as well.

## 16D Examples of application of the method

**16D-1 EXAMPLE 1: Cylindrical shell with nozzle under internal pressure and external forces (See figure 16D-1).**

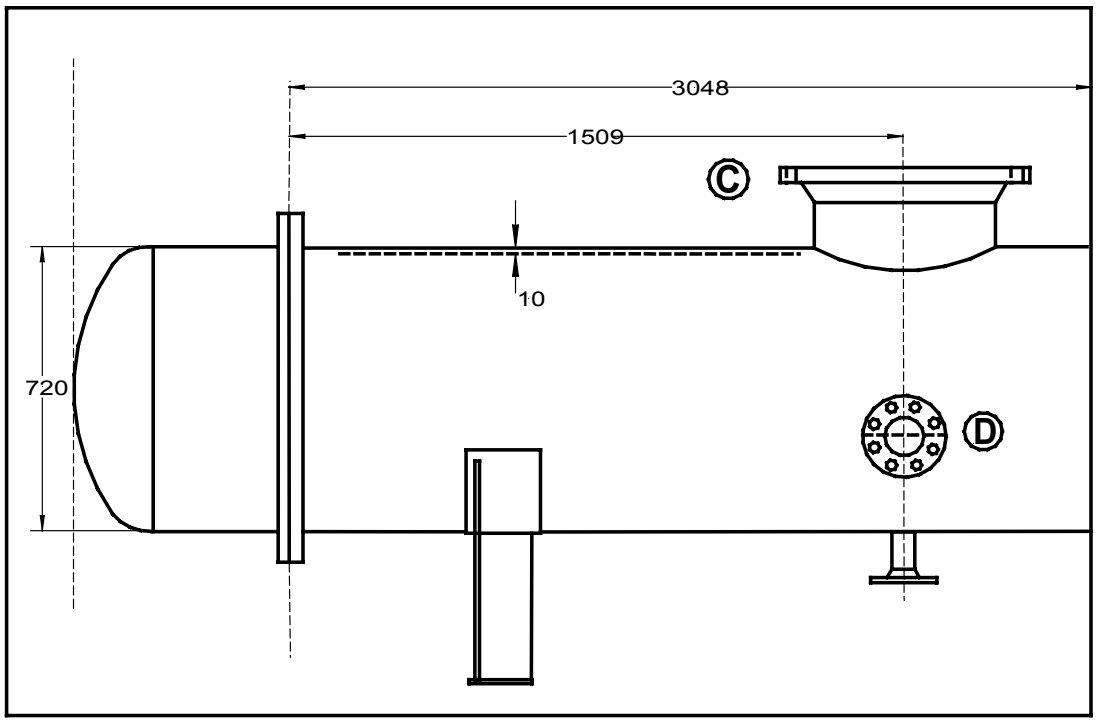


**Figure 16D-1: Cylindrical shell with nozzle C**

*16D-1a General data:*

**Design conditions:**

| Quantity | Symbol | Value | Unit | Paragraph of the standard/Remark |
|---|---|---|---|---|
| Testing group | | 1 | | See EN 13445-5 |
| Calculation temperature | $t$ | 150 | °C | |
| Calculation pressure (internal pressure) | $P$ | 0,9 | MPa | |
| Corrosion allowance at inside wall | $c$ | 1,0 | mm | |

**Materials:**

| Quantity | Symbol | Value | Unit | Reference |
|---|---|---|---|---|
| Steel grade for shell and nozzle C | | P265GH | | EN 10028-2 |
| Nominal design stress of shell | $f_s$ | 136,67 | MPa | |
| Nominal design stress of nozzle | $f_b$ | 136,67 | MPa | |

**Nozzle loads:**

| Quantity | Symbol | Value | Unit | Reference |
|---|---|---|---|---|
| Axial load | $F_z$ | 8000 | N | Clause 16<br>Figure 16.5-1 |
| Circumferential bending moment | $M_x$ | 6500 | N.m | |
| Longitudinal bending moment | $M_y$ | 0 | N.m | |
| Resulting nozzle moment | $M_b$ | 6500 | N.m | |

**Shell dimensions:**

| Quantity | Symbol | Value | Unit | Reference |
|---|---|---|---|---|
| Outside diameter | $D_e$ | 720,0 | mm | Clause 9 |
| Inside radius (as corroded) | $r_{is}$ | 351,0 | mm | |
| Mean diameter | $D$ | 711,0 | mm | |
| Actual thickness | $e_n$ | 10,0 | mm | |
| Analysis thickness | $e_a$ | 9,0 | mm | |
| Maximum length of shell contributing to opening reinforcement | $l_{so}$ | 79,99 | mm | Clause 9<br>Figure 9.5-2 |

**Nozzle dimensions:**

| Quantity | Symbol | Value | Unit | Reference of formula<br>Remark |
|---|---|---|---|---|
| Type of nozzle | | Flush nozzle | | |
| Outside diameter | $d_e$ | 457,0 | mm | |
| Actual nozzle thickness | | 10,0 | mm | |
| Analysis thickness | $e_b$ | 9,0 | mm | |
| Mean diameter | $d$ | 448 | mm | |
| Nozzle/shell weld leg size | | 0,0 | mm | Not taken into account |
| Actual length | $l_b$ | 150,0 | mm | |
| Length of nozzle contributing to reinforcement | $l_{bo}$ | 63,5 | mm | Clause 9<br>Formula (9.5-39) |

***16D-1b Results of computation:***

**Pressure load ratio:**

| Quantity | Symbol | Value | Unit | Reference/Remark |
|---|---|---|---|---|
| Shell stress loaded area | $Af_s$ | 800,9 | mm² | Clause 9<br>Formula (9.5-21) |
| Weld stress loaded area | $Af_w$ | 0 | mm² | Not taken into account |
| Nozzle stress loaded area | $Af_b$ | 571,5 | mm² | (9.5-42) |
| Pressure loaded area in shell | $Ap_s$ | 108281,3 | mm² | (9.5-23) |
| Pressure loaded area in nozzle | $Ap_b$ | 15913,3 | mm² | (9.5-45) |
| Distance | $a$ | 228,50 | mm | (9.5-26) |
| Allowable stress | $f_{ob}$ | 136,67 | MPa | (9.5-8) |
| Maximum pressure | $P_{max}$ | 1,502 | MPa | (9.5-10) |
| Pressure load ratio | $\Phi_P = \frac{P}{P_{max}}$ | 0,599 | - | Clause 16<br>Formula (16.5-9) |

**At edge of nozzle:**

| Quantity | Symbol | Value | Unit | Reference of formula Remark |
|---|---|---|---|---|
| Combined analysis thickness of the shell and reinforcing plate | $e_c = e_a$ | 9,00 | mm | No plate |
| Factor | $\lambda_C = \frac{d}{\sqrt{De_c}}$ | 5,600 | - | (16.5-1) |
| Factor | $\frac{e_a}{D}$ | 0,0127 | - | Applicability |
| Factor | $C_1$ | 5,848 | - | (16.5-4) |
| Allowable axial load | $F_{Z,max} = f\ e_c^2\ \max[C_1;1,81]$ | 64738 | N | (16.5-3) |
| Factor | $C_2$ | 7,124 | - | (16.5-6) |
| Allowable circumferential bending moment | $M_{X,max} = f \cdot e_c^2 \cdot \frac{d}{4} \cdot \max[C_2;4,90]$ | 8832 | N.m | (16.5-5) |
| Factor | $C_3$ | 31,321 | - | (16.5-8) |
| Allowable longitudinal moment | $M_{Y,max} = f \cdot e_c^2 \cdot \frac{d}{4} \cdot \max[C_3\ ;4,90]$ | 38833 | N.m | (16.5-7) |
| Axial load ratio | $\Phi_Z = \frac{F_Z}{F_{Z,max}}$ | 0,124 | - | (16.5-10) |
| Bending load ratio | $\Phi_B = \sqrt{\left(\frac{M_X}{M_{X,max}}\right)^2 + \left(\frac{M_Y}{M_{Y,max}}\right)^2}$ | 0,736 | - | (16.5-11) |
| Combined load ratio | $\sqrt{\left[\max\left(\left\lvert\frac{\Phi_P}{C_4} + \Phi_Z\right\rvert;\left\lvert\Phi_Z\right\rvert;\left\lvert\frac{\Phi_P}{C_4} - 0,2\,\Phi_Z\right\rvert\right)\right]^2 + \Phi_B^2} \leq$ | 0,994 | | (16.5-15) |

**Nozzle longitudinal instability check:**

| Quantity | Symbol | Value | Unit | Reference of formula Remark |
|---|---|---|---|---|
| Mean nozzle diameter | $d$ | 448,00 | mm | |
| Maximum longitudinal tensile stress | $\sigma$ | 16,41 | MPa | (16.5-26) |
| Elastic limit | $\sigma_e$ | 205,00 | MPa | Clause 8, paragraph 8.4 |
| E-modulus at temperature | $E$ | 203000,0 | MPa | |
| Ratio | $\frac{d}{e_b}$ | 49,777 | - | |
| Factor | $K$ | 24,071 | - | (16.14-15) |
| Ratio | $\frac{w}{l}$ | 0,010 | - | |
| Factor | $\alpha$ | 0,743 | - | (16.14-17) |
| Factor | $\Delta$ | 0,618 | - | (16.14-19) |
| Maximum allowable compressive stress | $\sigma_{c,all}$ | 126,68 | MPa | (16.14-20) |
| Instability load ratio | | 0,036 | - | (16.5-27) |

Since all load ratios are less than 1 the design is acceptable to EN 13445.

NOTE: Using the PD 5500 Annex G.2.2 calculation procedure one finds nearly identical results (max allowable values $F_Z$ = 8200 N and $M_B$ = 6990 N.m).

**16D-2 EXAMPLE 2: Cylindrical shell on 2 saddle supports (See figure 16D-2)**

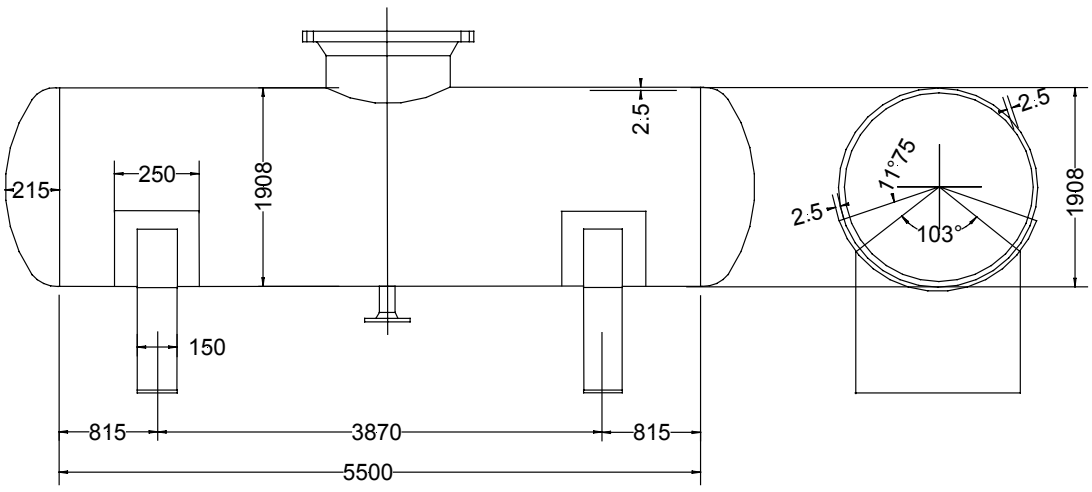


**Figure 16D-2: Cylindrical shell on 2 saddle supports**

***16D-2a General data***

**Design conditions:**

| Quantity | Symbol | Value | Unit | Remark |
|---|---|---|---|---|
| Testing group | | 1 | | See EN 13445-5 |
| Calculation temperature | $t$ | 50 | °C | |

| | | | | |
|---|---|---|---|---|
| Internal pressure at top level | | 0,1 | MPa | |
| Internal pressure at bottom level | | 0,119 | MPa | |
| Internal fluid density | $\rho$ | 1000,00 | Kg/m$^3$ | |
| Weld joint efficiency | $z$ | 1 | - | |
| Corrosion allowance at inside wall | $c$ | 0 | mm | |
| Wall tolerance | | 0,0 | mm | |

**Materials:**

| Quantity | Symbol | Value | Unit | Remark |
|---|---|---|---|---|
| Nominal design stress of shell and reinforcing plate | $f$ | 173,33 | MPa | X5CrNi18-10 Austenitic steel with rupture elongation > 35 % EN 10028-7 |
| Young's Modulus of shell and plate | $E$ | 193750 | MPa | |

**Shell dimensions:**

| Quantity | Symbol | Value | Unit | Remark |
|---|---|---|---|---|
| Outside diameter | $D_e$ | 1908,0 | mm | |
| Inside diameter | $D_i$ | 1903,0 | mm | |
| Corrosion allowance | $c$ | 0 | mm | |
| Length of cylindrical part | $L$ | 5500,0 | mm | |
| Inside depth of dished end | $H_i$ | 215,0 | mm | |
| Actual thickness | $e_n$ | 2,5 | mm | |
| Analysis thickness | $e_a$ | 2,5 | mm | |

**Saddle data:**

| Quantity | Symbol | Value | Unit | Remark |
|---|---|---|---|---|
| Saddle position | | type 'A' | | Vessel symmetrically on two saddles |
| Included angle of saddle | $\delta$ | 103,0 | degree | See figure 16.8-4 |
| Saddle width | $b_1$ | 150,0 | mm | See figure 16.8-4 |
| Distance to adjacent head | $a_1$ | 815,0 | mm | See figure 16.8-1 |
| Cantilever length | $a_3 = a_1 + \frac{2}{3} H_1$ | 958,3 | mm | See figure 16.8-1 |
| Distance between saddle centres | $l_1$ | 3870,0 | mm | See figure 16.8-1 |

**Reinforcing plate design data:**

| Quantity | Symbol | Value | Unit | Remark |
|---|---|---|---|---|
| Width of reinforcing plate | $b_2$ | 250,0 | mm | See figure 16.8-4 |

| | | | | |
|---|---|---|---|---|
| Critical width | $K_{11}D_i + 1{,}5b_1$ | 321,62 | mm | Equation (16.8-32) |
| Distance from saddle horn to reinforcing plate | $a_2$ | 195,00 | mm | See figure 16.8-4 |
| Included angle of reinforcing plate | $\delta_2$ | 126,50 | degree | See figure 16.8-4 |
| Thickness of reinforcing plate | $e_2$ | 2,50 | mm | See figure 16.8-4 |
| Combined effective thickness | $e_c$ | 3,54 | mm | Equation (16.8-35) |

***16D-2b Results of computation***

**Ratios and K-factors:**

| Quantity | Value | Equation |
|---|---|---|
| $L / D_i$ | 2,890 | |
| $D_i / e_a$ | 761,200 | |
| $K_2$ | 1,250 | |
| $K_{11}$ | 0,051 | (16.8-33) |
| $K_{12}$ | 1,456 | (16.8-12) |

Calculation case 1: width = $b_2$ angle = $\delta_2$ thickness = $e_a$

Calculation case 2: width = $b_1$ angle = $\delta$ thickness = $e_c$ (16.8-35)

| Quantity | Calculation case 1 | Calculation case 2 | Equation |
|---|---|---|---|
| $D_i / e_a$ | 761,2000 | 538,2497 | |
| $\beta$ | 3,2983 | 1,6641 | (16.8-16) |
| $\gamma$ | 0,0439 | 0,0522 | (16.8-15) |
| $K_3$ | 0,2500 | 0,2500 | (16.8-17) |
| $K_4$ | 0,3142 | 0,6115 | (16.8-18) |
| $K_5$ | 0,9338 | 1,1404 | (16.8-19) |
| $K_6$ | 0,2512 | 0,6367 | (16.8-20) |
| $K_7$ | 0,5608 | 0,8650 | (16.8-21) |
| $K_8$ | 0,1954 | 0,2761 | (16.8-22) |
| $K_9$ | 0,5814 | 0,5483 | (16.8-23) |
| $K_{10}$ | 0,3863 | 0,5912 | (16.8-24) |

**Determination of forces, moments and shear forces:**

| Quantity | Symbol | Value | Unit | Equation |
|---|---|---|---|---|
| Total weight of vessel | $W$ | 170000 | N | |
| Weight of content | $W_F$ | 161885 | N | |
| Load per unit vessel length | $q$ | 29,38 | N/mm | (16.8-1) |
| Edge moment | $M_0$ | 6331,9 | N.m | (16.8-2) |
| Vertical force at saddle i (saddle 1 or 2) | $F_i$ | 85000 | N | (16.8-3) |

| | | | | |
|---|---|---|---|---|
| Global bending moment at saddle i | $M_i$ | 7158,5 | N.m | (16.8-4) |
| Shear force at saddle i | $Q_i$ | 56846,2 | N | (16.8-5) |

**Allow compressive stress (vessel mid span):**

| Quantity | Symbol | Value | Unit | Equation or Clause |
|---|---|---|---|---|
| Assumed buckling | | 3870,0 | mm | |
| Ratio | $D/e_a$ | 761,200 | - | |
| Factor | $K$ | 1,831 | | (16.14-15) |
| Factor | $\alpha$ | 0,177 | | (16.14-16) |
| Ratio | $w/l$ | 0,020 | | |
| Factor | $\Delta$ | 0,162 | | (16.14-18) |
| Elastic limit stress | $\sigma_e$ | 168,000 | MPa | Clause 8, paragraph 8.4 |
| Maximum allowable | $\sigma_{c,all}$ | 27,218 | MPa | (16.14-20) |

**Shell stresses (between saddles):**

| Quantity | Symbol | Value | Unit | Equation or Clause |
|---|---|---|---|---|
| Moment between saddle 1 and 2 | $M_{12}$ | 47840 | N.m | (16.8-6) |
| Axial stress | $\sigma$ | 32,45 | MPa | (16.8-10) |
| Maximum allowable axial stress | $f_{max}$ | 173,33 | MPa | |
| Maximum allowable moment | $M_{max}$ | 194044 | N.m | (16.14-3) |

The design is satisfactory:

$\sigma \le f_{max}$

$|M_{12}| / M_{max} \le 1{,}0$

**Computation of allowable loads ($\sigma_{b,all}$ according to equation 16.6-6):**

Compute successively: $\upsilon_1, \upsilon_{21}, \upsilon_{22}, K_1, \sigma_{b,all}, F_2$ *or* $F_3$

| $\nu_1$ | $\nu_{2,1}$ | $\nu_{2,2}$ | $K_1$ | $\sigma_{b,all}$ | $F_2, F_3$ |
|---|---|---|---|---|---|
| - | - | - | - | MPa | kN |

a) Saddle 1: Calculation 1

| | | | | | | |
|---|---|---|---|---|---|---|
| Location 2 | -0,048 | -0,005 | 0,100 | 1,491 | 323,086 | 167,055 |
| Location 3 | -1,481 | 0,000 | 0,209 | 0,540 | 117,029 | 144,207 |

b) Saddle 1: Calculation 2

| | | | | | | |
|---|---|---|---|---|---|---|
| Location 2 | -0,142 | -0,003 | 0,071 | 1,436 | 311,088 | 221,503 |
| Location 3 | -1,477 | 0,000 | 0,148 | 0,541 | 117,273 | 109,169 |

ALLOWABLE LOAD $F_{2,max}$ = 167055 N (16.8-25)

ALLOWABLE LOAD $F_{3,\max}$ = 109169 N (16.8-26)

RESULTING ALLOWABLE LOAD = 109169 N (multiplication factor = 1,0 )

**Instability check (at saddles):**

| Quantity | Symbol | Value | Unit | Formula |
|---|---|---|---|---|
| Ratio | $L / R$ | 5,773 | - | |
| Equivalent axial force | $F_{\text{eq}}$ | 90389 | N | (16.8-29) |
| Ratio | $\lvert P \rvert / P_{\max}$ | 0 | | (8.4.2-5) |
| Maximum allowable axial force | $F_{\max}$ | 407334 | N | (16.14-2) |
| Ratio | $\lvert F_{\text{eq}} \rvert / F_{\max}$ | 0,2219 | | |
| Maximum allowable moment | $M_{\max}$ | 194044 | N.m | (16.14-3) |
| Ratio | $\lvert M \rvert / M_{\max}$ | 0,0369 | | |
| Maximum allowable | $Q_{\max}$ | 179183 | N | (16.8-30) |
| Ratio | $\left(\lvert Q \rvert / Q_{\max}\right)^2$ | 0,1006 | | |
| Summation load ratio | | 0,3594 | | |

The design is satisfactory according to EN 13445.

## 16E Validation of the method

The actual methods for dealing with non-pressure loads are based partially on simplified theoretical analyses and partially on existing standards. These standards, supported by the available experimental work have been used successfully for a long time.

The methods used in the EN13445 for the problem of non-pressure loads on nozzles in both spherical and cylindrical shells are new. Comparisons with other existing design methods, found in ref. [2, 3, 18] indicate that the new design method is less conservative than BS 5500. A comparison with WRCB 107 is difficult, as the effects of pressure are not considered in the latter method. If omitting the pressure it appears that the new method is more conservative than WRCB 107.

## 16F Conclusion

The European Design Code for dealing with the problem of external loads in combination with pressure provides a new set of rules. Generally those rules are based on limit analysis and as such a more consistent safety margin is obtained.

With regard to nozzles in cylindrical shells, the new method is considered conservative. Additional improvements could be obtained as soon as results of theoretical analyses and non-linear FE calculations become available.

## 16G Bibliography


[1] BS 5500: 1997 “Unfired fusion welded pressure vessels” British Standard

[2] WRCB 107 “Local Stresses in Spherical and Cylindrical Shells due to External Loadings” March 1979 by K.R. Whichman, A.G. Hopper and J.L. Mershon

[3] WRCB 297 “Local Stresses in Cylindrical Shells due to External Loadings on Nozzles - Supplement to WRCB No 107 (Revision 1) September 1987 by J.L. Mershon, K. Mokhtarian, G.V. Ranjan and E.C. Rodabaugh

[4] WRCB 34 “Computation of the Stresses from Local Loads in Spherical Vesseles or Pressure Vessel Heads” March 1957 by P.P. Bijlaard

[5] WRCB 49 “Stresses in a Spherical Vessel” April 1959 by P.P. Bijlaard

[6] WRCB 50 “Stresses in Spherical Vessels from Local Loads Transferred by a Pipe – Additional data on Stresses in Cylindrical Shells under Local Loading” May 1959 by P.P. Bijlaard

[7] WRCB 60 “Interpretive Commentary on the Application of Theory to Experimental Results” May 1960 by P.P. Bijlaard

[8] C.R. Steele “Reinforced Openings in Large Steel Pressure Vessels” Progress report submitted to PVRC, Shelltech May 15,1983

[9] ASME VIII Division 2: 1998 “Boiler & Pressure Vessel Code”

[10] Dr.-Ing. N. Kiesewetter, Dr.-Ing. Wölfel “Ermittlung der zulässigen Belastungen auf Stutzen in Behältern und Apparaten” Doc. 5 presented in subgroup “Local Loads” of CEN TC54 WG “C” 1994

[11] WRCB 90 “Stress Concentration Factors for the Stresses at Nozzle Intersections in Pressure Vessels” September 1963 by F.A. Leckie and R.K. Penny

[12] J. Decock “Reinforcement Method of Openings in Cylindrical Pressure Vessels Subjected to Internal Pressure” Report MT 104 WTCM-CRIF February 1975

[13] Dr.-Ing. Ziegenbalg G."Beanspruchung zylindrischer Apparatewandungen durch örtliche Lasten. Dissertation TU Dresden 1969

[14] Richtlinienkatalog Festigkeitsberechnungen (RKF) Behälter und Apparate, Teile 1 to 6

[15] TGL 32903/17 "Behälter und Apparate, Festigkeitsberechnung, Schalen bei Belastung durch Tragelemente" June 1982

[16] L.P. Zick “Stresses in Large Horizontal Cylindrical Pressure Vessels on Two Saddle Supports ” Welding Journal Research Supplement 30 (1951)

[17] Dr.-Ing. Wölfel “Horizontal Vessels on Ring Supports – Limit load calculations” Doc. 24 presented in subgroup “Local Loads” of CEN TC54 WG “C” April 1995

[18] AD-Merkblätter “Berechnung von Druckbehältern“

# 17 Simplified assessment of fatigue life

## 17A Introduction

In pressure vessel codes, assessment of fatigue loading is a matter for which generally only "extreme" solutions are given: on the one hand simplistic "exemption from fatigue analysis" conditions or "screening test" are proposed, which in most case are largely conservative, and on the other hand sophisticated rules for detailed fatigue analysis, which allow smaller conservatism but involve an important design effort due to the stress calculations and expertise they require.

The rules for simplified assessment of fatigue life aim to offer to users an intermediate approach, which does not require any stress analysis but nevertheless can give a good approximation of the fatigue life, with a reasonable safety margin.

The basic idea behind such rules is that the maximum stress in any component can be estimated knowing its actual thickness and the formula or rule which governs its design.

This idea has been applied in the (East) German rules TGL 32903/31 [1] based on the East European Standard N° 3648-82 of the Council for Mutual Economic Assistance (Comecon), and was improved and detailed in the RKF Catalogue [2]. In 1995, the AD code issued a revised version of AD-Merkblatt S1 "Simplified analysis for cyclic loading" [3] based on the TGL and RKF approach. The rules in clause 17 have been mainly based on these documents, with an adaptation to the context specific to EN13445-3, more particularly for consistency with the more general rules of clause 18 "Detailed assessment of fatigue life". Further to the CEN Enquiry on prEN13445, some input was also taken from the corresponding rules that had been issued in chapter C10.2 of CODAP [4] in the meantime.

As a consequence of their principle and implicit reference to Design by Formulas (DBF), all these rules cover only pressure loading. However provision has been made in clause 17 to make possible the consideration, in a conservative way, of additional thermal or external loads, the determination of the corresponding stresses being left to the user's responsibility (see 17.1.2).

## 17B Background of the simplified fatigue assessment approach

For assessing fatigue life at a potentially critical location in a vessel, two types of information have to be determined, whatever the method used, rough or refined:

– the stress (or strain) cycles, which characterise the loading action at the location under consideration,

– the fatigue strength of the material at same location.

Regarding *fatigue strength*, clauses 17 and 18 refer to same data and use basically the same rules:

- same distinction between welded and unwelded regions,
- same stress types used for fatigue assessment:
  - structural stress in welded details, together with the nominal stress on weld throat for fillet welds,
  - effective notch stress in unwelded regions,
- same classification of welded details,
- same set of fatigue curves for welds,

For details on all these aspects, see the paper by S. J. Maddox on clause 18.

The only significant difference between clauses 17 and 18 as regards characterisation of fatigue strength concerns the fatigue curve used for the unwelded regions, which is more conservative in clause 17 than in clause 18 (see 17B-2).

So, what is essentially different between simplified and detailed fatigue assessment is *stress evaluation*.

In the following, most of the comments are devoted to this subject, only a few of them being concerned with characterisation of fatigue resistance.

### 17B-1 Stress range estimate

In clause 17, the stress range $\Delta\sigma$ produced by a pressure fluctuation of range $\Delta P$ is given by:

$$\Delta\sigma = \frac{\Delta P}{P_{\max}} \cdot \eta \cdot f \qquad (17.6\text{-}1)$$

where: $\eta$ is the *stress factor* applicable to the vessel detail under study

$P_{\max}$ is the *maximum permissible pressure* of the component under consideration,

$f$ is the *nominal design stress* of the component, at calculation temperature.

This formula is based on the following:

– at the maximum permissible pressure $P_{\max}$, the maximum stress $\sigma_{\max}$ in the component is some multiple of the nominal design stress $f$. Let us designate this multiple by $\eta$. So we have:

$$\sigma_{\max} = \eta \cdot f$$

– for a pressure cycle between $P = 0$ and $P = P_{\max}$, the stress range $\Delta\sigma$ is then:

$$\Delta\sigma = \sigma_{\max} = \eta \cdot f$$

– for a different pressure variation, the corresponding stress range is now:

$$\Delta\sigma = \frac{\Delta P}{P_{\max}} \cdot \eta \cdot f$$

which is formula (17.6-1).

For application of that formula, $\Delta P$, $P_{\max}$ and $f$ are values that are known by the user. What is not know at first is the value of $\eta$. This is the central input clause 17 brings.

### *17B-1a Stress factors*

The stress factor $\eta$ is defined as an upper bound of the following ratio:

$$\frac{\text{maximum structural stress in detail under consideration under pressure } P_{max}}{\text{nominal design stress at calculation temperature}}$$

A "detail" may be a component, a region in a component or a junction between adjacent components. If a unique value $\eta$ is proposed for a detail, it must conservatively cover all possible geometrical configurations the design rule allows, as well as all possible critical points where the maximum stress may occur. Better, different $\eta$ values can in some cases be defined to cover different ranges of geometry or different locations within the detail.

The *structural stress* mentioned in the above ratio is defined as the stress determined using a stress-concentration-free model of the structure, i.e. a model which accounts for the global geometry of that structure but excludes the local discontinuities (notches). This type of stress is that which is naturally obtained when using plate or shell models, either through numerical or analytical calculations. According to these models, it has got a linear distribution across the thickness.

In welded joints, the notch effects associated to the weld profile at toes or surface irregularities are (statistically) included in the relevant fatigue curve. Therefore the stress increase due to the notches need not to be taken into account in the stress range.

In unwelded regions, whose fatigue curve does not include any notch effect, the stress range considered must be that of the *notch stress*; so when assessing unwelded regions, the stress range given by equation (17.6-1) shall be corrected with an appropriate stress concentration factor. The one used in clause 17 is $K_f$, the same *effective* stress concentration factor as used in clause 18.

The values of $\eta$ are listed in Table 17-1, together with their conditions of validity (if any). These values have got different origins. In a few simple cases, they can straightforwardly be deduced from the design formula(s) of the component, but more commonly they are based on structural analysis results available in the literature. Most of them were taken from TGL 32903/31 [1] or the RKF Catalogue [2]. Detailed information on their derivation can be found in the paper by B. Gorsitzke [5], which was published in support to the new version of AD-Merkblatt S1 [3] issued in 1995. Additional studies and calculations where performed by N. Kiesewetter when drafting EN13445-3, to complete the existing values or revise some of them for better adaptation to the EN13445-3 design rules. They are reported in CEN/TC54/WGC documents [6].

The structural stress that the factors $\eta$ reflect is supposed to be the *equivalent* structural stress, i.e. the stress calculated according to the Tresca or Von Mises criteria. This is the option used in the original German rules, and corresponds to the preference implicitly given to the equivalent stress option in clause 18 (the maximum principal stress option is also allowed in clause 18 but the associated tables for weld detail classification have been moved to an annex, Annex P).

Some stress factor values are specific to clause 17, due to different design rules in EN13445-3 compared to that in TGL, RKF or AD-Merkblatt, or due to some refinement EN13445-3 has brought in their determination. The details concerned are mainly the following:

- ***longitudinal and circumferential butt welds***

At these locations, the value of $\eta$ is the value which accounts for the true vessel shape, i.e. including the effect of the shape imperfections that may affect the stress at abutting walls: offset, ovality, and peaking. For conformity with clause 18, the corrections used have been adjusted to the values the general formulas of that clause give for calculation of the stresses due to shape imperfections (see 18.10.4). It must be noted that among these various types of imperfections, peaking is the most critical and results in a strong adverse influence on fatigue life of longitudinal welds; even when the tolerances are kept within the limits allowed in Part 4 the standard (see the comments on that point in S.J. Maddox's paper on clause 18).

Due to the presence of the weld joint coefficient $z$ in the design formulas for shells, the stress at seam welds is proportional to this coefficient and this must be accounted in the value of $\eta$. Its is the reason why $z$ has been introduced into the expression of the stress factors for seam welds.

- ***welded flat ends***

In EN13445-3, the design rule for welded flat ends requires that the shakedown criterion (stress limitation to $3f$) is fulfilled. As a consequence, the stress factor $\eta$ cannot exceed 3 at the shell-to-end junction. In the German rules, this criterion is not considered and the stress factor may reach highest values, up to 5.

It must be mentioned that in the amendments which are presently under study in TC54/WGC for next revision of EN13445-3, the possibility of designing welded flat ends with no consideration of shakedown will be made, under the condition that a simplified fatigue analysis is performed (the appropriate stress factor will be given). This will allow more economical design when possible.

- ***fillet welded junctions of components***

At such junctions, two types of fatigue cracking may occur:

– cracking from a weld toe: this is governed by the structural stresses at weld toes, whose maximum magnitude is normally accounted for in the applicable stress factor $\eta$;

– cracking from weld root: this is governed by the stress on the weld throat, which directly depends on the weld throat dimension (whereas the stresses at weld toes are only slightly influenced by the weld throat size). The problem is that no stress factors are presently available to account for this type of stress at the various junctions of components that can be found in pressure vessels. Only an empirical rule has been proposed, in general welded construction, to avoid cracking from weld root. It says that this type of cracking is not determinant in comparison with cracking from weld toe if the following condition is met:

$$a \geq 0{,}8\, e_{\min}$$

where:

$a$ is the weld throat size,

$e_{\min}$ is the thickness of the thinner connected plate.

Although not proved, this assumption has been considered as acceptable for vessels under pressure loading, at least as a provisional rule for solving the problem in the context of clause 17. On that basis, the following reasoning has been made to establish stress factors values representing the stress on weld throat:

– When a weld throat exactly meets the above condition, i.e. when $a = 0{,}8\, e_{\min}$, then the fatigue damage due to any given pressure cycle should be the same for both types of cracking. Knowing, that according to both clauses 17 and 18, the fatigue classes associated to weld toe cracking in fillet welds and root cracking are 63 and 32 respectively, the following equation holds for that case:

$$\frac{\eta_{\text{throat stress}}}{\eta} = \frac{32}{63} \qquad \text{which gives} \qquad \eta_{\text{throat stress}} = \frac{32}{63} \cdot \eta$$

where $\eta$ (the structural stress factor known for the detail) is supposed to reflect the maximum structural stress at weld toes.

– When the condition $a \geq 0{,}8\, e_{\min}$ is not met, at least $a \geq 0{,}7\, e_{\min}$ holds, due to the requirements for minimum weld size given in Annex A (Design of welded joints) or in Part 4 (Fabrication) of EN13445. Therefore when a fillet weld has got this minimum throat size, the corresponding throat stress factor has the value:

$$\eta_{\text{throat stress}} = \frac{0{,}8}{0{,}7} \frac{32}{63} \cdot \eta \quad \text{or} \qquad \eta_{\text{throat stress}} \approx 0{,}6 \cdot \eta$$

This last equation allows defining a throat stress factor when knowing the "normal" stress factor (structural stress factor) applicable to the weld detail.

Although these two stress factors have a fixed ratio, it is not possible to know in advance which of them will govern the fatigue assessment for a given weld, because the maximum permissible pressure $P_{\max}$ to be used with each of them is not the same. This is because the weld throat size depends on the thickness of the thinner connected component (through the rule $a \geq 0{,}7\, e_{\min}$) and not on the strength of the detail under consideration as a whole. Therefore the appropriate value of $P_{\max}$ to be used with $\eta_{\text{throat stress}}$ is that of the vessel wall of thickness $e_{\min}$, not that of the detail as a whole.

Consequently, two fatigue checks are asked for in clause 17 for fillet welded details having welds with $a \leq 0{,}8\,e_{\min}$ :

- one with $\eta$ associated with the value $P_{\max}$ of the detail as a whole (e.g. an opening, a flat end-to-shell junction, etc…), as for any other vessel detail;
- one with $\eta_{\text{throat stress}}$ associated to the value $P_{\max}$ of the wall of thickness $e_{\min}$ (e.g. nozzle wall or shell wall at an opening, shell wall at a flat end-to-shell junction).

The more penalising result must be retained for fatigue assessment.

In practice, the specific notation $\eta_{\text{throat stress}}$ has not been introduced in clause 17. In Table 17-1, the details for which the double calculation has to be made are those where the box which gives the stress factor is divided into two sub-boxes by a dotted line. The upper sub-box gives the $\eta$ value based on structural stress, and the lower one gives the $\eta$ value based on throat stress. The requirement about the need of a double check is given in note 8) to that table.

***17B-1b Maximum permissible pressure***

According to its general definition (given in clause 3), $P_{\max}$ is to be determined using the *analysis* thickness of the component or detail (in the corroded condition), i.e. the thickness which includes the existing extra-thickness present in the component or detail, if any.

This determination is straightforward when a formula for $P_{\max}$ is given in the design rule of the component/detail under consideration. When no formula is given (because no close-form expression can be proposed for $P_{\max}$), then iterative calculations are needed to get $P_{\max}$. For sake of simplicity, clause 17 allows in all cases the use of the calculation pressure $P$ instead of $P_{\max}$, because always conservative.

As a rule, $\eta$ is calculated for *internal pressure* with the pre-supposition that the design of the component is governed by gross plastic deformation. In cases where the design is governed by instability (which may be the case for thin dished ends under internal pressure, shells under external pressure), the allowable pressure is lower than it would be if gross plastic deformation only (which is controlled by the nominal design stress $f$) were considered. Application of equation (17.6-1) with $P_{\max}$ derived from an instability condition would then result in a higher $\Delta\sigma$, although the stresses in the component are lower than they would be if this component were designed by gross plastic deformation. This is obviously wrong. In such cases, the correct way to apply equation (17.6-1) is to consider the $P_{\max}$ value determined ignoring the instability criterion. For dished ends, this is specified by note 7) in Table 17-1[(1)].

In some cases, e.g. at junctions, there may be a doubt about the design formula to be referred to for calculation of $P_{\max}$. So Table 17-1 gives for each case the relevant equation or design procedure that must be used.

***17B-1c Nominal design stress***

When calculating the stress range $\Delta\sigma$ for a detail whose design rule involves only one value of $f$, equation (17.6-1) gives a result which is in fact independent from the particular value assumed for $f$, because $P_{\max}$ is always proportional to the value assumed. In other words, the ratio $\dfrac{f}{P_{\max}}$ does not depend on $f$, and consequently neither depends on the design temperature nor on the material. This is logical and reflects the fact that, for a given loading, the stresses in any structure are only dependent on the geometry of the structure, not on the resistance of the material (as far as elastic behaviour is concerned).

However 17.6.1.1 states that $f$ shall be taken at calculation temperature. This is only a practical rule which ensures that $f$ and $P_{\max}$ do correspond in equation (17.6-1).

---

(1) No such note is necessary to cover the case of shells under external pressure. The correct determination of $P_{\max}$ is always obtained using Table 17-1, because it makes reference to the equations for internal pressure design only.

When more than one value of $f$ are involved in the design rule of the detail, then $P_{max}$ becomes dependent on the various $f$ values, and there is no particular ratio $\frac{f}{P_{max}}$ which represents correctly the stress level in the detail. In that case, the only correct way to apply equation (17.6-1) is to use an arbitrary and unique value of $f$ for all parts of the detail, and derive the corresponding pressure $P_{max}$. This is mentioned in 17.6.1.1. For users who would not like to perform this fictitious calculation and would only use the more "normal" $P_{max}$ value based on real nominal design stresses, then the highest value of $f$ among the different parts shall be used, to ensure conservatism.

***17B-1d Plasticity correction***

Whenever the stress range $\Delta\sigma$ calculated according to equation (17.6-1) remains below the shakedown limit $3f$, elastic cycling is ensured after a few first cycles. When the shakedown limit is exceeded, then elastic-plastic conditions occur and the proportionality between stress and strain is lost. In that case $\Delta\sigma$ does not represent any longer the real strain range the material endures. To account for this effect, $\Delta\sigma$ shall be multiplied by the plastic correction factor $K_e$ defined in clause 18.

In practice, no detail having a stress factor $\eta \leq 3$ may be concerned by this correction, because the pressure range can never exceed the design pressure, resulting in a $\frac{\Delta P}{P_{max}}$ ratio never higher than 1[(2)]. For the details having a stress factor $\eta > 3$ (e.g. nozzles with reinforcing plate, possibly longitudinal welds with peaking imperfection), the plastic correction will generally apply for full pressure cycles, except if extra thickness is enough to increases $P_{max}$ to a level that can compensate the high value of $\eta$.

**17B-2 Fatigue curves and fatigue corrections**

As already mentioned, the fatigue curves used in clause 17 for welded joints are the same as in clause 18. Their background and derivation is explained in the paper on that clause.

The situation is different for unwelded regions. In Clause 18, the fatigue curve for an unwelded region depends on the tensile strength $R_m$ of the material, and four different corrections factors have to be applied to account for conditions different from those the fatigue curve covers: temperature (if > 100°C), thickness (if > 25mm), mean stress (if ≠ 0), surface finish (if the roughness $R_z$ is > 6μm). Moreover, the last three corrections depend on the allowable number of cycles. This makes the rules complex, and for application to clause 17 some simplification was deemed necessary.

So, for unwelded regions, it was decided to base the fatigue curve on the lowest $R_m$ value among all steel grades of EN10028-2 (i.e. P235GH), and to incorporate in this curve the maximum possible mean stress correction together with the surface finish correction based on rolled or extruded condition. The resulting curve is therefore a lower bound of the results that can be obtained with clause 18, and ensures a full consistency with detailed fatigue analysis.

A less conservative solution would have been to incorporate the corrections as explained above but in different curves for different values of $R_m$, to reduce conservatism. Such an improvement should be considered for a future revision of clause 17.

As regards the other corrections, that for temperature is the same as in clause 18, whereas that for thickness has also been simplified with respect to clause 18: the correction specific to the unwelded regions has been waved, so that the correction defined for welded regions applies to all regions.

---

(2) Nevertheless, this may not be true if the pressure fluctuation occurs between a positive pressure and a negative pressure (vacuum). In this case, the ratio $\frac{\Delta P}{P_{max}}$ may exceed 1.

### 17B-3 Weld details classification

According to general philosophy of clause 17 and meaning of the stress factor $\eta$ (see *17B-1a* above), the tables which give the weld details classification in clause 17 are the same as those given in clause 18 for fatigue assessment using the equivalent stress option.

Only a few changes had to be brought to them:

- the (few) cases showing unwelded details, e.g. crotch corner of openings with nozzles, were deleted, because no option for assessing unwelded regions with the fatigue class concept is made in clause 17.
- for attachments, the only classification given is that to be used with structural stress. The option for use of nominal stress which is permitted in clause 18 is not consistent with use of stress factor and then is not proposed in clause 17.
- class 32, which is to be used in conjunction with the stress on weld throat to assess fatigue failure from weld root in fillet welds, is never mentioned. This failure mode is dealt with through the double calculation required for fillet welded details, as explained in 17B-1a, third bullet point.

## 17C Conditions of applicability – Relation to inspection

The simplified fatigue analysis approach has been developed mainly to allow fatigue life assessment for vessels designed using the DBF rules of the Standard. Nevertheless its use is also permitted for assessment of vessel details designed via the DBA rules of Annex B or C, provided the stress range estimate given by equation (17.6-1) is replaced by the true stresses resulting from a detailed stress analysis.

Regarding inspection requirements and allowable defects, the conditions required in clause 17 are the same as in clause 18:

- restriction to testing groups 1,2 and 3 only. This is justified by the absence of requirements for NDT of welds other than visual inspection in testing group 4. Without NDT, embedded defects as well as undetected surface breaking defects or flaws may exist in welds, making the reference fatigue curves non relevant.
- mandatory application of Annex G of Part 5, which defines the additional prescriptions to be followed for vessels subject to cyclic loads. These prescriptions concern only the *critical areas*. These areas are defined (in both clauses 17 and 18) as those where the damage index $D$ $(= \sum \frac{n_i}{N_i})$ exceeds a given value $D_{max}$, which is a function of the cycle range in which the loading cycles act (low, medium or high cycle range):

  $D_{max} = 0{,}8$ for $500 < n_{eq} \leq 1\,000$

  $D_{max} = 0{,}5$ for $1\,000 < n_{eq} \leq 10\,000$

  $D_{max} = 0{,}3$ for $n_{eq} > 10\,000$

  where $n_{eq}$ is the number of equivalent full pressure cycles, defined in clause 5.

  The decrease of $D_{max}$ with increasing $n_{eq}$ accounts for the larger scatter the fatigue results exhibit at higher number of cycles.

## 17D Future developments

Examination of Table 17-1 shows that stress factors are missing for some vessel details, e.g. tubesheet-to-shell, tubesheet-to-channel and tubesheet-to-tube junctions, flange-to-crown junction in bolted domed ends, some types of jacket-to-shell junctions... Others have been set provisionally to very rough estimates, e.g. joggle joints, cylindrical shells at stiffening rings, set-in and set-on pads. One can imagine that more accurate factors could also be derived for the important case of openings, for which only a fixed value (3 or 4) is proposed.

May be not all these details can easily be assessed through simplified fatigue analysis, but surely additional solutions can be expected to cover more of them or get improved stress factors.

Progress on these points is not possible without further technical studies. Up to now they have not been placed in the list of work-items that CEN/TC54 intends to consider in a near future.

## 17E Concluding remark

Yet called "simplified", the fatigue assessment rules given in clause 17 may finally appear as rather complex to apply, even if simple in their principle. This may particularly be the opinion of a user who would like to limit conservatism to the minimum. With that respect, one important good practise is to avoid using the calculation pressure $P$ of the component instead of its maximum permissible pressure $P_{max}$, as permitted by the rules for easiness. But when doing so, the user must go through all $P_{max}$ calculations, which are iterative in a number of cases.

So it must be understood that practical application of clause 17 should preferably be made through dedicated software. The corresponding calculation sequences can easily be added to any computer programme which already handles the design rules of EN13445-3. Additional input from the user is then limited to the definition of the applied stress cycles, and to the fatigue class applicable to each welded details. With such well adapted tools, simplified fatigue assessment may become an easy task to perform.

## 17F Bibliography


[1] TGL 32903/31 – Behälter und Apparate. Festigkeitsberechnung. Ermüdung bei zyklischer Belastung. Ausgabe 1983.

[2] Richtlinienkatalog Festigkeitsberechnungen (RKF), Behälter und Apparate, Teil 5 und 6 – Ausgabe 1986, Linde-KCA-Dresden GmbH.

[3] AD-Merkblatt S1: Simplified analysis for fatigue loading, AD 2000 Code, issued by VdTÜV, Carl Heymanns Verlag.

[4] CODAP – French code for construction of unfired pressure vessels, edition 2000. - SNCT Publications

[5] Erläuterungen zum neuen AD-Merkblatt S1 "Vereinfachte Berechnung auf Wechselbeanspruchung" und ergänzende Hinweise, B. Gorsitzke, Z. TÜ 37 (1996) N° 6 (Teil 1) & N°7/8 (Teil 2).

[6] CEN/TC54/WGC Working documents N° 328 (July 1995), 361 (February 1996) and 376 (March 1996).


# 18 Detailed assessment of fatigue life

## 18A Introduction

Fatigue failures are comparatively rare in pressure vessels, as compared with most other structures subjected to fluctuating loading. However, the avoidance of fatigue is still an important design criterion and the fatigue design rules occupy around one sixth of Section 3 in EN 13445.

In common with other pressure vessel design rules, EN 13445 provides a 'screening test' to enable further fatigue analysis to be avoided, based on the limit of 500 to the number of pressure cycles expected during the design life of the vessel. If there are any sources of cyclic loading other than pressure, then either the simplified fatigue assessment procedure of Chapter 17 or the detailed procedure of Chapter 18 must be applied. The simplified procedure is based on assumptions about the loading, resulting stresses and fatigue resistance. The detailed fatigue analysis procedure is more comprehensive and adaptable. The background to this procedure is the subject of the present paper.

The overall aim of this paper is to describe the procedure laid down in Chapter 18, its background and, where appropriate, to compare and contrast it with the rules in other Standards, particularly ASME VIII (1) , BS PD 5500 (2) and AD-Merkblatt (3) since these have been the main source of material used in drafting the European Standard. Validation of the new rules is discussed by reference to available experimental data and areas of the rules needing improved or new guidance are highlighted. Initially, general aspects of the rules are discussed and then attention is focused on the specific assessment of weld details, plain material and bolting.

## 18B Development of fatigue design rules for pressure vessels

For many years all pressure vessel fatigue design rules followed the approach originally introduced by ASME in the early 1960s (4). They are based on the concept that the fatigue life of any component or structure can be estimated from the S-N curve for the material concerned, as obtained from fatigue tests on small polished specimens, by applying an appropriate fatigue strength reduction factor ($K_f$).

Initially, the design curves were obtained from low-cycle fatigue tests conducted under strain control and they covered lives up to only $10^6$ cycles. Later, they were extended to very long lives $10^{11}$ cycles, presumably to enable potential fatigue damage from vibration to be assessed. Even so, the overall design approach is clearly directed mainly at high-strain low-cycle fatigue conditions. Furthermore, little attention is paid to weld details as sources of fatigue, implying that non-welded features, such as crotch corners in nozzles, are expected to be the most critical locations.

It was this aspect of the ASME rules that, in the 1980s, led to a major departure from the approach used in their fatigue rules in BS 5500, the British Standard for the design of welded pressure vessels at that time (5). In particular, it was recognised that the original ASME concept, that the plain material S-N curve can be simply factored to produce a design curve for a structural detail, is not applicable to weld details (5,6). Consequently, completely different design data were provided for assessing weld details and plain material, with the former based on those developed for designing other welded structures (notably bridges and offshore structures). Subsequently, similar rules were adopted by AD-Merkblatt and CODAP, and finally also for EN 13445.

The data used to derive the design curves for weld details relate more to high-cycle than low-cycle fatigue, but sufficient data are available to confirm that they can be extrapolated into the low-cycle regime (7), as illustrated in Fig.18B-1. A condition is that shakedown occurs such that the highly-strained region under consideration is constrained by the surrounding elastic material to cycle under strain control. Then, strains can be expressed as pseudo-elastic stresses to achieve continuity from the high-cycle to the low-cycle regime. Limited experimental data indicate that the S-N curve eventually becomes horizontal at very low endurances, less than 1000 cycles, at stress ranges of the order of twice the material's yield strength. Thus, the curves should be used with caution in this regime.

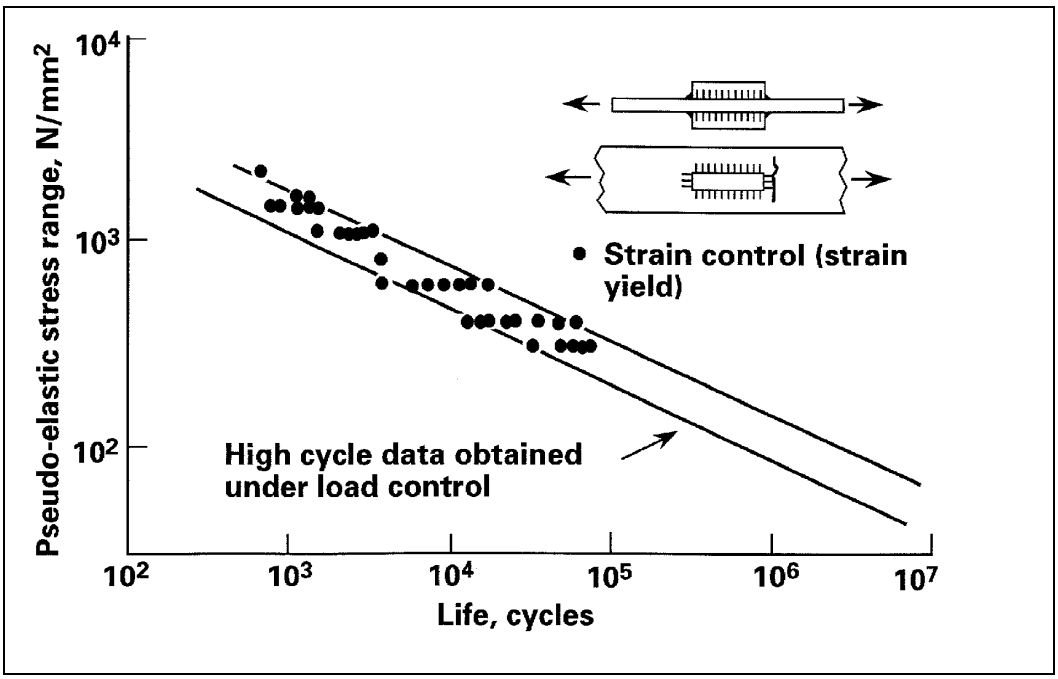


**Figure 18B-1 Low-cycle fatigue test results obtained under strain control from steel plate with longitudinal fillet welded attachments (7) compared with scatterband enclosing high-cycle fatigue data for the same weld detail.**

## 18C Fatigue design in EN 13445

### 18C-1 Basic method

As with all other major design Standards (8), fatigue design in EN 13445 is based on S-N curves used in conjunction with Miner's rule to sum the cumulative damage due to the various stresses expected to arise in service. The rules are presented in such a way that the user is expected to consider any detail or feature of the vessel that could act as a site for fatigue cracking and then ensure that it has sufficient fatigue resistance to survive the required design life. Thus, typical steps in an assessment are:

- Identify all potential sites for fatigue and undertake an assessment for each site

- Identify all sources of fatigue loading at that site and the corresponding stress history
- Determine the cyclic stress ranges ($\Delta\sigma_1$, $\Delta\sigma_2$,… $\Delta\sigma_i$) from an analysis of the stress history
- Determine the numbers of times ($n_i$) each stress range occurs.
- Deduce the limiting number of fatigue cycles ($N_i$) for each stress range from the design S-*N* curve
- Calculate the fatigue damage from each stress range ($n_i/N_i$)
- Sum the fatigue damage and compare it with the damage that could cause failure to ensure that:

$$\frac{n_1}{N_1}+\frac{n_2}{N_2}+\frac{n_3}{N_3}+\text{etc.}=\sum\frac{n}{N}\le 1 \text{ at the end of the required life}$$

The Standard provides S-N curves for plain and welded steel, and for bolting, with instruction on how to use them.

### 18C-2 Derivation of Design Curves

The S-N curves in EN 13445 are based on lower bounds to fatigue test results obtained from relevant test specimens. However, the method used to derive the design curves for assessing weld details and bolting was different from that used to derive the curves for plain material. In common with ASME, the curves for assessing plain steel were obtained by applying selected safety factors to the mean curves fitted to the test data (9,10). These factors were 1.5 on stress or 10 on life, compared with 2 on stress and 20 on life in the case of the ASME design curves. This approach results in curves that are non-linear even on a log-log basis, and the probability of survival they embody is unknown.

In contrast, the design curves for assessing weld details and bolting relate to statistical lower bounds to test data representing known probabilities of survival (11,12). Mean S-N curves were fitted to each dataset by the method of least squares, assuming a linear relationship between log (stress range, S) and log (life, N) and taking log N as the dependent variable. The resulting standard deviation of log N (SD) was then used to establish a design S-N curve, set some number of standard deviations below the mean curve. This approach is more in keeping with the design data in most modern fatigue design rules than the use of arbitrary safety factors. In the case of EN 13445, the design curves are based on the mean - 3 SD curves, corresponding to 99.8% probability of survival. The corresponding ASME curves are still based on the application of safety factors. The probability of survival adopted for EN 13445 is higher than that embodied in most design rules for structures, including BS PD 5500, where the mean - 2 SD curves, corresponding to 97.8% probability of survival, is more widely adopted (8).

### 18C-3 Material

At present, EN 13445 covers only steels, both ferritic and austenitic, although there are plans to extend it to cover aluminium alloys as well. In comparison some of the other codes also cover nickel, copper and aluminium alloys. However, there is no doubt that the main background information in all cases comes from fatigue testing of steels, mainly ferritic.

Apart from the material type, there might also be the need to consider the material's tensile strength. This is the case in EN 13445 in the assessment of plain steel and bolting, the basic assumption being that fatigue strength increases with increase in tensile strength. However, no such distinction is drawn in the assessment of weld details, as in most other fatigue design rules. This represents a major difference between the American and European codes for welded pressure vessels. It has been known for decades that the fatigue performance of a weld detail is not related to the S-N curve for the parent metal obtained from tests on small polished specimens by a simple fatigue strength reduction factor, as assumed by ASME (13,14). Indeed, such an assumption can be very misleading and result in unsafe fatigue life estimates for weld details, notably because it infers a beneficial effect of increased tensile strength when in fact no such benefit actually exists (5,6). The fundamental problem is that the fatigue life of the polished specimen is dominated by fatigue crack initiation process, whereas that in most weld details is dominated by fatigue crack growth from some pre-existing discontinuity, such as the minute intrusions that the welding operation leaves at the weld toe (14-16). The number of cycles needed to initiate a fatigue crack generally increases with increase in tensile strength. However, the rate of growth of the fatigue crack is independent of material tensile strength. Thus, observations of fatigue behaviour made using polished specimens can be very misleading when applied to situations where the fatigue life is dominated by crack growth, as in welded structures. Consequently, in common with most other design rules for welded structures (8), the European pressure vessel rules are based on fatigue test results obtained from actual welded specimens.

### 18C-4 Environment

In common with all other pressure vessel rules, EN 13445 requires correction of the design curves for operation at elevated temperature. Rather similar values are also given for the upper limit temperatures to which the rules apply, all below the creep regime. However, this is achieved simply on the basis of the reduction in elastic modulus in the ASME and BS rules. Higher factors, consistent with AD-Merkblatt and resulting in larger reductions in the design curves, are required by EN 13445, as illustrated in Fig.18C-1. It is understood that the basis of the AD-Merkblatt factor is fatigue test results obtained from plain polished specimens at various temperatures (9,10,). Other data more relevant to weld details, bolting and severely-notched components, including fatigue crack growth data, support the less severe elastic modulus based correction factor (17).

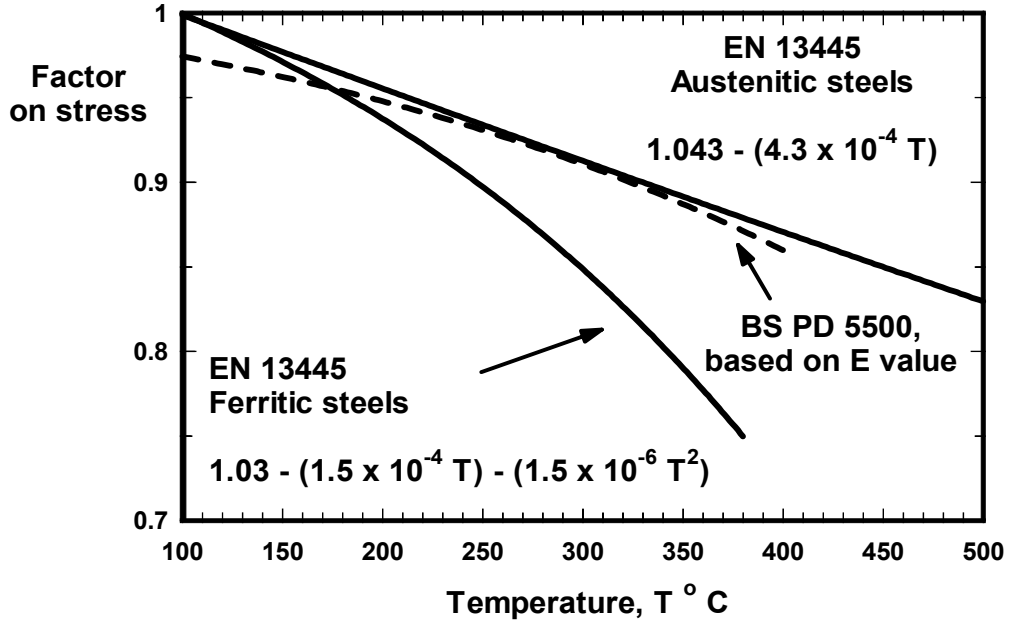


**Figure 18C-1 Comparison of temperature correction factors in EN 13445 and BS PD 5500.**

Although all the pressure vessel codes draw attention to the deleterious effect of a corrosive environment, none of them provides specific design data. Practical guidance from BS PD 5500 on the operation of vessels in corrosive conditions has been included in EN 13445, but the only specific guidance is reference to the need to maintain the magnetite layer in water conducting parts in non-austenitic materials at elevated temperature.

### 18C-5 Section Thickness

In line with most other modern fatigue design rules, EN 13445 recognises that fatigue strength tends to decrease with increasing section thickness, especially in the case of weld details. A size effect in fatigue resistance can be expected from statistical considerations, the larger the structure the greater the chance that a severe flaw will be encountered. However, more significant is the fact that a fatigue crack that is propagating through the section thickness from a surface stress concentration, notably from the toe of a weld, is affected by that stress concentration to a greater depth in a thick section than a thin one (14,18) Thus, correction factors are applied to the design curves when the section thickness exceeds a specified reference value. This reference value is usually the maximum thickness of the specimens used to generate the fatigue data used to derive the design curve, which is typically 12 to 25mm. The value specified in EN 13445 is 25mm, compared with 22mm in BS PD 5500. ASME requires no such correction.

### 18C-6 Stresses Used in Fatigue Design

A particular effort was made in EN 13445 to include clear descriptions of the stresses to be used in fatigue assessments. Principal stresses are the basis, the full stress range being used in any assessment. The use of the full stress range contrasts with the 'traditional' approach originating from the ASME of designing pressure

vessels on the basis of the stress amplitude, which is half the range. Most assessments are performed using the structural stress, defined as the 'linearly distributed stress across the section thickness that arises from applied loads and the corresponding reaction of the particular structural part'. Thus, it includes all stress concentration effects, such as those due to nozzles, vessel/end junctions or misalignment due to deviations from design shape, but not the notch effect of local structural discontinuities that give rise to non-linear stress distributions. The exception is if the applied loading produces a non-linear stress distribution, as can be the case with thermal loads. Then, to be conservative the total stress is used instead. In practice, the regions most likely to need a fatigue assessment will be on the surface of the vessel or component, in which case it is the value of the structural or total stress on the surface that is used in the fatigue assessment.

In some cases, including the assessment of bolting and some weld details, the nominal stress on the relevant section is used instead of the structural stress.

In common with ASME and most other pressure vessel design rules, in general assessments are based on an equivalent stress, calculated from the principal stresses. Any examples given in the code use the Tresca equivalent stress, but use of the von Mises stress is permitted. However, as discussed later, there can be advantages in using principal stresses directly and, as in BS PD 5500, this is an option in EN 13445.

### 18C-7 Mean stress

A mean stress correction is applied to the design curves for plain steel, in line with the effect of mean stress seen in fatigue tests on plain polished specimens (9,10). However, as is usually the case with fatigue design rules for welded structures (8), there is no need to take account of the applied mean stress when assessing weld details, even if the stress range is partly compressive. In the context of high-cycle fatigue, at stress levels below yield, this reflects the presence of high tensile residual stresses due to welding or assembly. These result in high effective tensile mean stresses regardless of the applied value (13). However, even in the absence of residual stress, applied mean stress is irrelevant if the loading conditions give rise to strain cycling above yield (low-cycle fatigue conditions). In the case of bolting, the design S-N curve is based on test data obtained at high tensile mean stresses (12) and therefore, again, there is no need to take operating mean stress into account.

### 18C-8 Complex Loading

Essentially the same guidance on the derivation of the required stress amplitude or range for multi-axial or combined loading is given in all the main pressure vessel codes. There is very little experimental evidence to validate the methods specified. Indeed, recent research has shown that although the method for considering proportional loading, when the principal stress directions remain constant throughout the loading cycle, seems to be acceptable, that for considering non-proportional loading, where the principal stress direction changes during a cycle, can be unsafe (19,20). Alternative design methods are being developed and revision to the codes is likely in future.

### 18C-9 Elastic-Plastic Conditions

As noted earlier, there is some evidence to indicate that shakedown is unlikely to occur if the cyclic stress range exceed twice yield, and the S-N curve becomes horizontal. EN 13445 includes a correction to be applied to the estimated stress, which effectively lowers the design curve, if the range exceeds twice yield. The same correction procedure has been adopted in BS PD 5500, but a different procedure is given in ASME. References 9, 10, 21 and 22 provide some background to these procedures, but there is still some doubt about their general applicability and they are likely to be reviewed in future.

### 18C-10 Cumulative Damage Calculations

As noted earlier, Miner's rule is the recommended approach for assessing the fatigue damage introduced under variable amplitude loading. An important step in applying this approach is conversion of the service stress history into recognisable cycles that can be compared with the design S-N curve. This is the process of cycle counting and the most widely used methods are 'Rainflow' or 'Reservoir' counting. EN 13445 provides guidance on the use of the Reservoir cycle counting method, which is also included in BS PD 5500 and other British Standards.

Like BS PD 5500, EN 13445 acknowledges the need to modify the design S-N curve in the high-cycle regime when performing cumulative damage calculations. This is to allow for the fact that stresses below the original constant amplitude fatigue limit (CAFL) become damaging once a fatigue crack has initiated under higher stresses in the spectrum. The commonly used approach, originally proposed by Haibach (23), of extrapolating the S-N curve beyond the fatigue limit at a shallower slope is adopted. EN 13445 then introduces an absolute cut-off fatigue limit for any loading conditions at stress ranges corresponding to $N$=$10^8$ cycles. Other Standards

are less precise about extrapolation of the curve beyond this endurance, but in practice this regime is only significant for very high-cycle fatigue situations, for example when vibrations could give rise to $10^{10}$ or more cycles. Since the ASME curves do not include a sharp cut off at the fatigue limit, in a sense they are already suitable for cumulative damage calculations.

It should be mentioned that there is now an extensive body of experimental data that throw doubt on the validity of Miner's rule and the method of allowing for the damaging effect of stress ranges below the fatigue limit (24). Clearly the latter is particularly relevant to high-cycle fatigue and may, therefore, be irrelevant for many pressure vessel assessments. However, the former is not restricted to any particular regime and so could be relevant to pressure vessel design. Present indications are that lives can be over-estimated by a factor of around two using Miner's rule (24,25). This is the subject of some research projects and revisions to the current cumulative damage approach may be introduced in future.

## 18D Fatigue assesment of weld details

### 18D-1 Design S-N Curves

EN 13445 offers very detailed rules for assessing weld details, reflecting the view that most vessels will be welded and the weld details will tend to be the most critical locations for potential fatigue cracking. In contrast, ASME provides very little guidance on the assessment of welds, recommending just one value of the fatigue strength reduction factor, namely 4 for fillet welds.

Eurocode 3 (26) and the IIW fatigue design recommendations (27) were the basis of the EN 13445 S-N curves for weld details. These were both developed largely on the basis of UK rules (8,24) and hence there are similarities with BS PD 5500. The design S-N curves were based on fatigue test data obtained from tests on actual welded joints (11,12). The specimens were mainly made from steel plate or I-section beams, typically 10 to 25mm thick, tested under either axial, or in the case of beams, bending. The criterion of failure in the plate specimens was complete fracture, generally corresponding to the attainment of a through-thickness crack. Bend tests on beams usually stopped when the deflection had increased significantly as a result of the presence of a fatigue crack, but again this usually corresponded to through-thickness cracking. Thus, the failure criterion in the tests would correspond to leakage of a vessel.

Although there are similarities between the new EN 13445 design curves and those in BS PD 5500, they are referred to differently. British Standards adopt an arbitrary lettering system (e.g. Class D, E, F etc.), but EN 13445 refers to each S-N curve in terms of the fatigue strength in $N/mm^2$ at 2 x $10^6$ cycles, as illustrated in Figure 18D-1. As in the case of Eurocode 3, IIW and BS PD 5500, all the S-N curves for assessing weld details in EN 13445 are parallel with a slope $m = 3$. This choice arises partly because the statistical analysis of test data suggested such a value, but also because it is consistent with the slope of S-N curve expected from a detail in which the fatigue life is dominated by crack growth (8,11,14). In the statistical analysis discussed in Section 3.2 the slope of $m = 3$ was imposed when deriving design curves. Thus, the design S-N curves are of the form $\Delta\sigma_R{}^3 . N = C$, where $\Delta\sigma_R$ is the appropriate stress range, $N$ is the fatigue life in cycles and $C$ is a constant dependent on the Class. These are based on fatigue data obtained from tests on actual welded specimens. Thus, the stress concentration effect of the weld detail in the test specimen is included in the S-N curve.

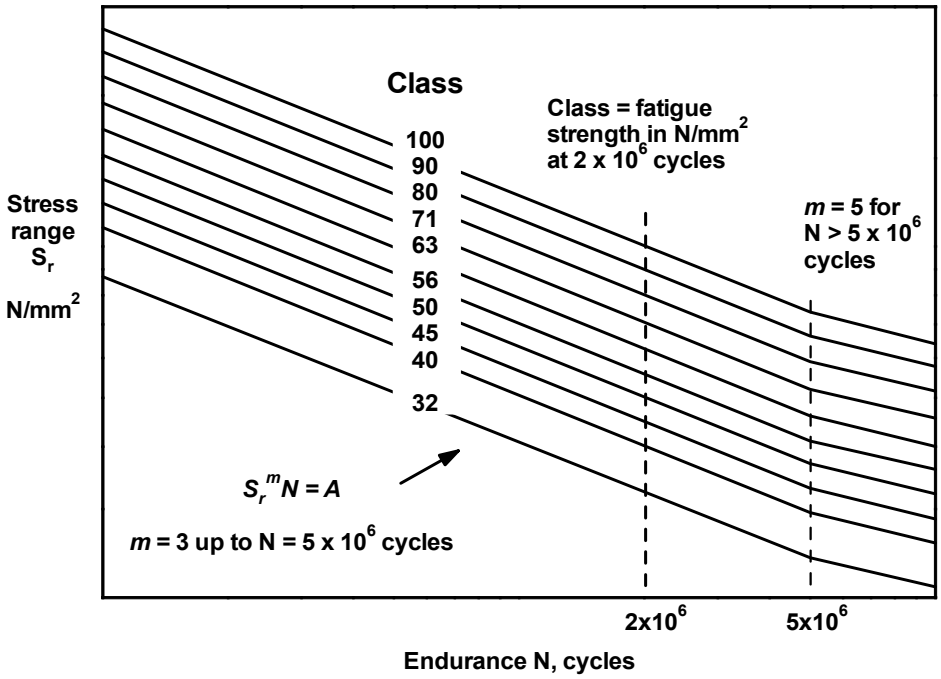


**Figure 18D-1 Fatigue design S-N curves for weld details in EN 13445**

### 18D-2 Classification System

In their original form (i.e. British Standards, Eurocode 3, IIW) the design curves refer to particular weld details, modes of fatigue failure and directions of loading. Tables are then provided with sketches linking these features and the appropriate design Class. The S-N curves are then used in conjunction with the relevant principal stress range (i.e. that acting normal to the plane of potential fatigue cracking). However, an important feature of EN 13445 is the preference for the use of the equivalent structural stress range, with direct use of the principal structural stress as an option. As a result, two tables are provided for classifying a weld detail, Table 18-4 for assessments made using equivalent stress ranges and the table in Annex P for assessments based on principal stress ranges. The disadvantage of the use of the equivalent stress is that no account can be taken of the weld orientation since, as a scalar quantity, the equivalent stress has no direction. This is important because the fatigue strength and hence design Class of a weld detail usually varies with the direction of loading. However, assessments based on equivalent stresses must make use of the lowest design Class for the detail concerned, which may be lower than the one most likely to govern the actual fatigue performance of the weld (see Figure 18D-2). Thus, more precise and less conservative fatigue design is possible using the principal stress. However, it seems that industries in some European countries still prefer use of the equivalent stress range since this is the stress used for static design of the vessel.

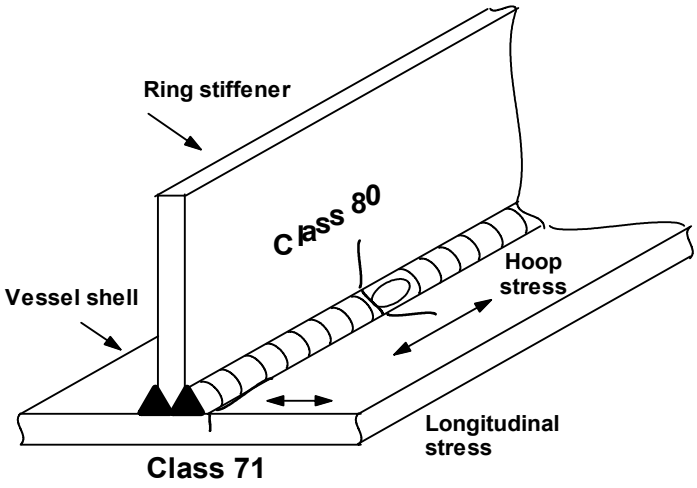


EN 13445 offers choice of using equivalent stress or principal stress. Since equivalent stress has no direction, a consequence is that the lowest detail Class must be assumed.
Thus, the joint shown would be designed as Class 71.

**Figure 18D-2 Effect of choice of stress, equivalent or principal, on weld detail classification in EN 13445**

### 18D-3 Derivation of Design Curves

As noted earlier, the original design curves were approximately two standard deviations below the mean, representing 97.7% probability of survival. When deriving the higher survival probability S-N curves required for EN 13445 it was noted that the Eurocode 3 or IIW design curves were approximately one standard deviation of log N apart. Thus, unless there was new evidence to change it, the Class chosen for a given detail and potential failure site in EN 13445 was one Class below the Eurocode 3/IIW Class.

### 18D-4 Fatigue Endurance Limit

As in the case of the Eurocode 3 design curves, those in EN 13445 are assumed to reach the CAFL at $N = 5\text{x}10^6$ cycles. In contrast, BS PD 5500 adopts the fatigue limit used in other British Standards, which corresponds to an endurance of $10^7$ cycles and is therefore lower. There is plenty of experimental evidence to show that some weld details will fail at stresses below that corresponding to $5\text{x}10^6$ cycles on the S-N curves (24). Thus, the BS design curves are considered to be more realistic than those in EN 13445, and indeed Eurocode 3, in the high-cycle regime.

As noted earlier, the CAFL is ignored in cumulative damage calculations and instead the S-N curve is assumed to be extrapolated, to $N = 10^8$ cycles in EN 13445, at a shallower slope. In EN 13445, the slope changes from $m = 3$ to 5, the same as in Eurocode 3 and the IIW recommendations. This is also the case in BS PD 5500, but the slope changes at $10^7$ cycles. However, as noted earlier, there are now serious doubts that this approach is sufficiently conservative, but this would only be relevant to high-cycle fatigue assessments of pressure vessels.

### 18D-5 Misalignment of Welded Joints

A feature of EN 13445, that follows BS PD 5500, is recognition of misalignment as a major source of stress concentration due to the introduction of local secondary bending when the misaligned joint is loaded. It was considered necessary to draw special attention to this because it was found that misalignment levels that were acceptable according to the manufacturing rules was sufficient to reduce the fatigue performance of a weld detail to a level below the design curve. In an extreme case, the local stress could be increased by a factor of 14 from secondary bending due to acceptable axial and angular misalignment. Guidance is therefore given on the calculation of the secondary bending stress due to the various types of misalignment relevant to pressure vessels (17,28). In contrast, an implicit assumption in rules that do not draw attention to this issue, including the ASME rules, is that allowable misalignment will not reduce the fatigue performance of a weld detail below that estimated using the rules.

The guidance on misalignment is essentially an application of the so-called fitness-for-purpose philosophy, whereby an imperfection in the structure can be considered to be acceptable as long as it does not reduce the strength of the structure below that required. BS PD 5500 encourages use of this same philosophy for assessing

the significance of welding flaws in general, making direct reference to BS7910 (17), that provides guidance on the application of the approach. It is planned to develop special acceptance criteria for welding flaws related to fatigue performance for EN 13445 in future.

### 18D-6 Weld Toe Grinding

Another novel feature of both EN 13445 and BS PD 5500 is the inclusion of guidance on the improvement of the fatigue performance of some weld details by weld toe grinding. The technique aims to remove the minute sharp imperfections that are known to exist at weld toes (15) and to reduce the stress concentration effect of the weld profile by blending the weld smoothly with the adjacent plate. Specific guidance on application of the technique is given, developed on the basis of both high- and low-cycle fatigue tests of welded specimens (29). Correct application justifies an increase in design Class. Clearly, it is only applicable in the case of potential fatigue cracking from a weld toe and care should be taken not to overlook other potential sites for fatigue cracking that might result in only marginal overall improvement in fatigue life.

### 18D-7 Structural Hot-Spot Stress

An important development that is likely to influence all the pressure vessel design rules in future is use of the structural hot-spot stress for designing weld details from the viewpoint of potential fatigue failure from the weld toe (30). Indeed, it is understood that the approach is currently being developed to allow major revision of the ASME fatigue rules for weld details (31).

The fatigue design curves given in EN 13445 are based on those given in fatigue design rules based on the so-called 'nominal stress approach'. As already explained, they incorporate the stress concentration effect of the weld detail tested to generate the data from which they were derived. In those cases where the main potential failure mode is by fatigue cracking from the weld toe, this consists partly of the local notch effect of the weld toe but also that due to the overall joint geometry. Thus, in practice the design curves are used in conjunction with the nominal stress near the weld detail, increased if necessary to allow for any other source of stress concentration. In the context of a pressure vessel this might be a nozzle that introduces an extra stress concentration factor near the weld toe of $K_t$. Then, the design curve would be used in conjunction with $K_t$ x nominal stress. However, without a precise definition of $K_t$ there is no guarantee that it really does account for all differences between the stress concentration effects of the test specimen and the real structure. However, this should be possible using the structural hot-spot stress.

The structural hot-spot stress is the structural stress at the weld toe. Since it includes all sources of stress concentration except that due to the local notch effect of the weld toe, it should be possible to correlate fatigue data obtained from any welded joint geometry that fatigue cracks from the weld toe. Such correlation has already been demonstrated for tubular joints and the hot-spot stress used in conjunction with a single design S-N curve has been the basis of their design for offshore applications for over 20 years. Some progress has been made in developing the same approach for other types of structure, but proposals are still tentative and awaiting further validation (32).

Preliminary guidance on the use of hot spot stress is given in EN 13445, based directly on that developed by the IIW (30). However, in view of the lack of experience in the use of the hot-spot stress approach or calculation of the structural hot-spot stress in pressure vessels, the cautious decision was made to use it in conjunction with the 'nominal stress approach' design S-N curves. This means that, with confidence from more experience and further experimental validation, it should be possible to use higher design curves for some details.

### 18D-8 Validation

Validation of the design method for assessing welds on the basis of fatigue data obtained from actual pressure vessels was an important step in the adoption of the method in BS PD 5500 (5,6). The original validation exercise was repeated recently and was extended to consider the EN 13445 rules (29,33). Again, the BS PD 5500 rules were validated, but limited evidence suggested that some small changes should be made to EN 13445. In particular, Class 100 should be reduced to Class 71 for assessing nozzle welds from the point of view of potential radial fatigue cracking from the root using the equivalent stress; Class 63 should be reduced to Class 50 for circumferential seam welds between the shell and vessel end; Class 36 should be reduced to Class 32 for assessing load-carrying fillet welds from the viewpoint of potential fatigue cracking in the weld throat. However, on the positive side the review showed that both fillet welded nozzle joints could be designed as the same Class as full penetration welds from the viewpoint of fatigue cracking from the weld toe. In the context of the structural hot-spot approach, it proved difficult to determine hot-spot stresses accurately from the information provided in the references available. This might explain why the data did not justify use of a higher design curve

than the 'nominal stress approach' one currently recommended in EN 13445. Ideally those data need to be re-analysed, preferably using finite element stress analysis.

Most of the pressure vessel fatigue data presented in the review were obtained around 30 years ago. A particularly valuable conclusion drawn in the review was that there was no evidence to indicate that those test vessels were unrepresentative of pressure vessels designed and manufactured to modern Standards. Thus, the fatigue test data they provided were suitable for validating the EN 13445 design S-N curves.

## 18E Fatigue assessment of plain material

### 18E-1 Design S-N Curves

EN 13445 provides a group of design curves, which come from the AD-Merkblatt code (3). They were originally derived from data obtained in fatigue tests of small-scale polished steel specimens, under stain control in the case of low-cycle fatigue data (9,10). It is reported that although most of these data relate to fatigue lives corresponding to complete failure of the test specimen, as in the case of the data for welded joints, those endurances correspond to crack initiation, or the presence of a 'technical incipient crack' in a real vessel, but the argument for this is unclear (10). The design curves were obtained by applying factors of 1.5 on stress and 10 on life to the mean curves fitted to the data. The corresponding probability of failure is unknown. Since the test database obtained from polished specimens showed an increase in fatigue life with increase in steel tensile strength, this has been reflected in the design curves. When applying the design curves, account must be taken of differences between the polished specimens and real structures. Thus, allowance must be made for all stress concentration effects, steel UTS, surface finish and applied mean stress, as well as thickness, temperature and plasticity.

The design curves are compared with the ASME curves, which also distinguish between low and high-strength steels, in Figure 18E-1. They are seen to be higher than the corresponding curves in ASME, but in practice would usually be lowered to allow for surface finish and for mean stress if this is not zero, whereas the ASME curves would not.

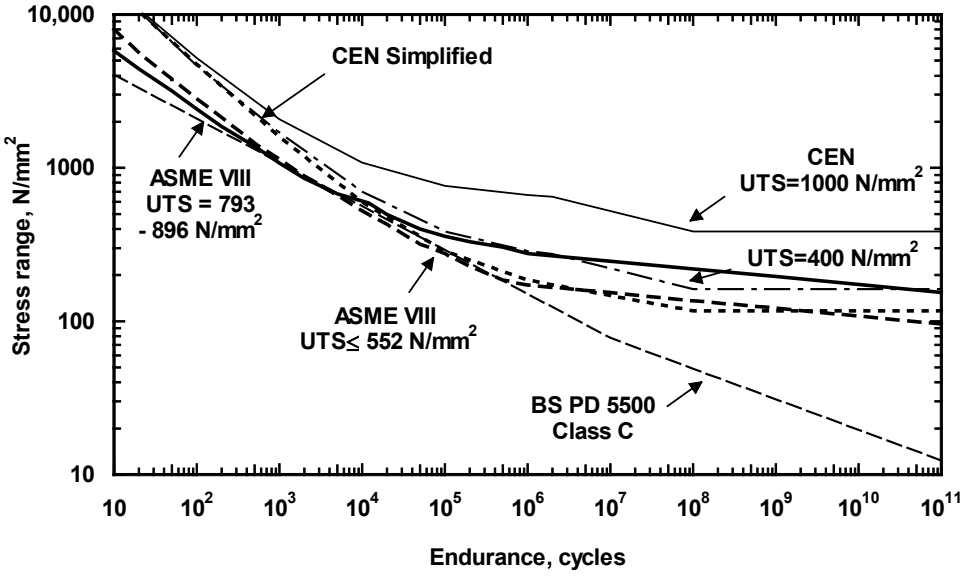


**Figure 18E-1 Comparison of pressure vessel design curves for plain steels (intermediate CEN curves for UTS of 600 and 800 N/mm$^2$ not shown)**

The EN 13445 and ASME curves are used in conjunction with equivalent stresses, the stress range in EN 13445 or the stress amplitude (half the range) in ASME. Both codes refer specifically to that based on the Tresca yield criterion (i.e the maximum shear stress, although twice its value, referred to as the 'stress intensity', is actually used in ASME). Any equivalent stress that 'produces the same fatigue damage as the applied multi-axial stress' is

allowed by EN 13445. However, an implicit assumption is that this is **not** the maximum principal stress and therefore that the direction in which it acts is not known.

With regard to the need to allow for all sources of stress concentration, plain steels are assessed using 'effective equivalent total stresses. This is obtained either by detailed stress analysis or by applying an appropriate fatigue strength reduction factor to allow for the notch effect of the local discontinuity to the equivalent structural stress range. The fatigue strength reduction factor given in EN 13445 (equation 18.7-2) is novel and was developed specially for the Standard.

BS PD 5500 provides a single design curve for assessing plain material, independent of UTS, surface finish and mean stress. In contrast to the other codes, it is used in conjunction with the maximum principal stress range. This curve was originally derived from fatigue test results obtained from welded specimens (11) and it is used in other British Standards to assess longitudinal welds as well as plain steel. A similar curve is provided in EN 13445, but only for use in a Simplified Fatigue Assessment using Chapter 17.

### 18E-2 Validation

The experimental data obtained from fatigue tests on actual pressure vessels used to validate the design curves for weld details also included many results for vessels that failed in plain steel. In the review referred to earlier these were compared with the EN 13445 design curves, as shown in Figure 18E-2. The EN 13445 curves include the maximum correction factor for surface finish; they would be higher for good surface finish. The lowest EN 13445 curve is the one that would be used in a Simplified Fatigue Assessment. Also shown for comparison is the BS PD 5500 design curve; the ASME curves included in Figure 18E-1 are omitted for clarity. It was surprising to find that whilst the lowest EN 13445 design curve, and indeed the lowest ASME, is consistent with this database, the EN 13445 curves for use in a Detailed Fatigue Assessment are not. The same is true for the ASME curve for high strength steels. It may also be noted that the database included vessels made from steels that ranged in tensile strength from 370 to 850 N/mm$^2$ but provided no evidence to support the distinction between different strength steels in the design curves (29,33). Thus, at this early stage in the life of the new European Standard, there is a clear need for review of the design curves for assessing plain steel. The single curve used for Simplified Assessments, or that from BS PD 5500, looks to be more suitable than those related to UTS.

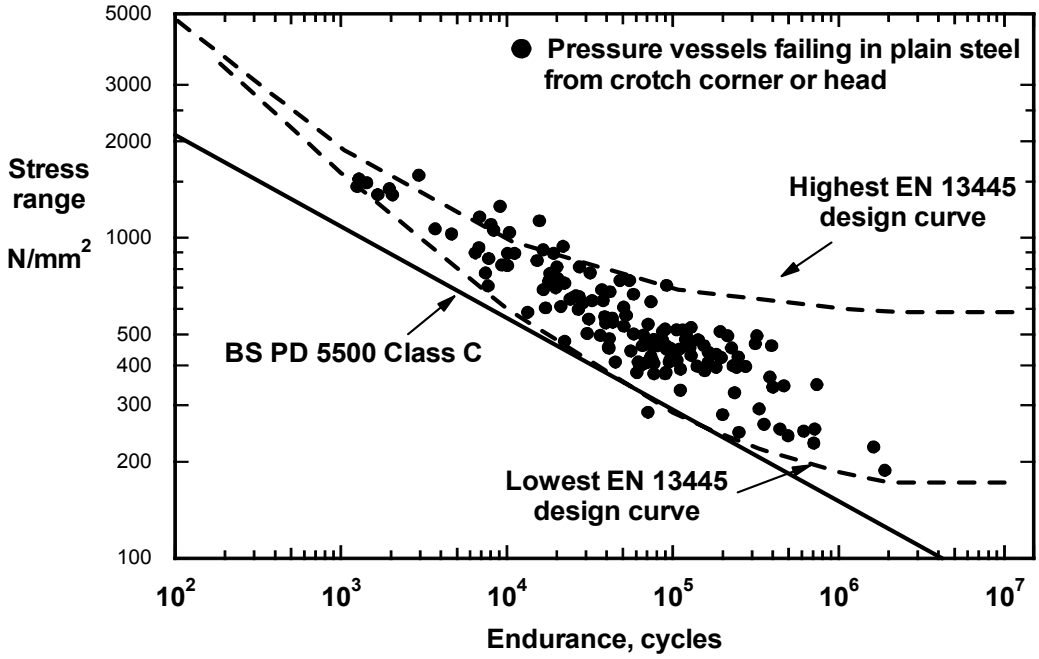

**Figure 18E-2 Fatigue test results from actual pressure vessels failing in plain, unwelded steel compared with EN 13445 and BS PD 5500 design curves (29).**

## 18F Fatigue assessment of bolts

### 18F-1 Design S-N Curves

The design curve for steel bolting in BS7608 (12), lowered to correspond to mean - 3 standard deviations of log N, was adopted for EN 13445. This was based directly on fatigue data obtained from actual (steel) bolts, some under moderately high tensile mean stresses. Thus, in this case, the design curve already incorporates the stress concentration effect of the thread root. Therefore, it is used in conjunction with the nominal axial stress on the minimum bolt cross-section due to applied tension and bending. In practice, the actual fluctuating stress in a pre-tensioned bolt may be lower than that applied, due to the need to overcome the resulting compressive stress that clamps together the parts joined.

ASME VIII and BS PD 5500 provide essentially the same rules for assessing bolts. In contrast to EN 13445, the ASME and British Standard design curves were obtained from tests on polished steel specimens. Therefore they must be used in conjunction with a fatigue strength reduction factor, 4 unless a lower value can be justified, to allow for the stress concentration effect of the thread root.

In all cases, it is assumed that the fatigue strength of a bolt increases with increase in material UTS, up to specified limits.

### 18F-2 Validation

The S-N curve for bolting in EN 13445 is expressed in terms of stress range/UTS. However, recent data (34) show that the fatigue lives of bolt threads are independent of the tensile strength of the steel. Therefore, there is no justification for assuming a higher design curve for higher strength bolts. However, the new data also suggest that the present design curves in EN 13445, BS PD 5500 and ASME are over-conservative, as seen in Figure 18F-1. A preliminary analysis indicates that a better design approach would be to have a conventional S-N curve (29,33); corresponding to Class 50.

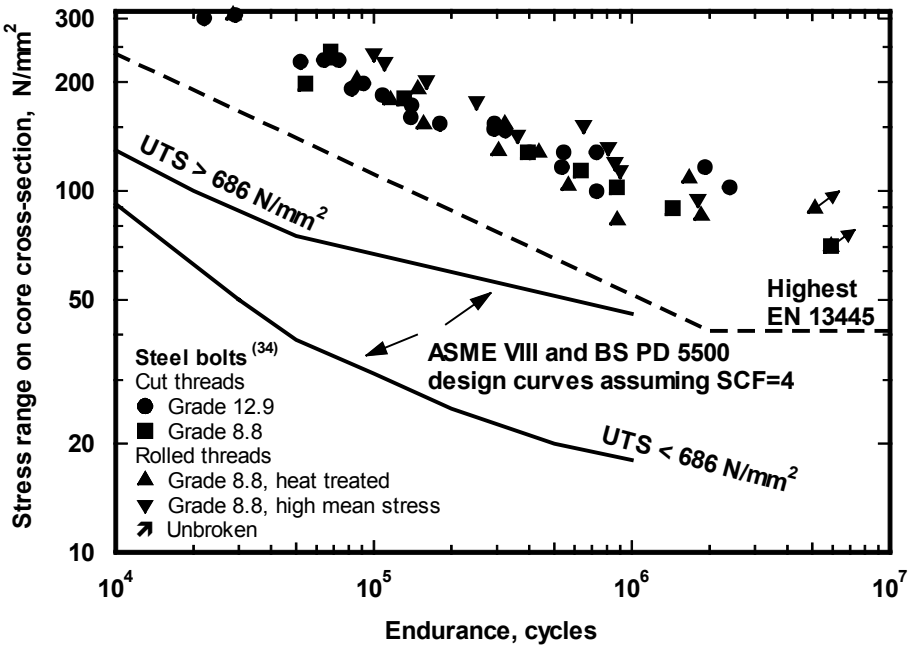


**Figure 18F-1 Comparison of fatigue test results obtained from steel bolts in tension and pressure vessel design curves**

## 18G Design by experimental methods

Only ASME provides guidance on the use of special fatigue testing to prove a particular vessel or part, as a substitute for design. Plans are in hand to provide a similar route in EN 13445. Meanwhile, EN 13445 provides similar guidance to that in BS PD 5500 on the use of special fatigue tests to validate or change a design curve for a particular detail. However, the factors to be applied to the fatigue life obtained from the tests, which depends on the number of tests performed, come from AD-Merkblatt (10). They are claimed to embody the same level of safety as the official design curves for plain steels with 95% confidence.

## 18H Fatigue design of expansion joints

Special rules are provided for the design of expansion joints, including consideration of fatigue, in Chapter 14. These follow the route originally proposed by the Expansion Joints Manufacturers Association (EJMA), which presents design S-N curves modelled on those in ASME. However, for EN 13445 use has been made of the larger database from fatigue tests now available. These were analysed to produce the same form of S-N relationship incorporating safety factors on the fitted mean S-N curve of 1.25 on stress and 3 on life. The stress used with the S-N curves is the equivalent stress range arising from cyclic pressure and deflection of the convolutions. As distinction is drawn between austenitic stainless steel, nickel alloy and copper-nickel alloy expansion joints that have or have not experienced cold work. On the basis that cold work increases the yield strength of the steel, the fatigue resistance of the latter is assumed to be higher than that of the former. However, no distinction seems to be drawn between joints that do or do not include longitudinal weld seams. Even so, both design curves are within the band of curves provided in Chapter 18 for assessing plain steels. In the case of expansion joints made from ferritic steel, the user of Chapter 14 is directed to Chapter 18. However, it is not clear if in the case of a welded component, he should use the appropriate S-N curve for welded joints or plain steel.

## 18I Future work

The following list reflects known deficiencies in the current EN 13445 rules, as discussed above, together with areas where new guidance is needed:

- 'Marriage' of stress analysis, especially FEA, and fatigue data.
- Generation of parametric hot-spot SCFs for pressure vessel details
- Revised rules for threads and bolts
- Treatment of elastic-plastic fatigue
- Effect of environment (corrosive, elevated temperature, hydrogen)
- Improved cumulative damage method
- Closer link between design and fabrication quality
- Guidance on experimental methods for design.

## 18J Bibliography


[1] ASME Boiler and Pressure Vessel Code, Section VIII, Rules for construction of pressure vessels, Division 2 - Alternative rules, ASME, 2003.

[2] BS PD 5500: 'Specification for unfired fusion welded pressure vessels', BSI Standards, London, 2000.

[3] AD-Merkblatter S1: 'Technical rules for pressure vessels', *Vereinigung der Technischen Uberachungs-Vereine e.V*, Essen, 1994.

[4] Langer, B F: 'Design of pressure vessels for low cycle fatigue', *J. Basic Eng. (Trans. ASME Series B),* Vol.84, 1962, p389-402.

[5] Harrison J D and Maddox S J: 'A critical examination of rules for the design of pressure vessels subject to fatigue loading' in *Proc. 4th Int. Conf. on 'Pressure Vessel Technology'*, IMechE, London, 1980.

[6] Maddox S J: 'Fatigue aspects of pressure vessel design' in *'Pressure Vessel Design-Concepts and Principles*', Spence J and Tooth A S (Editors), E & F N Spon, London, 1994, p.337.

[7] Harrison J D: 'Low-cycle fatigue tests on welded joints in high-strength steels*, Proc. Int. Conference 'Fatigue of Welded Structures'*, The Welding Institute, Abington Cambridge, 1971.

[8] Maddox S J: 'Fatigue design rules for welded structures', *Progress in Structural Engineering and Materials*, **1,** (2), Jan-Mar 2000, pp102-109.

[9] Gorsitzke B: 'Neuere Berechnungsvorschriften zum Ermudungsfestigkeitsnachweis von Druckbehaltern', *TÜ Bd. 36*, Part.1, No.6; Part 2, No.7/8, 1995.

[10] 'AD-Merkblatt S2, Fatigue Analysis, Annex 1 'Explanatory notes to AD-Merkblatt S2', RWTÜ*V*, Essen, March 1994.

[11] Gurney T R and Maddox S J: 'A re-analysis of fatigue data for welded joints in steel', *Welding Research International*, **3**, (4), 1973.

[12] BS 7608: 'Code of practice for fatigue design and assessment of steel structures', BSI Standards, London, 1993.

[13] Gurney T R: *'Fatigue of Welded Structures'*, Cambridge University Press, 2nd edition, 1979.

[14] Maddox S J: *'Fatigue Strength of Welded Structures'*, 2nd Edition, Abington Publishing, Cambridge, 1991.

[15] Signes E G, Baker R G, Harrison J D and Burdekin F M: 'Factors affecting the fatigue strength of welded high strength steels', *Brit. Weld. J*, **14**, (3), 1967, pp108-116.

[16] Harrison J D: *'Fatigue Performance of Welded High Strength Steels'*, The Welding Institute Report Series, The Welding Institute, Cambridge, 1974.

[17] BS 7910: 'Guide on methods for assessing the acceptability of flaws in metallic structures', BSI, London, 2000.

[18] Orjasaeter O: 'Effect of plate thickness on fatigue of welded components', IIW Document No.XIII-1582-95, 1995.

[19] Sonsino C M: 'An overview of the state of the art on multiaxial fatigue of welds', in 'E. Macha, W. Bedkowski and T. Lagoda '*Multiaxial Fatigue and Fracture'*, ESIS Publication 25, 1999, pp 195-217.

[20] Maddox S J and Razmjoo G R: 'Interim fatigue design recommendations for fillet welded joints under complex loading', *Fatigue Fract. Engng. Mater. Struct.*, **24**, 2001, pp 329-337.

[21] Neuber H: 'Theory of stress concentrations for shear strained prismatic bodies with arbitrary non-linear stress-strain law', *Trans. ASME J. of Applied Mechanics*, 1969, p544.

[22] Grandemange J M et al: 'Plasticity corrections in fatigue analysis', *AFIAP Conference*, **2**, 109, October 1992.

[23] Haibach E: 'Discussion', Proc. Int. Conference on '*Fatigue of Welded Structures'*, The Welding Institute, Abington, Cambridge, 1971, p.xxxv.

[24] Maddox S J: 'Key developments in the fatigue design of welded constructions', 2003 IIW Portvin Lecture, *Proc. IIW Int. Conf. on 'Welded Construction for Urban Infrastructure'*, ISIM, Timisoara, Romania, 2003.

[25] Niemi E: 'Random loading behaviour of welded components'. *Proc IIW Conf on 'Performance of Dynamically Loaded Welded Structures',* Welding Research Council, New York, (1997), p.339.

[26] Eurocode 3 - Design of steel structures - pr EN 1993, European Committee for Standardization, Brussels, 1992.

[27] Hobbacher A: *'Fatigue Design of Welded Joints and Components'*, International Institute of Welding, Abington Publishing, Abington, Cambridge, 1996.

[28] Maddox S J: 'Fitness for purpose assessment of misalignment in transverse butt welds subject to fatigue loading', IIW Document XIII-1180-85 (1985).

[29] Maddox S J: 'Assessment of pressure vessel design rules on the basis of fatigue test data' in *'Pressure Equipment Technology - Theory and Practice'*, Banks W M and Nash D H (Editors), Professional Engineering Publications Ltd., Bury St. Edmunds, 2003, p237-248.

[30] Niemi E: 'Stress *Determination for Fatigue Analysis of Welded Components'*, International Institute of Welding, Abington Publishing, Abington, Cambridge, 1996.

[31] Dong P, Hong J K, Osage D and Prager M: 'Assessment of ASME's FSRF rules for vessel and piping welds using a new structural stress method', IIW Doc. XIII-1929-02/XV-1118-03, 2003.

[32] Maddox S J: 'Recommended hot-spot stress design S-N curves for fatigue assessment of FPSOs', *Int. J Offshore and Polar Eng.* Vol. 12, No.2, June, pp134-141 (2002).

[33] Taylor N (Ed): 'Current practices for design against fatigue in pressure equipment', *EPERC Bulletin No.6*, European Commission, NL-1755ZG, Petten, The Netherlands, 2001.

[34] 'Fatigue tests on steel bolts', *Offshore Technology Report* OTO 97067, Health & Safety Executive, London, 1998.

# Annex A Design requirements for pressure bearing welds

Annex A aims at gathering in a single text all that the designer must know when he designs a pressure weld. Although this Annex cannot be exhaustive, it tries to cover the maximum of joints used in practice in the pressure vessel industry. A special attention has been brought to welded joints for tube to tubesheet (Table A-5).

The following details the content of the columns:

1. Design requirements are mainly dimensional requirements known to limit stress concentrations. Joints are represented in the finished condition.

2. The applicable weld testing group is related to non-destructive testing (NDT) and influences the design through the weld joint coefficient. Welds for which all testing groups can be used are given first. Then welds with partial penetration are given. For these, in general, the last two testing groups 3 or 4 or testing group 4 alone are permitted.

3. Fatigue class is that of the weld detail of Table 18-4 of Clause 18 having the same fatigue behaviour. It is the class for use with the structural equivalent stress range.

4. Lamellar tearing susceptibility considers two cases: A = no risk and B = possible risk.

5. If there is risk of corrosion, the letter S indicates that the joint is not permitted, while the letter N indicates normal conditions.

6. Help to the joint preparation is provided by a reference to prEN 1708-1.

# Annex B Design by Analysis - direct route

## BA General

The Design By Analysis (DBA) route is included in the standard

- as a complement to the common (and easy) Design By Formulae (DBF) route, for cases not covered by the DBF route, but also as an allowed alternative,
- as a complement for cases where superposition (of pressure actions) with environmental actions – wind, snow, earthquake, etc. – is required,
- as a complement for fitness-for-purpose cases where (quality related) allowed manufacturing tolerances are exceeded,
- as a complement for cases where local authorities require detailed investigations, e. g. in major hazards' situations or for environmental protection reasons.

Within this DBA route, there are two possibilities available:

- The so-called Direct Route (DR), and
- the Stress Categorization Route (SCR)

The second, the SCR, is the one, well-known from many national standards and technical regulations [1 ÷ 10], which requires categorization of stresses, or parts of stresses, into primary, secondary, and peak stresses. Because of the "familiarity" with this route, it is included in this standard as well, despite its also well-known drawbacks and problems – the problems associated with non-uniqueness of the choice of stress classification lines [11], and the problems associated with the categorization, the non- uniqueness of the determination of primary stresses [12 ÷ 14].

This approach, derived for assessing the results from thin shell theory, cannot easily be applied to results from 3-D (continuum) Finite Element Analyses, but it requires only linear-elastic analyses, with the advantages of uniqueness in the determination of stress results and the possibility of (linear) superposition of these results for different actions.

Because of the familiarity with this route, and with published problems, this route is not discussed here further.

## BB Direct Route - General

The main advantages of this route are:

- it overcomes all of the problems associated with the stress categorization route,
- it addresses failure modes directly, and, thus, gives better insight into critical failure modes and the corresponding safety margins – of special importance for in-service inspections – and thus, it may lead to improved design philosophy,
- it allows for direct incorporation of other actions than pressure, especially thermal and environmental ones,
- it is stated generally in general terms, allowing for different approaches

The disadvantages of this route are:

- non-linear calculations are required, leading to more computation time, and, because of this non-linearity,
- linear superposition is, in many checks, not possible anymore,
- quite often requires a good knowledge of the underlying theories.

To allow for easy incorporation of other actions than pressure, and especially the environmental ones – usually prescribed by local codes or regulations – this route follows, quite closely the Eurocode (for steel structures); like the Eurocode, it uses a multiple safety factor format (partial safety factor format).

## BC Direct Route - Notions

As in the Eurocode, distinction is made between principles and application rules:

**Principles** comprise general statements, definitions and requirements for which there is no alternative, and requirements and analytical models for which no alternative is permitted, unless specifically stated.

**Application rules** are generally recognised rules which follow the principles and satisfy their requirements; alternatives are allowed provided it is shown that they accord with the relevant principle.

Typical examples of application rules are the well-known primary, and primary plus secondary stress criteria of the SCR, which are stated, in slightly modified forms, as application rules.

As in the Eurocode, the old term loadings is consistently replaced by the term **actions**, which denotes all thermomechanical quantities imposed on the structure causing stress or strain, like forces (including pressure), temperature changes and imposed displacements.

Actions are classified by their variation in time:

- **permanent actions** (G),
- **variable actions** (Q),
- **exceptional actions** (E),
- **operating pressures and temperatures** (p, T).

Although pressures and temperatures are variable actions, they are considered separately to reflect their special characteristics – variation in time, random properties, limits influenced by safety devices.

The **characteristic values of an action** – there may be more than one for one action – depend on the action's statistical properties, and on the considered design check.

The **characteristic values of permanent actions** are usually their mean values (or extreme values) that can occur under reasonably foreseeable conditions.

The **characteristic values of variable actions** are defined as mean values or p % - percentiles of extreme values, or values specified as characteristic values (or extreme values) in relevant codes, e. g. national codes for wind, snow, earthquake.

The **upper characteristic value of pressure** shall not be smaller than the lesser of the set pressure of the (pressure) protecting device or the highest (credible) pressure that can occur under normal and reasonably foreseeable upset conditions; the **upper characteristic value of temperature** shall not be smaller than the highest reasonably foreseeable temperature (under the same conditions). There may be more than one pair of upper characteristic values for pressure and corresponding temperature.

The **characteristic values of exceptional actions** are not defined, leaving their determination open to the discretion of the interested parties.

The characteristic values of actions are used in the determination of the **design values of actions**.

The selection of the characteristic values must be done judiciously to ensure that a near-constant reliability can be obtained, care is required when incorporating actions from environmental codes, especially if these are not based on a partial safety factor format.

## BD Direct Route – Partial Safety Factors

To allow for an easy, straightforward incorporation of environmental actions into the design calculations, and, especially, to give the flexibility expected from a modern code to be able to adjust safety margins to differences in actions' variations, likelihood of combinations, and also to consequences of failure, differences in structural behaviour and consequences in different failure modes, and to uncertainties in analyses and material properties, a (**multiple – factor format**) or (**partial safety format**) was introduced.

The **partial safety factors of actions** depend on the action considered, on its combination with other actions, and on the considered failure mode – the considered design check.

The **partial safety factors of resistances** depend on the material – taking into account the dispersion in material parameters, the uncertainties of the relationship between material test parameters and those in the real structure, and the uncertainties due to the use of vicarious material parameters. They also they depend on the considered failure mode and the consequences of failure, and they depend, in principle, on the degree of inspection and control – of the material and of the structure.

To take into account

- the possible consequences of failure in terms of risk of life, injury, potential economic losses and the level of social inconvenience,
- the expense and effort to reduced the risk of failure
- the cause of failure

in the Eurocode the usage of the following classification is suggested:

- **Classe 1**: Risk to life low, economic and social consequences small or negligible
- **Classe 2**: Risk to life medium, economic or social consequences considerable
- **Classe 3**: Risk to life high, economic or social consequences very great,

and it is suggested to use additional **adjustment factors**, with which the partial safety factors of actions shall be multiplied, the "usual" one being 1.0 for Class 2 (0.9 for Class 1 and 1.2 for Class 3).

This notion of **risk** or **reliability classes** was not carried over into the pressure vessel standard explicitly, or, to put it in a different way: **All pressure vessels** were considered to be **in Class 2**.

This fact requires consideration when characteristic values or partial safety factors for actions are carried over from one standard, e. g. an environmental one, into a pressure vessel design investigation.

## BE Direct Route – Design checks

**Design checks** are investigations of the structure's safety under the influence of specified combinations of actions with respect to specified limit states; they are designated by the (main) failure mode they deal with.

The specified combinations of actions are called **design load cases**.

The specified limit states may represent one or more failure modes. For example, the design check against gross plastic deformation, which deals mainly with the failure mode gross plastic deformation, is intended to encompass also the failure mode of excessive local yielding – design details with possible strain concentration may require special consideration in the analysis' model.

In the design checks the **effects of design values of actions** (or of design functions) **on design models** (of the structure) are determined and compared with allowable values, or, in some cases, with **design resistances**.

**Design effects** are usually the stresses, maximum equivalent stresses, etc. in the structure, evaluated as response of the structure's model to design actions, or combination of design actions.

The expression for **design effects**

$$E_d = E\,(A_d, a_d, ...) = E\,(\gamma_P \cdot P, \quad \gamma_G \cdot G, \quad \gamma_Q \cdot Q, .. a_d \; .. X_d \; ..)$$

is a very general, symbolic one:

$E_d$ stands for an equivalent stress, a principal stress, a normal stress, a stress resultant, or even for an action itself.

The "variables" $P, G, Q$, etc., stand for possibly many different actions, or combination of actions, depending on the design load cases; $\gamma_P, \gamma_G, \gamma_Q$ , etc. stand for the corresponding partial safety factors of the actions.

The "variable" $a_d$ stands symbolically for design dimensions, and the "variable" $X_d$ for design material properties, essential in the model used for the determination of the design effect.

For **design values of geometrical data** (in the model) nominal values may be used. For **design values of material properties** (in the model), like modulus of elasticity, coefficient of linear thermal expansion, etc. nominal or mean values may be used. For strength related data design values are used, obtained by dividing material strength parameters, like $R_{eH}, R_p, R_m$, by the relevant partial safety factor. For the characteristic values of the material strength parameters the minimum guaranteed values specified in the material codes or material data sheets shall be used.

The **design values of actions** are obtained by multiplication of the actions' characteristic values with the relevant partial safety factors (of actions). In the case of design load cases involving combinations of actions of stochastic nature, the products of characteristic values and partial safety factors of actions may for stochastic actions additionally be multiplied by a **combination factor** (<1).

Within one design check, consideration of one design load case or more than one design load case may be required. In some cases, the design resistance may be obtained directly as (limit) response of the structures' model to the relevant combination of actions using for material strength parameter of the model not the characteristic values – given by the minimum guaranteed ones – but the design values (of material strength parameters), which are obtained by dividing the characteristic values by the partial safety factor of the resistance:

$$R_d = R\,(X_d / \gamma_R, a_d, \ldots)$$

The following design checks are included

- **gross plastic deformation (GPD) design checks**, with corresponding failure modes ductile rupture and excessive local strains
- **progressive plastic deformation (PD) design checks**
- **instability (I) design checks**
- **fatigue (F) design checks**
- **static equilibrium (SE) design checks**

In the **fatigue design check** the fatigue clauses of the DBF part of the standard are referred to as application rules, but the intention is that these DBF fatigue clauses should be used principally. In following this intention,

results of linear-elastic calculations are required only, which can then be used directly in the fatigue calculations in accordance with the procedures of these DBF fatigue clauses. In some cases, with dominant pressure action and negligible other actions, it may be possible to use only the rules of DBF's simplified fatigue analysis, but, of course, with loss of detailed knowledge of (fatigue) safety margins, and loss of knowledge of critical points – important for manufacturing, for pre-service checks, and especially for in-service inspections.

In the **instability design checks** details are given on partial safety factors and on reduction factors – often called knock-down factors, which relate the results of theoretical models to experimental results. Nevertheless, it is expected that the normal approach to the instability design check, used whenever structure and actions permit, will be via the instability clauses of the DBF part of the standard, referred to as application rules.

In the **static equilibrium design checks** details are given on partial safety factors, design load cases, i. e. actions' combination rules, for the usual investigation of the static equilibrium of the structure as a rigid body – safety margins against overturning and rigid body displacement. The obvious results of these checks are the required bolting and the maximum pressure on the foundation; investigations of the admissibility of design details – brackets, feet, rings, saddles, etc. -, via DBF rules for non-pressure loadings –, or via other DBA checks, may be part of these checks.

## BF Gross plastic deformation design checks

In these design checks the design models and the application of the actions are specified in detail:

The design actions shall be carried by the design model with

- proportional increase of all actions considered in the design load case under investigation
- a linear-elastic ideal-plastic constitutive law
- first-order theory
- Tresca's yield criterion and associated flow rule
- specified design strength parameters, obtained from minimum guaranteed values (in the material standards or material data sheets) of the yield or proof strength at specified temperature divided by the appropriate partial safety factors of resistances

with the maximum absolute value of principal structural strains less than a load case dependent limit value.

The **partial safety factors** are calibrated such that, for "normal" steels and pressure loading only, the same results as for the DBF route are obtained for cylinders and spheres. For high strength steels with a ratio of $R_{eH}$ or $R_{p\,0.2}$ to $R_m$ at ambient temperature above 0.8 the partial safety factors are increased in such a manner that at ambient temperature the "effective" value of $R_{eH}$ or $R_{p\,0.2}$ is given by 80% of $R_m$

Because of this strain limitation, it was necessary to specify the increase of actions as proportional – the limit action itself without this limitation is independent of the action path.

There are cases where this proportional increase seem to be inappropriate, or at least cumbersome, e. g. in cases of multiple actions where some actions are constant and one is interested only in maximum values of the others.

Tresca's yield criterion was specified for safety reasons, but especially to guarantee the calibration effect mentioned above – in the DBF route Tresca's yield criterion is used everywhere.

It is recognized that software allowing for Tresca's yield criterion is not, or not readily, available, and it is also well known that this criterion may lead to numerical (stability) problems, and that it is (computation) time consuming. Mises' yield criterion may be used instead, but then the design strength parameter shall be decreased by multiplication with $\sqrt{3}/2$ , i. e. decreased by 15.5%.

## BG Progressive plastic deformation design checks

For these checks the goal is specified:

On repeated application of specified action cycles progressive plastic deformation shall not occur for

- a linear-elastic ideal-plastic constitutive law
- first-order theory

- von Mises' yield criterion and associated flow rule
- specified design strength parameters (equal to the characteristic ones, the minimum guaranteed ones of material standards or material data sheets)

Here, Mises' yield criterion is allowed, in recognition of the fact that, because of material hardening, a less stringent criterion is deemed to be justified.

Here, the design strength parameters are equal to the materials' characteristic values – the partial safety factor of the resistances is in these design checks equal to unity.

Only the goal is specified, to use all the possibilities a (cumbersome) cycling of actions may be necessary, with all the numerical problems to show that definitely no further progressive plastic deformation occurs after a few cycles.

To prove that the structure shakes down under the cyclic action, e. g. using Melan's shakedown theorem, can in many cases be a way out of this dilemma. In applying Melan's shakedown theorem, solutions already obtained in the GPD design check together with corresponding linear-elastic ones can be used to obtain the self-equilibrating stress fields required in this approach [16].

Unfortunately the **ratcheting criterion** [15 et loc. cit], a variant of Melan's shakedown theorem stated in generalized stresses – the familiar stress resultants of the technical theories for beams, plates, shells – , **is not** a **generally valid** sufficient condition for non-occurance of progressive plastic deformation. It seems to be that it is not valid in cases where during unloading plastic strains occur.

On the other hand, this criterion uses the notion of generalized stresses – appropriate in technical theories – and, thus, leads to the very same problems of determination of stress classification lines encountered in the stress categorization route – this criterion belongs to the SCR, but there it is (usually) not used.

Modifications of the "usual" 3f-criterion, well known from the stress categorization route, are given as application rules. That these are based on a necessary condition only is recognised explicitly; they should be used with care. Unfortunately, these application rules treat (instationary) thermal stress problems very conservatively – to avoid problems associated with stress classification lines (and with stress linearization) the notions of (thermal) peak stresses and of equivalent linear stress distributions were not used. An improvement seems to be necessary, at least for thermal stresses.

## BH Remarks

Experience has shown that, with presently available software, it is quite easy to obtain Finite Element results, but to obtain reasonably correct ones is not so easy – the setting up to the appropriate model and the appropriate boundary conditions requires experience, know-how and good knowledge of the theory of structures.

Experience has also shown that it requires even more experience and know-how to evaluate obtained results.

DBA is a powerful tool in the design of pressure equipment, but like other powerful tools, it has to be used with care. This had been stated, and agreed upon by all experts, in the first drafts of this DBA route. This warning note could not be carried over into the (draft) standard, but it is repeated here:

**Design by analysis requires a great amount of expertise, in the analysis or the experimental stage, but especially in the evaluation stage. This route (DBA) should be used with care.**

If the DBA route is chosen, all of the stated design checks shall be considered – not all will require detailed calculation, some can be quite simple, with an obvious answer, but still all need consideration.

DBA is a powerful tool, giving much insight into the structural behaviour, into the safety margins against failure modes, but it is a pre-supposition that materials, manufacturing procedures and testing guarantee the required quality of the structure.

The Design By Analysis routes are contained in normative annexes. Because of the advanced approach of the Direct Route, a warning remark had been introduced at the beginning:

Due to the advanced methods applied, until sufficient in-house experience can be demonstrated, the involvement of an independent body, appropriately qualified in the field of DBA, is required in the assessment of the design (calculations) and the potential definition of particular NDT requirements.

## BI Bibliography


[1]: ASME Code, Section III

[2]: ASME Code, Section VIII, Div. 2, App. 4 and 5

[3]: AD-Merkblatt S 4

[4]: BS 5500, Appendix A

[5]: CODAP, Section C 10

[6]: KTA 3201.2, KTA 3211.2F

[7]: ÖNORM M7307

[8]: RCC-M (RB 3200), RCC-MR (RB 3200)

[9]: Richtlinienkatalog Festigkeitsberechnungen, BR-A1

[10]: STOOMWEZEN D 1200,

[11]: J L Hechmer & G L Hollinger, "Considerations in the calculations of the primary plus secondary stress intensity range for Code stress classification," "Codes & Standards and Applications for Design and Analysis of Pressure Vessel and Piping Components" Ed R Seshardi, ASME PVP Vol. 136, 1988.

[12]: A Kalnins & D. P. Updike, "Role of plastic limit and elastic plastic analyses in design," ASME PVP-Vol. 210-2 Codes and Standards and Applications for Design and Analysis of Pressure Vessel & Piping Components, Ed R Seshardi & J.T. Boyle, 1991. A Kalnins & D.P. Updike, "Primary stress limits on the basis of plasticity," ASME PVP-Vol. 230, Stress Classification, Robust Methods and Elevated Temperature Design, Ed R Seshardi & D.L. Mariott, 1992.

[13]: A Kalnins, Updike & Hechmer, "On Primary Stress in Reducers", ASME PVP Vol. 210-2, pp. 117-124

[14]: D. Mackenzie & J. T. Boyle, "Stress Classification: A Way Forward", IMechE presentation 5.5.92

[15]: J. L. Zeman, "Ratcheting limit of flat end to cylindrical shell connections under internal pressure", Int. J. Pres. Ves. & Piping **68** (1996) 293-298

[16]: J. L. Zeman, R. Preiss, "The deviatoric map - a simple tool in DBA", Int. J. Pres. Ves. & Piping.


# Annex C Design by Analysis - Method based on stress categories

## CA Introduction

"Design by Analysis" (DBA) is an approach which was first introduced in 1963 in Section III (Nuclear components) of the ASME Code [1], followed by Section VIII Div.2 (Pressure Vessels) in 1968 [2]. With time it has got a large success, so that today most of the national pressure vessel codes have incorporated such rules, always in a form very similar to that given in the ASME Code. This success has been favoured by the tremendous progress performance of computers has made in the last three decades, allowing a large development of structural analysis techniques and the coming on the market of user-friendly structural analysis software.

For pressure vessel designers familiar with "Design by Analysis", DBA is implicitly understood as *design based on elastic stress analysis* and *classification of stresses into categories.*

However, prior to starting examination of what are the corresponding rules in EN13445-3, it is important to mention that "DBA" has got a more general meaning in this Standard, because two different DBA routes have been introduced in EN13445-3. The first, which is that considered in this paper, keeps in line with the original ASME approach. The second, given in Annex B "DBA – Direct route", is based on individual checks of the relevant failure modes and is a novel one.

EN13445-3 does not give any precedence to one of these two routes. The choice between them is left to the user, depending on his specific needs, and within the respect of their respective scope. The intention of the EN13445-3 writers was to offer a standard that allow users, on one hand to apply rules with which they feel familiar and in which they can take advantage from their past experience (this apply to Annex C), and on the other hand to

benefit from more advanced design methods (this applies to Annex B). Doing so, when implementing the rules of the "classical" DBA method of Annex C, no particular effort was made to try to solve or overcome some of the well known difficulties encountered when facing the stress classification problem (definition of the reference plane or stress classification line, three dimensional stress classification, linearisation procedure, and mainly distinction between primary and secondary stresses). Only established solutions were adopted, with their advantages and drawbacks. It was considered that if applied by sufficiently trained users, these rules are reliable enough. In order to ensure that application of Annex C will really be made under that condition, a statement was placed to require that design by DBA shall be assessed by a qualified independent body (last paragraph in C.1).

## CB Origin of the rules

The rules in Annex C have been essentially taken from CODAP, the French Pressure Vessel Code [3]. Basically, they are in line with those that can be found in ASME VIII Div.2, PD5500, AD-Merkblatt S4 , the Dutch Code, the Swedish Code…, and more generally speaking in all codes that have implemented ASME-like DBA rules.

The background of these rules has been largely presented and discussed in the literature, and is now well known by pressure vessel designers. It will not be explained again here. The historical reference for it is the ASME criteria document published in 1969 [4], while a more recent presentation can be found in [5].

Although essentially conform to the ASME design by analysis concepts, the French rules and thus the European EN13445-3 rules exhibit some (slight) differences with them on some aspects. These differences are reviewed in the detailed comments on Annex C which are presented at point C-4 below.

## CC Scope and field of application

Sub-clause C.1 states that Annex C may be used either:

- as an alternative to Design by Formula (DBF),
- as a complement to Design by Formula for cases (structural shapes, loading) not covered by DBF, including cases where manufacturing tolerance according to Part 5 of the Standard are exceeded,
- as an alternative to the Design by Analysis direct route (Annex B).

An important difference with DBF lies in the fact that nowhere in Annex C the weld joint coefficient $z$ is considered. Consequently, to keep consistent with the basic shell design according to DBF, and to respect the general philosophy of the Standard, it has been required that whenever Annex C is used, the minimum thickness for pressure loading only shall not be less than that required by the DBF rules for shells and dished ends. The higher thicknesses that DBF requires, when values of $z$ lower than 1 apply, are thus maintained.

Annex C applies to all testing groups, including testing group 4 whose characteristic is that no NDT of the welds other than visual examination is required. For vessels which fall in the domain where that testing group may be used (i.e. vessels working essentially under static loading conditions, with not more than 500 full pressure cycles), this provision allows such vessels to be designed with account given to possible additional loads other than pressure.

As in all corresponding rules of other codes, fatigue failure, buckling and creep are not covered by Annex C.

As regards fatigue, although total stresses (i.e. primary + secondary + peak stresses) are considered in Annex C , the design criteria that are imposed concern only limitation of primary and primary + secondary stresses. The peak part is left apart, for possible use in fatigue assessment if required. Note that in EN13445-3, the consideration of peak stresses is only necessary when assessing unwelded zones, welded zones being assessed using structural stresses (see Clause 18).

As regards creep, no general temperature limit (by family of materials) has been imposed. Annex C is applicable as far as the nominal design stress based on time-independent characteristics governs upon that based on creep characteristics (the latter being defined in the amendment on creep design in preparation in CEN/TC54).

## CD Detailed comments on rules of Annex C

In the following, the comments are presented in the order in which the rules appear in Annex C, using the sub-clause numbering of the Standard.

### *C.2 Specific definitions*

Only a few definitions are given.

They are those of structural discontinuities: gross structural discontinuity,

local structural discontinuity,

and stress categories: primary stress ( $P_m$ , $P_L$ , $P_b$ ),

secondary stress ( $Q_m$ , $Q_b$ ),

peak stress ( $F$ ).

All these definitions are very close to that of all other codes. The only difference which must be mentioned concerns the secondary stress: although the general definition given for the secondary stress is the usual one, Annex C makes a formal distinction between the membrane and bending parts of that stress, denoting them with separate symbols $Q_m$ and $Q_b$ . But a note has been placed which explains, that except for particular cases, only consideration of the sum $Q_m + Q_b$ is needed. The particular cases where a distinction is required are those where instability is likely to occur and has to be checked. In such cases, classifying membrane thermal stresses as secondary could result in membrane yielding, which would invalidate the elastic stress pattern on the basis of which the instability check is normally made.

Other basic terminology (equivalent stress, equivalent stress range, supporting line segment) is introduced further on in the rules.

### *C.3 Specific symbols and abbreviations*

Nothing worth mentioning for that point, except that two different symbols have been introduced to allow a distinction the stress components due to an individual load ( $\sigma_{ij}$ ) from those resulting from superposition of all loads acting simultaneously at a given instant ( $\Sigma_{ij}$ ). This helps for expressing the successive steps of the detailed stress analysis procedure described at point C.6 of Annex C.

### *C.4 Representative stresses*

Annex C calls "representative stresses" all those stress quantities that are used in the method, from the initial decomposition of the stress into parts, up to the final checks against allowable limits.

- ***equivalent stress and equivalent stress range:***

– the *equivalent stress* $\sigma_{eq}$ is the "*stress intensity*" according to the ASME terminology,

– the *equivalent stress range* $\Delta\sigma_{eq}$ is the "*stress intensity range*" according to the ASME terminology again.

In EN13445-3, these stresses may be determined using either the maximum shear stress theory (Tresca criterion) or the maximum distortion energy theory (Von Mises criterion). Formulas for calculation according to both criteria are given.

In the ASME code, the rule for calculation of the stress intensity range (which is a misleading word since the value calculated is not the range of the stress intensity!) is not given in the appendix on DBA but in that on fatigue analysis, and there two different calculation procedures are defined, depending upon whether the principal stress directions change or not from one extreme load condition to the other. In EN13445-3, only one calculation procedure is given: the most general one, which covers all cases.

- ***total stress, elementary stresses, decomposition of stresses:***

These sub-clauses describe in which way the membrane, bending, linear and non-linear parts of the stresses have to be determined from the stresses obtained by elastic calculations. For this, Annex C defines:

– the *supporting line segment*

– the system of axes attached to it, in which the *elementary stresses* (i.e. the stress components) are expressed.

Figures are given to illustrate the notion of supporting line segment and of stress decomposition into parts.

Each stress part is given a precise mathematical definition, in the form of an integral of the stress distribution through the thickness. The linearisation method used in Annex C asks for linearisation of all stress components, regardless of their type (normal stress or shear) or their direction with respect to the vessel wall. Other types of linearisation have been proposed in the literature, where the shear stresses and the direct stress normal to the wall are treated differently. That of Annex C is not better than the others, but has the advantage to be simple.

In addition to the linearisation problem, the problem of giving a non ambiguous definition of the supporting line segment is also a problem not well solved in Annex C, just like in all other similar rules. Annex C defines the supporting line as "the smallest segment joining the two sides of the wall" and states that "outside the gross structural discontinuities, the supporting line segment is normal to the wall mean surface". In fact, these two definitions do not always coincide.

Linearisation and selection of appropriate supporting line segments must be seen as weak points of the method. The problem is particularly complex when the structure has no rotational symmetry and/or when stresses are calculated using solid finite element models. These problems have generated a number of studies and some practical recommendations have been published, but with limited practical guidance. An interesting review and discussion of all these matters can be found in chapter 2 of the "DBA Manual" [6] the European Commission published to make available the results of the European research project "DBA" undertaken in parallel with the work of CEN when preparing EN13445.

One can imagine that more hints should probably have been given in Annex C for a proper selection of the supporting line segment in gross structural discontinuities, despite no rigorous answer can be proposed. Here experience and expertise really help for making reasonable choices.

To finish with decomposition of the stresses, let us add that a figure (C-3) has been placed especially to prevent users from making confusion between wall bending and global bending of a whole component, the latter resulting in negligible wall bending.

- ***requirements relating to the methods for determining stresses:***

This sub-clause is intended to give some guidance about selection of appropriate models for performing stress calculations to be used in the frame of Annex C.

### *C.5 Classification of stresses*

- ***stress classification table:***

As in all other codes, the general definitions which are given for the various stress categories are completed by a classification table (Table C-2, reproduced herein) that gives the correct interpretation which must be made of these general definitions, for a set of vessel locations/load cases which covers most of the usual vessel details and loading.

This table has been built on a logic different from that which is behind the well known ASME table.

The ASME table lists those *types of stress* that have to be considered for a given component and location, depending on the load source, and allocate to them the stress category which has to be used. Doing so, not all possible types of stress are mentioned for the different cases (component + location), and not all load sources are always taken into account. In addition, the types of stress used are sometimes confusing. As an example, this is the case for the ASME stress classification for nozzles, in which two different types of "bending" stresses are considered: wall bending (for the location "nozzle wall") and global component bending (for the location "cross section perpendicular to nozzle axis").

The EN13445-3 logic is to present a stress classification which, at each considered location, systematically associates a stress category to both membrane and bending parts of the stress, as resulting from the general decomposition scheme given in the rules (C.4.4) and as obtained from finite element calculations (either readily from shell/plate models, or through the linearisation procedure if solid elements are used). With that presentation, users always know how to do with those two stress parts.

This table assigns categories only for membrane and bending stresses. It has been considered, as a rule, that the peak stress is always the non-linear part of the stress distribution, and never needs to be taken into account, because having an influence only on fatigue behaviour (not covered by Annex C).

- ***stress categories assignments specific to EN13445-3*** *(and to CODAP as well)**:***

In the classification table C-2, it can be seen that a stress classification has been proposed for cases which are not considered in the ASME table. The added cases concern:

- stresses due to external local loads (in all vessel regions, far from discontinuities or not),
- stresses in plane walls (not only circular flat ends), including the vicinity of openings.

For the first case, the category proposed for the bending part of the stress is basically $P_b$, for conservatism, but a note states that $Q_b$ is also permitted, provided the local plastic deformation that may result from using that

category is acceptable for the service of the vessel. This leaves some flexibility to the user, allowing him to decide for a more economical design, when possible.

The second case is one for which the classification to be proposed is not obvious at all, particularly at the vicinity of edges. At edges of plane walls, bending stresses due to pressure have been classified as $Q_b$ (while bending stresses due to external loads are classified $P_b$ [3] as in all other vessel discontinuities, with a possible change for $Q_b$ as explained just before). This is based on the following reasoning:

– for circular flat ends, which are usually much thicker than the connected shell, the bending stress at edge is always lower than that at centre, and then cannot govern the end thickness; so classifying it as $Q_b$ is not a problem. What matters is the classification assigned to the bending stress at the end of the connected cylindrical shell: if classified as $Q_b$, yielding of the end-to-shell junction is possible; when it occurs, it would tend to increase the bending stress at the centre of the end above the value obtained from the elastic stress calculations, and then would render the evaluation of $P_b$ non conservative at that point[4]. Despite this difficulty, the classification of bending stresses into category $Q_b$ at edge can be considered as acceptable. An estimate of the possible effect of that choice can be got by studying the two extreme boundary conditions that may exist at the end-to-shell junction:

  - for built-in conditions (shell thickness > end thickness): the criterion $P_b \leq 1{,}5f$ at centre leads to an under-thickness of ≈ 4,5% compared to the limit load criterion with a safety factor of 1,5; the criterion $P+Q \leq 3f$ at edge does not govern.

  - for simply supported conditions (no connected shell): the criterion $P_b \leq 1{,}5f$ at centre leads to an over-thickness of ≈ 11% compared to the limit load criterion with same safety factor.

  Since the true boundary conditions are in most case closer to simply support edge than to built-in edge, it can be assumed that the design resulting from the classification proposed is correct. It is only when the shell thickness is close to that of the flat end that this classification could result in some (very limited) under-conservatism.

– for rectangular vessel walls, where the thickness of all sides is generally similar, classifying the edge bending stresses as $Q_b$ leads to producing plastic bending deformation along the edges. As a result, the shape of the cross section of the vessel is modified in such a way that second order geometrical effects become significant: the plastic deformation at edges induces a curvature of the walls, which allows them to develop some membrane resistance in addition to their initial bending resistance. This effect has been studied (see e.g. [7]) and the conclusions driven tend to justify that a less conservative classification than $P_b$ can be proposed in practice for these cases.

Even if questionable on some aspects, these proposals for stress classification in flat walls were considered as acceptable.

In fact, the difficulty comes mainly from the different behaviour bending stresses exhibit in plates and shells: in shells, the bending stresses which occur at component discontinuities (junctions, openings) are produced by discontinuity forces and moments and they naturally vanish when increasing the distance from the discontinuity, whereas in plates the bending stresses which occur at edges and gross discontinuities like openings always correspond to bending moments which propagate over the whole plate. So the DBA classification concepts are better adapted to shell structures than to plate structures.

### *C.6 Stress analysis procedure*

This sub-clause describes step by step the sequence of successive operations the user must follow when applying Annex C. It has been written with the aim to be as clear and comprehensive as possible, in order to avoid misapplication of the method.

---

(3) For that case, table C-2 presently indicates $Q_b$. This is an editing mistake, which should be corrected

(4) In the ASME code, note [2] in the classification Table 4-120.1 relates to this problem. But since it is attached to the case "Flat end – Junction to shell", the bending stress concerned may be understood as that in the end instead of that in the shell. This is misleading.

### *C.7 Assessment criteria*

The assessment criteria of Annex C are those given in all DBA rules based on stress categories. The limits on $P_m$, $P_L$, $P_m + P_b$ and $P_m + P_b + Q$ are of course the same as in all these rules. Note that the limit on $P_m + P_b + Q$ is $3f$, with no possibility for using the alternative value $2R_{p/t}$ permitted in the ASME code when the material has a $R_p / R_m$ ratio lower than 0,7. Apart from this, what is different and particular to Annex C is:

– the temperature at which the nominal design stress $f$ shall be taken for assessment of the primary + secondary stress range; this temperature is not the mean temperature of the cycle, but a weighted average temperature $t^*$ defined by:

$$t^* = 0{,}75\, t_{max} + 0{,}25\, t_{min}$$

– the criterion for prevention of the risk of brittle fracture attached to tri-axial stress states is:

$$\max(\sigma_1; \sigma_2; \sigma_3) \leq R_{p/t} \ ,$$

and shall apply when the smallest tensile principal stress exceeds half the highest principal tensile stress.

This criterion has been taken from AD-Merkblatt S4 [8]. It is different from the ASME one, which is limitation of the hydrostatic component of the stress $\frac{\sigma_1 + \sigma_2 + \sigma_3}{3}$ to the maximum value $\frac{4}{3} S_m$.

In addition, it is worth noticing that for assessment of local primary membrane stresses, a detailed explanation is given (through figure C-4) to describe how the extent of a primary membrane stress region shall be measured when the two sides of the vessel discontinuity have got different shell radius ($R_1$ and $R_2$) and different thickness ($e_1$ and $e_2$). The principle is that this extent is not limited by fixed distances (like $\sqrt{R_1 \cdot e_1}$ and $\sqrt{R_2 \cdot e_2}$ on each side), but only by its total allowable length $\frac{\sqrt{R_1 \cdot e_1} + \sqrt{R_2 \cdot e_2}}{2}$. This gives more flexibility to the rule.

The possibility of using the so-called *simplified elastic-plastic analysis* also exists in EN13445-3, under the same conditions as in all similar code rules. Yet the plasticity correction to be applied in conjunction with this analysis is not defined in Annex C, but in clause 18 on detailed assessment of fatigue life. Two corrections factors are defined: $K_e$ applicable to stresses of mechanical origin, and $K_\nu$ applicable to thermal stresses. The latter plays the same role as the Poisson's ratio correction required in the ASME code when plastic analysis is chosen. The former is different from that of ASME and gives less conservative values (see paper on clause 18).

Simplified elastic-plastic analysis is the only alternative to the fulfilment of the normal assessment criteria which is detailed in Annex C. For users who would like to deviate from these criteria by using plastic or limit load analysis, the logic of EN13445-3 would normally be to skip to Annex B "Design by Analysis – Direct route". However application of Annex B is not strictly required. Annex C only states that the alternative method used shall prove the same safety margin against gross plastic deformation and progressive deformation as required in Annex B.

Lastly, the rules for prevention of thermal stress ratchet given in Annex C are those commonly known.

## CE Future developments

For the need of the additional rules which are under study in CEN/TC54 to extend the scope of EN13445 to the creep domain, design criteria for assessment of creep behaviour using stress categorisation are in preparation. They will complete Annex C in the near future.

May we foresee other improvements or complements to the stress categorisation approach? For the majority of the CEN/TC54 experts who are in charge of the evolution of EN13445-3, further development of that approach is not a priority. Two main reasons can explain this position:

– firstly, nobody is expecting solid improvements of the method. The fact that no significant change has been brought to its practical rules since they were first proposed tends to confirm this point of view. In any case, if progress can still be made, it could only result from important research programmes. This is outside the goal

of normal standardisation work, which can only establish rules of industrial practice using up-to-date but available technical knowledge.

– secondly, all experts are convinced that the highest potential for innovation and possible progress in direction of more advanced design rules lies in the DBA–Direct route of Annex B, even for deriving revised DBF solutions.

Then it can be anticipated that Annex C will not be given particular interest in the near future. This tool was necessary in EN13445-3, because world-wide known and applied. It is a useful tool having some limits and should be used within these limits.

## CF Bibliography


[1] ASME Boiler and Pressure Vessel Code – Section III: Nuclear Power Plants components

[2] ASME Boiler and Pressure Vessel Code – Section VIII Div.2: Pressure Vessels - Alternative Rules

[3] CODAP – French code for construction of unfired pressure vessels, edition 2000. - SNCT Publications

[4] Criteria of the ASME Boiler and Pressure Vessel Code for Design By Analysis in Sections III and VIII, Division 2 - ASME (1969)

[5] "Fundamental Concepts behind Section III Design-by-Analysis" by G. C. Slagis, Tenth ICPVT Conference, Vienna, Austria, July 2003.

[6] The Design-by-Analysis Manual – European Commission, DG-JRC/IAM, Petten, The Netherlands, 1999.

[7] "Rectangular Pressure Vessels of Finite Length" by A.E. Blach, V.S. Hoa, C.K. Kwok and A.K. Ahmed, J. of Pressure Vessel Technology, vol. 112, Feb. 1990.

[8] AD-Merkblatt S4: Evaluation of stresses determined by way of calculation and experimental stress analysis, AD 2000 Code, issued by VdTÜV, Carl Heymanns Verlag


# Annex D Verification of the shape of vessels subject to external pressure

No comment.

# Annex E Procedure for calculating the departure from the true circle of cylinders and cones

No comment

# Annex F Allowable external pressure for vessels outside circularity tolerance

The method leads to $P_q$, a theoretical lower bound of the collapse pressure. Equation (F-1) merely provides a smooth transition with the rules in clause 8:

$$P_{ra} = P_q + (P_a - P_q)\frac{0{,}005\,R}{w_{max}} \le P_a \qquad \text{(F-1)}$$

# Annex G Alternative design rules for flanges and gasketed flange connections

## GA Introduction

Since more than sixty years the traditional calculations of flange connections are based on estimated required gasket forces for assemblage and working conditions; and it is assumed that the actual forces are equal the required forces (c.g. AD-Merkblatt B8, ASME VIII, PD 5500 and EN13445-3, Clause 11).

Already in 1951 in [1] it was stated " ... that the actual conditions existing in a bolted joint will be considerably different from those assumed ... "; but there was not detected a consequence of this knowledge in an official flange calculation method. Similar knowledge was found in [2]; however the planned norms was realised for several parts of vessels, but not for flange connections.

The works [4] to [8] consider both essentials for the calculation of flange connections:

(1) The actual forces shall be not greater than the allowable forces (usual strength calculation).

(2) The actual forces shall bc not less than the required forces (required for leak tightness).

Both conditions may bc written as the following general condition for bolted connections:

$$\textit{Required forces} \leq \textit{Actual forces} \leq \textit{Allowable forces} \qquad \text{(GA-1)}$$

The required forces are determined for no loss of contact (force greater equal zero) or for a minimum gasket pressure necessary for tightness.

The actual forces may be calculated under the assumption of elastic deformations between assemblage and subsequent load cases, where only the assemblage condition may be assumed.

The allowable forces in all cases are limited by an assumed safety against the limit load, where the limit load should be calculated for ductile materials of flanges and bolts.

These principles were applied in the calculation methods [4], [6], [8] with convincing success: At no of the so designed (and correspondingly manufactured) flange connections untightness occur. For some cases of untightness at existing flange connections (designed anyhow) the calculation methods show possible reasons for the untightness, and these reasons was justified in practice. (An example for the latter was a heat exchanger, designed for ca. 40 bar and ca. 400 °C according to AD-Merkblatt. Calculation with [8] shows it should be tight, although some times it was untight: The flange to gasket surfaces was not correct flat. After re-machining these surfaces was flat enough and since this time the untightness is removed.)

NOTE: The methods [4], [6], [8] do not include modern tightness parameters. Its tightness criterions are no other than e.g. in DIN 2505 [3]. Untightness there is e.g. an acoustic or optic phenomenon.

## GB Elasticity of flange connections

### GB-1 Axisymmetric shell

The most flanges are ring like parts welded to an axisymmetric shell. The shell may be cylindrical, conical or spherical. Figure GB-1 shows such a system.

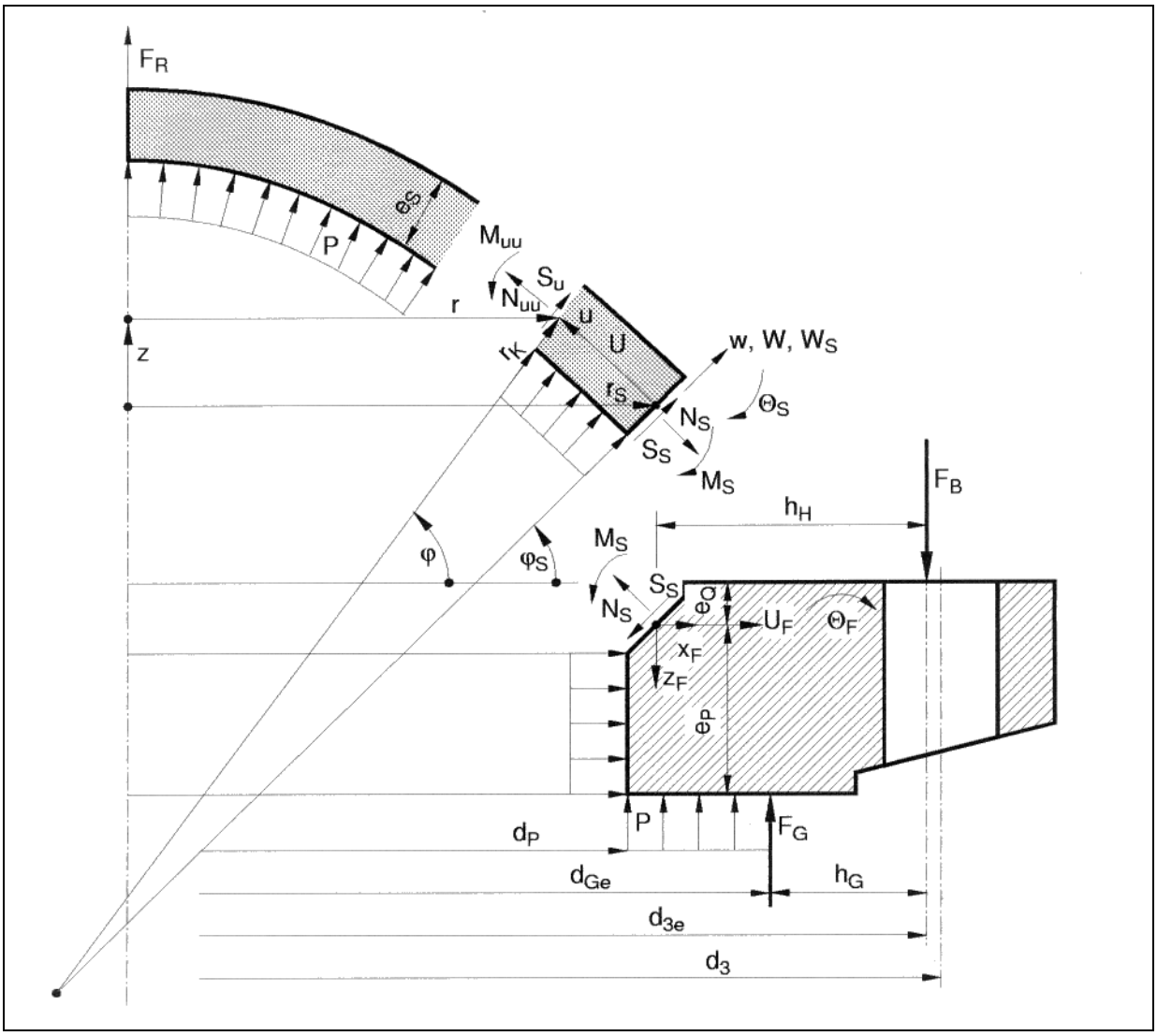


**Figure GB-1 Flange ring and shell**

Coordinates are u (meridional), v (circumferential) and w (normal to the middle surface) or r (radius) and z (axial distance) respectively.

U, V, W are displacements corresponding to u, v, w. Θ = W' = dW/du is an inclination.

Forces per length unit are $N_{uu}$, $S_u$ and $N_{vv}$; Moments per length unit $M_{uu}$ and $M_{vv}$.

Values at the end of the shell are designated by a subscript S (shell). (In the case of $S_S$ - to avoid negative signs - the direction is assumed opposite to $S_u$ .)

Geometry:

$$r' = dr/du = -\sin\varphi\,; \qquad z' = dz/du = +\cos\varphi \tag{GB.1-1}$$

$$du = r_K \cdot d\varphi \qquad r_K = \text{const}\,. \tag{GB.1-2}$$

Equilibrium conditions:

$$\left(r \cdot N_{uu}\right)' + \sin\varphi \cdot N_{vv} + r \cdot S_u / r_K = 0 \tag{GB.1-3}$$

$$\left(r \cdot S_u\right)' - \cos\varphi \cdot N_{vv} - r \cdot N_{uu} / r_K + P \cdot r = 0 \tag{GB.1-4}$$

$$\left(r \cdot M_{uu}\right)' + \sin\varphi \cdot M_{vv} - r \cdot S_u = 0 \tag{GB.1-5}$$

Elastic relations:

$$N_{uu} = \left[+U'-U\cdot\nu\cdot\sin\varphi/r + W\cdot\left(1/r_K + \nu\cdot\cos\varphi/r\right)\right]\cdot E_S\cdot e_S/\left(1-\nu^2\right) \quad \text{(GB.1-6)}$$

$$N_{vv} = \left[+U'\cdot\nu - U\cdot\sin\varphi/r + W\cdot\left(\nu/r_K + \cos\varphi/r\right)\right]\cdot E_S\cdot e_S/\left(1-\nu^2\right) \quad \text{(GB.1-7)}$$

$$M_{uu} = \left[-W'' + W'\cdot\nu\cdot\sin\varphi/r\right]\cdot E_S\cdot e_S^3/\left[12\cdot\left(1-\nu^2\right)\right] \quad \text{(GB.1-8)}$$

$$M_{vv} = \left[-W''\cdot\nu + W'\cdot\sin\varphi/r\right]\cdot E_S\cdot e_S^3/\left[12\cdot\left(1-\nu^2\right)\right] \quad \text{(GB.1-9)}$$

From equations (GB.1-5, -8, -9) the shear force is:

$$S_u = \left[-W''' + W''\cdot\sin\varphi/r + W'\cdot\left(\nu\cdot\cos\varphi/\left(r\cdot r_K\right) + \sin^2\varphi/r^2\right)\right]\cdot E_S\cdot e_S^3/\left[12\cdot\left(1-\nu^2\right)\right] \quad \text{(GB.1-10)}$$

From the given equations are derived two differential equations for the displacements U and W. These are solved approximately with the following general result:

$$U = A_0 + A_1\cdot u/l_S + \left[A_2\cdot\cos\left(u/l_S\right) + A_3\cdot\sin\left(u/l_S\right)\right]\cdot\exp\left(-u/l_S\right) \quad \text{(GB.1-11)}$$

$$W = C_0 + C_1\cdot u/l_S + \left[C_2\cdot\cos\left(u/l_S\right) + C_3\cdot\sin\left(u/l_S\right)\right]\cdot\exp\left(-u/l_S\right) \quad \text{(GB.1-12)}$$

$$l_S = \left\{\frac{4r^2\cdot e_S^2}{\left[12\left(1-\nu^2\right)\cdot\cos^2\varphi\right]}\right\}^{1/4} \quad \left(r\approx r_S;\ \varphi\approx\varphi_S\right) \quad \text{(GB.1-13)}$$

With the given deformations $W_S$ and $\Theta_S$ at the boundary $u$ = 0 ($r$=$r_S$; boundary conditions), and writing $r$=$r_S$=$d_S$/2, the following results were found:

$$S_S = \left[\left(W_S - W_0\right)\cdot k_1\cdot 2l_S + \left(\Theta_S - \Theta_0\right)\cdot k_2\cdot l_S^2\right]\cdot E_S\cdot e_S\cdot 2\cos^2\varphi_S/d_S^2 \quad \text{(GB.1-14)}$$

$$M_S = \left[\left(W_S - W_0\right)\cdot k_2\cdot l_S^2 + \left(\Theta_S - \Theta_0\right)\cdot k_3\cdot l_S^3\right]\cdot E_S\cdot e_S\cdot 2\cos^2\varphi_S/d_S^2 \quad \text{(GB.1-15)}$$

$$N_s = \frac{S_s\cdot\sin\varphi_s + \left(F_s + F_R\right)/\left(\pi\cdot d_s\right)}{\cos\varphi_s} \quad \text{(GB.1-16)}$$

$$F_S = P\cdot d_S^2\cdot\frac{\pi}{4} \text{ (preliminary abbreviation)} \quad \text{(GB.1-17)}$$

$$W_0 = \frac{F_S\cdot k_4 + F_R\cdot k_6}{\pi\cdot E_S\cdot e_S\cdot\cos^2\varphi_S} + \frac{\alpha_S\cdot\Delta T_S\cdot d_S}{2\cos\varphi_S} \quad \text{(GB.1-18)}$$

$$\Theta_0 = \frac{F_S\cdot k_5 + F_R\cdot k_7}{\pi\cdot E_S\cdot e_S\cdot l_S\cdot\cos^2\varphi_S} \quad \text{(GB.1-19)}$$

The additional coefficients $k_1$ to $k_7$ and the value $\Theta_0$ are included to facilitate numerical comparison with the analytical solution, for which:

$$k_1 = k_2 = k_3 = 1;\quad k_5 = k_7 = 0;\quad (\Theta_0 = 0) \quad \text{(GB.1-20)}$$

$$k_4 = 1 + k_6;\quad k_6 = -\frac{\nu + r_s/\left(r_K\cdot\cos\varphi_s\right)}{2} \quad \text{(GB.1-21)}$$

**GB-2 Conical hub with cylindrical shell**

The elastic stiffness of the system sketched in Figure GB-2 has been calculated numerical. (Computer program ROSCHA, TU Dresden).

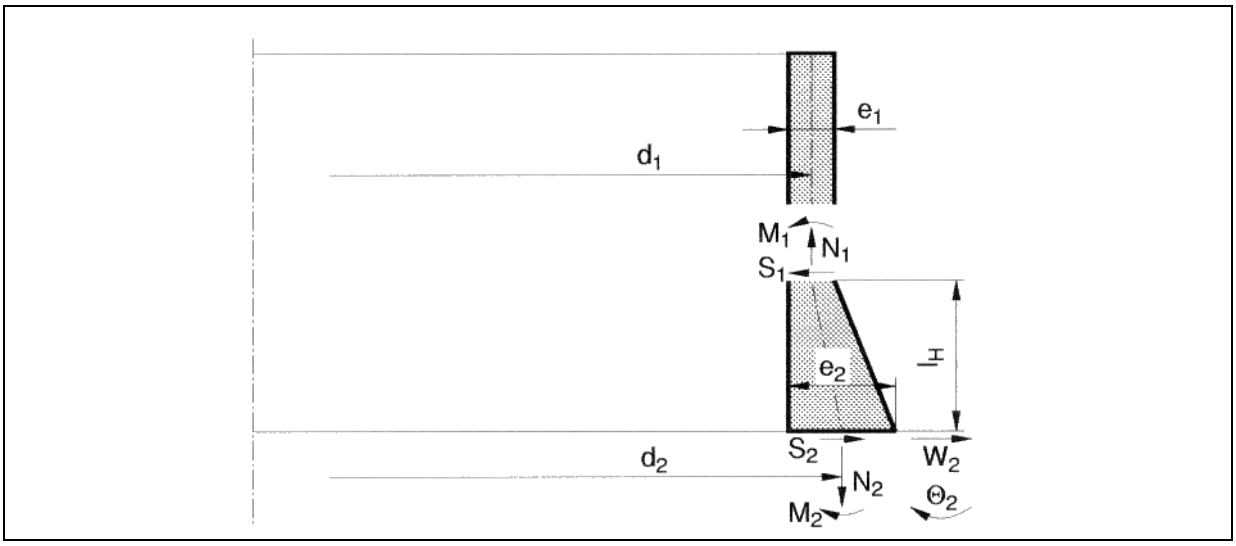


**GB-2 Conical hub with cylindrical shell**

For simplicity it was assumed that the system could be represented by an equivalent cylindrical shell as follows:

$e_1 = e_E = e_2$; $\quad r_E = r_0 + e_E/2$

From equations (GB.1-14,-15) with $\cos\varphi_S = 1$ and $W_0 = 0$, $\Theta_0 = 0$ it follows:

$$S_2 = \left[W_2 \cdot k_1 \cdot 2l_1 + \Theta_2 \cdot k_2 \cdot l_1^2\right] \cdot E_S \cdot \frac{e_1}{2r_1^2} = \left[W_2 \cdot 2l_E + \Theta_2 \cdot l_E^2\right] \cdot E_S \cdot \frac{e_E}{2r_E^2} \qquad \text{(GB.2-1)}$$

$$M_S = \left[W_2 \cdot k_2 \cdot l_1^2 + \Theta_2 \cdot k_3 \cdot l_1^3\right] \cdot E_S \cdot \frac{e_1}{2r_1^2} = \left[W_2 \cdot l_E^2 + \Theta_2 \cdot l_E^3\right] \cdot E_S \cdot \frac{e_E}{2r_E^2} \qquad \text{(GB.2-2)}$$

$$l_1 = \left[\frac{4r_1^2 \cdot e_1^2}{12\left(1-\nu^2\right)}\right]^{1/4} \qquad l_E = \left[\frac{4r_E^2 \cdot e_E^2}{12\left(1-\nu^2\right)}\right]^{1/4} \qquad \text{(GB.2-3)}$$

Calculations were performed for the following values:

$d_1/e_1$=10 … 1000; $\quad \beta = \frac{e_2}{e_1} = 1{,}5;\quad 2{,}0;\quad 3{,}0;\quad 4{,}0;\quad 6{,}0.$

ν=0,30; $\quad \chi = \frac{l_H}{\sqrt{2r_1 \cdot e_1}} = 0{,}55;\quad 1{,}10;\quad 2{,}20;\quad 4{,}40.$

From the results the factors $k_1$, $k_2$, $k_3$ are obtained.

Then by comparison of the coefficients in equations (GB.2-1, -2) it follows:

$$\frac{e_E}{e_1} = \frac{r_E}{r_1} k_1^{2/3}; \qquad \frac{e_E}{e_1} = \left(\frac{r_E}{r_1}\right)^{1/2} k_2^{1/2}; \qquad \frac{e_E}{e_1} = \left(\frac{r_E}{r_1}\right)^{1/5} k_3^{2/5} \qquad \text{(GB.2-4)}$$

Each set of parameters gives three different results for $e_E/e_1$. However the differences are not large and therefore neglected. All results are fitted approximately by the following formula:

$$\frac{e_E}{e_1} = 1 + (\beta - 1)\frac{\chi}{\beta/3 + \chi} \qquad \text{(GB.2-5)}$$

For β = 1 and for χ = 0 this formula gives $\frac{e_E}{e_1} = 1$; for $\chi \Rightarrow \infty$ $\frac{e_E}{e_1} = \beta$, all as required.

The effective diameter $d_E$ is limited as follows:

$$d_{E,\max} = \min\left\{d_1 - e_1 + e_E;\, d_2 + e_2 - e_E\right\} \qquad \text{(GB.2-6a)}$$

$$d_{E,\min} = \min\left\{d_1 + e_1 - e_E;\, d_2 - e_2 + e_E\right\} \qquad \text{(GB.2-6b)}$$

For all cases shall be used the mean value:

$$d_E = \frac{d_{E;\max} + d_{E;\min}}{2} \qquad \text{(GB.2-7)}$$

This may be shown to be exact for cylindrical inner surface, cylindrical outer surface and cylindrical middle surface also.

### GB-3 Flange ring without shell

For simplicity is assumed that the radial section of the flange ring remains undeformed. Its total radial displacement $U_F$ and rotation $\Theta_F$ (Figure GB-1) cause a tangential stress $\sigma_{vv}$ with a resultant force and a resultant moment in the radial section as follows:

$$\sigma_{vv} = \left(U_F - r_S \cdot a_F \cdot \Delta T_F - \Theta_F \cdot z_F\right) \cdot E_F / \left(r_S + x_F\right) \qquad \text{(GB.3-1)}$$

$$R_F = +\iint \sigma_{vv} \cdot dA = +\left(U_F - r_S \cdot a_F \cdot \Delta T_F\right) \cdot E_F \cdot A_F / r_F - \Theta_F \cdot E_F \cdot B_F / r_F \qquad \text{(GB.3-2)}$$

$$M_F = -\iint \sigma_{vv} \cdot z_F dA = -\left(U_F - r_S \cdot a_F \cdot \Delta T_F\right) \cdot E_F \cdot B_F / r_F + \Theta_F \cdot E_F \cdot C_F / r_F \qquad \text{(GB.3-3)}$$

$$\frac{A_F}{r_F} = \iint \frac{1}{r_S + x_F} dA \qquad \text{(GB.3-4a)}$$

$$\frac{B_F}{r_F} = \iint \frac{z_F}{r_S + x_F} dA \qquad \text{(GB.3-4b)}$$

$$\frac{C_F}{r_F} = \iint \frac{z_F^2}{r_S + x_F} dA \qquad \text{(GB.3-4c)}$$

Equilibrium conditions ring:

$$R_F = -\left(N_S \sin\varphi_S + S_S \cos\varphi_S\right) r_S + P \cdot \int r\left(z_F\right) dz_F \qquad \text{(GB.3-5)}$$

$$M_F = +\left(N_S \cos\varphi_S - S_S \sin\varphi_S\right) \cdot r_S \cdot h_H - M_S \cdot r_S + \frac{F_G}{2\pi} \cdot h_G + P \cdot \left\{\iint \left(r_{3e} - r\right) \cdot r dr - \int r\left(z_F\right) \cdot z_F dz_F\right\} \qquad \text{(GB.3-6)}$$

Integration regions: $0 \le z_F \le e_P$; $\frac{d_0}{2} \le r \le \frac{d_{Ge}}{2}$.

Equilibrium conditions shell:

$$\left(N_S \cos\varphi_S - S_S \sin\varphi_S\right) r_S = \frac{F_R}{2\pi} + P \frac{\left(d_S - e_S \cos\varphi_s\right)^2}{8} \qquad \text{(GB.3-7)}$$

Using

$$F_Q = P \cdot d_{Ge}^2 \cdot \frac{\pi}{4} \qquad \text{(GB.3-8)}$$

the following equations are found (with minor simplifications):

$$R_F = +P \cdot e_P \cdot \frac{d_P}{2} - \left(N_S \sin\varphi_S + S_S \cos\varphi_S\right) \frac{d_S}{2} \qquad \text{(GB.3-9)}$$

$$M_F = +\frac{F_G \cdot h_G + F_R \cdot h_H + F_Q\left(h_H - h_P\right)}{2\pi} - M_S \cdot \frac{d_S}{2} \qquad \text{(GB.3-10)}$$

For a flange ring with rectangular cross section the following holds (with $r_S + x_F \approx \frac{d_F}{2}$):

$$A_F = b_F\left(e_P + e_Q\right) = b_F \cdot e_F \qquad \text{(GB.3-11a)}$$

$$B_F = b_F \frac{\left(e_P^2 - e_Q^2\right)}{2} = b_F \cdot e_F^2 \cdot \frac{1 - 2\lambda}{2} \qquad \text{(GB.3-11b)}$$

$$C_F = b_F \frac{\left(e_P^3 + e_Q^3\right)}{3} = b_F \cdot e_F^3 \cdot \frac{1 - 3\lambda + 3\lambda^2}{3} \qquad \text{(GB.3-11c)}$$

$$e_F = e_P + e_Q; \qquad \lambda = \frac{e_Q}{e_P} \qquad \text{(GB.3-12)}$$

Within the flange width $b_F$ the bolt holes are subtracted partially by

$$d_{5e} = d_5\sqrt{\frac{d_5}{p_B}}\ ; \qquad p_B = \frac{\pi \cdot d_3}{n_B} \tag{GB.3-13}$$

This is based on a proposal in DIN 2505 in 1972 [3]. It is exact in both extreme cases $\frac{d_5}{p_B} \Rightarrow 0$ and $\frac{d_5}{p_B} \Rightarrow 1{,}0$; therefore it is assumed general.

The effective bolt circle diameter $d_{3e}<d_3$ takes account of the difference between chord and arc in the calculation of lever arms. A simple geometric estimation gives:

$$d_{3e} = d_3\left(1-\frac{2}{n_B^2}\right) \tag{GB.3-14}$$

**GB-4 Flange ring connected to shell**

To connect flange ring and shell the following conditions are to be realized (Figure GB-1):

$$W_S = \frac{U_F}{\cos\varphi_S}\ ; \qquad \Theta_S = \Theta_F \tag{GB.4-1}$$

Equations (GB.3-2,-3,-9,-10) and (GB.1-14,-15,-16) then gives two equations for $U_F$ and $\Theta_F$. Their solution for $\Theta_F$ ($U_F$ later is not required) is:

$$\Theta_F = \left\{F_G \cdot h_G + F_Q \cdot \left(h_H - h_P + h_Q\right) + F_R \cdot \left(h_H + h_R\right) + E_S \cdot \pi \cdot r_S \cdot e_S \cdot h_S \cdot \left(a_S \cdot \Delta T_S - a_F \cdot \Delta T_F\right)\right\} \cdot \frac{Z_F}{E_F} \tag{GB.4-2}$$

In the method Annex J (with respect to the equivalent cylindrical shell, see GB-2) is simplified:

$a_S \cdot \Delta T_S = a_F \cdot \Delta T_F$ and $E_S=E_F$

(These simplifications in a future edition should be waived.) Note that the parameters $h_Q$ and $h_R$ (defined in the method) contain some effects of deformation without a moment on the flange ring.

The simplified equation (GB.4-2) is presented also in the method (equation (G.8-16)). It is basically for the calculation of forces in the different load cases. For a flat closure (blank flange, plate with flange ring) an equal equation may be derived, where only some parameters are different (given in the method).

A loose flange and its stub or collar may be calculated also with the same equation, again with slightly different parameters only. For the loose flange the equation is more simple:

$$\Theta_L = \left\{F_B \cdot h_L\right\} \cdot Z_F / E_F \tag{GB.4-3}$$

**GB-5 Elastic stiffness of bolts**

The axial elastic elongation of the bolts shall be:

$$U_B = \frac{F_B \cdot X_B}{E_B} \tag{GB.5-1}$$

Here is (see Figure G.3-2):

$$X_B = \left\{\frac{l_s}{d_{Bs}^2} + \frac{l_e}{d_{Be}^2} + \frac{0{,}8}{d_{B0}}\right\} \cdot \frac{4}{\pi \cdot n_B} \tag{GB.5-2}$$

The last term in the brackets is an approximation for the elastic deformation of the two nuts or one nut and bolt head.

**GB-6 Elastic stiffness of the gasket**

The axial elastic diminution of the thickness of the gasket shall be:

$$U_G = F_G \cdot \frac{X_G}{E_G} \tag{GB.6-1}$$

Here as an approximation was found:

$$X_G = \frac{(e_G / A_{Gt}) \cdot (b_{Gt} + e_G / 2)}{b_{Ge} + e_G / 2} \qquad \text{(GB.6-2)}$$

The last factor is based on the assumption that the axial compressed width of the gasket is linear increased (with an angle of 45°) from the effective width $b_{Ge}$ maximum up to the theoretical width $b_{Gt}$.

The possible creep of the gasket is approximately taken into account by a "creep factor" $g_C$, using $E_G \cdot g_c$ instead of $E_G$ . Always $E_G = E_o + K_1 \cdot Q$ is the unloading modulus of the gasket after being taken to pressure load $Q$. (This is for unloading of the gasket after assemblage is typical for flange connections.)

**GB-7 Elastic deformation of the whole flange connection**

In the assembly condition all parts of the flange connection are coupled by internal forces (assembly bolt load). For no loss of contact is allowed in all subsequent load conditions the following geometric relation must be hold (see Figure G.3-1 and Figure GB-1):

$$\begin{Bmatrix} [\Theta_F \cdot h_G + \Theta_L \cdot h_L]_{Flange1} + [\Theta_F \cdot h_G + \Theta_L \cdot h_L]_{Flange2} + U_B + U_G \end{Bmatrix}_{(I=0)} = \\ \begin{Bmatrix} [\Theta_F \cdot h_G + \Theta_L \cdot h_L]_{Flange1} + [\Theta_F \cdot h_G + \Theta_L \cdot h_L]_{Flange2} + U_B + U_G + \Delta U_I \end{Bmatrix}_{(I \neq 0)} \qquad \text{(GB.7-1)}$$

(For integral flanges and for blank flanges is $\Theta_L \cdot h_L = 0$ .)

The equations for $\Theta_F$ and $\Theta_L$ (given above) and the global equilibrium condition for all load cases (all I)

$$F_B = F_G + F_Q + F_R \qquad \text{(GB.7-2)}$$

then give:

$$F_{G(0)} \cdot Y_{G(0)} + F_{Q(0)} \cdot Y_{Q(0)} + F_{R(0)} \cdot Y_{R(0)} = F_{G(I)} \cdot Y_{G(I)} + F_{Q(I)} \cdot Y_{Q(I)} + F_{R(I)} \cdot Y_{R(I)} + \Delta U_{(I)} \qquad \text{(GB.7-3)}$$

**This is the fundamental equation relating force changes in the flange connection.**

The flexibility parameters $Y_G$, $Y_Q$, $Y_R$ are positive; they (and $\Delta U_I$,) are defined in Annex G. (Slightely deviating from Annex G here the load condition identifier I (or 0) is written in brackets. This seems to be more clear and it announces that this information may be waived - as done in G.7.)

In general is $F_{Q(0)} = 0$ (no fluid pressure in assemblage). If preliminary all loads additional to the fluid pressure are ignored ($F_{R(0)} = F_{R(I)} = 0$ and $\Delta U_{(I)} = 0$) then it follows (assume $F_{Q(I)} > 0$ for $P_{(I)} > 0$):

$$F_{B(0)} = F_{G(0)}\,; \quad F_{G(0)} \cdot Y_{G(0)} = F_{G(I)} \cdot Y_{G(I)} + F_{Q(I)} \cdot Y_{Q(I)} \qquad \text{(GB.7-4)}$$

This equation shows, that with an increasing internal fluid pressure the gasket force always decreases.

For traditional flange connections in general is $h_H > h_G$ and $Y_{Q(I)} > Y_{G(I)} \approx Y_{G(0)}$. Then it follows:

$$F_{B(I)} = F_{G(I)} + F_{Q(I)} = F_{G(0)} \cdot \frac{Y_{G(0)}}{Y_{G(I)}} + F_{Q(I)} \cdot \left(1 - \frac{Y_{Q(I)}}{Y_{G(I)}}\right) < F_{B(0)} \qquad \text{(GB.7-5)}$$

In these cases with an increasing internal fluid pressure the bolt load also decreases. (This is not general, but often so.)

If (to ensure leak tightness) the required gasket force in a subsequent condition $F_{G(I)}$ is known, then from the general equation (GB.7-3) follows a required gasket force in the assembly condition:

$$F_{G(0)} \geq \frac{F_{G(I)} \cdot Y_{G(I)} + F_{Q(I)} \cdot Y_{Q(I)} + F_{R(I)} \cdot Y_{R(I)} - F_{R(0)} \cdot Y_{R(0)} + \Delta U_{(I)}}{Y_{G(0)}} \qquad \text{(GB.7-6)}$$

(Here is included the usual presupposition $F_{Q(0)}$=0.) This corresponds to equation (G.6-10).

Annex G, equation (G.6-9) defines the required force $F_{G(I)}$ by the maximum of two values. The first represents the tightness at the gasket, the second is to avoid loss of contact at the bolts. (The bolt load theoretical could be $F_{B(I)} < 0$ for cases with negative fluid pressure and/or external load.)

# GC Limit loads of flange connections

## GC-1 Axisymmetric shell

Description and figure see Annex GB-1. Only different is the following task: instead of the elastic deformation now shall be calculated the load carrying capacity, which is given by the limit load.

Dimensionless forces and moment are used as follows:

$$n_{uu} = \frac{N_{uu}}{(f_S \cdot e_S)}; \quad n_{vv} = \frac{N_{vv}}{(f_S \cdot e_S)}; \quad s_u = \frac{S_u}{(f_S \cdot e_S)}; \tag{GC.1-la}$$

$$m_{uu} = 4\frac{M_{uu}}{(f_S \cdot e_S^2)}; \quad m_{vv} = 4\frac{M_{vv}}{(f_S \cdot e_S^2)}; \tag{GC.1-lb}$$

As in EN13445-3 defined here $f_S$ is the nominal design stress of the shell, used for allowable loads instead of the yield stress for the real limit loads.

If the fluid pressure is small ($P/f_s$ « 1) the following limit load condition shall be fulfilled for all sections in all axisymmetric shells. (It is based on the Mises criterion):

$$\psi = \left[1 - \left(n_{uu}^2 - n_{uu} \cdot n_{vv} + n_{vv}^2 + 3s_u^2\right)\right]^2 + \frac{3}{4}\left(m_{uu} \cdot n_{vv} - m_{vv} \cdot n_{uu}\right)^2 - \left(m_{uu}^2 - m_{uu} \cdot m_{vv} + m_{vv}^2\right) \geq 0 \tag{GC.1-2}$$

To write the equilibrium conditions equation (GB.1-3 to -5) for the dimensionless forces and moments equation (GC.1-la, -lb) the following dimensionless coordinate and modified notation is used:

$$\xi = \frac{u}{(r_S \cdot e_S)^{1/2}}; \quad \rho = \frac{r}{r_S}; \quad \kappa = \frac{r_S}{r_k \cdot \cos\varphi_S} \tag{GC.1-3}$$

$$(\quad)' = d(\quad)/du \rightarrow (\quad)^{\circ} = d(\quad)/d\xi = (\quad)' \cdot (r_S \cdot e_S)^{1/2} \tag{GC.1-4}$$

Equations (GB.1-3 to -5) now become:

$$w \cdot (\rho \cdot n_{uu})^{\circ} + \sin\varphi \cdot n_{vv} + (\rho \cdot s_u) \cdot \kappa \cdot \cos\varphi_S = 0 \tag{GC.1-5}$$

$$w \cdot (\rho \cdot s_u)^{\circ} - \cos\varphi \cdot n_{vv} - (\rho \cdot n_{uu}) \cdot \kappa \cdot \cos\varphi_S + \frac{P}{f_S} \cdot \frac{r}{e_S} = 0 \tag{GC.1-6}$$

$$w \cdot (\rho \cdot m_{uu})^{\circ} + \sin\varphi \cdot m_{vv} - (\rho \cdot s_u) \cdot 4w^2 = 0 \tag{GC.1-7}$$

The parameter $w = \sqrt{\frac{r_S}{e_S}}$ indicates which terms are important.

With these equations $n_{uu}$, $n_{vv}$ and $s_u$ can be expressed by $m_{uu}$ and $m_{vv}$ (including derivatives). For the shell is not very flat (sinφ/w « 1 is negligible) and the plastic zone is small ( $\rho \approx 1$ and $\varphi \approx \varphi_S$ ) were found the following approximations:

$$n_{uu} = \frac{\delta_Q}{2} + \delta_R \tag{GC.1-8}$$

$$n_{vv} = \delta_Q - \kappa \cdot n_{uu} + \frac{m_{uu}^{\circ\circ}}{4\cos\varphi_S} \tag{GC.1-9}$$

The here used loading parameters correspond to Annex G, equations (G.7-10, -11):

$$\delta_Q = \frac{P \cdot r_S}{f_S \cdot e_S \cdot \cos\varphi_S}; \quad \delta_R = \frac{F_R}{f_S \cdot 2\pi r_S \cdot e_S \cdot \cos\varphi_S} \tag{GC.1-10}$$

Equations (GC.1-8, -9) are based on the equilibrium conditions and they do not include $m_{vv}$.

For such case this value may be determined by optimisation of the limit load condition equation (GC.1-2):

$$\frac{\partial \Psi}{\partial m_{vv}} = 0 \rightarrow m_{vv} = m_{uu} \cdot \frac{1 - (3/2) \cdot n_{uu} \cdot n_{vv}}{2 - (3/2) \cdot n_{uu}^2} \tag{GC.1-11}$$

Substitution of this $m_{vv}$ into equation (GC.1-2) and neglecting $s_u$ gives the following limit load condition:

$$m_{uu}^2 \le \frac{4}{3}\cdot\left(1-\frac{3}{4}n_{uu}^2\right)\cdot\left[1-\left(n_{uu}^2 - n_{uu}\cdot n_{vv} + n_{vv}^2\right)\right] \qquad \text{(GC.1-12)}$$

Solving equation (GC.1-12) for $n_{vv}$ and equating equation (GC.1-9) gives a differential equation for $m_{uu}^{\circ\circ}$ (depending on $m_{uu}^2$ and $n_{uu}^2$) which despite its complicated form can be integrated analytical with the following result (j = ±1 is determined later):

$$\left(m_{uu}^{\circ}\right)^2 = 8\cos\varphi_S\sqrt{\frac{4}{3}\left(1-\frac{3}{4}n_{uu}^2\right)^3}\cdot\left[j\cdot f(m_*) - n_*\cdot m_*\right] + const. \qquad \text{( GC.1-13)}$$

$$m_* = \sqrt{\frac{3}{4}}\frac{m_{uu}}{1-\frac{3}{4}n_{uu}^2} \qquad \text{(GC.1-14a)}$$

$$n_* = \frac{\delta_Q - (\kappa+1/2)n_{uu}}{\sqrt{1-\frac{3}{4}n_{uu}^2}} \qquad \text{(GC.1-14b)}$$

$$f(m_*) = \frac{1}{2}\left[\arcsin(m_*) + m_*\sqrt{1-m_*^2}\right] \qquad \text{(GC.1-14c)}$$

$$\frac{\partial f(m_*)}{\partial m_*} = \sqrt{1-m_*^2} \qquad \text{(GC.1-14d)}$$

Equation (GC.1-7) with the mentioned simplifications gives

$$\left(m_{uu}^{\circ}\right)^2 = 16\cdot(s_u)^2\cdot\frac{r_S}{e_S} \qquad \text{(GC.1-15)}$$

Equations (GC.1-13, -15) give the shear force $s_u$, as a implicite function of the coordinate ξ. The plastic zone may have the following boundaries:

$$\xi = 0: \quad m_* = m_{*0} = m_{*S}\,; \quad s_u = s_{u0} = -s_S \qquad \text{(GC.1-16a)}$$

$$\xi = \xi_1: \quad m_* = m_{*1}\,; \quad s_u = s_{u1} = 0 \qquad \text{(GC.1-16b)}$$

The value $s_{u0}$ shall be maximum. The unknown value $m_{*1}$ is determined from $\frac{\partial(s_{u0})^2}{\partial m_{*1}} = 0$, giving:

$$-j\cdot\sqrt{1-m_{*1}^2} + n_* = 0\,; \quad m_{*1} = k_1\cdot\sqrt{1-n_*^2}\,; \quad k_1 = \pm 1 \qquad \text{(GC.1-17)}$$

Then for the changed direction $s_S = -s_{u0}$ (see figure GB-1) and with $j_s = \text{sign}(s_S)$ it was found:

$$m_S = \frac{4M_S}{f_S\cdot e_S^2} = k_M\cdot c_M\,; \quad -1 \le k_M \le +1 \qquad \text{(GC.1-18)}$$

$$s_S = \frac{S_S}{f_S\cdot e_S} = j_S\cdot\sqrt{\frac{e_S}{d_S}\cos\varphi_S\cdot c_M\cdot c_S\cdot(1+j_S\cdot k_M)} \qquad \text{(GC.1-19)}$$

The variable $k_M$ ($-1 \le k_M \le +1$) is defined by $m_{*0} = m_{*S} = k_M\sqrt{1-n_*^2}$. The factor $c_M$ then follows immediately from the above formulae; $c_S$ is found after some simplifications.

It is used κ = 0 for conical and cylindrical shell; κ = 1 for spherical shell.

(For more details may be asked the CEN REPORT [9] to EN 1591-1.)

### GC-2 Cortical hub with cylindrical shell

To obtain an equivalent cylindrical shell thickness $e_D$ such that its limit load is equal to the real shell $e_1$ with hub $e_2$, $1_H$, the system in Figure GB-2 is analysed.

For very small hub length $\chi = \frac{1_H}{\sqrt{d_1\cdot e_1}} \ll 1$ based on the foregoing was found the following:

$$\frac{e_D}{e_1} \approx 1 + 2{,}33\chi \qquad \text{(GC.2-1)}$$

For median hub length a numerical procedure gave some results as follows:

$$\frac{e_D}{e_1} = \sqrt{\frac{m_2}{m_1}}\ ; \quad \frac{e_D}{e_1} = \left(\frac{s_2}{s_1}\right)^{\frac{2}{3}} \qquad \text{(GC.2-2)}$$

For very large hub length the asymptotic result is known:

$$\frac{e_D}{e_1} = \frac{e_2}{e_1} = \beta \qquad \text{(GC.2-3)}$$

All these results finally are represented by the following approximation (similar equation (GB.2-5)):

$$\frac{e_E}{e_1} = 1 + \frac{(\beta - 1)\cdot\chi}{\left[(\beta/3)^4 + \chi^4\right]^{1/4}} \qquad \text{(GC.2-4)}$$

### GC-3 Flange ring without shell

The ring to be calculated is shown in Figure GB-1; it is assumed to have a rectangular cross section. Its allowable design stress is $f_F$, and the assumed stress distribution is as follows:

$$\sigma_{vv} = \pm f_F \quad \text{for} \quad -e_Q \le z_F \le z_0 \qquad \text{(GC.3-1a)}$$

$$\sigma_{vv} = \mp f_F \quad \text{for} \quad z_0 \le z_F \le +e_P \qquad \text{(GC.3-1b)}$$

The coordinate for the sign change $z_F = z_0$ is yet unknown.

The resultant force and the resultant moment in the rectangular radial section are as follows:

$$R_F = +\iint \sigma_{vv} dA = \pm f_F \cdot b_F \cdot \left(2z_0 + e_Q - e_P\right) \qquad \text{(GC.3-2)}$$

$$M_F = -\iint \sigma_{vv} \cdot z_F dA = \pm f_F \cdot b_F \cdot \left[\left(e_Q^2 + e_P^2\right)/2 - z_0^2\right] \qquad \text{(GC.3-3)}$$

$$z_0 = \frac{\pm\dfrac{R_F}{f_F \cdot b_F} + e_P - e_Q}{2} \qquad \text{(GC.3-4)}$$

$$M_F = \pm f_F \cdot b_F \cdot \left\{ \frac{(e_Q + e_P)^2}{4} \mp \frac{R_F}{f_F + b_F} \cdot \frac{e_P - e_Q}{2} - \frac{\left(\dfrac{R_F}{f_F + b_F}\right)^2}{4} \right\} \qquad \text{(GC.3-5)}$$

With $e_Q + e_P = e_F$ and a sign variable $j_m = \pm 1$ this gives the limit load condition for the ring:

$$j_m \cdot \left[ M_F \cdot \frac{4}{f_F + b_F + e_F^2} + \frac{R_F}{f_F + b_F + e_F} \cdot \left(4\frac{e_P}{e_F} - 2\right) \right] + \left(\frac{R_F}{f_F + b_F + e_F}\right)^2 \le 1 \qquad \text{(GC.3-6)}$$

The actual loadings are given in equations (GB.3-7,-9,-10) and may be written as follows:

$$R_F = +P \cdot e_P \cdot \frac{d_P}{2} - \left\{ \left[ \frac{F_R}{2\pi} + \frac{P \cdot (d_S - e_S \cdot \cos\varphi_S)^2}{8} \right] \cdot \tan\varphi_S + S_S \cdot \frac{d_S}{\cos\varphi_S} \right\} \qquad \text{(GC.3-7)}$$

$$M_F = +\frac{F_G \cdot h_G + F_R \cdot h_H + F_Q \cdot (h_H - h_P)}{2\pi} - M_S \cdot \frac{d_S}{2} \qquad \text{(GC.3-8)}$$

### GC-4 Flange ring connected to shell

Equations (GC.1-18,-19) give:

$$M_S = \left(f_S \cdot e_S^2/4\right) \cdot k_M \cdot c_M\ ; \quad -1 \le k_M \le +1 \qquad \text{(GC.4-1)}$$

$$S_S = (f_S \cdot e_S) \cdot j_S \cdot k_S \cdot \sqrt{\frac{e_S}{d_S} \cdot \cos\varphi_S \cdot c_M \cdot c_S \cdot (1 + j_S \cdot k_M)} \qquad \text{(GC.4-2)}$$

Here is introduced a new factor $k_S$ ( $0 \le k_S \le 1$ ). This is for equation (GC.1-19) calculates the maximum or minimum possible shear force in the shell, but equation (GC.4-2) represents the actual force between shell and ring, which need not to be a maximum or minimum.

For use of equation (GC.3-6) a new parameter Ψ is defined and with equation (GC.3-7) written as follows:

$$\Psi = -\frac{R_F}{f_F \cdot b_F \cdot e_F} \qquad \text{(GC.4-3)}$$

$$\Psi = \frac{f_S \cdot e_S \cdot d_S \cos\varphi_S}{2 f_F \cdot b_F \cdot e_F} \cdot \left[ \left( \frac{\delta_Q}{2} + \delta_R \right) \tan\varphi_F - 2\delta_Q \cdot e_P \cdot \frac{d_P}{d_S^2} + \frac{S_S}{f_S \cdot e_S \cdot \cos^2\varphi_S} \right] \qquad \text{(GC.4-4)}$$

Equation (GC.3-6) now may be written:

$$j_m \cdot \frac{F_G \cdot h_G + F_R \cdot h_H + F_Q \cdot (h_H - h_P)}{2\pi} \le \left[ 1 + j_M \cdot \Psi \cdot \left( \frac{4e_P}{e_F} - 2 \right) - \Psi^2 \right] \cdot f_F \cdot b_F \cdot \frac{e_F^2}{4} + j_M \cdot M_S \cdot \frac{d_S}{2} \qquad \text{(GC.4-5)}$$

The left side of this equation may be understand as the load and right side as the resistance. Variation of Ψ increasing from zero increases the resistance up to a maximum at $\Psi = \Psi_{opt}$ (optimum value):

$$\Psi_{opt} = j_M \left( \frac{2e_P}{e_F} - 1 \right) \qquad \text{(GC.4-6)}$$

As Ψ depends on parameters $j_M$, $j_S$, $k_M$, $k_S$, the method Annex G gives some rules to find the best values. The load ratio $\Phi_F$ is the ratio of actual load to resistance. Since the resistance is influenced by the load, there is no exact proportionality in the sense

(*Permitted load*) = (*Actual load*)/ $\Phi_F$.

Only for $\Phi_F = 1{,}0$ such an equation is always true.

For a flat flange (blank flange, plate with flange ring) comparable limit load equations are derived, where the influence of the shell (if it exists) is ignored. However an additional check is provided for a potentially critical section with a thickness $e_X < e_F$. (For integral flanges in general may be presupposed $e_X > e_2$; then such a check is not necessary).

For loose flanges and their stub or collar the calculation as for integral flanges is applicable (some parameters correspondingly changed). An question is the actual diameter $d_7$ for the load transfer between loose flange and stub or collar. For this is proposed to apply the optimum value for each load condition.

This not agrees with the diameter $d_{70}$ being applied in the calculation of forces; however the calculated forces may be approximations only, the load carrying capacity should be calculated as correct as possible. Especially for thin walled collars an possible improvement of the load carrying capacity is presented by equation (G.7-31), taking account of a supporting moment from the clamping on a flat gasket.

### GC-5 Limit load of bolts

The maximum permissible tensile force of the bolts (sum for $n_B$ equal bolts) is:

$$F_B = f_B \cdot A_B \qquad \text{(GC.5-1)}$$

$$A_B = (n_B \cdot \pi / 4) \cdot \{\min(d_{Be}; d_{Bs})\}^2 \qquad \text{(GC.5-2)}$$

$$d_{Be} = \frac{d_{B2} + d_{B3}}{2} \qquad \text{(GC.5-3)}$$

The last equation represents ISO effective diameter.

Bolt tightening by torque-wrench causes a torsion moment in the bolt. In the usual design of bolted joints this torsion moment is neglected. However in the discussion to EN 1591-1 and EN 13445-3, Annex G, it was demanded to respect this torsion moment minimum for the assemblage. This is done and explained in subclause G.8.4.

### GC-6 Limit load of the gasket

The gasket is assumed to be a plastic deformable strip (design stress $f_G$) between two rigid planes. For $e_G \ll b_G$ the stresses $\sigma_{xx} = \sigma_{yy}$ and $\sigma_{zz} = -Q$ are functions of x only, independent of y and z. The system is sketched in Figure GC-1.

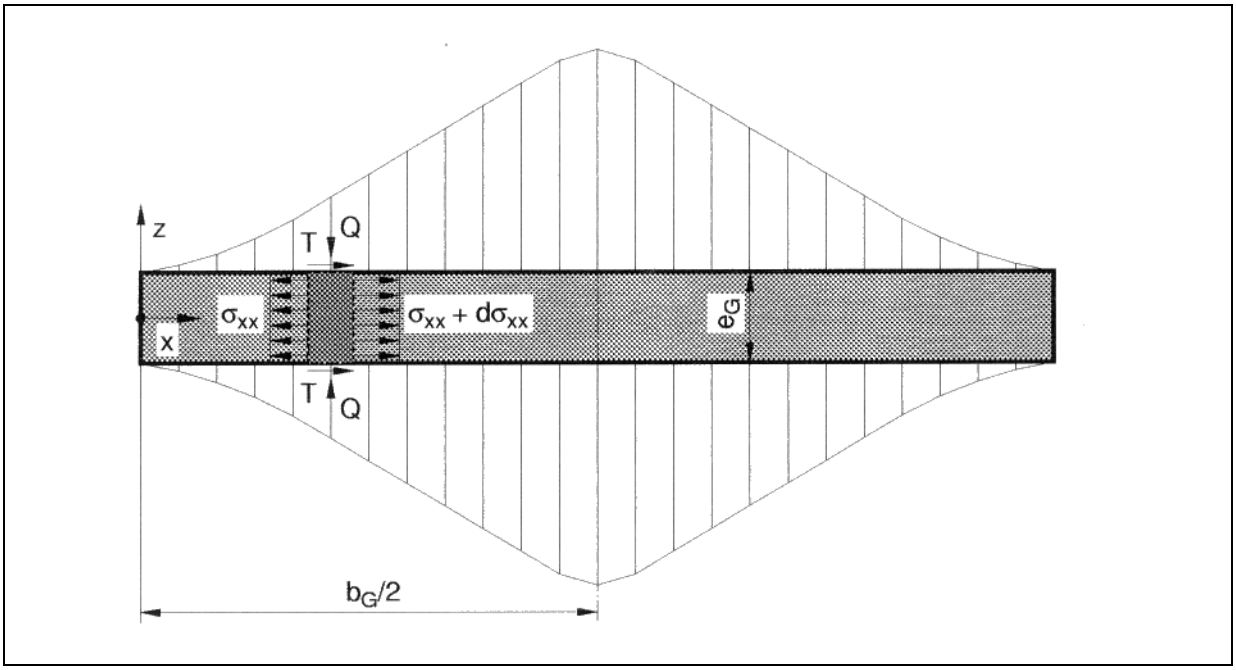


**Figure GC-1 Limit load of a gasket**

Dimensionless force-values are defined as follows:

$$p = \frac{Q}{f_G}; \quad n_{xx} = \frac{\sigma_{xx}}{f_G}; \quad n_{yy} = \frac{\sigma_{yy}}{f_G} \tag{GC.6-1}$$

In the given case is $n_{yy} = n_{XX}$ and the limit load condition becomes:

$$n_{xx} + p \le 1; \quad p \le 1 - n_{xx} \tag{GC.6-2}$$

Equilibrium condition:

$$e_G \frac{\partial \sigma_{xx}}{\partial x} + 2T = 0 \quad \rightarrow \quad \frac{\partial n_{xx}}{\partial x} + 2\frac{T}{f_G \cdot e_G} = 0 \tag{GC.6-3}$$

Surface condition (Coulomb friction and Tresca shear limit):

$$T \le \min\left\{\mu_G \cdot Q; \frac{f_G}{2}\right\}; \quad Limit: p \cdot 2\mu_G = 1 \tag{GC.6-4}$$

First solution of equations (GC.6-3,-4):

$$\frac{\partial n_{xx}}{\partial x} + (1 - n_{xx}) \cdot 2\frac{\mu_G}{e_G} = 0 \tag{GC.6-5}$$

$$n_{xx} = 1 - \exp\left(x \cdot 2\frac{\mu_G}{e_G}\right)$$

$$p = 1 - n_{xx} = \exp\left(x \cdot 2\frac{\mu_G}{e_G}\right) \tag{GC.6-6}$$

This solution includes the boundary condition $n_{xx(x=0)} = 0$. (Always is $n_{xx} \le 0$ and $p \ge 0$.) It is valid for

$$p \le \frac{1}{2 \cdot \mu_G} \text{ or } \frac{x}{e_G} \le \frac{1}{2\mu_G} \ln\left(\frac{1}{2\mu_G}\right)$$

Second solution of equations (GC.6-3, -4):

$$\frac{\partial n_{xx}}{\partial x} + \frac{1}{e_G} = 0 \qquad \text{(GC.6-7)}$$

$$n_{xx} = Const. - \frac{x}{e_G}$$

$$p = 1 - n_{xx} = \frac{1 + \ln(2\mu_G)}{2\mu_G} + \frac{x}{e_G} \qquad \text{(GC.6-8)}$$

This solution is valid for $p \geq \frac{1}{2\mu_G}$ or $\frac{x}{e_G} \geq \frac{1}{2\mu_G} \ln\left(\frac{1}{2\mu_G}\right)$.

For $\mu_G = 0{,}20$ the limit between both solutions is at $x/e_G = 2{,}29$. Therefore for $\mu_G \leq 0{,}20$ the second solution occurs only for $b_G/e_G > 4{,}5$, and for $\mu_G \leq 0{,}10$ it occurs only for $b_G/e_G > 16$.

The average pressure over the whole gasket width is:

$$p_{av} = \frac{2}{b_G} \int p dx \; ; \quad \left(0 \leq x \leq \frac{b_G}{2}\right) \qquad \text{(GC.6-9)}$$

The first solution gives:

$$p_{av} = \frac{e_G}{b_G \cdot \mu_G} \cdot \left[\exp\left(\frac{b_G \cdot \mu_G}{e_G}\right) - 1\right] = 1 + \frac{\frac{b_G \cdot \mu_G}{e_G}}{2} + \frac{\left(\frac{b_G \cdot \mu_G}{e_G}\right)^2}{6} + \ldots \qquad \text{(GC.6-10)}$$

The linear term for $\mu_G = 0{,}10$ gives the factor $c_G$ in Annex G. For $\mu_G < 0{,}50$ it is always conservative. It is of practical importance e.g. for thin aluminium gaskets in high pressure vessels at high temperatures.

## GD Diverse special effects

### GD-1 Effective width of gaskets

If a flat gasket with a large width is used in a connection with thin flanges (e.g. traditional piping flanges) the gasket pressure (compressive stress on the gasket surfaces) varies over its width; partially the gasket pressure may be zero, for the gasket surfaces are separated from the flange surfaces. The calculation of this effect in the following is shown for the assemblage condition.

The calculated effective gasket width then is assumed to be unchanged for all subsequent load conditions. This is not exact but for simplicity it is assumed to be a reasonable approximation. (For this assumption full face gaskets are excluded.)

(a) For a flat gasket the calculation model is shown in Figure GC-2.

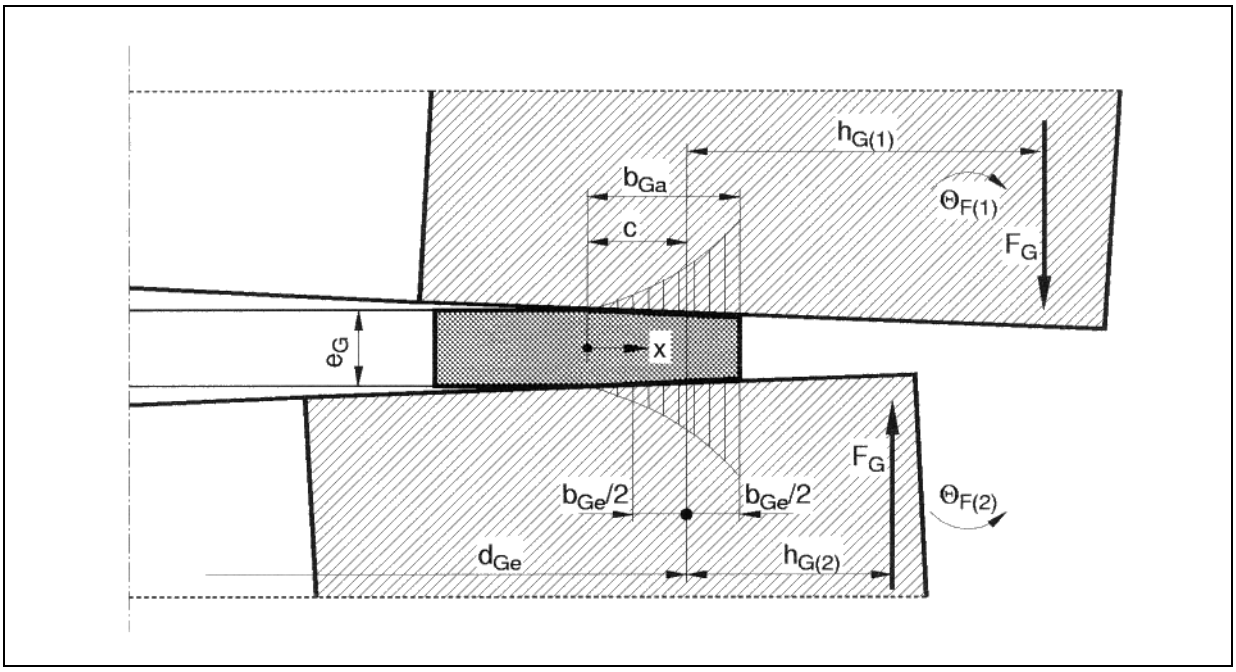


**Figure GC-2 Effective width of a flat gasket between two flanges**

Notation: $b_{Ga}$ = contact width; $b_{Gi}$ = interim (ideal, calculated) width;

$b_{Ge}$ = effective width; $b_{Gt}$ = theoretical width;

Q = gasket pressure = comprssive stress.

Elastic rotation of both flanges:

$$\Theta_{F(1)} + \Theta_{F(2)} = F_G \cdot \left[ \left( \frac{Z_F \cdot h_G}{E_F} \right)_{(1)} + \left( \frac{Z_F \cdot h_G}{E_F} \right)_{(2)} \right] \qquad \text{(GD.1-1)}$$

Elastic deformation of gasket (for $0 \le x \le b_{Ga}$):

$$\varepsilon = \frac{\left(\Theta_{F(1)} + \Theta_{F(2)}\right) \cdot x}{e_G} = k \cdot x \qquad \text{(k = abbreviation)} \qquad \text{(GD.1-2)}$$

$$E_G = \frac{dQ}{d\varepsilon} = E_0 + K_1 \cdot Q \qquad \text{(GD.1-3)}$$

$$Q = \left[\exp\left(K_1 \cdot \varepsilon\right) - 1\right] \cdot \frac{E_0}{K_1} \approx E_0 \cdot \varepsilon \cdot \left(1 + K_1 \cdot \frac{\varepsilon}{2}\right) \qquad \text{(GD.1-4)}$$

The resultant gasket force is

$$F_G = \pi \cdot d_{Ge} \cdot \int Q_{(x)} dx \qquad \left(0 \le x \le b_{Ga}\right) \qquad \text{(GD.1-5)}$$

acting at x = c, given by:

$$c \cdot \int Q_{(x)} dx = c \cdot \int Q_{(x)} \cdot x dx \quad \left(0 \le x \le b_{Ga}\right) \qquad \text{(GD.1-6)}$$

From this follows step by step:

$$F_G = \frac{1}{2} \pi \cdot d_{Ge} \cdot E_0 \cdot k \cdot b_{Ga}^2 \cdot \left(1 + \frac{K_1 \cdot k \cdot b_{Ga}}{3}\right) \qquad \text{(GD.1-7)}$$

$$c = \frac{2}{3} b_{Ga} \cdot \frac{1 + \frac{8}{3} K_1 \cdot k \cdot b_{Ga}}{1 + \frac{1}{3} K_1 \cdot k \cdot b_{Ga}} \qquad \text{(GD.1-8)}$$

$$b_{Ga} = \sqrt{\frac{2F_G \cdot e_G}{\pi \cdot d_{Ge} \cdot E_0 \cdot \left(\Theta_{F(1)} + \Theta_{F(2)}\right) \cdot \left(1 + \frac{K_1 \cdot k \cdot b_{Ga}}{3}\right)}} \qquad \text{(GD.1-9)}$$

$$b_{Gi} = 2\left(b_{Ga} - c\right) = \frac{2}{3} b_{Ga} \cdot \frac{1 + \frac{K_1 \cdot k \cdot b_{Ga}}{4}}{1 + \frac{K_1 \cdot k \cdot b_{Ga}}{3}}$$

$$b_{Gi} = \sqrt{\frac{F_G \cdot e_G \cdot \frac{8}{9} F(k)}{\pi \cdot d_{Ge} \cdot E_0 \cdot \left(\Theta_{F(1)} + \Theta_{F(2)}\right)}} \qquad \text{(GD.1-10a)}$$

$$\text{where } F(k) = \frac{\left(1 + \frac{K_1 \cdot k \cdot b_{Ga}}{4}\right)^2}{\left(1 + \frac{K_1 \cdot k \cdot b_{Ga}}{3}\right)^3} \qquad \text{(GD.1-10b)}$$

For $K_1 \cdot k \cdot b_{Ga} \ll 1$ is

$$F(k) = \frac{1}{1 + \frac{K_1 \cdot k \cdot b_{Ga}}{2}} \qquad \text{(GD.1-11)}$$

With $F_G = \pi \cdot d_{Ge} \cdot b_{Ge} \cdot Q$, where $Q$ is an average value, equation (GD.1-7) gives

$$E_0 \cdot k \cdot b_{Ga} = \frac{2Q \cdot b_{Ge}}{b_{Ga} \cdot \left(1 + \frac{K_1 \cdot k \cdot b_{Ga}}{3}\right)} \qquad \text{(GD.1-12)}$$

This value is required only in $F$(k) and connected to the (not very essential factor) $K_1$. Therefore the only rough approximation $E_0 \cdot k \cdot b_{Ga} \approx Q$ may be accepted. Further is simplified $\sqrt{\frac{8}{9}} \approx 1$. Then:

$$b_{Gi} = \sqrt{\frac{F_G \cdot e_G}{\pi \cdot d_{Ge} \cdot \left(\Theta_{F(1)} + \Theta_{F(2)}\right) \cdot \left(E_0 + K_1 \frac{Q}{2}\right)}} = b_{Ge(el)} \qquad \text{(GD.1-13)}$$

This is the equation for the elastic behaviour of the gasket, where $\left(\Theta_{F(1)} + \Theta_{F(2)}\right)$ are to be substituted by equation (GD.1-1). For the plastic behaviour is assumed:

$$b_{Ge(pl)} = \frac{F_G}{\pi \cdot d_{Ge} \cdot Q_{\max}} \qquad \text{(GD.1-14)}$$

True elasto-plastic deformation gives an effective width greater than for pure elastic and pure plastic deformation; approximately:

$$b_{Ge} = \sqrt{b_{Ge(el)}^2 + b_{Ge(pl)}^2} = b_{Gi} \qquad \text{(GD.1-15)}$$

The denomination $b_{Gi}$ is used for the real effective width is limited as follows:

$$b_{Ge} \min\left\{b_{Gi}; b_{Gt}\right\} \qquad \text{(GD.1-16)}$$

Note that the elastic modulus $E_G = E_0 + K_1 Q$ it is defined and measured for unloading/reloading (see GB-6). Here it is used for initial loading also, because validated data for loading are missed.

(b) For a gasket with curved surfaces (simple contact) the following was calculated:

For elastic deformation (Hertzian contact) the contact width and the maximum contact pressure are:

$$b_{Ga}^2 = \frac{32}{\pi} \cdot F_G \cdot r_2 \cdot \frac{1 - \nu^2}{E_G \cdot \pi \cdot d_{Ge}} \qquad \text{(GD.1-17)}$$

$$Q_{\max} = \frac{4}{\pi} \cdot \frac{F_G}{\pi \cdot d_{Ge} \cdot b_{Ga}} \qquad \text{(GD.1-18)}$$

It is assumed this maximum contact pressure $Q_{\max}$ within the contact width $b_{Ga}$ is equal the mean contact pressure $Q$ over the effective gasket widt $b_{Ge}$:

$$Q_{\max} = Q = \frac{F_G}{\pi \cdot d_{Ge} \cdot b_{Ga}} \qquad \text{(GD.1-19)}$$

Therefore:

$$b_{Ge} = b_{Ga} \cdot \frac{\pi}{4} \qquad \text{(GD.1-20)}$$

$$b_{Ge} = \sqrt{2\pi F_G r_2 \cdot \frac{1-\nu^2}{\pi E_G d_{Ge}}} \qquad \text{(GD.1-21)}$$

Finally here is simplified $2\pi\left(1-\nu^2\right) \approx 6$ (similar to 8/9 ≈1 for flat gaskets). The plastic effects are assumed equal as for flat gaskets.

### GD-2 Required internal forces

The required internal forces in flange connections are given by two general requirements:

(1) No loss of contact at all contact surfaces in all load conditions.

(2) Sufficient gasket pressure to prevent leakage in all load conditions.

In all subsequent conditions both requirements are represented by the following formula (G.6-9):

$$F_{G(I)\min} = \max\left\{A_{Ge} \cdot Q_{(I)\min};\ -\left(F_{Q(I)} + F_{R(I)}\right)\right\} \qquad \text{(GD.2-1)}$$

In the assembly condition with I = 0 this formula also should be respected (although $Q_{(0)min}$ is under discussion), however it is not sufficient:

Only by a sufficient large bolt load in assemblage the required gasket forces in the subsequent conditions can be guaranteed. Therefore it must be {Formulae (GB.7-6) and (G.6-10), (G.6-11)}:

$$F_{G(0)} \geq \frac{\left\{F_{G(I)\min} \cdot Y_{G(I)} + F_{Q(I)} \cdot Y_{Q(I)} + F_{R(I)} \cdot Y_{R(I)} - F_{R(0)} \cdot Y_{R(0)} + \Delta U_{(I)}\right\}}{Y_{G(0)}} = F_{G\Delta} \qquad \text{(GD.2-2)}$$

or

$$F_{G(0)} \geq \max\left\{F_{G(0)\min};\ F_{G\Delta}\right\} = F_{G(0)req} \qquad \text{(GD.2-3)}$$

### GD-3 Scatter of bolt-load in assemblage

All bolt-tightening methods involve some degree of inaccuracy. The real bolt load in the assemblage load condition (after bolt-tightening) therefore more or less deviates from the intended bolt load. The deviations have a statistic character. The scatter-values are named by $\varepsilon$. They are assumed to decrease if the number of bolts increases. Possibly the scatter values $\varepsilon_+$ above the nominal load are different from the scatter values $\varepsilon_-$ below the nominal load.

For a connection with $n_B$ bolts the scatter depending relations are (see G.6.5.2):

$$F_{B0,\min} \leq F_{B0,nom} \leq F_{B0,\max} \qquad \text{(GD.3-1)}$$

$$F_{B0,\min} = F_{B0,nom} \cdot \left(1-\varepsilon_{n-}\right); \qquad F_{B0,\max} = F_{B0,nom} \cdot \left(1+\varepsilon_{n+}\right) \qquad \text{(GD.3-2)}$$

$$\varepsilon_{n-} = \varepsilon_{1-} \cdot \frac{1+\frac{3}{\sqrt{n_B}}}{4}; \qquad \varepsilon_{n+} = \varepsilon_{1+} \cdot \frac{1+\frac{3}{\sqrt{n_B}}}{4} \qquad \text{(GD.3-3)}$$

To ensure that the flange connection is tight (also for the minimum forces) and not overloaded (also for the maximum forces) the following relations should be met (compare (GA-1)):

$$F_{B0,req} \leq F_{B0,\min} \leq F_{B0,nom} \leq F_{B0,\max} \leq F_{B0,allowable} \qquad \text{(GD.3-4)}$$

Therefore the bolting up parameters are to be defined for $F_{B0,nom}$ with the following conditions:

$$F_{B0,req} \le F_{B0,nom}\left(1-\varepsilon_{n-}\right) \qquad \text{(GD.3-5)}$$

**GD-4 Plastic deformation after assemblage, multiple assemblages**

Due to the foregoing requirements {equations (GD.2-3) and (GD.3-5) } the real bolt load in assemblage always is higher (may be considerably higher) than that required for the subsequent load conditions. Therefore a limited lowering of the bolt load due to small plastic deformations may and shall be permitted. The design for subsequent load conditions could be based on $F_{G(0)} = F_{G\Delta}$. However repeated plastic deformation due to repeated dismounting and reassemblage must be avoided. To avoid progressive distortion the plastic deformation is to be limited: The design for subsequent load conditions should be based on $F_{G(0)} = F_{G(0)d}$, where the design assembly gasket load $F_{G(0)d}$ may be greater than $F_{G\Delta}$.

The following considerations gives an estimation for $F_{G(0)d}$ :

Assemblage with a bolt load $F_{B(0)max}$ produces a maximal strain $\varepsilon_{max}$. (Do not interchange $\varepsilon_{max}$ and the scatter value $\varepsilon_{\pm}$). $N_R$ -times change of the bolt load from $F_{B(0)max}$ to a lower actual bolt load $F_{B(0)act}$ and back, in the worst case is connected with a cumulative strain change:

$$\Delta\varepsilon_R \approx N_R \cdot \varepsilon_{\max} \cdot \left(1-\frac{F_{B(0)act}}{F_{B(0)\max}}\right) \qquad \text{(GD.4-1)}$$

It should be limited

$$\Delta\varepsilon_R \le C \cdot \varepsilon_{\max} \qquad \text{(GD.4-2)}$$

$$F_{B(0)act} \ge F_{B(0)\max}\left(1-\frac{C}{N_R}\right) \qquad \text{(GD.4-3)}$$

For usual materials the nominal design stresses are such that $\varepsilon_{max} \le 0{,}001 \ldots 0{,}002$, while the elongations

at rupture are $\varepsilon_{rupt} \ge 0{,}1 \ldots 0{,}2$. Therefore the factor $C$ could be assumed (conservative) as follows:

$$C \approx 10 \qquad \left(C \approx 5...20\right) \qquad \text{(GD.4-4)}$$

If for subsequent load conditions is used a design load $F_{B(I)d}$, the usual safety factor 1,50 against yield stress guarantees that plastic deformations will not occur for $F_{B(I)act} < 1{,}5\ F_{B(I)d}$. Therefore the minimum design assembly bolt load to define the calculation bolt load in subsequent load conditions is assumed:

$$F_{B(0)d,\min} \approx \frac{2}{3} F_{B(0)act} \approx \frac{2}{3} F_{B(0)\max} \cdot \left(1-\frac{C}{N_R}\right) \qquad \text{(GD.4-5)}$$

This gives immediately:

$$F_{G(0)d} = \max\left\{F_{G\Delta}; \left[\frac{2}{3} F_{B(0)\max}\left(1-\frac{C}{N_R}\right) - F_{R(0)}\right]\right\} \qquad \text{(GD.4-6)}$$

Based on the foregoing considerations an important hint to useful application of the method shall be given:

Normally for flange connections three or more load conditions are considered: Assemblage-, Test- and Operating (one or more) conditions. The test pressure is higher than the operating pressures and therefore (by $F_{G\Delta}$) it determines the required bolt load in assemblage. If one calculation is made for all three or more load conditions, the test condition may be applied at any time, also after some operating cycles; the high bolt load required for test is conserved over the operation cycles. This however in general is not necessary.

Normally the test pressure applies only once after assemblage, not after operating cycles. Therefore it may be useful to make two calculations as follows: one for assemblage and all operating conditions, and a second for assemblage and test condition. The second gives the more strong and therefore governing assemblage requirements. During operating conditions possibly (not necessary) the bolt load lowers and the test pressure then should not be allowed. However - if $F_{B(0)d,min}$ is met - this is no problem: After dismounting and reassemblage all requirements are fulfilled!

**GD-5 Load transfer diameter for loose flanges**

The load transfer diameter $d_7$ is the diameter of the circle where the resultant force ($F_B$) between the loose flange and the stub or collar acts. The value $d_7$ is yet undetermined but limited: $d_{7,min} \le d_7 \le d_{7,max}$. For large internal fluid pressure $P$ and/or positive additional force $F_R$ obviously $d_7$ will be near $d_{7,min}$. For assemblage without $P$ and $F_R$ may be expected $d_7$ near $d_{7,max}$. If there is a flat soft gasket over the whole width of the stub or collar, the

diameter $d_7$ may be calculated for equal rotation of loose flange and stub or collar: $\Theta_L = \Theta_F$ . In assemblage with $F_Q = F_R = 0$ it follows:

$$\Theta_L = F_{B(0)} \cdot h_L \cdot \frac{Z_L}{E_{L(0)}}; \quad \Theta_F = F_{B(0)} \cdot h_G \cdot \frac{Z_F}{E_{F(0)}} \tag{GD.5-1}$$

$$h_L = \frac{d_{3e} - d_7}{2}; \quad h_G = \frac{d_7 - d_{Ge}}{2} \tag{GD.5-2}$$

$$d_7 = \frac{d_{Ge} + d_{3e} \cdot \kappa}{1 + \kappa} = d_{7(0)}; \quad \kappa = \frac{Z_L \cdot E_{F(0)}}{Z_F \cdot E_{L(0)}} \tag{GD.5-3}$$

In equation (G.5-63) this equation is combined with the basic limits $d_{7,min} \leq d_{7(0)} \leq d_{7,max}$.

**GD-6 Conditions of applicability**

The method Annex G gives many restrictions and validity limits. Some of them are short repeated and explained in the following:

- The whole assembly is axisymmetric. Small deviations such as those due to a finite number of bolts are permitted. There are four or more identical, uniformly distributed bolts.

  - Axisymmetric geometry and loading are basically for all included calculations.
  - Identical bolts are normally in use. The minimum number four is a compromise.

- The circular gasket is located entirely within the bolt circle on plane surfaces and compressed axially. Its modulus of elasticity may increase with the compressive stress $Q$ on the gasket.

  - Full face gaskets (bolt holes within the gasket width) for simplicity are not taken into account.

  Otherwise it would be necessary the effective gasket width to determine different for each load condition. Gaskets outside the bolt circle are omitted for their only exceptional use.

  - Gaskets on plane surfaces are mentioned for possible unexpected leakages at uneven surfaces.
  - Gaskets compressed axially are mentioned for e.g. radially tightening gaskets are not respected.
  - The variable modulus $E_G = E_0 + K_1 Q$ is an approximation for a more general behaviour.

It is necessary to respect that in each case always must be $E_G > 0$. ($E_0 < 0$ is unacceptable!).

- The flange dimensions met the following conditions:

$0{,}2 \leq b_F/e_F \leq 5{,}0$; $0{,}2 \leq b_L/e_L \leq 5{,}0$ and $e_F \geq \max \{e_2 ; d_{B0}; p_B \cdot \{(0{,}01 \ldots 0{,}10) \cdot p_B/b_F\}^{1/3}$

  - The first limits are estimated for the acceptance of the ring with an undeformed cross section. For $b_F/e_F \leq 0{,}1$ commonly are assumed calculations for shells; for $10 \leq b_F/e_F$ those for plates. The reduced allowable load ratio $\Phi_{max} < 1{,}0$ for $d_4/d_0 > 2{,}0$ equation (G.7-2) has a similar reason.

  It was introduced in TGL 32903/13 [8] for safety reasons; probably it can be waived.

  - The last limit (more precise in G.8.1) is intended to restrict the non-uniformity of the gasket compressive stress. It is based on a conservative estimate for the non-axisymmetric deformation of the flange ring. It was included after discussion in CEN; probably it can be waived. An alternative could be a comparable estimate to include in the check for tightness.

- The shell met the condition $\cos\varphi_S \geq 1/\{ 1+0{,}01 \cdot d_s / e_s \}$

  - This limit is introduced for the analytic solution for the elastic shell is approximately only (see Annex GB-1 here). A numerical verification with two different computer programs shows no serious contradictions, but it gave no better or more general solution.

**GD-7 Experimental verification**

The CEN REPORT [9] to EN 1591-1 in its Annex B gives information about measurements for bolt load and/or tightness of nearly 20 flange connections (diameter 50mm, 100mm, 400mm, up to 1200mm). All measurements more or less precise verify the basic calculations for required and actual forces.

## GE Future work

(1) The simplification of equal elastic moduli and equal temperatures for flange and shell shall be omitted. Different materials and temperatures of flange and shell should be respected. This requires (instead of the used equivalent cylindrical shells) more precisely to investigate conical hub and shell, both for elastic deformation and for limit load.

(2) Possibly present washers shall be explicitly included in the calculation. This includes to define dimensions and material properties of the washers, but it is no problem.

(3) Some corrections could be recommendable to be compatible with future "Heat exchanger tubesheet flange connections" (see Annex J-5). This includes e.g. to calculate a circular plate with a thicker flange at the outer diameter, where the midplane of the plate is not those of the flange.

Also flange connections with non axisymmetric loadings could be calculated (also Annex J-5).

Instead of the limitation G.8.1 this effect then could be included in the check for tightness.

(4) It will be necessary to update the method so that the results of new gasket investigations may be applied (e.g. [11], probably a new edition of EN 1591-2 [10]). However surely then again new gasket parameters will be required which are not available, e.g. data for irreversible deformation.

(5) Possibly the effective gasket width could be calculated variable with the loading and depending on the load cases. Then the to day open questions for full-face flanges and for spacer-seated flanges may be solved.

## GF Bibliography


[1] Wesstrom, D.B. and Bergh, W.D.: "Effect of Internal Pressure on Stresses and Strains in BoltedFlanged Connections"; Transactions of the ASME, July, 1951.

[2] Materialy k edinym normam i metodam rasceta na procnost sosudov i apparatov.

(Basics to unifyed normes and methods for strength calculation of vessels and apparates.)

Sovjet Ekonomiceskoj Vsaimopomoshci, Postojannaja Komissija po Mashinostroeniju, Sekcija

No. l2 (COMECON, Permanent Commission for Engineering, Section No. 12), Moskva, 1963:

6: "Flancevije sojedinenija" (Clause 6: Flange connections): Authors: Karasev, L.P. i Perzev, L.P.

[3] DIN 2505 (Vornorm Okt.1964, Entwurf Nov.1972, Vornorm Jan. 1986, Entwurf April 1990)

"Berechnung von Flanschverbindungen". Teil 1: Berechnung; Teil 2: Dichtungskennwerte.

[4] RichtlinienKatalog Eestigkeitsberechnungen (RKF), Behälter und Apparate; Teil 1, BR-A13:

"Apparatebauelemente. Flanschverbindungen" (Flange connections); Dresden 1971. 1973;

VEB Komplette Chemieanlagen Dresden, 1979 (Author: J.Wölfel).

[5] Wölfel, J. und Räbisch, W.: "Berechnung und Standardisierung von Flanschverbindungen"

Chemische Technik, Leipzig, August 1975.

[6] TGL 20360 (1977) "Flanschverbindungen. Berechnung auf Festigkeit und Dichtigkeit"

[7] Wölfel, J.: "Berechnung der Festigkeit und Dichtigkeit von Flanschverbindungen" Maschinenbautechnik, Berlin, Juni 1985.

[8] TGL 32903/13 (1983) "Behälter und Apparate. Festigkeitsberechnung. Flanschverbindungen"

[9] CR 13642 (1999): CEN REPORT: "Flanges and their joints - Design rules for gasketed circular

flange connections - Background information"

[10] EN 1591-1: 2001: "Flanges and their joints - Design rules for gasketed circular flange connections

Part 1: Calculation method" (EN 1591-2: Gasket parameters.)

[11] PERL = Pressure Equipment, Reduction of Leak rate: Gasket parameters measurement.

Project funded by the European Community (1998-2002). Coordinator: ASE Ltd Cambridge UK.

# Annex H Table H-1 Gasket factors m and y

No comments.

# Annex I Additional information on heat exchanger tubesheet design

No comments.

# Annex J Alternative methods for the design of heat exchanger tubesheets

## JA Introduction

The calculation of heat exchanger tubesheets in the last sixty years in Germany mainly was based on semi-empirical formulae [1]. Some trials to use modern theory of elasticity ([2], [3]) gave results contradicting to long experiences. Therefore limit load calculations was tested and gave excellent results corresponding to the experiences ([3], [4]). These methods are used in a Standard of COMECON and in TGL 32903-23 [5]. An improved form is given in EN 13445-3, Annex J.

## JB Basic assumptions

### JB-1 Design principles

The assumed design principles corresponds to EN 13445-3, Annex B. Especially this means:

- Design for maximum static loads in any load condition (load case) is based on limit load analysis.

  Slightely generalized here is included design against instability. It uses the design loads.

- Design for cyclic load changes is based on linear elasticity. This is provided similar to fatigue assessment in clauses 17 and 18. It uses the operating loads (not the design loads).

### JB-2 Design details

Main components of all tubular heat exchangers are the tubebundle, shell and channels, including connected vessel flanges. Mainly considered is the tubebundle, consisting of the following parts:

- Tubesheets (Plates, subscript P), per heat exchanger in general two, in U-tube-types only one.
- Tubes (Subscript T), a large number $N_T$ ; equal dimensions $d_T \cdot e_T \cdot L_T$ .
- Baffles; their distances define the buckling length of the inner tubes.

The tubesheets are calculated as flat plates with a constant thickness $e_p$. The tubed region is nearly homogeneous weakened by a large number of tube holes (diameter $d_0$, equal pitch $p$). Outside the tubed region is an untubed rim with the same thickness $e_p$, and outside this may be a flange. The tubesheets may be supported (connected) by the inner tubes. All mentioned parts are assumed to be axisymmetric.

The method applies to the following loads:

- Fluid pressures tube side ( $P_T$ ) and shell side ( $P_S$ ), both arbitrary internal or external;
- Boundary moments at the outside boundary of tubesheets;
- Weight of the vertical tubebundle;
- Axial thermal expansion (to be calculated only for fixed tubesheets without expansion bellows).

### JB-3 Notations

The explanations in Annex J are to be completed as follows:

Allowable loads (and otherwise load limited single values) are indicated by inclusion in square brackets. Examples: [F] = allowable force; [M] = allowable moment; [P] = allowable pressure.

**JB-4 Tubes as plate supports**

The boundary between the tubed and the untubed region is approximated by a circle with the diameter $d_1$. This should be not the outermost circle around all tubes but a "realistic" average. It is calculated by use of the real number of tubes $N_T$ and an additional number of ideal possible tubes $N_I$ as follows:

$$d_1 = 2 \cdot p \cdot \{(N_T + N_I)/(\pi \cdot \Theta)\}^{1/2} \qquad \text{(JB.4-1)}$$

The determination of $N_I$ is not easy and requires some judgement. For safety reasons is proposed to calculate two or more variants using different values $d_1$, where the most unfortunate is to be used. (Such strong requirement is necessary while no calculation for a non-axisymmetric tubed region is available.)

For tubebundles having two tubesheets and straight tubes between them, within the tubed region an effective fluid pressure $P_E$ is used. It is less than the direct difference of both pressures $P_D$:

$$P_D = P_T - P_S\,; \qquad P_E = P_T \cdot x_T - P_S \cdot x_S \qquad \text{(JB.4-2)}$$

The values $x_T$ and $x_S$ are also contents of the subclauses 13.5 and 13.6.

The tube support per area unit is determined by the relative tube cross section area within the tubed region:

$$\vartheta = x_T - x_S = 4 \cdot N_T \cdot (d_T - e_T) \cdot e_T / d_I^2 \qquad \text{(JB.4-3)}$$

The support force per area unit is named by Q and limited as follows:

$$-[Q_c] = +\vartheta \cdot [\sigma_{x,\min}] \le Q = +\vartheta \cdot \sigma_\chi \le +[Q_t] = +\vartheta \cdot [\sigma_{x,\max}] \qquad \text{(JB.4-4)}$$

The maximum allowable tensile stress in the tubes $[\sigma_{x,\max}] = +f_{T,t}$ is limited by the Tresca criterion.

The minimum allowable compressive stress in the tubes $[\sigma_{x,\min}] = -f_{T,c}$ $(f_{T,c} > 0)$ also respects the Tresca criterion, however govern is the elastic buckling:

Elastic buckling of tubes was investigated in a special work:

The calculation system is shown in Figure JB-1. The tube between the two clamped ends has a total free length $L_T, N_{B,e}$ effective supporting baffles and $N_{B,e}+1$ regions. The cross section $d_T \cdot e_T$ and all material properties are constant.

The tube is loaded by an axial compressive force $F_c$, an internal fluid pressure $P_i = P_T$, and an external fluid pressure $P_e = P_S$. The total bending deformation of the (theoretical straight) axis is $V = V_{(z)}$.

The unloaded tube has an initial deformation $V_{(0)}$ which shall meet the same boundary conditions as the final total deformation *V*.

The elastic deformation is calculated generally for arbitrary lengths $l_j$. The required minimum eigenvalues are numerical calculated for equal distances between the baffles, q.e. $l_2 = l_3 = \ldots$ ; only $l_1$ and $l_{Ne+1}$ may be different. (These lengths in Annex J are denominated by $l_B$ and $l_A$, $l_C$.) From the eigenvalues are derived the effective bucking lengths, which are given by a simple approximation formula (Table J-1).

Based on assumed initial deformations (Herve, see clause 13) the total stresses in the tubes are calculated. Between the both asymptotes "Plastic limit" and "Elastic instability" then is applied an asymptotic exact quadratic interpolation. If the asymptotes are correct, then all values between it are good approximated. This are the basics for Annex J, equation (J.7.3-2).

The strength of the connection between tube and tubesheet may be less than the strength of the tube itself. Such situation is unfortunately allowed, so it must be taken into account. For this reason is defined a fictitious nominal design stress $f_x$ for the connection, to be used as follows:

$$[Q_c] = +\vartheta \cdot \min\{f_X; f_{T,c}\}\,; \quad [Q_t] = +\vartheta \cdot \min\{fx; f_{T,t}\} \qquad \text{(JB.4-5)}$$

The calculation of $f_x$ is based on limit load approximations with the models of Figure JB-2.

For expanded and welded tubes the rule $f_X = f_{XW} + 0{,}6 \cdot f_{XE}$ is taken from TGL 32903/23 (based on a COMECON-Standard).

### JB-5 Tubesheets as weakened plates

An effective diameter of tubeholes in some tubesheet calculation methods is assumed either by the outside tube diameter $d_T$ or by the inside tube diameter $d_T - 2 \cdot e_T$. The first assumption may be unsafe, if the tubes are welded only and the gap $d_0 - d_T$ is not small; but it may be too conservative also, if the attachment length $l_X$ is large or the tubesheet thickness is very small. In the applied final assumption the second assumption is accepted as a limit for safety reasons:

$$d_{0,e} = \max \left\{ d_0 - 2 \cdot \delta_X \cdot A_X / e_p ; d_T - 2 \cdot e_T \right\} \qquad \text{(JB.5-1)}$$

The perforated tubesheet is calculated as an unperforated plate with reduced strength. The ratio of the reduced to the non reduced strength is the "ligament efficiency", in Germany called "weakening factor". Figure JB-3 shows the calculation model used in the following, where $d_E = d_{0,e}$.

Limit loads for one ligament in the perforated tubesheet are calculated as follows:

Allowable limit bending moment for one ligament:

$$[M_b] = [\sigma]_P \cdot b_E \cdot e_P^2 / 4 \qquad \text{(JB.5-2)}$$

Allowable limit torsion moment for one ligament as a long beam (Figure left):

$$[M_t] = [\tau]_p \cdot \left(b_E - e_p / 3\right) \cdot e_p{}^2 / 4 \qquad \text{for } b_E \geq e_p \qquad \text{(JB.5-3a)}$$

$$[M_t] = [\tau]_p \cdot \left(e_p - b_E / 3\right) \cdot b_E{}^2 / 4 \qquad \text{for } b_E \leq e_p \qquad \text{(JB.5-3b)}$$

$$[\tau]_p = (0{,}500 \ldots 0{,}577) \cdot [\sigma]_p \qquad \textit{(Tresca…Mises)} \qquad \text{(JB.5-4)}$$

Allowable limit torsion moment for one ligament as a short beam (Figure right):

$$[M_t] = [\tau]_Q \cdot b_E \cdot e_p{}^2 / 4 = \kappa_p \cdot [M_b] \qquad \text{(JB.5-5)}$$

$$\kappa_p{}^2 = (b_E / p) \cdot (1 - b_E / p) \qquad \text{for } b_E / p \leq 0{,}5 \qquad \text{(JB.5-6a)}$$

$$\kappa_p{}^2 = 1/4 \qquad \text{for } b_E / p \geq 0{,}5 \qquad \text{(JB.5-6b)}$$

The last equations are found from the worst section y = constant in Figure JB-3.

The allowable limit torsion moment for a short beam (JB.5-5) in nearly all practical cases is greater than those for a long beam (JB.5-3a,b). Both are static admissible; therefore the better remit is used always. (If in exceptional cases the long beam gives the better result, then the used result is conservative and also acceptable).

Limit loads for the equivalent quasi homogeneous plate are calculated as follows:

For a really homogeneous plate the following limit load condition is valid (Tresca):

$$\max \left\{ |M_1| ; |M_2| ; |M_1 - M_2| \right\} \leq [M]_P = [\sigma]_p \cdot b_e \cdot e_p{}^2 / 4 \qquad \text{(JB.5-7)}$$

For the perforated plate with an arbitrary orientation of the ligament (Figure, angle $\psi$) the following

equilibrium conditions hold:

$$M_b = p \cdot \left(M_1 \cdot \cos^2 \psi + M_2 \cdot \sin^2 \psi\right) \qquad \text{(JB.5-8a)}$$

$$M_t = p \cdot (M_1 - M_2) \cdot \sin \psi \cdot \cos \psi \qquad \text{(JB.5-8b)}$$

The general limit load condition for the ligament is (Tresca and/or Mises):

$$\{M_b / [M_b]\}^2 + \{M_t / [M_t]\}^2 \leq 1 \qquad \text{(JB.5-9)}$$

Substitutions and abbreviations:

$$[M_b] = [M]_P \cdot b_E \; ; \qquad [M_t] = [M]_P \cdot b_E \cdot \kappa_p \qquad \text{(JB.5-10)}$$

$$\varphi_p = b_E / p = 1 - d_E / p \; ; \qquad \kappa_p = [\kappa]_Q / [\sigma]_p \qquad \text{(JB.5-11)}$$

$$m_1 = M_1 / \left([M]_P \cdot \varphi_P\right) \; ; \qquad m_2 = M_2 / \left([M]_P \cdot \varphi_p\right) \qquad \text{(JB.5-12)}$$

$$m_m = (m_1 + m_2)/2 \ ; \qquad m_d = (m_1 - m_2)/2 \qquad \text{(JB.5-13)}$$

From the given equations is evaluated the solution for the worst orientation of the ligament. However for realistic plates the governing solution is not that for the worst orientation of the ligaments but an average between the worst and the best. Such a solution is given by the following limit load equation:

$$\max\left\{|m_1|;|m_2|;|m_1 - m_2|/(2\cdot\kappa_p)\right\} \le 1 \qquad \text{(JB.5-14)}$$

Figure JB-4 shows examples of these results and those for the worst orientation.

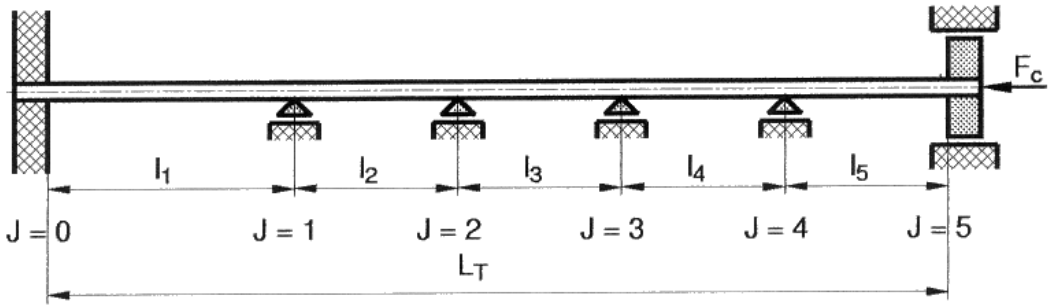


One tube with $N_{B,e} = M = 4$ effective supporting baffles

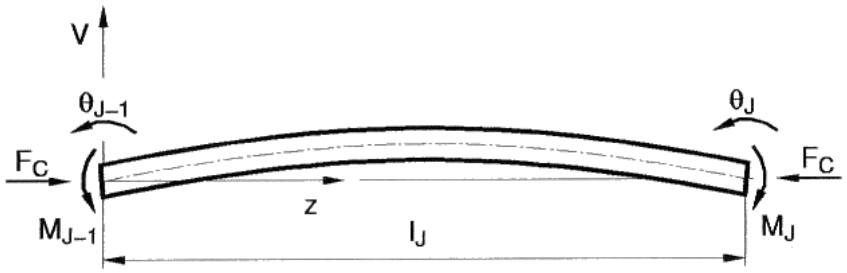


One region of the tube between two supporting baffles

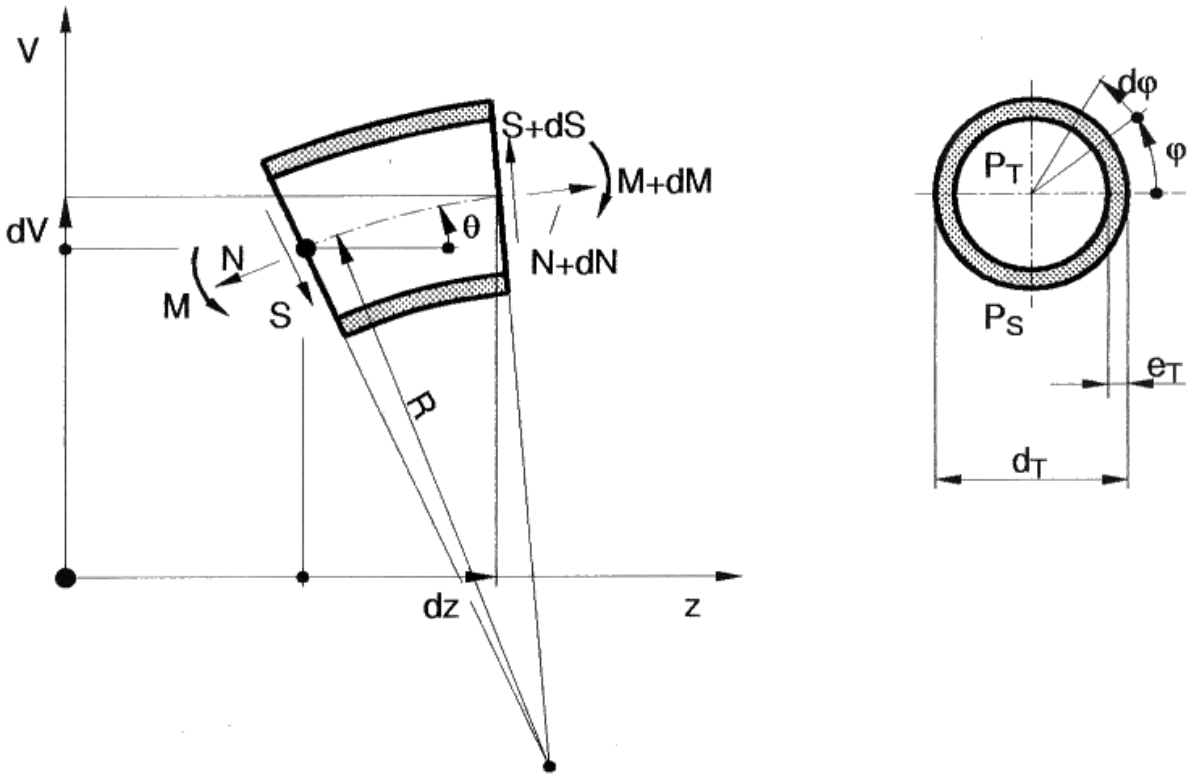


Details within one region of the tube

**Figure JB-1: Tube loaded by axial compressive force** $F_c$

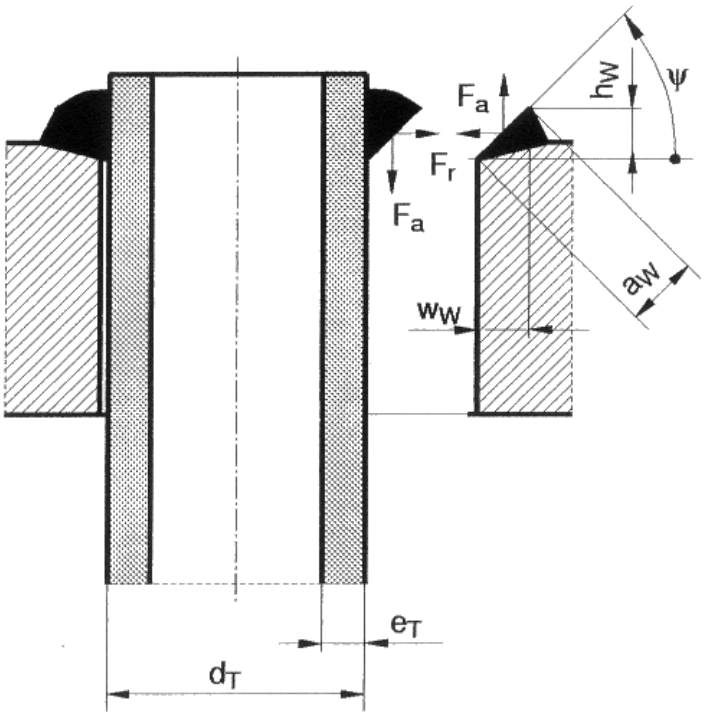


Tube-to-tubesheet-connection welded only

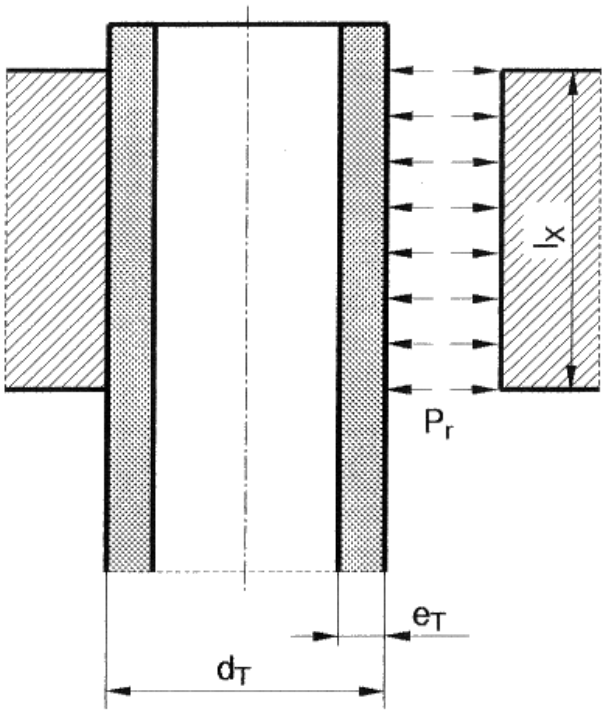


Tube-to-tubesheet-connection expanded only

**Figure JB-2: Tube-to-tubesheet-connections**

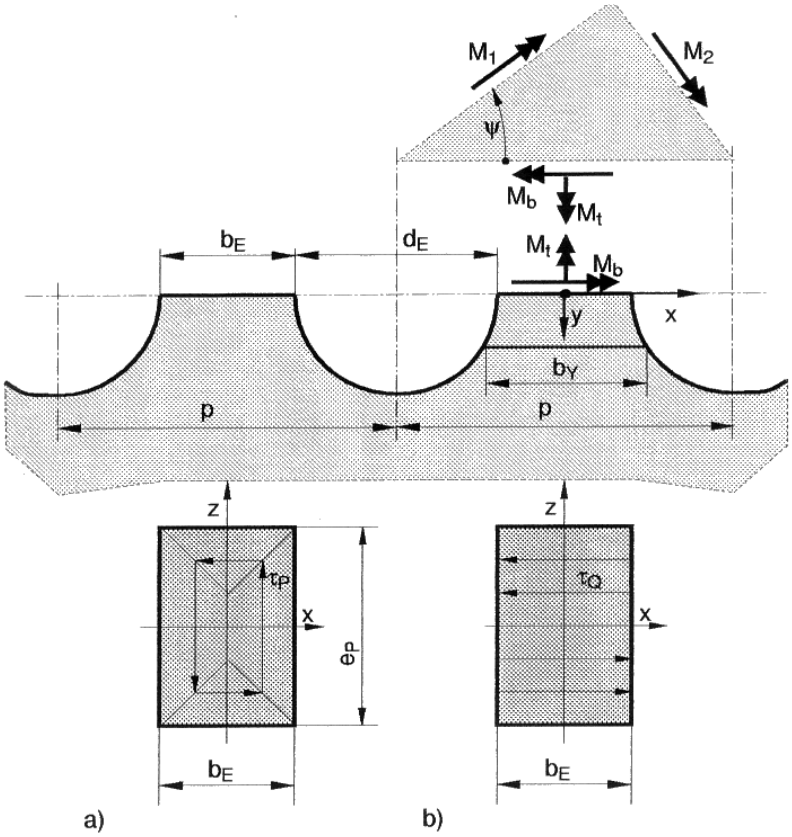


**Figure JB-3: Weakened plate/Ligaments**

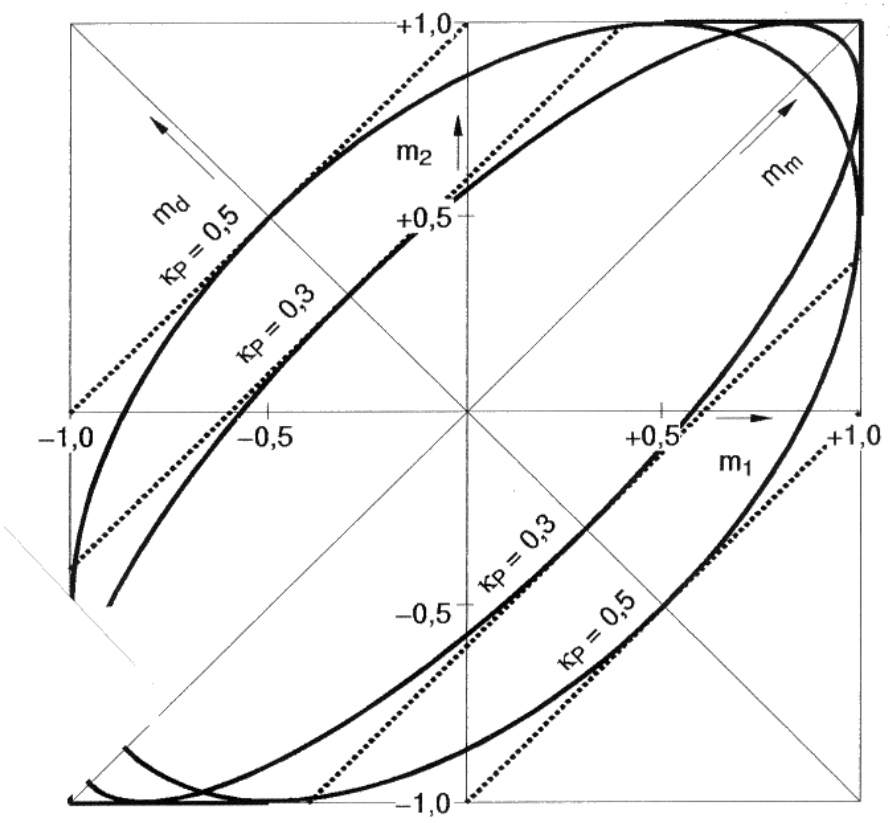


**Figure JB-4: Limit load curves for weakened plates**

## JC Limit loads of the tubebundle

### JC-1 Limit load of the axisymmetric tubed region

The geometric axisymmetric tubebundle is axisymmetricly loaded by the boundary shear force $S_1$, the boundary bending moment $M_1$ and the effective fluid pressure $P_E$.

Figures JC-1 and JC-2 show the calculation model for the whole tubebundle (two tubesheets and many tubes) and for a single tubesheet. First is calculated its central tubed region $0 \le r \le r_1$.

The reactions of the tubes are $Q_X$; they are assumed to be constant within each of two zones:

$0 \le r < \zeta \cdot r_1$ : $Q_X = Q_I$ *(English: Inner zone; German: Innen-Zone)*

$\zeta \cdot r_1 < r \le r_1$ : $Q_X = Q_A$ *(English: Outer zone; German: Auβen-Zone)*

The parameter $\zeta (0 \le \zeta \le 1)$ defines the boundary between both zones. It will be calculated below.

Resultant tubebundle loads (forces per area unit): $P_X = P_E + Q_X$ :

$0 \le r < \zeta \cdot r_1$ : $P_X = P_I = P_E + Q_I$ (JC.1-1)

$\zeta \cdot r_1 < r \le r_1$ : $P_X = P_A = P_E + Q_A$ (JC.1-2)

Equilibrium conditions :

Forces : $(r \cdot S_r)_{|r} - P_X \cdot r = 0$ (JC.1-3)

Moments : $(r \cdot M_{rr})_{|r} - M_{\varphi\varphi} + (r \cdot S_r) = 0$ (JC.1-4)

NOTE: The symbol $(\ )_{|r}$ means the differentiation $d(\ )/dr$

Limit load conditions :

Tubes: $-[Q_c] \le Q_X \le +[Q_t]$ (JC.1-5)

Plates: $\max\left\{|M_{rr}|; |M_{\varphi\varphi}|; |M_{rr} - M_{\varphi\varphi}| / (2 \cdot \kappa_p)\right\} \le \varphi_P * [M]_p$ (JC.1-6)

Allowable (limit) bending moment (unpierced, non-weakened plate):

$$[M]_P = f_P \cdot {e_P}^2 / 4 \quad \text{(JC.1-7)}$$

The tube reactions from the limit load condition of the tubes and looking at Figure JC-6 follows:

For $-[Q_t] \le P_E \le +[Q_c]$:

$$Q_1 = -P_E \quad \rightarrow \quad P_1 = 0 \quad \text{(optimum case)} \quad \text{(JC.1-8)}$$

Then:

For $S_1 > 0$: $Q_A = +[Q_t]$ (JC.1-9a)

For $S_1 < 0$: $Q_A = -[Q_c]$ (JC.1-9b)

For $+[Q_c] \le P_E$:

$$Q_I = -[Q_c] \quad \rightarrow \quad P_1 > 0 \quad \text{(JC.1-10)}$$

Then for equilibrium it is necessary $S_1 > 0 \quad \rightarrow$

$$Q_A = +[Q_t] \quad \text{(JC.1-11)}$$

For $P_E \le -[Q_t]$:

$$Q_I = +[Q_t] \quad \rightarrow \quad P_1 < 0 \quad \text{(JC.1-12)}$$

Then for equilibrium it is necessary $S_I < 0 \quad \rightarrow$

$$Q_A = -[Q_c] \quad \text{(JC.1-13)}$$

**Dimensionless basic equations** are used for the following solutions:

Parameters:

$\rho = r / r_1 \quad (0 \le \rho \le 1)$ ( $\zeta$ and $\eta$ are special values of $\rho$ ) (JC.1-14)

$m_{XX} = M_{XX} / [M]_P$ (Subscript X here is used as a general subscript) (JC.1-15)

$s_X = S_X \cdot r_1 / (2 \cdot [M]_p)$ (JC.1-16)

$p_X = p_X \cdot {r_1}^2 / \cdot (4 \cdot [M]_p)$; (JC.1-17)

$q_X = Q_X \cdot {r_1}^2 / (4 \cdot [M]_P)$ (JC.1-18)

Equilibrium conditions:

$(\rho \cdot s_r)|_\rho - 2 \cdot p_X \cdot \rho = 0$ (JC.1-19)

$(\rho \cdot m_{rr})|_\rho - m_{\varphi\varphi} + 2 \cdot \rho \cdot s_r = 0$ (JC.1-20)

Limit load conditions:

$-[q_c] \le qx \le [q_t]$ (JC.1-21)

$\max\left\{|m_{rr}|; |m_{\varphi\varphi}|; |m_{rr} - m_{\varphi\varphi}| / (2 \cdot \kappa_p)\right\} \le \varphi_p$ (JC.1-22)

**General solutions:**

First equilibrium condition for $p_x = const.$:

$$(\rho \cdot s_r) = +p_x \cdot \rho^2 + const. \quad \text{(JC.1-23)}$$

Centre of plate $(\rho = 0)$: $s_{r(\rho=0)} = 0 \quad \rightarrow$

$0 \le \rho \le \zeta$: $(\rho \cdot s_r) = +p_I \cdot \rho^2$ (JC.1-24)

$\zeta \le \rho \le 1$: $(\rho \cdot s_r) = +p_I \cdot \zeta^2 + P_A \cdot (\rho^2 - \zeta^2) = +p_I \cdot \rho^2 + (p_A - p_I) \cdot (\rho^2 - \zeta^2)$ (JC.1-25)

Boundary $(\rho = 1) \quad (1 \cdot s_1) = +p_I \cdot 1 + (p_A - p_I) \cdot (1 - \zeta^2) = p_R \quad \rightarrow$

$$\zeta^2 = (p_A - s_1)/(p_A - p_I) = (p_A - p_R)/(p_A - p_I) \quad \text{(JC.1-26)}$$

The here introduced equivalence

$$s_1 = p_R \tag{JC.1-27}$$

replaces the shear force $s_1$ by a corresponding pressure $p_R$.

The parameter $\zeta$ is independent of the design (thickness $e_p$) of the tubesheets and also of the edge moments applied to them. This independence is what makes it possible to calculate each tubesheet separately and give them different thicknesses.

From the obviously general requirement $0 \le \zeta \le 1$ it follows

$$\textit{either} \quad 0 \le p_I \le p_R \le p_A \quad \textit{or} \quad p_A \le p_R \le p_I \le 0 \tag{JC.1-28}$$

By use of a sign variable

$$j = sign(p_A) = sign(p_R) = \pm 1 \tag{JC.1-29}$$

equation (JC.1-28) becomes :

$$0 \le j \cdot p_I \le j \cdot p_R \le j \cdot p_A \tag{JC.1-30}$$

From the second equilibrium condition and from the limit load condition for the plate it follows:

$$0 \le \rho \le \eta : \quad m_{\varphi\varphi} = j \cdot \varphi_P \quad \text{and} \quad m_{rr(\rho=0)} = m_{\varphi\varphi(\rho=0)} \rightarrow$$

$$(\rho \cdot m_{rr}) = j \cdot \rho \cdot \varphi_P - 2 \cdot \int (\rho \cdot s_r) \cdot d\rho \tag{JC.1-31}$$

$$\eta \le \rho \le 1 : \quad m_{\varphi\varphi} = m_{rr} + j \cdot 2 \cdot \kappa_p \cdot \varphi_P \quad \text{and} \quad m_{rr(\rho=1)} = +m_1 \rightarrow$$

$$m_{rr} = j \cdot 2 \cdot \kappa_p \cdot \varphi_P \cdot \ln \rho - 2 \cdot \int s_r \cdot d\rho \tag{JC.1-32}$$

Further details depend on the relation between the parameters $\zeta$, $\eta$, and 1. (At $\rho = \zeta$ is the boundary between the tube reactions $Q_I$ and $Q_A$ and at $\rho = \eta$ is the boundary where the second respective third term of the limit load condition (JC.1-22) is valid.)

Results (without details of the derivation)are given in the following cases 1 to 3.

**Case 1** : $0 \le \xi \le 1 \le \eta$ : (Whole plate (tubed region) with $m_{\varphi\varphi} = j \cdot \varphi_P$ )

$$0 \le \rho \le \zeta : \quad (\rho \cdot s_r) = +p_I \cdot \rho^2 \tag{JC.1-33}$$

$$m_{rr} = j \cdot \varphi_P - p_I \cdot (2/3) \cdot \rho^2 \tag{JC.1-34}$$

$$\zeta \le \rho \le 1 : \quad (\rho \cdot s_r) = +p_I \cdot \rho^2 + (p_A - p_I) \cdot (\rho^2 - \zeta^2) \tag{JC.1-35}$$

$$m_{rr} = j \cdot \varphi_P - p_I \cdot (2/3) \cdot \rho^2 - (p_A - p_I) \cdot (2/3) \cdot (\rho^2 - 3 \cdot \zeta^2 + 2 \cdot \zeta^3 / \rho) \tag{JC.1-36}$$

At the boundary $\rho = 1, m_{rr} = m_1$ $\rightarrow$

$$(2/3) \cdot \{(p_A - p_I) \cdot (1 - 3 \cdot \zeta^2 + 2 \cdot \zeta^3) + p_I\} + m_1 = j \cdot \varphi_P \tag{JC.1-37}$$

This is the limit load equation of Case 1.

**Case 2** : $0 \le \zeta \le \eta \le 1$ : (Characteristic of $m_{\varphi\varphi}$ changes at $\rho = \eta$ )

$$0 \le \rho \le \zeta : \quad (\rho \cdot s_r) = +p_I \cdot \rho^2 \tag{JC.1-38}$$

$$m_{rr} = j \cdot \varphi_P - p_I \cdot (2/3) \cdot \rho^2 \tag{JC.1-39}$$

$$\zeta \le \rho \le \eta : \quad (\rho \cdot s_r) = +p_I \cdot \rho^2 + (p_A - p_I) \cdot (\rho^2 - \zeta^2) \tag{JC.1-40}$$

$$m_{rr} = j \cdot \varphi_P - p_I \cdot (2/3) \cdot \rho^2 - (p_A - p_I) \cdot (2/3) \cdot (\rho^2 - 3 \cdot \zeta^2 + 2 \cdot \zeta^3 / \rho) \tag{JC.1-41}$$

$$\eta \le \rho \le 1 : \quad (\rho \cdot s_r) = +p_I \cdot \rho^2 + (p_A - p_I) \cdot (\rho^2 - \zeta^2) \tag{JC.1-42}$$

$$m_{rr} = m_1 + j \cdot \kappa_p \cdot \varphi_P \cdot \ln \rho^2 + p_I \cdot (1 - \rho^2) + (p_{A-} p_I) \cdot [(1 - \rho^2) + \zeta^2 \cdot \ln \rho^2] \tag{JC.1-43}$$

Equal values $m_{rr} = j \cdot (1 - 2 \cdot \kappa_P) \cdot \varphi_P$ at $\rho = \eta$ $\rightarrow$

$$(p_A - p_I) \cdot (\eta^2 - 3 \cdot \zeta^2 + 2 \cdot \zeta^3 / \eta) + p_I \cdot \eta^2 = j \cdot 3 \cdot \kappa_P \cdot \varphi_P \tag{JC.1-44}$$

$$(p_A - p_I) \cdot [(1 - \eta^2) + \zeta^2 \cdot \ln \eta^2] + p_I \cdot (1 - \eta^2) + m_1 = j \cdot [1 - \kappa_P \cdot (2 + \ln \eta^2)] \cdot \varphi_P \tag{JC.1-45}$$

$$(p_A - p_I)\cdot\left[1-3\cdot\zeta^2+2\cdot\zeta^3/\eta+\zeta^2\cdot\ln\eta^2\right]+p_I+m_1 = j\cdot\left[1+\kappa_P\cdot\left(1-\ln\eta^2\right)\right]\cdot\varphi_P \quad \text{(JC.1-46)}$$

The last equation is the sum of the first two ; is the limit load equation of Case 2.

The parameter $\eta$ is as yet unknown. It is calculated from the first of these three equations, which is independent of the edge moment $m_1$ :

$$(p_A - p_I)\cdot\left(\eta^2-3\cdot\zeta^2+2\cdot\zeta^3/\eta\right)=(p_A-p_I)\cdot(\eta-\zeta)^2\cdot(1+2\cdot\zeta/\eta)=j\cdot3\cdot\kappa_P\cdot\varphi_P-p_I\cdot\eta^2$$
$$(p_A - P_I)\cdot\left(\eta^2-\zeta^2\right)^2=\left(j\cdot3\cdot\kappa_P\cdot\varphi_P-p_I\cdot\eta^2\right)\cdot(\eta+\zeta)^2/(1+2\cdot\zeta/\eta)$$
$$(p_A - p_I)\cdot\left(\eta^2-\zeta^2\right)^2=\left\{\left(j\cdot3\cdot\kappa_P\cdot\varphi_P-p_I\cdot\left[\left(\eta^2-\zeta^2\right)+\zeta^2\right]\right\}\cdot\left\{\left(\eta^2-\zeta^2\right)+\zeta^2\cdot2\cdot(\eta+\zeta)/(\eta+2\cdot\zeta)\right\}$$
$$\left(\eta^2-\zeta^2\right)^2\cdot p_A-\left(\eta^2-\zeta^2\right)\cdot\left[\left(j\cdot3\cdot\kappa_P\cdot\varphi_P-p_I\cdot\zeta^2\right)-p_I\cdot\zeta^2\cdot w\right]=\left(j\cdot3\cdot\kappa_P\cdot\varphi_P-p_I\cdot\zeta^2\right)\cdot\zeta^2\cdot w \quad \text{(JC.1-47)}$$

$$w=2\cdot(\eta+\zeta)/(\eta+2\cdot\zeta)=2{,}000\ldots1{,}333 \quad \text{for} \quad \zeta/\eta=0\ldots1 \quad \text{(JC.1-48)}$$

$$\left(\eta^2-\zeta^2\right)\cdot p_A=\left[\left(j\cdot3\cdot\kappa_p\cdot\varphi_P-p_I\cdot\zeta^2\right)-p_I\cdot\zeta^2\cdot w\right]/2+$$
$$\pm\left\{\left(j\cdot3\cdot\kappa_P\cdot\varphi_P-p_I\cdot\zeta^2\right)-p_I\cdot\zeta^2\cdot w\right]^2/4+\left(j\cdot3\cdot\kappa_P\cdot\varphi_P-p_I\cdot\zeta^2\right)\cdot\zeta^2\cdot w\cdot p_A\Big\}^{1/2} \quad \text{(JC.1-49)}$$

For $p_A>0$ and $\eta>\zeta$ the positive values always are true.

For $\zeta=0$ and for $\zeta=\eta$ respectively it follows immediately from equation (JC.1-44) that :

$$\eta^2=j\cdot3\cdot\kappa_P\cdot\varphi_P/p_A=\eta^2_{\min} \quad \text{(JC.1-50a)}$$
$$\eta^2=j\cdot3\cdot\kappa_P\cdot\varphi_P/p_I=\eta^2_{\max} \quad \text{(JC.1-50b)}$$

**Case 3:** $0\le\eta\le\zeta\le1$ : (Characteristic of $m_{\varphi\varphi}$ changes at $\rho=\eta$ )

$$0\le\rho\le\eta: \quad (\rho\cdot s_r)=+p_I\cdot\rho^2 \quad \text{(JC.1-51)}$$
$$m_{rr}=j\cdot\varphi_P-p_I\cdot(2/3)\cdot\rho^2 \quad \text{(JC.1-52)}$$
$$\eta\le\rho\le\zeta: \quad (\rho\cdot s_r)=+p_I\cdot\rho^2 \quad \text{(JC.1-53)}$$
$$m_{rr}=m_1+j\cdot\kappa_P\cdot\varphi_P\cdot\ln\rho^2+p_I\cdot\left(1-\rho^2\right)+(p_A-p_I)\cdot\left[\left(1-\zeta^2\right)+\zeta^2\cdot\ln\zeta^2\right] \quad \text{(JC.1-54)}$$
$$\zeta\le\rho\le1: \quad (\rho\cdot s_r)=+p_I*\rho^2+(p_A-p_I)*\left(\rho^2-\zeta^2\right) \quad \text{(JC.1-55)}$$
$$m_{rr}=m_I+j\cdot\kappa_P\cdot\varphi_P\cdot\ln\rho^2+p_I\cdot\left(1-\rho^2\right)+(p_A-p_I)\cdot\left[\left(1-\rho^2\right)+\zeta^2\cdot\ln\rho^2\right] \quad \text{(JC.1-56)}$$

Equal values $m_{rr}=j\cdot(1-2\cdot\kappa_P)\cdot\varphi_P$ at $\rho=\eta \quad \rightarrow$

$$p_I\cdot\eta^2=j\cdot3\cdot\kappa_P\cdot\varphi_P \quad \text{(JC.1-57)}$$
$$(p_A-p_I)\cdot\left[\left(1-\zeta^2\right)+\zeta^2\cdot\ln\zeta^2\right]+p_I\cdot\left(1-\eta^2\right)+m_1=j\cdot\left[1-\kappa_P\cdot\left(2+\ln\eta^2\right)\right]\cdot\varphi_P \quad \text{(JC.1-58)}$$
$$(p_A-p_I)\cdot\left[\left(1-\zeta^2\right)+\zeta^2\cdot\ln\zeta^2\right]+p_I+m_1=j\cdot\left[1+\kappa_P\cdot\left(1-\ln\eta^2\right)\right]\cdot\varphi_P \quad \text{(JC.1-59)}$$

The last equation is the sum of the first two; it the limit load equation of Case 3.

The parameter $\eta$ is as yet unknown. It is calculated from the first of these three equations:

$$\eta^2=j\cdot3\cdot\kappa_P\cdot\varphi_P/p_I\left(=\eta^2{}_{\max}\right) \quad \text{(JC.1-60)}$$

**Summary for Cases 1,2,3:**

The following definitions for a new resultant effective “pressure” shall be used:

$$\text{Case 1:} \quad P_{Q(1)}=(p_A-p_I)\cdot\left(1-3\cdot\zeta^2+2\cdot\zeta^3\right)+p_I \quad \text{(JC.1-61)}$$
$$\text{Case 2:} \quad P_{Q(2)}=(p_A-p_I)\cdot\left[1-3\cdot\zeta^2+2\cdot\zeta^3/\eta+\zeta^2\cdot\ln\eta^2\right]+p_I \quad \text{(JC.1-62)}$$
$$\text{Case 3:} \quad P_{Q(3)}=(p_A-p_I)\cdot\left[\left(1-\zeta^2\right)+\zeta^2\cdot\ln\zeta^2\right]+p_I \quad \text{(JC.1-63)}$$

For Case 2 and Case 3 define a new parameter:

$$k_P=\kappa_P\cdot\left(1-\ln\eta^2\right) \quad \text{(JC.1-64)}$$

Then for these three cases the following limit load equations are valid :

Case 1:

$$j \cdot \left\{ (2/3) \cdot p_{Q(1)} + m_1 \right\} \le \varphi_P \qquad \text{(JC.1-65)}$$

Case 2 and Case 3:

$$j \cdot \left\{ p_{Q(2,3)} + m_1 \right\} \le (1 + k_P) \cdot \varphi_P \qquad \text{(JC.1-66)}$$

Boundaries between these three cases are as follows:

Case 1 / Case 2: $\eta = 1 \quad \rightarrow \quad j \cdot m_1 = (1 - 2 \cdot \kappa_P) \cdot \varphi_P \quad \rightarrow$ (JC.1-67)

$$j \cdot p_{Q(1)} = j \cdot p_{Q(2)} = 3 \cdot \kappa_P \cdot \varphi_P \qquad \text{(JC.1-68)}$$

Case 2/Case 3: $\eta = \zeta \quad \rightarrow \quad j \cdot p_I \cdot \zeta^2 = 3 \cdot \kappa_P \cdot \varphi_P \qquad \text{(JC.1-69)}$

Case 3/Case 1: No common boundary, except for $p_A = p_I$, where $p_{Q(1)} = p_{Q(2)} = p_{Q(3)} = p_I$.

The following boundary condition applies for all cases:

$$|m_1| \le \varphi_P \qquad \text{(JC.1-70)}$$

**Special case without tube support:**

Without tube support ("tubesheets unsupported by tubes"):

$$Q_A = Q_I = 0 \qquad \textit{and} \qquad \text{(JC.1-71)}$$

$$P_A = P_I = P_D \quad (\underline{\textit{not}} = P_E \textit{, for the tubes are effective closed by their curvature}). \qquad \text{(JC.1-72)}$$

Then due to $P_A = P_I = P_D$ and $p_A = p_I = p_D$ it follows:

$$p_{Q(1)} = p_{Q(2)} = p_{Q(3)} = p_D \qquad \text{(JC.1-73)}$$

If $p_I = p_A$ it follows that $p_R = p_A$ and the parameter $\zeta$ is not defined, whereas the parameter $\eta$ is required.

It may be assumed that $\zeta = \eta$. Then the most complicated Case 2 may be waived and from Case 1 and Case 3 it follows that

$$\eta^2 = \min\left\{1{,}0;\ j \cdot 3 \cdot \kappa_p \cdot \varphi_P / p_I\right\} \qquad \text{(JC.1-74)}$$

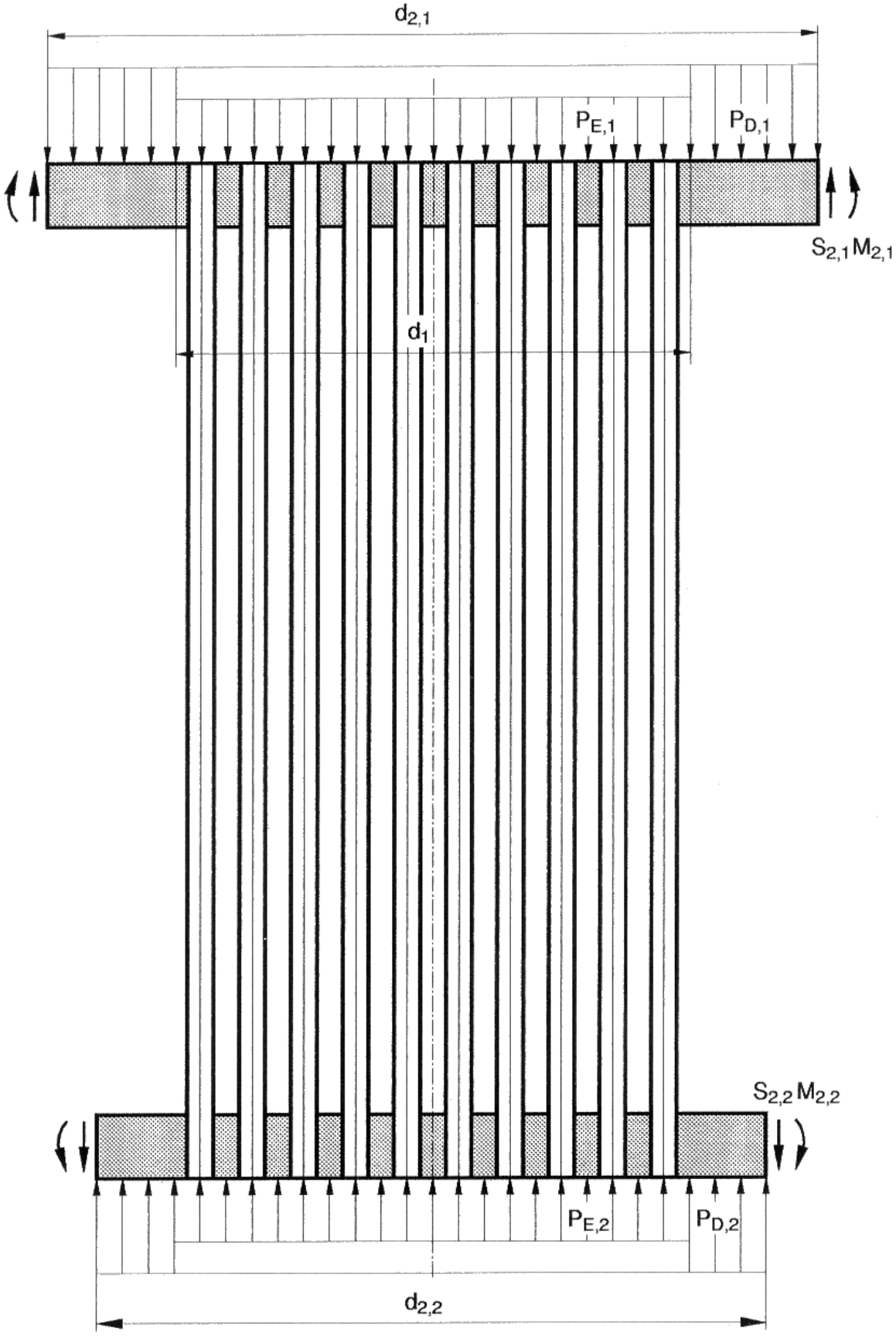


**Figure JC-1: Tubebundle (two tubesheets) with untubed rims**

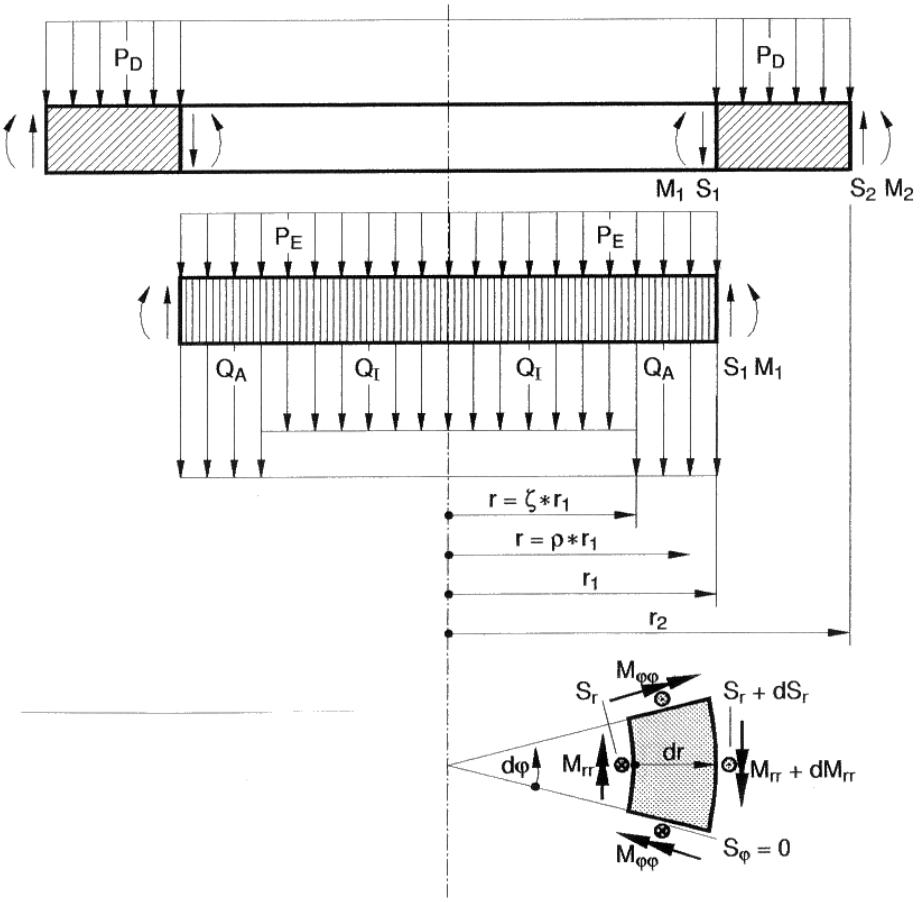


**Figure JC-2: Calculation model local axisymmetric tubesheet**

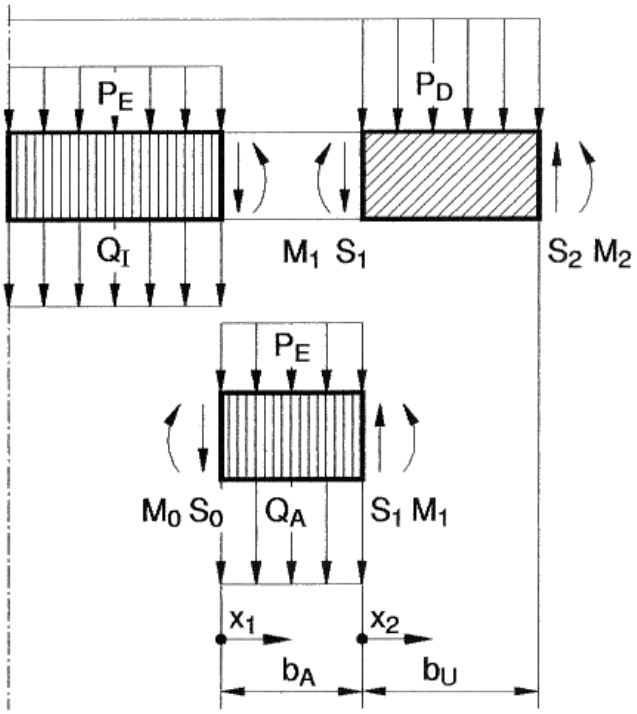


**Figure JC-3: Calculation model local untubed region (strip)**

### JC-2 Limit load of the axisymmetric untubed rim

**Dimensionless basic equations** are based on those in JC-1.

Special parameters:

$$\lambda_R = (d_2 - d_1)/d_1 \;;\; \varphi_P = 1{,}0 \;;\; \kappa_P = 0{,}5 \qquad \text{(JC.2-1)}$$

$$P_X = P_D \;;\; \rightarrow \; p_X = p_D \qquad \text{(JC.2-2)}$$

Equilibrium conditions:

$$(\rho \cdot s_r)_{|\rho} - 2 \cdot p_D \cdot \rho = 0 \qquad \text{(JC.2-3)}$$

$$(p \cdot m_{rr})_{|\rho} - m_{\varphi\varphi} + 2 \cdot \rho \cdot s_r = 0 \qquad \text{(JC.2-4)}$$

Boundary conditions:

$$\rho = 1: \qquad s_r = s_1 \;;\; m_{rr} = m_1 \qquad \text{(JC.2-5)}$$

$$\rho = 1 + \lambda_R: \quad s_r = s_2 \;;\; m_{rr} = m_2 \qquad \text{(JC.2-6)}$$

Limit load condition:

$$\max\left\{|m_{rr}| \,;\, |m_{\varphi\varphi}| \,;\, |m_{rr} - m_{\varphi\varphi}|\right\} \le 1 \qquad \text{(JC.2-7)}$$

Solutions

For $m_{\varphi\varphi}$ = const. from the equilibrium conditions and the boundary conditions at $\rho = 1$ it follows that:

$$\rho \cdot s_r = s_1 + p_D \cdot \left(\rho^2 - 1\right) \qquad \text{(JC.2-8)}$$

$$\rho \cdot m_{rr} = m_1 + \left(m_{\varphi\varphi} - 2 \cdot s_1\right) \cdot (\rho - 1) - p_D \cdot (2/3) \cdot (\rho - 1)^2 (\rho + 2) \qquad \text{(JC.2-9)}$$

Boundary conditions at $\rho = 1 + \lambda_R$:

$$(1 + \lambda_R) \cdot s_2 = s_1 + p_D \cdot \left(2 \cdot \lambda_R + {\lambda_R}^2\right) \qquad \text{(JC.2-10)}$$

$$(1+\lambda_R)\cdot m_2 = m_1 + (m_{\varphi\varphi} - 2\cdot s_1)\cdot\lambda_R - p_D\cdot(2/3)\cdot\lambda_R{}^2(3+\lambda_R) \quad \text{(JC.2-11)}$$

Definition:

$$m_R = m_2\cdot(1+\lambda_R) + s_1\cdot 2\cdot\lambda_R + p_D\cdot 2\cdot\lambda_R{}^2\cdot(1+\lambda_R/3) \quad \text{(JC.2-12)}$$

Then the limit load equation of the untubed rim is:

$$m_1 = m_R - m_{\varphi\varphi}\cdot\lambda_R \quad \text{(JC.2-13)}$$

The value $m_{\varphi\varphi} = \text{const.} = \pm 1 \ldots (\pm 1 + m_{rr})$ shall be determined below.

NOTE: A variable moment $m_{\varphi\varphi} = \pm 1 + m_{rr}$ here is not considered (for simplicity) but approximated by a constant value, because within the small range $\rho = 1 \ldots 1+\lambda_R$ the moment $m_{rr}$ varies only not considerable between $m_1$ and $m_2$ and it may approximated by $m_{rr} = (m_1 + m_2)/2$.

**JC-3 Limit load of the whole axisymmetric tubebundle**

**Basis relationships**, taken from the foregoing subclauses:

$$j\cdot\{(2/3)\cdot p_{Q(1)} + m_1\} \le \varphi_P \quad \text{(JC.3-1)}$$

$$j\cdot\{p_{Q(2,3)} + m_1\} \le (1+k_p)\cdot\varphi_P \quad \text{..(JC.3-2)}$$

$$|m_1| \le \varphi_p \quad \text{(JC.3-3)}$$

$$m_1 = m_R - m_{\varphi\varphi}\cdot\lambda_R \quad \text{(JC.3-4)}$$

A given boundary moment $m_2$ corresponds to a given value $m_R$.

The moment $m_1$ is to be determined optimum for the desired limit load as follows:

(1) For $j\cdot p_Q \Rightarrow$ Max! (Axial force is desired to be maximum.):

$$j\cdot(2/3)\cdot p_{Q(1)} \le \varphi_P - j\cdot m_1 \quad \text{=> Max!} \quad \rightarrow \quad j\cdot m_1 \text{ => } Min!$$

$$j\cdot p_{Q(2,3)} \le (1+k_p)\cdot\varphi_p - j\cdot m_1 \text{ => Max!} \quad \rightarrow \quad j\cdot m_1 \text{ => } Min! \rightarrow$$

$$j\cdot m_1 = \max\{-\varphi_P; j\cdot m_R - j\cdot m_{\varphi\varphi}\cdot\lambda_R\} \rightarrow \quad j\cdot m_{\varphi\varphi} \text{ => } Max! \rightarrow$$

The limit load condition of the untubed rim gives the possible maximum of $j\cdot m_{\varphi\varphi}$ as follows:

$$j\cdot m_{\varphi\varphi} = 1 + k_R; \quad k_R = \min\{0; j\cdot m_{rr}\}; \quad (k_R \le 0; \text{definition of } k_R) \quad \text{(JC.3-5)}$$

$$j\cdot m_1 = \max\{-\varphi_P; j\cdot m_R - (1+k_R)\cdot\lambda_R\} \rightarrow \quad \text{(JC.3-6)}$$

$$j\cdot(2/3)\cdot p_{Q(1)} = \min\{2\cdot\varphi_P; \varphi_P + (1+k_R)\cdot\lambda_R - j\cdot m_R\} \quad \text{(JC.3-7)}$$

$$j\cdot p_{Q(2,3)} = \min\{(2+k_p)\cdot\varphi_P; (1+k_p)\cdot\varphi_P + (1+k_R)\cdot\lambda_R - j\cdot m_R\} \quad \text{(JC.3-8)}$$

(2) For $j\cdot m_2$ => *Max*! or $j\cdot m_R$ => *Max*! (Boundary moment is desired to be maximum.):

$$j\cdot m_R = j\cdot m_1 + j\cdot m_{\varphi\varphi} \text{ => } Max! \quad \rightarrow$$

(a) $j\cdot m_1$ => *Max*! $\rightarrow$

$$j\cdot m_1 = \min\{+\varphi_P; \varphi_P - j\cdot(2/3)\cdot p_{Q(1)}; (1+k_P)\cdot\varphi_p - j\cdot p_{Q(2,3)}\} \quad \text{(JC.3-9)}$$

(b) $j\cdot m_{\varphi\varphi}$ => *Max*! $\rightarrow$

For $j\cdot m_1 = +\varphi_P$ is $j\cdot m_{rr} > 0$ and therefore $j\cdot m_{\varphi\varphi} = +1$ $\rightarrow$

$$j\cdot m_R = \min\{\varphi_P + \lambda_R; \varphi_P + (1+k_R)\cdot\lambda_R - j\cdot(2/3)\cdot p_{Q(I)}; (1+k_p)\cdot\varphi_P + (1+k_R)\cdot\lambda_R - j\cdot p_{Q(2,3)}\} \quad \text{(JC.3-10)}$$

The foregoing limitations for $p_{Q(1)}$, $p_{Q(2,3)}$ and $m_R$ are equivalent to the following five conditions:

$$j\cdot(2/3)\cdot p_{Q(1)} \le 2\cdot\varphi_P \quad \text{(JC.3-11)}$$

$$j \cdot p_{Q(2,3)} \le (2 + k_p) \cdot \varphi_P \qquad \text{(JC.3-12)}$$

$$j \cdot \{(2/3) \cdot p_{Q(1)} + m_R\} \le \varphi_P + (1 + k_R) \cdot \lambda_R \qquad \text{(JC.3-13)}$$

$$j \cdot \{p_{Q(2,3)} + m_R\} \le (1 + k_p) \cdot \varphi_P + (1 + k_R) \cdot \lambda_R \qquad \text{(JC.3-14)}$$

$$j \cdot m_R \le \varphi_P + \lambda_R \qquad \text{(JC.3-15)}$$

The first two conditions correspond to $j \cdot m_1 = -\varphi_P$. However Case 1 is valid for $j \cdot m_1 \ge (1 - 2 \cdot \kappa_P) \cdot \varphi_P \ge 0$ only. Therefore the first of these conditions is waived, and in the third it follows $k_R = 0$.

For $k_R = 0$ the third and the fifth condition may be connected as follows:

$$\max\{|(2/3) \cdot p_{Q(1)} + m_R|; |m_R|\} = |(1/3) \cdot p_{Q(1)} + m_R| + |(1/3) \cdot p_{Q(1)} + m_R| \le \varphi_P + \lambda_R \qquad \text{(JC.3-16)}$$

The fourth condition (JC.3-14) requires a value for $k_R$, which is estimated as follows:

$$k_R = \min\{0; j \cdot m_{rr}\}; \quad j \cdot m_{rr} = (j \cdot m_1 + j \cdot m_2)/2;$$

$$j \cdot m_1 = j \cdot m_R - j \cdot m_{\varphi\varphi} \cdot \lambda_R; \quad j \cdot m_{\varphi\varphi} = 1 + j \cdot m_{rr} \qquad \rightarrow$$

$$k_R = \min\{0; [j \cdot m_R + j \cdot m_2 - \lambda_R]/(2 + \lambda_R)\}. \qquad \text{(JC.3-17)}$$

IF $j \cdot m_{rr} > 0$ THEN

$$k_R = 0$$

$$j \cdot (p_{Q(2,3)} + m_R) \le (1 + k_p) \cdot \varphi_P + \lambda_R. \qquad \text{(JC.3-18)}$$

ELSE $j \cdot m_{rr} < 0$

$$k_R = [j \cdot (m_R + m_2) - \lambda_R]/(2 + \lambda_R)$$

$$j \cdot \{(p_{Q(2,3)} + m_R) - (m_R + m_2) \cdot \lambda_R/(2 + \lambda_R)\} \le (1 + k_p) \cdot \varphi_P + \lambda_R - \lambda_R{}^2/(2 + \lambda_R)$$

Slightly simplified for $\lambda_R^2$ « 1 and $m_2 \cdot \lambda_R \approx m_R \cdot \lambda_R$:

$$j \cdot \{(p_{Q(2,3)} + m_R) - m_R \cdot \lambda_R\} \le (1 + k_P) \cdot \varphi_P + \lambda_R \qquad \text{..(JC.3-19)}$$

END

Both results (JC.3-18) and (JC.3-19) connected:

$$|p_{Q(2,3)} + m_R \cdot (1 - \lambda_R/2)| + |m_R \cdot \lambda_R/2| \le (1 + k_p) \cdot \varphi_P + \lambda_R \qquad \text{(JC.3-20)}$$

All results {conditions (JC.3-12), (JC.3-16) and (JC.3-20)) together:

$$\max\left\{\begin{matrix} |p_Q|/[(2 + k_p) \cdot \varphi_p]; (|p_Q + m_R \cdot (1 - \lambda_R/2)| + |m_R \cdot \lambda_R/2|)/[(1 + k_p) \cdot \varphi_P + \lambda_R] \\ (|(1/3) \cdot p_Q| + |(1/3) \cdot p_Q + m_R|)/[\varphi_P + \lambda_R] \end{matrix}\right\} \le 1 \qquad \text{(JC.3-21)}$$

This limit load condition for the whole axisymmetric tubebundle corresponds to the limit load condition $\Phi_B \le 1$ (eq.(J.9.1-14)) in Annex J .

For thick tubesheets an additional check shall be made by a load ratio for shear:

The shear force $S_1 = P_R \cdot r_1/2$ at $r = r_1$ is divided by the corresponding allowable shear force (Tresca)

$[S_1] = 0{,}500 \cdot fp \cdot e_p \cdot \varphi_P$ :

$$\Phi_S = |P_R| \cdot d_1/(2 \cdot f_p \cdot e_p \cdot \varphi_P) \le 1 \qquad \text{(JC.3-22)}$$

As usual there is assumed no interaction between the load ratios $\Phi_S$ and $\Phi_B$.

**JC-4 Additional effect of weight**

**Tube support moments per area unit:**

The tube support forces per area unit are very efficient against axial forces, but nearly without effect to cover the weight of the vertical tubebundle. Contrary, the tube support moments per area unit are less effective against the axial forces (therefore neglected for these cases), but important to cover the weight:

The allowable reactive axial tensile force of one tube is $[F_x]_T = \pi \cdot (d_T - e_T) \cdot e_T \cdot [\sigma]_T$ .

Similar the allowable reactive bending moment of one tube (linear elastic limit) is:

$$[M_b]_T = \pi \cdot (d_T - e_T)^2 \cdot e_T \cdot [\sigma]_T / 4 \qquad \text{(JC.4-1)}$$

From this may be defined an allowable reactive bending moment per area unit:

$$\lfloor M_{pa} \rfloor = [Q_t] \cdot (d_T - e_T) / 4 = \vartheta \cdot [\sigma]_T \cdot (d_T - e_T) / 4 \qquad \text{(JC.4-2)}$$

Here (for simplification) the influences of fluid pressures are ignored.

**Axisymmetric tubed region:**

The calculation model Figure JC-2 and subclause JC-1 are to be modified as follows:

$Q_I = Q_A = 0$ ;

$P_X = P_E \Rightarrow P_W$ (weight per area unit)

$M_{pa}$ (additional moment per area unit, directed as $dM_{rr}$ )

Equlibrium conditions:

Forces: $$(r \cdot S_r)_{|r} - P_W \cdot r = 0 \qquad \text{(JC.4-3)}$$

Moments: $$(r \cdot M_{rr})_{|r} - M_{\varphi\varphi} + (r \cdot S_r) + r \cdot M_{pa} = 0 \qquad \text{(JC.4-4)}$$

General solutions for $P_W = \text{const.}$, $M_{\varphi\varphi} = \text{const.}$, $M_{pa} = -R_{pa} \cdot r / r_1$ for the whole tubed region:

$$S_r = P_W \cdot r / 2 \qquad \text{(JC.4-5)}$$

$$M_{rr} = M_{\varphi\varphi} + (R_{pa} / r_1 - P_W / 2) \cdot r^2 / 3 \qquad \text{(JC.4-6)}$$

If the assumed reactive moment per area unit $R_{pa}$ is less than the allowable $\lfloor M_{pa} \rfloor$, then it may be $R_{pa} / r_1 - P_W / 2 = 0$ and $M_{rr} = M_{\varphi\varphi} = \text{const.}$, for the whole tubesheet $0 \le r \le r_1$ . If at $r = r_1$ is

$$M_{rr} = M_{\varphi\varphi} \le [M]_P \cdot \varphi_P \qquad \text{(JC.4-7)}$$

(limit load condition), then this may be true for the whole tubed region if

$$(\lfloor M_{pa} \rfloor / r_1 - P_W / 2) \ge 0 \qquad \text{(JC.4-8)}$$

Calculating the weight only for the tubes (densitiy $\rho_T$ *;* weight of the tubesheets comparable small and neglected) then this condition becomes:

$$\lfloor M_{pa} \rfloor / r_1 - P_W / 2 = \vartheta \cdot [\sigma]_T \cdot (d_T - e_T) / (2 \cdot d_1) - \vartheta \cdot \rho_T \cdot g \cdot L_T / 2 \ge 0 \qquad \text{(JC.4-9)}$$

By application of equation (J.5.1-3) to eliminate $d_1$ from this follows:

$$N_T + N_I \le (\pi \cdot \Theta) \cdot [\{[\sigma]_T \cdot (d_T - e_T)\} / \{\rho_T \cdot g \cdot L_T \cdot 2 \cdot p\}]^2 \qquad \text{(JC.4-10)}$$

If this condition is met, the bending strength of the tubes covers their own weight (as desired above).

Numerical values for usual tubular heat exchangers:

$\pi \cdot \Theta = (3{,}14...3{,}63)$ $\quad [\sigma]_T \approx (80...160)\text{MPa}$

$\rho_T \cdot g \approx 8000\text{kg/m}^3 \cdot 9{,}81\text{m/s}^2 \approx 80000\text{N/m}^3 = 0{,}080\text{MN/m}^3$

$L_T \le (6...12)\text{m}$ $\quad p / (d_T - e_T) \le (1{,}4...1{,}8)$

The condition then gives:

$$N_T + N_I \le 1700...51000 \qquad \text{(JC.4-11)}$$

Only for very large exchangers with very low tube strength this condition possibly is not met. Therefore this condition is been presupposed, and in "Conditions of applicability" is introduced the following simplified and more conservative condition:

$$N_T \le 30 \cdot \{(f_T / MPa)/(L_T / m)\}^2 \qquad \text{(JC.4-12)}$$

**Axisymmetric untubed rim:**

Corresponding to JC-2 with the small simplification $p_D = 0$ results:

$$m_R = m_2 \cdot (1+\lambda_R) + s_1 \cdot 2 \cdot \lambda_R = m_1 + m_{\varphi\varphi} \cdot \lambda_R \qquad \text{(JC.4-13)}$$

$$s_1 = S_1 \cdot r_1 / (2 \cdot [M]_P) = F_W / (4\pi \cdot [M]_P) \ldots \qquad \text{(JC.4-14)}$$

$$m_1 = M_1 / [M]_P \le +\varphi_P \qquad \text{(JC.4-15)}$$

$$m_{\varphi\varphi} = M_{\varphi\varphi} / [M]_P \le +1 \qquad \text{(JC.4-16)}$$

$$S_1 \cdot 2 \cdot \lambda_R \le \varphi_P + \lambda_R - m_2 \cdot (1+\lambda_R). \qquad \text{(JC.4-17)}$$

Any active boundary moment $m_2 \neq 0$ (e.g. due to flange bolting) is already covered in subclause JC-2. Possible reactive moments $m_2 < 0$ for simplicity and safety will be neglected, q.e. $m_2 = 0$. Then for the whole tubebundle follows:

$$F_W \cdot 2 \cdot \lambda_P / (\pi \cdot fp \cdot e_P^2) \le \varphi_P + \lambda_R. \qquad \text{(JC.4-18)}$$

or a load ratio $\Phi_W$ for the additional effect of weight:

$$\Phi_W = |F_W| \cdot 2 \cdot \lambda_R / \{\pi \cdot fp \cdot ep^2 \cdot (\varphi_P + \lambda_R)\} \le 1 \qquad \text{(JC.4-19)}$$

**JC-5 Limit load of local untubed regions**

**Definition of the problem (task):**

To be calculated is a "long" strip of a plate. Its geometry and loading is variable only in one direction. Figure JC.-3 shows the calculation model. It is very similar to Figure JC-2:

Instead of the one coordinate *r* now are used different coordinates $x_J$ (J = 0, 1, 2).

Instead of $b_R$ now is used $b_U$ (This untubed region $b_U$ is investigated more extensive than the former $b_R$) and now $b_A$ is used instead of the former $(1-\zeta)\cdot r_1$.

Instead of $M_{rr}$, $S_r$ now are used $M_{xx}$, $S_x$, and $M_{\varphi\varphi}$ is to be dropped.

An essential presupposition is $P_I = 0$ (sufficient high load carrying capacity of the central tubes).

If for the untubed width $b_U$ is assumed the maximum width, this calculation model is always conservative.

**Original basic equations.**

Resultant tubebundle loads:

$$\textit{Region of } x_0: \quad P_{X(0)} = P_E + Q_I = 0 \quad (\textit{essential presupposition}) \qquad \text{(JC.5-0)}$$

$$\textit{Region of } x_1: \quad P_{X(1)} = P_E + Q_A = P_A \qquad \text{(JC.5-1)}$$

$$\textit{Region of } x_2: \quad P_{X(2)} = P_D \qquad \text{(JC.5-2)}$$

Equilibrium conditions:

$$\textit{Forces}: \quad S_{x|x} - P_X = 0 \qquad \text{(JC.5-3)}$$

$$\textit{Moments}: \quad M_{xx|x} + S_x = 0 \qquad \text{(JC.5-4)}$$

Limit load conditions:

$$\textit{Tubes}: \quad -[Q_c] \le Q_A \le +[Q_t] \qquad \text{(JC.5-5)}$$

$$\textit{Plate region } x_1: \quad |M_{xx}| \le \varphi_P \cdot [M]_P \qquad \text{(JC.5-6)}$$

$$\textit{Plate region } x_2: \quad |M_{xx}| \le 1 \cdot [M]_P \qquad \text{(JC.5-7)}$$

**Solutions of the equilibrium conditions:**

*Region of* $x_0$ : $S_0 = 0$ (JC.5-8)

*Region of* $x_1$ : $S_x = S_0 + P_A \cdot x_1$ (JC.5-9)

$M_{xx} = M_0 - S_0 \cdot x_1 - P_A \cdot x_1^2 / 2$ (JC.5-10)

$x_1 = b_A$ : $S_1 = P_A \cdot b_A$ (JC.5-11)

$M_1 = M_0 - P_A \cdot b_A^2 / 2$ (JC.5-12)

*Region of* $x_2$ : $S_X = S_1 + P_D \cdot x_2$ (JC.5-13)

$M_{xx} = M_1 - S_1 \cdot x_2 - P_D \cdot x_2^2 / 2$ (JC.5-14)

$x_2 = b_U$ : $S_2 = S_1 + P_D \cdot b_U$ (JC.5-15)

$M_2 = M_1 - S_1 \cdot b_U - P_D \cdot b_U^2 / 2$ (JC.5-16)

*Within* $0 \le x_2 \le b_U$ *an extremum of* $M_{xx}$ *is possible*:

$d(M_{xx})/dx_2 = 0 \quad \rightarrow \quad x_2 = x_E = -S_1 / P_D \quad \rightarrow$ (JC.5-17)

$M_{xx}(x_E) = M_3 = M_1 + (S_1)^2 / (2 \cdot P_D)$ (JC.5-18)

This last equation is valid only if $0 \le x_E \le b_U$ . An other of these equations gives the support width:

$b_A = S_1 / P_A$ (JC.5-19)

**Dimensionless special equations:**

$m_J = M_J / [M]_P$ for J = 0, 1, 2, 3. (JC.5-20)

$s = S_1 \cdot b_U / [M]_P$ (JC.5-21)

$p = P_D \cdot b_U^2 / [M]_P$ ; $q = P_A \cdot b_U^2 / [M]_P$ (JC.5-22)

Bending moments (by elimination of the width $b_A$ ):

$m_1 = m_0 - s^2 / (2 \cdot q)$ (JC.5-23)

$m_2 = m_1 - p/2 - s$ (JC.5-24)

$m_3 = m_1 + s^2 / (2 \cdot p)$ {valid only if $0 \le (x_E / b_U = -s/p) \le 1$} (JC.5-25)

Limit load conditions plate:

$|m_0| \le \varphi_P$ (JC.5-26)

$|m_1| \le \varphi_P$ (JC.5-27)

$|m_2| \le 1$ (JC.5-28)

$|m_3| \le 1$ (JC.5-29)

**Solutions:**

(0) General

The boundary moment $m_2$ is assumed to be admissible. Then $m_1$ may be substituted as follows:

$m_1 = m_2 + p/2 + s \quad \rightarrow$ (JC.5-30)

$|m_0| = |m_2 + p/2 + s + s^2/(2 \cdot q)| \le \varphi_P$ (JC.5-31)

$|m_1| = |m_2 + p/2 + s| \le \varphi_P$ (JC.5-32)

$|m_3| = |m_2 + p/2 + s + s^2/(2 \cdot p)| \le 1$ (JC.5-33)

(1) Case 1: For $p$ => Max !

There are to be expected the following signs (Figure JC-3):

$p > 0; \quad q < 0; \quad s < 0$ (JC.5-34)

From this follows $m_0 < m_1 < m_3$ and $m_0 = -\varphi_P$ and either $m_1 = +\varphi_P$ or $m_3 = +1 \quad \rightarrow$

$m_0 = m_2 + p/2 + s + s^2/(2 \cdot q) = -\varphi_P$ (JC.5-35)

$$m_1 = m_2 + p/2 + s = (\leq) + \varphi_P \qquad \text{(JC.5-36)}$$

$$m_3 = m_2 + p/2 + s + s^2/(2\cdot p) \leq (=) + 1 \qquad \text{(JC.5-37)}$$

Without $m_3$ it follows:

$$m_0 - m_1 = s^2/(2\cdot q) = -2\cdot\varphi_P \quad \rightarrow$$

$$s = -\{-4\cdot q\cdot\varphi_P\}^{1/2} \qquad \text{(JC.5-38)}$$

$$p/2 = +\varphi_P - m_2 - s = +\varphi_P - m_2 + \{-4\cdot q\cdot\varphi_P\}^{1/2} \qquad \text{(JC.5-39)}$$

Without $m_1$ it follows

$$m_0 - m_3 = s^2\cdot\{1/(2\cdot q) - 1/(2\cdot p)\} = -(1+\varphi_P) \quad \rightarrow$$

$$s = \{-2\cdot p\cdot[(1+\varphi_P)/(1-p/q)]\}^{1/2} \qquad \text{(JC.5-40)}$$

$$m_3 = m_2 + p/2 - \{2\cdot p\cdot[(1+\varphi_P)/(1-p/q)]\}^{1/2} + [(1+\varphi_P)/(1-p/q)] = +1 \quad \rightarrow$$

$$p/2 = -\left\{[(1+\varphi_P)/(1-p/q)]^{1/2} + (1-m_2)^{1/2}\right\}^2 \qquad \text{(JC.5-41)}$$

(2) Case 2: For $p$ => Min!

There are to be expected the following signs (Figure JC-3):

$$p < 0;\quad q > 0;\quad s > 0 \qquad \text{(JC.5-42)}$$

From this follows $m_0 > m_1 > m_3$ and $m_0 = +\varphi_P$ and either $m_1 = -\varphi_P$ or $m_3 = -1$ $\rightarrow$

$$m_0 = m_2 + p/2 + s + s^2/(2\cdot q) = +\varphi_P \qquad \text{(JC.5-43)}$$

$$m_1 = m_2 + p/2 + s = (\geq) - \varphi_P \qquad \text{(JC.5-44)}$$

$$m_3 = m_2 + p/2 + s + s^2/(2\cdot p) \qquad (\geq) = -1 \qquad \text{(JC.5-45)}$$

Without $m_3$ it follows:

$$m_0 - m_1 = s^2/(2\cdot q) = +2\cdot\varphi_P \quad \rightarrow$$

$$s = +\{4\cdot q\cdot\varphi_P\}^{1/2} \qquad \text{(JC.5-46)}$$

$$p/2 = -\varphi_P - m_2 - s = -\varphi_P - m_2 - \{4\cdot q\cdot\varphi_P\}^{1/2} \qquad \text{(JC.5-47)}$$

Without $m_1$ it follows

$$m_0 - m_3 = s^2\cdot\{1/(2\cdot q) - 1/(2\cdot p)\} = +(1+\varphi_P) \quad \rightarrow$$

$$s = \{-2\cdot p\cdot[(1+\varphi_P)/(1-p/q)]\}^{1/2} \qquad \text{(JC.5-48)}$$

$$m_3 = m_2 + p/2 + \{-2\cdot p\cdot[(1+\varphi_P)/(1-p/q)]\}^{1/2} - [(1+\varphi_P)/(1-p/q)] = -1 \quad \rightarrow$$

$$p/2 = -\left\{[(1+\varphi_P)/(1-p/q)]^{1/2} + (1+m_2)^{1/2}\right\}^2 \qquad \text{(JC.5-49)}$$

(3) Summary of both cases:

The parameter $p$ is the "dimensionless" allowable fluid pressure difference; it may be positive or negative (logical result of both cases). Also other parameters and results are positive or negative.

To avoid negative parameters in the final formulae shall be made some changes of nominations:

| | | | | |
|---|---|---|---|---|
| Used up to here (above): | $+m_2$ | $+p$ | $+q$ | $+s$ |
| Case (1) later (below): | $-m_2$ | $+p$ | $-q$ | $-s$ |
| Case (2) later (below): | $+m_2$ | $-p$ | $+q$ | $+s$ |

After these changes the results of both cases becomes equal, and the new parameters should be always as possible maximum. The allowable pressure $p$ therefore is the minimum of both possibilities:

$$p/2 = \min\left( \left\{ \varphi_P + m_2 + \left(4 \cdot q \cdot \varphi_P\right)^{1/2} \right\}; \left\{ \left[ \left(1+\varphi_P\right)/\left(1+p/q\right) \right]^{1/2} + \left(1+m_2\right)^{1/2} \right\}^2 \right) \qquad \text{(JC.5-50)}$$

The best results are obtained for the maximum (new) values $m_2$ and $q$:

Case (1):

$$m_2 = -M_{2,\min}/[M]_P; \qquad q = -P_A \cdot {b_U}^2/[M]_P = -\left(-[Q_c]+P_E\right)\cdot {b_U}^2/[M]_P \qquad \text{(JC.5-51)}$$

Case (2):

$$m_2 = +M_{2,\max}/[M]_P; \qquad q = +P_A \cdot {b_U}^2/[M]_P = +\left(+[Q_t]+P_E\right)\cdot {b_U}^2/[M]_P \qquad \text{(JC.5-52)}$$

To avoid numerical problems at the limits $P_E \approx +[Q_c]$ or $P_E \approx -[Q_t]$ in the method the allowable loads $[Q_X]$ are multiplicated by a factor 1,1. This corresponds to a slightly decreased safety for these local loadings, which should be acceptable. (Compare e.g. clause 13 for stability of tubes).

In the above formula for $p/2$ (JC.5-50) the second term may be calculated by iteration only. If in the right side $p$ is assumed too large, the left side gives $p$ too small (and vice versa). If finally the second term is govern, the first term is too large, therefore it may be used as an allowable (conservative) approximation for the right side of the second term.

Finally an other interesting parameter is the width of pressurised region $b_A$ (two possibilities):

$$b_A/b_U = +s/q = \left(4 \cdot \varphi_P/q\right)^{1/2} \qquad \text{(JC.5-53)}$$

$$b_A/b_U = +s/q = \left[2 \cdot p \cdot \left(1+\varphi_P\right)/\left(1+p/q\right)\right]^{1/2}/q \qquad \text{(JC.5-54)}$$

Numerical calculations show, the second formula always is govern for large support parameters $q$; the corresponding results are $b_A/b_U < 1$. Contrary the first formula is govern for small $q$, giving $b_A/b_U > 1$ only for $q < 4\varphi_P$, which in practice is very rarely .Therefore it is presupposed, that the available width $b_A$ within the tubed region always is greater than this required width $b_A$. Consequently these formulae and a corresponding check are not included in the method.

In the method Annex J is renamed $p/2 => \chi$. The load ratio $\Phi_U$ then is calculated as follows:

$$\Phi_U = |P_D|/[P_D]; \qquad [P_D] = p \cdot [M]_P/{b_U}^2 \qquad \rightarrow$$

$$\Phi_U = |P_D| \cdot 2 \cdot {b_U}^2/\left\{\chi \cdot f_P \cdot {e_P}^2\right\} \le 1 \qquad \text{(JC.5-55)}$$

For the given calculation is essential independent from the whole axisymmetric tubebundle the should be assumed no interaction between $\Phi_U$ and another load ratio.

The calculation of $\Phi_U$ is an additional check to guarantee the safety in special cases of thin tubesheets which are possible under the applied presupposition $P_I = 0$.

## JD Different types of vessels and flanges

### JD-1 Global forces

#### General remarks

The six main types of tubular heat exchangers are shown in the method EN 13445-3, Annex J, Figures J-1 to J-6. The forces $S_1$ at the diameter $d_1$ (boundary of the tubed region) in these figures are sketched very small without its symbol. Figure JC-2 (here) shows the definitions of $S_1$ and $M_1$ as well.

In the following for these main types of heat exchangers are described in general and written in detail the axial equilibrium conditions, being basically for the “Active resultant pressure” in the method.

There in general are two or more possibilities to determine the required equilibrium conditions. Given is as possible the most simple variant; the other variants should have the same final results.

Because the effects of weight (constructive parts and operating fluids as well) is separated from the effects of fluid pressures, the following calculations are restricted to the effects of fluid pressures, the effects of weight are ignored. Therefore the fluid pressures at both tubesheets are assumed to be equal.

As already mentioned before, the shear force $S_1$ is replaced by an equivalent pressure $P_R$ as follows:

$$S_1 \cdot \pi \cdot d_1 = P_R \cdot \pi \cdot d_1^2 / 4 \qquad \text{(JD.1-0)}$$

**Figure J-1 : U-tube type**

This type has only one tubsheet and one channel.

Equilibrium condition for axial forces at the tubebundle :

$$S_1 \cdot \pi \cdot d_1 = (P_T - P_S) \cdot d_1^2 \cdot \pi / 4 \qquad \text{(JD.1-1)}$$

Note: Forces in the tubebundle are independent of the vessel (shell and channel).

**Figure J-2: Immersed floating head**

The immersed floating head has no contact to the shell ; it is free for axial displacement.

Equilibrium condition for axial forces at the tubebundle including the closed floating head (This is the same conditions as for U-tube type, because all forces at the floating head balance itself.) :

$$S_1 \cdot \pi \cdot d_1 = (P_T - P_S) \cdot d_1^2 \cdot \pi / 4 \qquad \text{(JD.1-2)}$$

NOTE : Forces in the tubebundle are independent of the vessel (shell and channel).

**Figure J-3: Externally sealed floating head**

The externally sealed floating head exchanger has a closed head at the second tubesheet. This head/channel is moveable together with the second tubesheet. The sealing (with the possible axial displacement) is between this head and the shell (or constructive parts welded to the shell). At the package (diameter $d_K$ ) are radial normal forces and (due to axial movements) axial friction forces, which are neglected.

Equilibrium condition for axial forces at the tubebundle including the closed floating head:

$$S_1 \cdot \pi \cdot d_1 = \left\{P_T \cdot d_1^2 + P_S \cdot \left(d_K^2 - d_1^2\right)\right\} \cdot \pi / 4 \qquad \text{(JD.1-3)}$$

NOTE: For $d_K = d_1$ indeed the shell side pressure $P_S$ has no influence on $S_1$ .

**Figure J-4: Internally sealed floating head**

The " internally sealed floating head " has no closed floating head at the second tubesheet; the second head/channel is not moveable connected to the shell. The sealing (with the possible axial displacement) is between the second tubesheet (or constructive parts welded to it) and the shell or the second head/channel at the shell. At the package (diameter $d_K$ are radial normal forces and (due to axial movements) axial friction forces, which are neglected.

Equilibrium condition for axial forces at the whole shell including both heads:

$$S_1 \cdot \pi \cdot d_1 = (P_S - P_T) \cdot \left(d_K^2 - d_1^2\right) \cdot \pi / 4 \qquad \text{(JD.1-4)}$$

NOTE: For $d_k = d_1$ indeed the force $S_1$ becomes zero.

**Figure J-5: Fixed tubesheets with expansion bellows**

The relative axial thermal displacements between the two tubesheets are compensated by the elastic expansion bellows within the shell. The elastic deformation of the expansion bellows causes an axial force, which in general is small compared to the other axial forces; therefore in the following it is neglected. The fluid pressure inside the expansion bellows causes an axial force which may be assumed as follows:

$$F_S = -P_S \cdot \left(d_K^2 - d_S^2\right) \cdot \pi / 4 \qquad \text{(JD.1-5)}$$

Here $d_K$ is the mean inside diameter of the expansion bellows. (For the definition of $F_S$ compare J-6).

Equilibrium condition for axial forces at the one or other channel:

$$S_1 \cdot \pi \cdot d_1 = \left\{P_T \cdot {d_1}^2 + P_S \cdot \left({d_K}^2 - {d_1}^2\right)\right\} \cdot \pi / 4 \qquad \text{(JD.1-6)}$$

This equation may be found by substitution of equation (JD.1-5) into equation (JD.1-8).

NOTE: Equation (JD.1-6) is remarkably equal equation (JD.1-3).

**Figure J-6: Fixed tubesheets without expansion bellows**

Without special elements to compensate the thermal axial deformation, the axial force in the shell $N_S$ is static indetermined. $N_S$ is the axial membrane force in the shell [N/mm], tensile force positive.

The total axial force in the shell is ( $d_S$ is the inside diameter of the shell):

$$F_S = \pi \cdot \left(d_S + e_S\right) \cdot N_S \qquad \text{(JD.1-7)}$$

Equilibrium condition for axial forces at the one or other channel:

$$S_1 \cdot \pi \cdot d_1 = \left\{P_T \cdot {d_1}^2 + P_S \cdot \left({d_S}^2 - {d_1}^2\right)\right\} \cdot \pi / 4 - F_S \qquad \text{(JD.1-8)}$$

To get more information, first are defined two abbreviations :

$$A_R = {d_1}^2 \cdot \pi / 4 \qquad \text{(JD.1-9)}$$

$$F_R = \left\{P_T \cdot {d_1}^2 + P_S \cdot \left({d_S}^2 - {d_1}^2\right)\right\} \cdot \pi / 4 \qquad \text{(JD.1-10)}$$

Then with equation (JD.1-0) from equation (JD.1-8) follows:

$$P_R \cdot A_R = F_R - F_S \qquad \text{(JD.1-11)}$$

The load carrying capacities of the tubebundle and the shell are limited as follows (Figure JC-2):

$$-\left[Q_c\right] \le P_R - P_E \le +\left[Q_t\right] \qquad \text{(JD.1-12)}$$

$$-\left[F_c\right] \le F_S \le +\left[F_t\right] \qquad \text{(JD.1-13)}$$

Replacing $F_S$ by equation (JD.1-11) in the last equation follows:

$$P_E - \left[Q_c\right] \le P_R \le P_E + \left[Q_t\right] \qquad \text{(JD.1-14)}$$

$$F_R - \left[F_t\right] \le P_R \cdot A_R \le F_R + \left[F_c\right] \qquad \text{(JD.1-15)}$$

These two equations gives the equations (J.7.5-7) in Annex J.

**All types**

Some times is required a formula for the total shell force $F_S$ . This for all types is found from the equilibrium of axial forces at the stationary tubesheet as follows:

$$F_S = \left\{P_T \cdot {d_1}^2 + P_S \cdot \left({d_S}^2 - {d_1}^2\right) - P_R \cdot {d_1}^2\right\} \cdot \left(\pi / 4\right)$$

$$F_S = \left\{P_S \cdot {d_S}^2 + \left(P_D - P_R\right) \cdot {d_1}^2\right\} \cdot \left(\pi / 4\right) \qquad \text{(JD.1-16)}$$

## JD-2 Edge bending moments

### Introduction

The four types of tubesheet edges are shown in the method EN 13445-3, Annex J, Figures J-10 to J-13. There the axial forces $S_2$ and the bending moments $M_2$ at the diameter $d_2$ (outside the boundary of the untubed rim) in these figures are sketched without its symbols. Figure JD-2 (here) shows the definitions of $S_2$ and $M_2$ . Figures J-10 to J-13 show for each type two variants: a) $b_S > 0$ and b) $b_S < 0$ . The calculation of the global forces requires to respect the whole heat exchanger. The determination of the edge bending moments $M_2$ may be done for a single tubesheet. The adjacent flange and/or shell must be respected. At the end of this subclause are determined resultant and optimum edge bending moments.

$M_A + M_B$ **= active bending moments**

In the following are determined the sums of the active bending moment from flange bolt load $M_A$ and actions of fluid pressures outside the diameter $d_2$ , causing the moment $M_B$ .

**Figure J-10: Both sides integral**

Equilibrium conditions for the total axial forces $F_C$ in the channel and $F_S$ in the shell:

$$F_C = +P_T \cdot {d_C}^2 \cdot (\pi / 4) \quad \text{(JD.2-1)}$$

$$F_S = \left\{P_S \cdot {d_S}^2 + (P_D - P_R) \cdot {d_1}^2\right\} \cdot (\pi / 4) \quad \text{(see equation (JD.1-16)} \quad \text{(JD.2-2)}$$

Variant a) $b_S > 0: \; d_C = d_2 + 2 \cdot b_S$

$$(M_A + M_B) \cdot \pi \cdot d_2 = +F_C \cdot (b_S + e_C / 2) - F_S \cdot e_S / 2 - P_T \cdot \left({b_S}^2 / 2\right) \cdot \pi \cdot (d_2 + b_S)$$

$$(M_A + M_B) \cdot \pi \cdot d_2 \approx +P_T \cdot b_S \cdot d_2 \cdot (d_2 + 2 \cdot b_S) \cdot (\pi / 4)$$

Variant b) $b_S < 0: \quad d_S = d_2 - 2 \cdot b_S$ (JD.2-3)

$$(M_A + M_B) \cdot \pi \cdot d_2 = +F_C \cdot e_C / 2 - F_S \cdot (-b_S + e_S / 2) + P_S \cdot \left({b_S}^2 / 2\right) \cdot \pi \cdot (d_2 - b_S)$$

$$(M_A + M_B) \cdot \pi \cdot d_2 \approx \left\{P_S \cdot d_2 \cdot (d_2 - 2 \cdot b_S) + (P_D - P_R) \cdot {d_1}^2\right\} \cdot (\pi / 4) \cdot b_S \quad \text{(JD.2-4)}$$

Here the small lever arms $e_C / 2$ and $e_S / 2$ are neglected.

**Figure J-11 : Both sides flanged**

Equilibrium conditions for the axial forces at the flange connection:

$$F_B = F_{GC} + P_T \cdot {d_{GC}}^2 \cdot (\pi / 4) \quad \text{(JD.2-5)}$$

$$F_B = F_{GS} + P_S \cdot \left({d_{GS}}^2 - {d_S}^2\right) \cdot (\pi / 4) + F_S$$

$$F_B = F_{GS} + \left\{P_S \cdot {d_{GS}}^2 + (P_D - P_R) \cdot {d_1}^2\right\} \cdot (\pi / 4) \quad \text{(JD.2-6)}$$

Variant a) $b_S > 0: \; d_{GC} = d_2 + 2 \cdot b_S$

$$(M_A + M_B) * \pi * d_2 = -F_{GC} * b_S - P_T * \left({b_S}^2 / 2\right) * \pi * (d_2 + b_S)$$

$$(M_A + M_B) \cdot \pi \cdot d_2 \approx -F_B \cdot b_S - P_T \cdot b_S \cdot d_2 \cdot (d_2 + 2 \cdot b_S) \cdot (\pi / 4) \quad \text{(JD.2-7)}$$

Variant b) $b_S < 0: \; d_{GS} = d_2 + 2 \cdot b_S$

$$(M_A + M_B) \cdot \pi \cdot d_2 = -F_{GS} \cdot b_S + P_S \cdot \left({b_S}^2 / 2\right) \cdot \pi \cdot (d_2 - b_S)$$

$$(M_A + M_B) \cdot \pi \cdot d_2 \approx -F_B \cdot b_S + \left\{P_S \cdot d_2 \cdot (d_2 - 2 \cdot b_S) + (P_D - P_R) \cdot {d_1}^2\right\} \cdot (\pi / 4) \cdot b_S \quad \text{(JD.2-8)}$$

**Figure J-12: Channel flanged**

Equilibrium conditions for axial forces (as in the both cases before):

$$F_B = F_{GC} + P_T \cdot {d_{GC}}^2 \cdot (\pi / 4) \quad \text{(JD.2-9)}$$

$$F_S = \left\{P_S \cdot {d_S}^2 + (P_D - P_R) \cdot {d_1}^2\right\} \cdot (\pi / 4) \quad \text{(JD.2-10)}$$

Variant a) $b_S > 0: \; d_{GC} = d_2 + 2 \cdot b_S$

$$(M_A + M_B) \cdot \pi \cdot d_2 = +F_B \cdot (d_{3e} - d_2) / 2 - F_{GC} \cdot b_S - P_T \cdot \left({b_S}^2 / 2\right) \cdot \pi \cdot (d_2 + b_S) - F_S \cdot e_S / 2$$

$$(M_A + M_B) \cdot \pi \cdot d_2 \approx +F_B \cdot (d_{3e} - d_2) / 2 + P_T \cdot b_S \cdot d_2 \cdot (d_2 + 2 \cdot b_S) \cdot (\pi / 4) \quad \text{(JD.2-11)}$$

Variant b) $b_S < 0: \; d_S = d_2 - 2 \cdot b_S$

$$(M_A + M_B) \cdot \pi \cdot d_2 = +F_B \cdot (d_{3e} - d_{GC}) / 2 - F_S \cdot (-b_S + e_S / 2) + P_S \cdot \left({b_S}^2 / 2\right) \cdot \pi \cdot (d_2 - b_S)$$

$$(M_A + M_B) \cdot \pi \cdot d_2 \approx +F_B \cdot (d_{3e} - d_{GC}) / 2 + \left\{P_S \cdot d_2 \cdot (d_2 - 2 \cdot b_S) + (P_D - P_R) \cdot {d_1}^2\right\} \cdot (\pi / 4) \cdot b_S \quad \text{(JD.2-12)}$$

Here the small lever arm $e_S / 2$ is neglected.

**Figure J-13: Shell flanged**

Equilibrium conditions for axial forces (as in the both cases before):

$$F_C = +P_T \cdot {d_C}^2 \cdot (\pi / 4) \quad \text{(JD.2-13)}$$

$$F_B = F_{GS} + P_S \cdot \left(d_{GS}{}^2 - d_S{}^2\right) \cdot (\pi/4) + F_S = F_{GS} + \left\{P_S \cdot d_{GS}{}^2 + \left(P_D - P_R\right) \cdot d_1{}^2\right\} \cdot (\pi/4) \qquad \text{(JD.2-14)}$$

Variant a) $b_S > 0$: $d_C = d_2 + 2 \cdot b_S$

$$\left(M_A + M_B\right) \cdot \pi \cdot d_2 = -F_B \cdot \left(d_{3e} - d_2\right)/2 + F_C \cdot \left(b_S + e_C/2\right) - P_T \cdot \left(b_S{}^2/2\right) \cdot \pi \cdot \left(d_2 + b_S\right)$$

$$\left(M_A + M_B\right) \cdot \pi \cdot d_2 \approx -F_B \cdot \left(d_{3e} - d_{GC}\right)/2 + P_T \cdot b_S \cdot d_2 \cdot \left(d_2 + 2 \cdot b_S\right) \cdot (\pi/4) \qquad \text{(JD.2-15)}$$

Variant b) $b_S < 0$: $d_{GS} = d_2 - 2 \cdot b_S$

$$\left(M_A + M_B\right) \cdot \pi \cdot d_2 = -F_B \cdot \left(d_{3e} - d_2\right)/2 - F_{GS} \cdot b_S - F_C \cdot e_C/2 + P_S \cdot \left(b_S{}^2/2\right) \cdot \pi \cdot \left(d_2 - b_S\right)$$

$$\left(M_A + M_B\right) \cdot \pi \cdot d_2 \approx -F_B \cdot \left(d_{3e} - d_2\right)/2 + \left\{P_S \cdot d_2 \cdot \left(d_2 - 2 \cdot b_S\right) + \left(P_D - P_R\right) \cdot d_1{}^2\right\} \cdot (\pi/4) \cdot b_S \qquad \text{(JD.2-16)}$$

Here the small lever arm $e_C/2$ is neglected.

**$M_C$ = reactive bending moment from connected components**

Here are given some explanations to the reactive bending moment $M_C$ from adjacent flange and shells.

Both are taken from the alternative method for calculation of flange connections:

EN 13445-3, Annex G: Subclause G.7.4: Integral flange… : $W_F$ => $M_C \cdot \pi \cdot d_2$ →

$$\left\{f_F \cdot 2 \cdot b_F \cdot e_F{}^2 + f_E \cdot d_E \cdot e_E{}^2 \cdot c_M\right\}/4 \;\Rightarrow\; M_C \cdot d_2 \qquad \text{(JD.2-17)}$$

Not required values here are put equal 0 or 1 respectively.

The first term is for the tubesheet flange:

$$M_C = \left\{\left(f_F \cdot e_F{}^2\right)/4\right\} \cdot 2 \cdot b_F / d_2 \qquad \text{(JD.2-18)}$$

The second term is for an adjacent shell (or channel):

$$M_C = \left\{f_E \cdot d_E \cdot e_E{}^2/4\right\} \cdot c_M \qquad \text{(JD.2-19)}$$

At the tubesheets is to be replaced $f_E \cdot d_E \cdot e_E$ => $f_S \cdot d_S \cdot e_S$ and/or $f_E \cdot d_E \cdot e_E$ => $f_C \cdot d_C \cdot e_C$.

The factor $c_M$ respects the decrease of load carrying capacity due to the direct action of a fluid pressure and/or an axial force. For flanges it is given by a relative complicated formula. For tubesheets (respecting its relative small influence) it is simplified to respect only pressure (not force) and further simplified from the Mises criterion in the direction to the Tresca criterion (more conservative):

Original formula for flanges, only for fluid pressure $P_E$:

$$c_M = \left\{(4/3) \cdot \left[1 - (9/16) \cdot \delta_Q{}^2\right] \cdot \left[1 - (3/4) \cdot \delta_Q{}^2\right]\right\}^{1/2} \qquad \text{(JD.2-20)}$$

Simplified formula tubesheets:

$$c_T = \left[1 - (3/4) \cdot \delta_Q{}^2\right]^{1/2} \qquad \text{(JD.2-21)}$$

In both cases:

$$\delta_Q = \left(P_E \cdot d_E\right)/\left(2 \cdot f_E \cdot e_E\right) \qquad \text{(JD.2-22)}$$

A comparison of both formulae is given in the following small table:

| | | | | | | | |
|---|---|---|---|---|---|---|---|
| $\delta_Q$ = | 0,000 | 0,200 | 0,400 | 0,600 | 0,800 | 0,900 | 1,000 |
| $c_T$ = | 1,000 | 0,985 | 0,938 | 0,854 | 0,721 | 0,626 | 0,500 |
| $c_M$ = | 1,155 | 1,133 | 1,067 | 0,953 | 0,781 | 0,659 | 0,520 |
| $c_T/c_M$ = | 0,866 | 0,869 | 0,879 | 0,896 | 0,923 | 0,950 | 0,962 |

As to be expected all results for tubesheets are more conservative than the results for flanges.

**$M_D$ = reactive bending moment limitation by the tubesheet**

Limit load equation Tresca for uniaxial stresses:

$$\sigma^2 + \tau^2 = [\sigma]^2 = f_P{}^2 \qquad \text{(JD.2-23)}$$

Bending moment and sharing force at $r = d_2/2$:

$$M_2 = \sigma \cdot e_P{}^2/4\,; \quad S_2 = \tau \cdot e_P \qquad \text{(JD.2-24)}$$

From both equations follows:

$$M_2 = \left(f_P \cdot e_P{}^2/4\right) \cdot \left\{1 - \left[S_2 \cdot 2/\left(f_P \cdot e_P\right)\right]^2\right\}^{1/2} \qquad \text{(JD.2-25)}$$

Knowing $S_1 = P_R \cdot d_1/4$ and simplifying $S_2 \approx S_1$ for $M_2$ => $M_D$ follows:

$$M_D = \left(f_P \cdot e_P{}^2/4\right) \cdot \left\{1 - \left[P_R \cdot d_1/\left(2 \cdot f_P \cdot e_P\right)\right]^2\right\}^{1/2} \qquad \text{(JD.2-26)}$$

In this equation additional may be respected the possibility of a local reduction for $e_P$ at $d = d_2$.

Replacing $d_1$ by $d_2$ equation (JD.2-26) becomes a little bit more conservative.

**Resultant and optimum edge bending moments**

The reactive bending moments $M_C$ and $M_D$ may act in any direction (positive or negative) and they not necessary act with its possible maximum absolute value. Therefore the resultant bending moment $M_2$ may vary within the range $M_{2,\min} \le M_2 \le M_{2,\max}$.

$$M_{2,\max} = \min\left\{M_A + M_B + M_C; +M_D\right\} \qquad \text{(JD.2-27)}$$

$$M_{2,\min} = \max\left\{M_A + M_B + M_C; -M_D\right\} \qquad \text{(JD.2-28)}$$

Due to small plastic deformations the real value $M_2$ approximates a value $M_{2,opt}$, being optimum for the limit load. These values are calculated as follows:

The moment $M_2$ shall be determined such that the load ratio for bending $\Phi_B$ becomes minimum.

Based on equation (JC.3-21) then the requirement (task) is:

$$\max\{L1; L2; L3\} \quad \Rightarrow \text{Min !} \qquad \text{(JD.2-29)}$$

By use of modified parameters L1, L2, L3 (modified in comparison to Annex J.9.1) this means:

$$L1 = 1/\left(2 + k_p\right); \qquad L2 = \left\{\left|1 + x \cdot (1 - a)\right| + \left|x \cdot a\right|\right\}/\left(1 + k_p + b\right); \qquad L3 = \left\{1/3 + \left|1/3 + x\right|\right\}/(1 + b)$$

$$a = \lambda_R/2\,; \quad b = \lambda_R/\varphi_P\,; \quad x = m_R/p_Q \text{ (asked value)} \qquad \text{(JD.2-30)}$$

$L1$ is independent of $x$ and therefore the extreme minimum possible value. The next question is to find solutions for $L2 = L1$ and $L3 = L1$. There indeed are real applicable solutions in the following region:

$$-(1+b)/\left(2 + k_p\right) \le x \le -(1-b)/\left|\left(2 + k_p\right) \cdot \left(1 - \lambda_R\right)\right| \qquad \text{(JD.2-31)}$$

For $\lambda_R = 0$ both limits are equal. This solution is selected for the method. Equation (JC.2-12) gives:

$$m_{2,opt} \cdot \left(1 + \lambda_R\right) = -2 \cdot \left\{P_Q/\left[2 \cdot \left(2 + k_P\right)\right] + p_R \cdot \lambda_R + p_D \cdot \lambda_R{}^2 \cdot \left(1 + \lambda_R/3\right)\right\} \qquad \text{(JD.2-32)}$$

$$M_{2,opt} = -\left\{P_Q/\left[2 \cdot \left(2 + k_P\right)\right] + P_R \cdot \lambda_R + P_D \cdot \lambda_R{}^2 \cdot \left(1 + \lambda_R/3\right)\right\} \cdot d_1{}^2/\left\{8 \cdot \left(1 + \lambda_R\right)\right\} \qquad \text{(JD.2-33)}$$

The calculated moment $M_{2,opt}$ may be outside the above defined possible range. Therefore the real bending moment $M_2$ is to be restricted as follows:

$$M_2 = \max\left\{M_{2,\min,}; \min\left(M_{2,opt}; M_{2,\max}\right)\right\} \qquad \text{(JD.2-34)}$$

The pressure finally representing the moment is defined thus (again us of equation (JC.2-12):

$$p_M = m_R/2 = \left\{m_2 \cdot \left(1 + \lambda_R\right) + p_R \cdot 2 \cdot \lambda_R + p_D \cdot 2 \cdot \lambda_R{}^2 \cdot \left(1 + \lambda_R/3\right)\right\}/2 \qquad \text{(JD.2-35)}$$

$$P_M = M_2 \cdot 8 \cdot \left(1 + \lambda_R\right)/d_1{}^2 + P_R \cdot \lambda_R + P_D \cdot \lambda_R{}^2 \cdot \left(1 + \lambda_R/3\right) \qquad \text{(JD.2-36)}$$

After determination of this last value all limit load conditions for the tubebundle may be checked.

**JD-3 Fatigue for fixed tubesheet heat exchangers without expansion bellows**

**Exemption for fatigue analysis**

The given condition

$$\left|\alpha_T \cdot t_T - \alpha_S \cdot t_S\right| < 0{,}2 \cdot 10^{-3} \qquad \text{(JD.3-1)}$$

is based on general experiences which are written in TGL 32903/31 [6] as follows:

"Changes of temperature differences between adjacent parts less than 15K for ferritic steels and 20K for austenitic steels…may be ignored for fatigue proofs."

From this rule the right side of the given criterion were $< (0{,}18...0{,}32) \cdot 10^{-3}$.

It shall be noted, the influence of fluid pressures here is ignored, however in the following simplified fatigue analysis it is respected.

**Simplified fatigue analysis**

The given condition

$$\left|\Delta P_F\right| < \left\{2 \cdot (e_P/L_T)^{1/2} + 0{,}5 \cdot {b_R}^2/(L_T \cdot e_P)\right\} \cdot \vartheta \cdot \Delta\sigma_R/K_{e2} \qquad \text{(JD.3-2)}$$

is taken from TGL32903/23 [5] with only some changes of symbols.

A minor change in contents results from the following substitution: $2{,}2 \cdot [\sigma_A]_P/\xi$ => $\Delta\sigma_R/K_{e2}$.

The "new" $\Delta\sigma_R \approx 2 \cdot [\sigma_A]_P$ $(\text{range} \approx 2 \cdot \text{amplitude})$ is taken according to EN 13445-3, clauses 17, 18. The figure for determination of $K_{e2}$ is (with simplifications) also taken from TGL 32903/23.

The formula which defines $\left|\Delta P_F\right|$ is also with only minor corrections from the same source. It shall be noted, that a direct comparable formula for $P_e$ is given in EN 13445-3, subclause 13.5 (Fixed tubesheet heat exchangers), but there with the simplification $\lambda_R = 0$ (without untubed rim).

**Detailed fatigue analysis**

The formulae to calculate the ranges of forces and moments are based on

Richtlinienkatalog Festigkeitsberechnungen (RKF), Behälter und Apparate; Teil 4 [3], BR-W 3: "Wärmeübertrager. Rohrbündelwärmeübertrager mit festem Rohrbündel" (Heat exchangers with fixed tubesheets); Dresden 1970, 1976; VEB Komplette Chemieanlagen Dresden, 1983 (Author: J.Wölfel).

For EN 13445-3, Annex J, unchanged adopted are e.g. $1_R, \lambda_R, \omega_R, \gamma_R; B_{RJ}, H_J (J = 1{,}2{,}3)$ and $M_2$.

Other details are approximated to TGL 32903/23, e.g the acceptance limit. The values $D^*, E^*, \nu^*$ and $k_C, k_S$ are taken from EN 13445-3, clause 13.

While in RKF the formulae for the calculation of stresses was restricted to thin tubesheets (large $\omega_R$, very good for $\omega_R > 4$, in East Germany common design) for Annex J they are extended to all cases. The approximation formulae for $H_1, H_2, H_3$ and $C_1, C_2$ was made by the author in 1996, they are based on numerical results elaborated by the author in 1966 (using a computer ZRA1).

Subclause J.10.3 as subclause 13.5 are based on the linear theory of elasticity, special for quasi homogeneous (weakened) thin plates on elastic foundation. The solutions for axisymmetric loaded circular plates are given by the special Bessel functions ber( ), bei( ); they are basis of both methods.

Main differences between both methods are as follows:

(a) Subclause 13.5 takes not into account the untubed rim.

(b) Subclause 13.5 is intended to calculate static strength, not to make fatigue analysis.

## JE Future work

In 2004 are planned three work items to improve Annex J:

(1) "To determine more accurately the leak tightness and strength of flanged extensions to tubesheets by calculating more precisely the interaction of the tubesheet-flange connection."

(2) "To design flanged extension which are thicker than the tubesheet."

(3) "To design tubesheets with large untubed rims (i.e. with an effective tubed region which is symmetrical about a tubesheet diameter but not symmetrical about its axis)."

From the work items (1) and (2) shall result a common generalisation of Annex G and Annex J. A short title may be: "Heat exchanger tubesheet flange connections". Such a method is already mentioned and missed in subclause J.4.3. (Several editorial details remain open.)

From the work item (3) shall result a generalisation of Annex J, subclauses J.9.1 to J.9.3. A short title may be: "Non axisymmetric tubebundles". (Non axisymmetric flanges probably will be not calculated.)

**JF Bibliography**

[1] AD-Merkblätter "Berechnung von Druckbehältern"

[2] Wölfel, J.: "Elastisch gekoppelte, ungleiche Kreisplatten in der Festigkeitsberechnung von Rohrbündelwärmeübertragern" Mitteilungen Industrie-Forschungszentrum Chemieanlagen, 1969.

[3] RichtlinienKatalog Festigkeitsberechnungen (RKF), Behälter und Apparate; Teil 4: "Wärmeübertrager. Rohrbündelwärmeübertrager……"(Heat exchangers ……); Dresden 1970, 1976; VEB Komplette Chemieanlagen Dresden, 1983 (Author: J.Wölfel).

[4] Wölfel, J.: "Tragfähigkeitsnachweise für Rohrbündelwärmeübertrager" Wissenschaftliche Zeitschrift der Technischen Hochschule Otto von Guericke Magdeburg, 1977.

[5] TGL 32903/23 (1986) "Behälter und Apparate. Festigkeitsberechnung. Rohrbündel- Wärmeübertrager" (ST RGW 4782-84)

[6] TGL 32903/31 (1983) "Behälter und Apparate. Festigkeitsberechnung. Ermüdung bei zyklischer Belastung" (ST RGW 3684-82)

## Annex K Additional information on expansion bellows design

No comments.

## Annex L Basis for design rules related to non-pressure loads

No comments.

## Annex M Measures to be adopted in service

No comments.

## Annex N Bibliography to Clause 18

No comments.

## Annex O Physical properties of steels

No comments.

## Annex P Classification of weld details to be assessed using principal stresses

No comments.

## Annex Q Simplified procedure for fatigue assessment of unwelded zones

No comments.

## Annex ZA Clauses of this European Standard addressing essential requirements or other provisions of the EU Directives

Harmonised standards provide a presumption of conformity with the essential requirements, of the Directive when their reference has been published in the Official Journal.

Annex ZA in a harmonised standard is the link between the standard and the directive. The directive places full responsibility on the manufacturer to comply with the Essential Safety Requirements (ESRs). Benefit is gained from the use of harmonised European standards as the manufacturer may presume conformity with some or all of the ESRs. Annex ZA lists in a table the clauses in the standard and the ESRs in Annex I of the directive to which they refer.

EN 13445-3 is linked to the ESRs about design (Annex I, section 2 of directive 97/23/CE, plus some quantitative requirements from section 7). By reading Table ZA.1, we are informed of those ESRs which are nor dealt with (e.g. experimental design method in the version of 2002).